Across the Irish Sea: Dental Affinities between Irish and British Populations from the Neolithic to Medieval Periods

Gabriel Peter Reavey

Thesis submission in partial fulfilment of requirements for the degree of Doctor of Philosophy

Liverpool John Moores University

MARCH 2026

Contents

List of Figures

List of Tables

House Farm, Poulton, GLC= St. Owen's Church Gloucester, GLRC= London Road, Gloucester, LDG= Great House Farm, Llandough, ATE= site 92, Atlantic Trading Estate, Barry, BRS= Brownslade Barrow, Castlemartin, STG= Strath Glebe chambered cairn, Skye, DIS= Distillery Cave, Oban, RAS= Raschoille Cave, Oban, SGR= Southgreen, Kildare, PKN= Parknahown 5, Co. Laois, KLY= Killeany 1, Co. Laois, BFL= Bushfield/Lismore, Co. Laois

Table 8: Trait percentages of numbers of individuals scored for a sub-set of 22 traits by sample. NOR= Norton Priory, Runcorn, POU= Chapel House Farm, Poulton, GLC= St. Owen's Church Gloucester, GLRC= London Road, Gloucester, LDG= Great House Farm, Llandough, ATE= site 92, Atlantic Trading Estate, Barry, BRS= Brownslade Barrow, Castlemartin, CLV= Culver Hole, Llangennith, TKW= Tinkinswood Burial Chamber, St. Nicholas, STG= Strath Glebe chambered cairn, Skye, DIS= Distillery Cave, Oban, RAS= Raschoille Cave, Oban, WHIT= Whithorn Priory, Dumfries and Galloway, SGR= Southgreen, Kildare, PKN= Parknahown 5, Co. Laois, KLY= Killeany 1, Co. Laois, BFL= Bushfield/Lismore, Co. Laois. 297

Table 9: Trait percentages of numbers of individuals scored for sub-set of 22 traits by global population sample. WE= Western Europe, NoE= Northern Europe, NA= North Africa, WA= West Africa, SA= South Africa, KH=Khoisan, CM= China-Mongolia, Jo= Jomon, RJ= Recent Japan, NES= Northeast Siberia, SS= South 299

Siberia, AA= American Arctic, NWA= Northwest America, NSAI= N. & S. American Indian, SEE= Southeast Asia (Early), SER=Southeast Asia (Recent), PO= Polynesia, MI= Micronesia, AU= Australia, NG= New Guinea, ML= Melanesia

Abstract

Migrations into and between Britain and Ireland have been attested to throughout history such as those of the Anglo-Saxons and Vikings, and the Scotti of Dál Riata in Early Medieval times. Archaeological material also shows patterns of shared material culture across Ireland and western Britain throughout the Neolithic to the medieval period. This thesis improves the understanding of the biological diversity in these regions and explore the causes.

Following the Arizona State University Dental Anthropology System (ASUDAS), dental non-metric trait data were collected for 36 traits in 570 individuals from 17 British and Irish samples that ranged from the Neolithic to the medieval period in date. The data were analysed using Principal Components Analysis (PCA), Kendall's tau-b correlation coefficient and mean measure of divergence (MMD) to compare the samples and determine the biological similarity and dissimilarity among populations. Multidimensional Scaling (MDS) was used to graphically illustrate the inter-sample relationships. MMD and geographic distance matrices were compared using Mantel test.

Results revealed a degree of homogeneity among the samples (36-trait MMD range 0.000-0.127; 17-trait MMD range 0.000-0.390) while MDS

revealed regional grouping among the samples. It was found that there is no significant difference between British and Irish populations, although phenetic patterns may differ to patterns in the archaeological record. The MMD distances align with the archaeological record to suggest close relationships between Ireland and Scotland. The findings, while suggesting Anglo-Saxon migration contributed to the gene-pool in the English samples to some degree, are consistent with population continuity in England. There is no strong positive relationship between MMD and geographic distances suggesting that patterns of gene flow and migration are more complex than a linear "stepping-stone" model.

Declaration

I, Gabriel Peter Reavey, confirm that no portion of the work referred to in this thesis has been submitted in **s**upport of an application for another degree or qualification of this or any other university or other institute of learning

Declaration of AI use

I, Gabriel Peter Reavey, confirm that ChatGPT has been used in the writing of this thesis for the purposes of improving grammar only.

Acknowledgements

Firstly, I must thank my director of studies, Prof. Joel Irish whose support and guidance throughout the duration of this project has been invaluable. Furthermore, I would also like to thank the other members of my supervisory team, Dr. Richard Jennings and Dr. Mark Grabowski, who have also provided their guidance.

I would also like to thank the Poulton Research Project, Museum of Gloucester and Liverpool John Moores University who enabled access to the Poulton and Gloucester collections housed at the university. Further thanks is given to: Norton Priory Trust, in particular Lynn Smith for access to the Nortion Priory collection ; Jody Deacon for enabling access to collections at National Museum Cardiff; Dr. Matthew Knight; for enabling access to collections at National Museum of Scotland Archaeological Consultancy Services Unit, Drogheda, in particular Glenn Gibney, for enabling access to collections stored at their premises; Dr. Alison Sheridan and Angela Boyle for enabling access to the Strath Glebe collection

I am also thankful to all my friends and family who have provided constant encouragement throughout the duration of this project. A special thanks goes out to my partner, Ellen, and my mother, Teresa, whose encouragement and support (and much patience) this project would not have been possible without.

Chapter 1: Introduction

A series of historical migrations into Britain is documented but understanding how they affected the genetic composition of the British population is an open question (Schiffels et al., 2016). The impact of these migrations is important because they can create divisions or dualities in perceptions of those populations and their cultures, e.g., the Romans contrasted with native British (Hingley et al., 2018).

These perceptions can influence policies such as education, with the National Curriculum in England focusing on the Romans and being criticised for neglecting prehistory (English Heritage 2010; Hingley et al., 2018). The National Curriculum in Wales stresses the 'Celtic Iron Age and Celtic Origins of the Welsh,' and since 2008 has offered the choice between 'Iron Age Celts **or** the Romans' (Hingley et al., 2018). These approaches influenced both government and general public sentiment during the Brexit campaign, with the Roman Empire used as an analogy for the EU by both pro-remain and pro-leave supporters (Hingley et al., 2018).

Previous studies have attempted to understand population structure through biological affinity analyses or modern genome sampling—which rely on participants having several generations within a defined area to assume samples are representative of pre-modern populations (Harvey et al., 1986; Leslie et al., 2015). However, the latter studies have issues such as the state of indigenous and immigrant populations both being unknown, so they must estimate both simultaneously. Specifically, migrations are difficult to

quantify if the source population is genetically close to the indigenous populations. Similarly, for Anglo-Saxons it is difficult to distinguish the effects of this migration from other migratory influences from northwest continental sources (Martiniano et al., 2016; Schiffels et al., 2016).

Recent studies assessed the impact of Anglo-Saxon migrations in Britain (Martiniano et al., 2016; Schiffels et al., 2016). The main issue with these studies is the availability of aDNA, due to both cost and issues of preservation. Both studies have small sample sizes to compare against modern samples with Schieffels et al. (2016) generating genomes for 10 samples from three sites and Martiniano et al. (2016) utilising nine ancient genomes from three sites. Even though many data were collected individually, small sample sizes mean that they might not be representative of the overall population from which they originate.

As with Britain, the population structure and impact of historic migrations in Ireland are largely unknown. Early research was conducted in the 1930s by the 'Harvard Irish Mission' using archaeology, and biological and social anthropology (Nash, 2006; Hooton, 1940; Hooton and Dupertius, 1955), but it has been criticised for its use of racial type language (Nash, 2006). Further studies (Bittles and Smith, 1991; Relethford, 1983; Relethford, 1988; Relethford, 1991; Relethford and Crawford, 1980; Relethford and Crawford, 1981) have been criticised as well because the subjects and methods still imply models of national and biological difference, despite dropping the language of racial types (Nash, 2006).

In 2000, a programme called ‘Irish Origins: the Genetic History and Geography of Ireland’ was begun by the Genetic Anthropology Committee in Ireland and focused on contemporary genome sampling to reconstruct prehistoric migration pathways. In this programme, Hill et al. (2000) examined variations on the Y-chromosome, and reconstructed population history by partitioning samples into Surname origin. This study was criticised for needing to be more archaeologically/historically situated and sensitive to issues of origins, ethnicity and cultural identity (Cooney, 2000a; Cooney 2000b).

Attempts at describing genetic structure have primarily used uniparental markers (Gilbert et al., 2017). The main issue with this is that the assumption has to be made that patterns seen in only one sex are representative of the genetic character of the population as a whole.

Furthermore, autosomal studies were unable to identify population structure (Cronin et al., 2007), although have been able to identify differences from European and neighbouring English and Scottish populations (O’Dushlaine et al., 2010). As noted by Gilbert et al. (2017), these studies were limited by a lack of geo-coded data sampling to allow analyses between regions.

Recently, Gilbert et al. (2017) identified fine-scale population structure using the ‘Irish DNA Atlas’ and ‘People of the British Isles’ datas with those from 6760 European individuals and two ancient Irish genomes as references. The study revealed 10 geographically stratified genetic clusters; seven are of ‘Gaelic’ Irish ancestry and two of mixed Irish-British ancestry with a genetic barrier in Ulster (Gilbert et al., 2017). Additionally, they

detected admixture events evidencing Norse-Viking activity and the Ulster Plantations (Gilbert et al., 2017). High levels of North-West French-like and West Norwegian-like ancestry were also observed (Gilbert et al., 2017).

Despite developments in genetic studies, without direct analysis of archaeological data, some events remain poorly understood. Anglo-Norman interactions in Wales and Ireland have been discussed by historians using the writings of Anglo-Norman chroniclers, such as Gerald of Wales as evidence (Sposato, 2009; Lilley 2002). Sposato (2009) argues that systems of lordship and governance in Leinster and Meath indicates Anglo-Norman communities remained separate from native populations. Lilley (2002) applied post-colonial theory to posit Anglo-Normans 'othered' Welsh and Irish populations,and would be little different from European colonisation in Africa, Asia and the Americas.

Similarly for Scotland, the origins of the kingdom of Dál Riata have been questioned. It is posited that written sources present differing narrative traditions so they should not be considered history (Campbell, 2001; Dumville, 2002). Furthermore, the absence of archaeology does not support migration but absence in linguistics does not support purely dynastic takeover (Campbell, 2001).

The Picts are another group in Scotland that are poorly understood. This is because there are very few Pictish historical documents (Noble et al., 2013). Similarly, archaeological material is difficult to interpret as investigation of monuments is rare and poor preservation at Pictish designated cemeteries means little anthropological study has been conducted (Noble et al., 2013).

In this thesis, another approach will be employed. Specifically, dental non-metric traits were scored following the Arizona State University Dental Anthropology System (ASUDAS) in a total of 570 individuals from 17 samples across western Britain and Ireland (areas that encompassed by a region of shared archaeological material culture known as the Irish Sea Pronvince (see chapter 2). The trait data were then compared using principal components analysis (PCA), which reduces the dimensionality to identify the most important directions of variance; mean measure of divergence (MMD), a dissimilarity measure in which low values indicate higher similarity and high values indicate greater inter-sample phenetic distances (Irish, 2010). Multidimensional scaling (MDS) was used to graphically illustrates the inter-sample relationships. Mantel's permutation test, which calculates the correlation between matrices, was used to compare MMD distance and geographic distance matrices to test the isolation by distance model (IBD). Further details about the methods used in this study can be found in Chapter 5.

Previous research has implied there is a significant genetic component to dental non-metric traits and so phenetic affinities based on these traits have been proposed to approximate genetic relatedness (Turner et al. 1991; Scott and Turner, 1997; Irish, 1997). Recently, Irish et al., (2020), using traits in the Arizona State University Dental Anthropology System (ASUDAS), found a close ASUDAS/SNP (single nucleotide polymorphisms) association based on MMD distances and F_{ST} Mantel correlations. The r_m-values ranged between 0.72 globally and 0.84 in Africa; as well, an association with geographical distances from 0.86 for 36 trait African MMD to 0.77 for

F_{ST} was reported. These results imply that ASUDAS traits are a reliable proxy for genetic data. On this basis dental morphological data will be used to address the following research questions and hypotheses.

Research Questions

1. Do British and Irish populations exhibit phenetic variation patterns that support the concept of the Irish Sea Province?

2. Were Scottish populations genetically influenced by Irish populations in the Early Medieval?

3. Were English populations genetically affected by Roman activity in the Iron Age and the Viking and Anglo-Saxon activity in the Early Medieval?

4. Are the morphological differences between the samples explained by the isolation by distance model?

Hypotheses

In order to address these questions, the following hypotheses were tested using principal components analysis (PCA), mean measurement of divergence (MMD) and isolation by distance (IBD) modelling to determine whether significant differences in 36 non-metric dental traits occur between the total samples followed by a second round of analyses using a sub-set of 17 traits.

For the first question:

H_o: There is no difference in the non-metric frequencies based on the MMD distances between the British and Irish samples.

H_1: There is a difference in the non-metric frequencies between the British populations and the Irish populations suggesting that there is low MMD biological affinity between the populations of Western Britain and those of Ireland.

For the second question:

H_o: There is no significant difference in the non-metric frequencies based on MMD distances among Early Medieval Irish populations and Scottish populations.

H_1: There is a significant difference in non-metric frequencies based on MMD distances among Early Medieval Irish populations and Scottish populations suggesting population continuity in population continuity and low/no admixture between the regions

For the third question:

H_o: There is no significant difference in the non-metric frequencies based on MMD distances among English populations and other populations.

H_1: There is a significant difference among English populations and the populations from other regions based on MMD distances suggesting population discontinuity in English populations.

For the fourth question:

H_o: There is no strong positive relationship between the MMD and geographical distances among the British and Irish populations.

H_1: There is a strong positive relationship between the MMD and geographical distances among the British and Irish populations suggesting

that isolation by distance was the main process causing the observed variation.

Significance

In this study dental non-metric traits will be used to estimate biological affinities, i.e., providing a proxy for aDNA evidence to identify population structures and improve understanding of continuity/discontinuity in British Isles populations. This approach avoids the limitations of modern DNA sampling, for example, there is no need for additional inclusion criteria in order to assume that samples represent pre-modern populations because the samples are archaeological and, therefore, come from pre-modern populations. It also avoids several limitations of ancient genome sampling as teeth are more likely to be preserved, macroscopic analysis is non-destructive and traits are largely not sexually dimorphic (Turner et al. 1991; Irish, 2020).

Furthermore, as this study directly observes archaeological populations, it will provide a biological perspective to migrations that have been confined to archaeology and history. A biological perspective can provide clarity to issues that may be unclear due to conflicting written evidence, and archaeological material that it is difficult to interpret.

To date, there has been limited study of dental non-metric traits in Britain and Ireland (Lloyd-Jones, 1995; Lloyd-Jones, 1999; Adler, 2005; Anctil, 2016; Weets, 2004; Weets, 2009). Additionally, regional variability of these traits in Europe has not been researched to the same extent as other regions, so the nature and patterning of these variations are largely unknown (Anctil,

2016). This study will contribute to filling the gap of knowledge in these areas.

Organisation of the Thesis

Chapter 2 outlines the historical and archaeological background regarding the concept of the Irish Sea Province. Archaeological evidence that demonstrates cultural contact between the different regions throughout the periods between the Neolithic and the medieval and whether these may represent cultural diffusion (trade only) or migration is detailed.

Chapter 3 outlines the methodological background of dental affinities analyses.

Chapter 4 details the samples that are included in the study. Background information for each sample is provided.

Chapter 5 describes methods used for data collection and the statistical methods chosen for this study, with a rationale for their use provided.

Chapter 6 provides a brief explanation of the results. This includes the results from Fisher's exact tests for intra-observer error tests, results from PCA, MMD, MDS for the biodistance analysis and results of Mantel test comparing MMD and geodistance matrices for isolation by distance.

Chapter 7 presents an in-depth discussion of the results and their interpretations. Each research question is addressed in turn and conclusions of the study are provided. This is followed by a consideration for possible further work that could be undertaken such as additional analyses.

Chapter 8 provides a summary and the conclusions of the study. The limitations of the research and considerations for future research is detailed.

Appendix I provides an overview of the ASUDAS scoring procedures including figures showing ASUDAS scoring plaques.

Appendix II includes an example of the ASUDAS recording sheet used for data collection.

Appendix III presents the results of Fisher's exact tests used to test for intra-observer error.

Appendix IV provides the inter-trait correlations determined by Kendall's tau-b

Appendix V presents the frequencies and numbers for 22 traits among the British and Irish samples and global populations.

Appendix VI presents graphs that visualize the frequencies for 22 traits among the British and Irish samples and global populations

Chapter 2: Archaeology between Britain and Ireland

The Irish Sea Province/Zone, also often referred to as the Irish Sea Cultural Province/Zone, is a relatively nebulous term used to describe areas in Britain and Ireland—typically the western and eastern coastal regions, respectively—that appear to share cultural elements in the archaeological record rather than forming a geographical or historical political entity. The boundaries of this proposed province/zone vary between researchers. For example, Phythian-Adams (1993) considers it to comprise Cheshire, Lancashire, South Westmorland, and the Isle of Man, defining a cultural province as "a zone occupied by more than one local society; which has a 'persistent existence, defined by the major watersheds'" (Phythian-Adams, 1993; Swallow, 2016). However, when studying the Neolithic period, Cummings (2009) employs a contextual definition based on the distribution of chambered tombs to avoid arbitrary cut-off points that might exclude relevant material.

For the purpose of this study, the initial criterion for defining the Irish Sea Zone was close proximity to the western coastline of Britain and the eastern coastline of Ireland, both of which border the Irish Sea. However, this boundary has been extended based on archaeological evidence and accessibility to the Irish Sea, justifying the inclusion of sites near the Bristol Channel, such as those in South Wales and Gloucester. This approach aims to establish a relatively well-defined region that provides a clear scope while

minimizing arbitrary boundaries that might otherwise exclude relevant sites, similar to the approach taken by Cummings (2009).

The significance of the Irish Sea was largely ignored by antiquarians of the 18th and 19th centuries, as well as by archaeologists in the early 20th century, who favoured theories emphasizing Atlantic and Mediterranean contacts with Ireland (Waddell, 1993). Research into the Irish Sea region began in earnest in the mid-20th century, trending toward the view that the Irish Sea functioned as a unifying rather than a dividing force. For example, Fox (1947) observed that "there is a definite tendency for the shores of the Irish Sea to form a cultural province," while Margaret Davies (1946), in her study of the diffusion and distribution of megalithic tombs, stated that "the borderlands of the Irish Sea and its north gateway formed a broad cultural province knit together by the sea, just as were the English and French shores of the Channel in the Middle and Late Bronze Age."

Much of the research on the Irish Sea Province has focused on the Neolithic period, as new technologies, artifacts, and practices emerged in both Britain and Ireland around 4000 BC. Sheridan (2004) proposed that spatial and chronological patterns in the region can be characterized by several key factors: commonality of origins—meaning the earliest communities shared a common continental ancestry and brought these traditions to Britain and Ireland—regular or sporadic contact between communities on either side of the Irish Sea, and relatively long-distance, exclusive connections.

Furthermore, Sheridan (2004) divides the concept of common origins into hypothetical diasporas: the 'Atlantic movement,' from southern Brittany up

the Irish Sea and along the west coast of Scotland and the north coast of Ireland; 'Cross-Channel-West,' from northern Brittany and Normandy to southern England; and 'Cross-Channel-East,' from several areas along the Channel, stretching from Haute-Normandie to the Netherlands. These distinct migration patterns from different regions of the continent to different parts of Britain and Ireland provide a framework for understanding cultural similarities and differences across these areas. As a result, they also imply that biological relationships in these regions should follow similar trends.

Evidence for the 'Atlantic movement' includes small, closed polygonal megalithic chambers and simple passage tombs found along the coasts of Wales, western Scotland, and Ireland. These structures form the starting point for the complex development of passage tombs (Sheridan, 2004). The design and construction of these tombs appear to parallel those in the Morbihan area of Brittany, and pottery found in a tomb at Achnacreebeag in Scotland has been identified as late Castellic style, which was used in simple passage tombs in Morbihan (Sheridan, 2000; 2004).

Clyde cairns in western Scotland and court tombs in Ireland have also been compared for their similarities and differences. While they share the same basic plan, the Irish tombs tend to be more elaborate, whereas Scottish tombs feature minor characteristics absent from Irish examples (Waddell, 1993; Corcoran, 1972). These similarities could be attributed to a shared common ancestry, as mentioned earlier. However, using Case's (1976) proposal that children were important assets to early farmers—both as

labourers and as a means of extending kinship through marriage—Waddell (1993) suggests that these similarities may instead reflect a complex system of kinship and allegiances.

Similarly, Cummings (2009) notes that megalithic monuments around the Irish Sea are situated in similar landscape settings and argues that the similarities in their structures are deliberate; otherwise, greater variation would be expected (Cummings, 2016). Cummings (2016) further suggests that these similarities in form, use, and setting were intentional expressions of affinities with broader communities beyond western Scotland. Along with Waddell's argument, this challenges the idea that such similarities arose purely from common ancestry and instead supports the notion that sustained contact between these areas was maintained throughout long periods of the Neolithic.

Other finds from the Neolithic period also suggest regular contact across the Irish Sea. Decorated pottery styles associated with tombs on both sides of the Irish Sea exhibit notable parallels. For example, Necked Vessels found at Beacharra on the Mull of Kintyre, Clachaig in Arran, and Bickers Houses on Bute closely resemble Irish Necked Style 1B, whereas those from Achnacree, Nether Largie, and Glenvoidean correspond to Irish Style 1C (Herity, 1982). However, no Exotic Vessels or Globular Bowls have been found in Scottish tombs, as they are exclusive to Irish court tombs (Herity, 1982). This suggests that while contact between these communities was frequent enough to facilitate the exchange of items and ideas, it was not

constant enough to eliminate regional variation, indicating that these communities maintained distinct identities.

Additionally, evidence of raw material movement further supports the existence of regular contact. Porcellanite axeheads from sources in County Antrim have been found in Scotland, England, Wales, and the Isle of Man (Cooney and Mandel, 1998; Sheridan, Cooney and Grogan, 1992). Similarly, Antrim flint has been found in southwestern Scotland (Saville, 1999), Arran pitchstone has been discovered in Ireland (Simpson and Meighan, 1999), and non-porcellanite axes in Ulster may have originated in southwestern England (Cooney, Mandel and Byrnes, 1999). Regarding porcellanite axes, Sheridan (1986) argues that the lack of a clear concentration away from their source suggests that these materials were dispersed through community networks rather than centralized redistribution.

Commonalities in pottery extend from the Neolithic into the Bronze Age. Decorated Irish bowls, found with both unburnt and cremated burials dating to 2300–1800 BC, are well represented in the north of Ireland and Leinster. They also occur in southwest Scotland, particularly in Argyll and Galloway, with fewer examples found on the Isle of Man and southwest Wales (Waddell, 1993). It has been noted that their distribution in Scotland is concentrated along important trade routes (Simpson, 1979). However, Waddell (1993) observes that most pottery vessels are made from local clays, suggesting that their association with burials more likely represents a spread of ritual practice rather than an exogenous movement of potters.

The early Bronze Age saw the introduction of Cinerary Urns, a new funerary tradition characterized by wide-mouthed pottery with narrow bases, inverted over cremated remains. These coexisted with existing Food Vessels before eventually replacing them (Lynn, 1993). Lynn (1993) argues that since no prior burial practices suggest that these rites could have developed locally, and since earlier funerary wares continued to be used alongside some forms of Cinerary Urns, the practice was likely intrusive to Ireland. Additionally, the general concentration of their distribution in northeast Ireland suggests that the main area of influence was southwest Scotland.

Among the Cinerary Urns, two types are particularly notable within the Irish Sea Province. The first is the Collared Urn, which was in use from 2000–1300 BC (Waddell, 1993). This pottery type initially developed over a wide area of England and Wales before spreading to Scotland and Ireland (Longworth, 1984).

The second series of this pottery developed into two main styles: the Northwestern style, centred in northwest England and extending into western Wales, northeastern Ireland, northeastern England, and Scotland; and the Southeastern style, mainly distributed across southern and eastern England (Longworth, 1984). The Southeastern style includes bipartite forms that are absent from Ireland, with type BIII not found outside England and type BII found only rarely in northwest England, Scotland, and Wales (Kavanagh, 1976; Longworth, 1984).

Collared Urns tend to be made using raw materials sourced near their final deposition sites (Longworth, 1984), suggesting that only the ideas were transmitted rather than the pottery or the people themselves. However, Longworth (1984) also notes a strong conservatism in styles and decorative motifs, alongside a lack of localized styles, which implies the existence of strong communication networks with the "main style zones."

The other significant type of Cinerary Urn is the Cordoned Urn, estimated to have been in use from 1800–1300 BC (Waddell, 1993). The distribution of these urns is generally centred in Scotland and northeast Ireland, with additional finds from islands such as Aran (west Ireland), Bute (Scotland), and Anglesey (north Wales). The distribution extends southward into southeast Ireland and southwest Wales (Kavanagh, 1976; Waddell, 1993).

The similarities in form between Cordoned Urns and Collared Urns, combined with the earlier use of Collared Urns, suggest that the former developed out of the latter tradition (Kavanagh, 1976). Some Cordoned Urns have also been found associated with razors, a common association with urns found in Britain (Kavanagh, 1976). Given this distribution, it has been suggested that Cordoned Urns most likely originated in Britain, particularly in Scotland.

Metalwork is another important aspect of the Bronze Age, with a notable shift around 1300 BC, when ritual practices involving pottery appear to cease (Waddell, 1993). This shift may correspond to a transition toward deposition in watery contexts, a practice observed across a northwest

European zone that includes Northern France and the Low Countries, which also share similar technologies and traditions (Champion, 2009).

While Chalcolithic and Early Bronze Age Ireland is often noted for its abundance of gold artifacts compared to neighbouring regions, the tin and copper content of Irish gold artifacts is often higher than typical for native Irish gold (Standish et al., 2015). A study by Standish, Hawkesworth, and Pike (2015) analysing 50 Chalcolithic and Early Bronze Age gold artifacts found that, while lead (Pb) isotope analysis suggested a source in southwest Ireland, further elemental analysis indicated that the most likely origin was the alluvial deposits of southwest Britain.

One notable type of metal artifact is the lock-ring, a penannular object with a triangular cross-section and a circular central opening, from which a slot extends to the edge (Eogan, 1969). Eogan (1969) identifies four regional distributions of these finds: the "Irish Group," concentrated around the Lower Shannon; the "Northern British Group," including Scotland south of Angus, the northeast English counties bordering the North Sea, Lancashire, and North Wales; the "Southern British Group," located in southern England; and the "French Group," comprising three find locations in northwestern France.

Analysis of these groups reveals specific patterns: the absence of side plates links the Irish, Southern British, and French groups, whereas the presence of tube and side-plating formed from a single sheet connects North Wales, northern England, and Scotland. Decorated faceplates are characteristic of the Irish, Southern British, and French groups, while the Northern British

examples are often undecorated. A binding strip with a C-shaped cross-section is found in the Irish Group and sometimes in the Northern British Group but is absent from the Southern British and French examples (Eogan, 1969). Based on this analysis, Eogan (1969) concludes that lock-rings developed in Ireland around the mid-8th century BC, continued in production through the 7th century BC, and were primarily produced in the Lower Shannon area. Lower-quality versions were exported northward to North Wales via Anglesey, then onward to northeast England and Scotland, and separately southeastward to southern England and France.

Similarly, gold torc bars are primarily found in Ireland and Britain, with additional finds in northwest France (Waddell, 1993). Waddell (1993) suggests that their distribution may indicate alliances across the North Channel and the southern half of the Irish Sea, with North Wales playing a central role.

One notable type of Bronze Age sword is the Ballintober type, which is concentrated in the Thames Valley, though sporadic finds extend north into eastern England, westward into the Upper Thames Valley and Somerset, and across to South Wales and Ireland. In Ireland, the main distribution is north of a line from Dublin to County Mayo (Colquhoun and Burgess, 1988). Colquhoun and Burgess (1988) propose that Ballintober swords are Irish/British adaptations of tongue-shaped and rectangular-hilt tang rod-tanged swords that no longer feature rod-tangs. The absence of Irish examples with a spike or tongue projecting from the hilt tang suggests that this type originally developed in England. Waddell (1993) speculates that

the distribution and sequence of these swords indicate the importance of the Bristol Channel in maintaining political alliances, particularly between southeast England and Ireland. However, it is also noted that, as offensive weapons, their distribution may not solely reflect peaceful interaction.

There is limited evidence of contact during the Roman period. Most Roman finds in Ireland are numismatic, primarily in the form of coinage. Other materials, such as pottery—particularly Samian ware—and fibulae, are likely the result of trade with Britain (Bateson, 1973). Burials also provide evidence of contact; for example, the long cist graves at Bray Head suggest familiarity with Roman burial customs. Additionally, burials on Lambay Island containing Roman and British objects are believed to be those of refugees from Britain (Bateson, 1973).

Several well-documented migrations occurred between Britain and Ireland during the Early Medieval period. Two notable migrations involved Irish populations moving to Britain: the expansion of the Dalriadic Scotti from northeastern Ireland into western Scotland, which is thought to have taken place in the 5th century AD, and the movement of the Déisi from Ireland to southwestern Wales, particularly Dyfed. The latter migration has been tentatively dated to the late 4th or early 5th centuries based on comparisons of Irish and Welsh genealogies (Alcock, 1970). However, it is suggested that there was little transfer of material culture to Dalriadic Scotland or Dyfed, with existing evidence indicating only superficial contact (Alcock, 1970).

A range of stone monuments has been proposed as evidence of contact between Britain and Ireland. Several inscriptions on stones in Wales contain translations that demonstrate the use of Irish names. For example, a standing stone from Llanfaelog in Anglesey, which was re-used in the 5th–6th century, and a re-used inscribed stone found in a curvilinear ditch in Bodedern, Anglesey, bear names that have been linguistically dated to the late 5th or 6th century AD (Edwards, 2001).

Furthermore, Nash-Williams' Group II cross-decorated stones, dated to the 7th–9th centuries, are described as characteristic of Ireland, Scotland, Wales, and the Isle of Man. These stones are potentially linked to the spread of Irish monasticism, and their western distribution in Wales suggests contact across the Irish Sea (Edwards, 2001).

Ogham inscriptions provide strong evidence of cultural contact between Ireland and Britain during this period. Ogham is a script that developed in southern Ireland in the 3rd or 4th century AD (Connelly, 2015; Thomas, 1973). There are 454 known inscriptions in Britain and Ireland, 440 of which are inscribed on ogham stones. The vast majority are found in Ireland (367 inscriptions, including 360 stones), with notable concentrations in Wales (35 inscriptions, all on stones) and Scotland (39 inscriptions, 32 of which are stones) (Connelly, 2015).

The use of Ogham inscriptions on monuments in Ireland is dated to the 5th century AD (Connelly, 2015; McManus, 1991), spreading to southern Britain in the 6th century AD and later to Scotland, where it remained in use from the 6th to the 11th century AD (Connelly, 2015). It has been argued

that Ogham held marginal status in Ireland and was declining in popularity by the 7th century AD, even as it gained prestige in Scotland (Connelly, 2015; Forsyth, 1996), which could indicate limited cultural contact. Similarly, the shorter Ogham inscriptions found on bilingual stones in Wales, compared to their British-Latin counterparts, suggest that Irish may have been spoken less frequently (Alcock, 1970).

Evidence of material culture transfer in the form of pottery during the Early Medieval period primarily consists of grass-marked pottery found in Cornwall. This type of pottery has been argued to be an offshoot of Ulster souterrain ware, which developed in the 6th century AD due to settlers migrating from Ulster to western Cornwall (Thomas, 1968). However, this connection has been disputed due to the lack of a clear chronology and the argument that the grass-marking technique could have developed independently (Alcock, 1970; Ryan, 1973). Additionally, outside of these examples, scholars have noted an overall absence of distinct native pottery styles in Britain and Ireland during this period (Alcock, 1970; Ryan, 1973).

During the Anglo-Saxon and Viking periods of the Early Medieval era, there is evidence of contact across both sides of the Irish Sea. Scandinavian settlement on either side is documented in historical accounts, particularly the expulsion of the Norse from Dublin in 902 and their subsequent settlement in northwestern England. This is supported by the *Irish Fragmentary Annals* and the *Welsh Annals*, which describe Ingimund's unsuccessful attempt to settle in Wales between 902 and 903, followed by the Norse settlement of western Cheshire, particularly in the northern part of the Wirral Peninsula (Griffiths, 2004).

Trade between Dublin and Britain in the 10th and 11th centuries AD is evidenced by the presence of Chester ware pottery alongside East Anglian wares, as well as the importation of salt and Anglo-Saxon metalwork, such as disc brooches (Griffiths, 1991). Additionally, it has been suggested that metalwork from Chester and Meols was produced in Dublin during this period, supported by evidence of metalworking activities there (Griffiths, 1991).

Similarly, excavations in Waterford revealed a row of three houses along Peter Street, which closely resembles a Phase IV house excavated at Lower Bridge Street in Chester. The settlement also demonstrates strong connections with southwestern England and France, with pottery largely represented by Severn Valley wares (Griffiths, 1991). Furthermore, it has been suggested that early 10th-century trade between southwestern England and Ireland may have been routed through Gloucester (Griffiths, 1991).

"Viking" insular weapon burials are found throughout Britain, Ireland, and the Isle of Man (Harrison, 2015). These burials were concentrated along the western seaboard, in northern and western Scotland, and around the Irish Sea basin. While they were related to burial practices in Scandinavia, local variations in weapon types and quantities suggest the influence of regional traditions (Harrison, 2015).

In summary, there are numerous similarities between the archaeological material found in Britain and Ireland across various periods:

- In the Neolithic, similarities are evident in megalithic structures, pottery, and other lithic materials (Cooney and Mandel, 1998;

Cooney, Mandel and Byrnes, 1999; Corcoran, 1972; Herity, 1982; Saville, 1999; Sheridan, 2000, 2004; Sheridan, Cooney and Grogan, 1992; Simpson and Meighan, 1999; Waddell, 1993).

- In the Bronze Age, pottery and metalwork serve as the primary indicators of connections between the regions (Colquhoun and Burgess, 1988; Eoghan, 1969; Hawkesworth and Pike, 2015; Kavanagh, 1976; Longworth, 1984; Lynn, 1993; Simpson, 1973; Standish et al., 2015; Waddell, 1993).

- During the Iron Age and Roman period, connections are mainly represented by the presence of Roman coins and other Roman and British objects (Bateson, 1973).

- In the Early Medieval period, contact between Britain and Ireland is evidenced by the founding of the kingdoms of Dyfed and Dál Riata, though archaeological evidence for these remains limited (Alcock, 1970). Historical sources also document the Viking expulsion from Ireland and their subsequent settlement in Britain (Griffiths, 2004). Archaeological evidence of contact and cultural similarity is further supported by inscribed stone monuments bearing Irish names, ogham inscriptions, pottery, metalwork, and burial practices (Connelly, 2015; Edwards, 2001; Griffiths, 1991; Harrison, 2015; McManus, 1991; Ryan, 1973; Thomas, 1968).

Chapter 3: Methodological Background of Biodistance Studies

Biodistance

Biological distance, shortened to biodistance, reflects population relatedness by measuring the differences and similarities in morphological variation between populations (Buikstra et al., 1990; Hefner et al. 2016). The traits that are measured are generally considered polygenic. Polygenic traits have both an environment and genetic component so can be used to reflect genetic and environmental differentiation (Buikstra et al., 1990).

Hefner et al. (2016) posit that there are a number of purposes for which biodistance studies have been performed. Firstly, the results can be used to answer evolutionary questions and secondly, the results can used to answer questions about social structure and as a comparison to other archaeological methods These studies have previously been subdivided into pre-determined levels of analysis: intra-site or inter-site specific, global variation and regional continuity.

The main underlying assumption is that groups that have similar morphological features have a common ancestry compared to groups with fewer similarities (Hefner et al. 2016). Several other underlying assumptions were described by Stonajowski and Schillachi (2006): Firstly, allele frequencies within and between geographically proximate populations are affected by genetic drift and gene flow; secondly, populations are accurately represented by samples which are temporal aggregates and not natural populations; thirdly, changes in allele frequencies results in visible skeletal changes; fourthly, the environmental effects on phenotypic variation is

minimal; fifthly, inheritance of phenotypic variation is additive and there is a close resemblance between relatives.

Some have warned against a reliance on any single type of data (Corruccini, 1974; Smith, 1972). This is because different types of data may provide different interpretations (Corruccini, 1974; Smith, 1972).

Dental Non-metric Traits

Dental non-metric traits, like those used in the present study, are observable variations in the morphology of tooth crowns and roots; crown traits appear as accessory ridges, tubercles, styles and cusps while root traits appear as variation in root number (Scott and Turner, 1988). These morphological variations are usually discrete and quasi-continuous (Scott and Turner, 1988).

A quasi-continuous characteristic is a continuous variable with a polygenic mode of inheritance, and, like a polygenic trait, underlying and visible expressions are separated by a threshold. (Grüneberg, 1952; Scott, 1973; Scott and Irish, 2017). The underlying scale is the genetic variation, whereas the visible scale is the variation observed when the threshold is exceeded; those with slight trait expression will be closer to the threshold than those with a pronounced expression (Scott, 1973).

Early researchers such as von Carabelli (1842), Owen (1840) and Tomes (1914) described dental non-metric traits. Early research in dental morphology from the 19th century was focused on phylogeny and taxonomy, and, subsequently, in the 20th century the focus shifted to population variability (Alt et al., 1998).

Hrdlička (1920) described and classified degrees of shovel shaped incisors in human and non-human populations. In this study, the presence of trait called shovelling was divided into groups: 'shovel-shaped' for all incisors with an enamel rim and well-developed fossa on the lingual surface, 'semi-shovel' for incisors with an enamel rim but less defined fossa, 'trace shovel' for incisors which exhibited distinct traces of enamel rim but could not be classified as 'semi-shovel', and 'no shovel' for incisors with no trace of enamel rim or fossa (Hrdlička, 1920). This study also noted the similarities between Native Americans and Asians through the distribution of this trait (Hrdlička, 1920).

Dahlberg (1956) created a series of reference plaques to standardise the observation of non-metric traits which was followed by the creation of a series of references plaques for deciduous dentition by Hanihara (1961; 1963). These plaques were distinguished from one another by Hanihara (1961) as the 'D series' for the deciduous dentition plaques and 'P series' for Dahlberg's permanent dentition plaques (Hanihara, 1961). This highlighted the need for standardisation in the field as subjectivity in scoring was later recognised as leading to intra-observer error (Sofaer et al. 1972).

Turner et al. (1991) devised a 24-rank scale series of plaques with detailed description and scoring sheets. This became known as the Arizona State University Dental Anthropology system and became firmly established as the standard for dental anthropologists. It has since been used in a number of studies into the biological affinities of populations from across the globe (Cucina et al., 1999; Irish 2005, 2006; Irish and Guatelli-Steinberg, 2003; Scott et al. 2018a).

The introduction of ASUDAS was significant as prior to its introduction studies primarily focused on a single population, whether using a single trait (Bang and Hasund, 1971, 1973) or multiple traits (Nelson, 1938; Goldstein, 1948). This is important as the accuracy of the analysis is affected by the number of traits examined (Livingstone, 1991).

There are number of benefits to the ASUDAS system. Firstly, the traits that are included are the most easily and reliably observed which helps reduce intra- and inter-observer error; secondly, the traits selected are the most persistent and so remain more likely to be observable despite factors such as wear; thirdly, the traits have been observed to have low or no sexual dimorphism, so sexes can be combined to expand sample size without bias; fourthly, the traits are evolutionarily stable and so appear in both modern and archaeological populations; sixthly, there is a large amount of comparable data; seventhly, the traits have been shown to have a high degree of heritability that typically ranges between 40-80% (Dempsey and Townsend, 2001; Hanihara, 2008, 2010; Irish et al., 2020; Scott and Irish, 2017; Stojanowski et al. 2018, 2019; Turner et al., 1991).

There are several evolutionary processes that play a role in the development of dental non-metric traits: selection, genetic drift, and gene flow. Dental traits are polytypic and polymorphic, and there has been considerable discussion regarding the extent to which selection plays a role in maintaining these polymorphisms (Scott and Turner, 1997).

A number of traits have been suggested to function as adaptations that add mass to the tooth, thereby increasing strength and durability. Examples

include incisal shovelling, Carabelli's cusp, cusp 5 on the upper molar (UM), and cusp 6 on the lower molar (LM) (Dahlberg, 1963; Cadian, 1973; Townsend et al., 1986). Furthermore, incisal shovelling and Carabelli's cusp have been shown to have significant associations with temperature (Mizoguchi, 1985, 1993), suggesting adaptation to selective pressures rather than being solely the result of genetic drift.

More recently, shovelling of the upper incisor 1 (UI1), double shovelling of UI1, and cusp number on the lower molar 2 (LM2), as well as the mesial ridge of the upper canine (UC) to a lesser degree, have been found to be associated with the ectodysplasin A receptor gene (EDAR) (Kimura et al., 2009; Park et al., 2012; Tan et al., 2014; Peng et al., 2016). EDAR is a genomic region that has been shown to be under positive selection (Bryk et al., 2008). However, EDAR also has pleiotropic properties, as it influences the development of other ectodermal derivatives such as hair, sweat glands, and sebaceous glands. Consequently, it has been proposed that these dental phenotypes may be "hitchhiking" rather than being the direct targets of selection (Park et al., 2012).

Scott and Turner (1997) argue that the effects of selection on a small proportion of loci within datasets do not significantly bias historical reconstructions. Alternatively, efforts have been made to identify combinations of traits that best preserve neutral genetic signals in order to reduce potential biases from traits affected by selection (Rathmann and Reyes-Centeno, 2019).

Scott and Turner (1997) also posit that the divergence in dental trait frequencies is considered more likely to result from processes such as founder effect, genetic drift, and the influence of population structure. Furthermore, the primary process that is proposed to likely to affect trait frequencies is gene flow, although its impact is greater at local or regional scales than at continental or global levels.

Dental non-metric trait data have been shown to correlate to genetic data (Hubbard, 2012; Hubbard, Guatelli-Steinberg, and Irish, 2015; Irish et al. 2020). Hubbard (2012) and Hubbard, Guatelli-Steinberg and Irish (2015) found that an overall agreement between the biodistances from genetic data and those from dental morphological data, although genetic data may provide greater resolution to overall among-group relationships. Meanwhile, Irish et al. (2020) found that MMD/F_{ST} correlations provided greater similarity between genetic data and dental data than results from previous studies. However, it has been found that the resolution that dental non-metric data provides is too low to detect close genetic relationships (Stojanowski and Hubbard, 2017, Ricaut et al.2010) and also provides low predictive power for genetic ancestry of individuals (Delgado et al., 2019).

Recently, an application called rASUDAS was devised that uses a naïve Bayes classifier algorithm to assign posterior probabilities to estimate ancestry of an individual by using data from 21 dental non-metric traits (Scott et al., 2018b). This has subsequently been expanded in an iteration called rASUDAS2 to include four additional traits and seven back-up traits (Scott et al., 2024). Both rASUDAS and rASUDAS2 assign an unknown

individual to one of seven biographic groups (Scott et al., 2018, Scott et al., 2024).

Statistical Methods

The statistical methods that have been used in relation to biodistance studies have changed gradually over time.

Pearson (1926) created the coefficient of racial likeness (CRL) which was a measure of similarity and dissimilarity using craniometric, anthropometric and odontometric measurements. The coefficients from CRL start at zero and increase in value. These values are then categorised into degrees of association or degrees of divergence. For association, categories ranged from ‘Very Intimate Association to ‘Doubtful Association’ and for divergence categories ranged from ‘Slight Divergence’ to ‘Very Wide Divergence’ (Pearson, 1926).

CRL received a number of criticisms. Seltzer (1937) criticized it for several reasons: firstly, it does not take the correlations between measurements in account and treats them as statistically independent; secondly, it assumes a single deviation for all groups, thereby assuming the groups are alike in variability and homogeneity; thirdly, the number of variables affects the coefficient calculation as the coefficient values get smaller as the number of variables increases and vice versa (Seltzer, 1937). Furthermore, Fisher (1936) criticized CRL as only being a test of significance and, therefore, only calculates probability and not racial divergence.

Mahalanobis (1936) introduced the generalised distance D^2 statistic. The D^2 statistic is a sum of squares of differences between the corresponding values

of two sets of suitably weighted measurements (Burnaby, 1966). The statistic was subsequently adapted to include a tetrachoric correlation matrix, referred as pseudo-D^2, and so adjusts for phenotypic correlation unlike the original (Konigsberg, 1990). The latter can be used for non-metric traits including those from the ASUDAS.

Penrose (1952) also created a distance statistic. Penrose distance is computed using means and there is both a 'shape' component for non-metric traits and 'size component for metric traits. This statistic, however, was criticized because it was difficult to interpret between the shape and size distances (Berry, 1979) and some argued that that shape distance did not represent actual biological similarities between populations (Rohlf and Sokal, 1965).

The mean measure of divergence statistic (MMD) is a dissimilarity measure in which low values represent closer phenetic similarity between samples and high values represent greater phenetic distance. MMD was first devised by Smith for use in mice by Grewel (1962) and was first used in humans by Berry and Berry (1967). Following this, MMD has been modified for shortcomings including small sample size, variance stabilisation, and fixed trait frequencies (Berry and Berry, 1967; Berry 1969; Sjøvold 1973; Green and Suchey 1976 and Souza and Houghton, 1977). The statistic has also been compared against pseudo-D^2 and found to both be comparable with some caveats towards use case (Edgar, 2004; Irish, 2010). MMD is preferable over D^2 for several reasons: it contains a correction for small samples; excessive missing data can lead to variable deletion affecting the results of D^2 but MMD uses summary count data so cases can be included

despite being incomplete; MMD produces more probable inter-sample patterning when using a large number of traits; MMD includes a test of significance (Irish, 2010).

Model-free and Model-bound Analyses

Analyses into biodistance are often referred to as either being model-free or model-bound. Model-free analyses typically precede model bound ones due to exploring the morphological affinities of populations and/or patterns in variation (Irish, 2010; Relethford and Lees, 1982). Model-bound analyses, on the other hand, typically investigate the causes of variation patterns through either admixture estimation or kinship estimation (Relethford and Lees, 1982). Therefore, the main difference between the two is that model-free analyses are descriptive and must be supplemented with other data such as archaeological material to facilitate interpretation whereas model-bound analyses can test hypotheses. Both a model-free analysis and model-bound analysis are used in this study.

The main issue that model-bound methods have compared to model-free is that they typically require more assumptions to be made (Relethford and Lees, 1982). Despite this, and model-free methods being still common, model bound approaches are becoming more frequently used as they serve as a way for biodistance analyses to counter the criticism that they are descriptive and typological (Armelagos and Ven Gerven, 2003).

The most common models that are used in biodistance studies include the ‘relationship (r) matrix model’ for genetic frequencies by Harpending and

Jenkins' (1973) and Harpending and Ward (1982), the modified 'r-matrix model' by Relethford and Blangero (1990) for quantitative traits and Konigsberg (2006) for discrete traits and, lastly, the isolation by distance model by Wright (1943).

The 'relationship (r) matrix' by Harpending and Ward (1982) was developed for use with allele frequency data. The model works by computing an expected heterozygosity and a regional mean and the expected heterozygosity is compared against observed heterozygosity with direction and magnitude of the difference providing information about gene flow from outside the region (Harpending and Ward, 1982; Relethford and Blangero, 1990).

Isolation by distance was a term introduced by Wright (1940; 1943). It refers to the patterns of genetic variation that result from spatially limited gene flow, this results in a decrease in the genetic similarity between populations decreasing as the geographical distance increases (Wright, 1940; Wright, 1943; Jensen, Bohonak and Kelly, 2005).

Summary

Biodistance studies aim to assess population relatedness by measuring the similarities and dissimilarities of the morphological variation between populations which is done using metric and non-metric data. Dental non-metric traits have been observed since the 19th century and procedures standardised over the course of the 20th century (see pages 48 and 49) and these dental data have been shown to correlate with genetic data (Irish et al., 2020). Numerous statistics for use in biodistance studies have been

developed; MMD and D^2 statistics being the most common for use with non-metric traits. It is MMD that will be used in this study (see Chapter 5). Several model-bound approaches have also been developed; isolation-by-distance will be used in this study.

Chapter 4: Materials

This chapter outlines the skeletal collections that are used in this study. Data were collected in a total of 570 individuals from 17 collections. Sample sizes for any given trait may, however, be much smaller than this due to factors such as missing teeth and dental wear impeding observation. An overview of the samples can be seen in Table 1 and the location of all sites is shown in Figure 1 below. Data from additional samples were intended to be collected, however, issues such as the Covid19 pandemic resulted in this not being possible (see Chapter 8 for further details).

Figure 1: Map showing all sample site locations. NOR= Norton Priory, Runcorn, POU= Chapel House Farm, Poulton, GLC= St. Owen's Church Gloucester, GLRC= London Road, Gloucester, LDG= Great House Farm, Llandough, ATE= site 92, Atlantic Trading Estate, Barry, BRS= Brownslade Barrow, Castlemartin, CLV= Culver Hole, Llangennith, TKW= Tinkinswood Burial Chamber, St. Nicholas, STG= Strath Glebe chambered cairn, Skye, DIS= Distillery Cave, Oban, RAS= Raschoille Cave, Oban, WHIT= Whithorn Priory, Dumfries and Galloway, SGR= Southgreen, Kildare, PKN= Parknahown 5, Co. Laois, KLY= Killeany 1, Co. Laois, BFL= Bushfield/Lismore, Co. Laois.

The skeletal collections were selected based on modern regions (i.e. England, Wales, Scotland and Ireland). Four sites represent the samples from England, totalling 245 individuals: Norton Priory, Runcorn (NOR), Chapel House Farm, Poulton (POU), St. Owen's church, Gloucester (GLC) and London Road, Gloucester (GLRC). Skeletal material that was assessed from these collections consisted of 79 individuals from Norton Priory, 68 individuals from Chapel House Farm, Poulton, 58 individuals from St Owen's, Gloucester, and 40 individuals from London Road, Gloucester.

Five sites represented the samples from Wales, totalling 148 individuals: Great House Farm, Llandough (LDG), Site 92, Atlantic Trading Estate, Barry (ATE), Brownslade Barrow, Castlemartin (BRS), Culver Hole, Llangennith (CLV), and Tinkinswood burial chamber, St. Nicholas (TKW). The skeletal material assessed from the collections was comprised of 41 individuals from Great House Farm, Llandough, 33 individuals from Site 92, Atlantic Trading Estate, 33 individuals from Brownslade Barrow, 24 individuals from Culver Hole and 17 composite individuals from Tinkinswood burial chamber.

Four sites represented the samples from Scotland, totalling 78 individuals: Strath Glebe chambered cairn, Skye (STG), Distillery Cave, Oban (DIS), Raschoille Cave (RAS) and Whithorn Priory, Dumfries and Galloway (WHIT). The skeletal material assessed from these collections consisted of 32 individuals from Strath Glebe chambered cairn, 11 individuals from Distillery Cave, 14 individuals from Raschoille Cave and 21 individuals from Whithorn Priory.

Four sites represented the samples from Ireland, totalling 99 individuals: Southgreen, Kildare (SGR), Parknahown 5, Co. Laois (PKN), Killeany 1, Co. Laois (KLY) and Bushfield/Lismore, Co. Laois (BFL). The skeletal material that was assessed from these collections consisted of 20 individuals from Southgreen, Kildare, 31 individuals from Parknahown 5, 20 individuals from Killeany 1 and 28 individuals from Bushfield/Lismore.

Table 1: Overview of samples used in the study

SITE	REGION	PERIOD	NUMBER OF INDIVIDUALS
NORTON PRIORY, RUNCORN	Cheshire, England	Medieval	79
CHAPEL HOUSE FARM, POULTON	Cheshire, England	Medieval	68
ST. OWEN'S CHURCH, GLOUCESTER	Gloucestershire, England	Medieval	58
LONDON ROAD, GLOUCESTER	Gloucestershire, England	Roman	40
GREAT HOUSE FARM, LLANDOUGH	Vale of Glamorgan, Wales	Early Medieval	41
SITE 92, ATLANTIC TRADING ESTATE, BARRY	Vale of Galmorgan, Wales	Late Roman/Early Medieval	33
BROWNSLADE BARROW, CASTLEMARTIN	Pembrokeshire, Wales	Early Medieval	33

CULVER HOLE, LLANGENNITH	Swansea, Wales	Bronze Age	24
TINKINSWOOD BURIAL CHAMBER, ST. NICHOLAS	Cardiff, Wales	Neolithic	17
STRATH GLEBE CHAMBERED CAIRN	Isle of Skye, Scotland	Neolithic	32
DISTILLERY CAVE, OBAN	Argyll and Bute, Scotland	Neolithic	11
RASCHOILLE CAVE, OBAN	Argyll and Bute, Scotland	Neolithic	14
WHITHORN PRIORY, WHITHORN	Dumfries and Galloway	Medieval	21
SOUTHGREEN, KILDARE	Kildare, Republic of Ireland	Early Medieval	20
PARKNAHOWN 5, PARKNAHOWN	Co. Laois, Republic of Ireland	Early Medieval	31
KILLEANY 1, KILLEANY	Co. Laois, Republic of Ireland	Early Medieval	20
BUSHFIELD/LISMORE	Co. Laois, Republic of Ireland	Early Medieval	28

Site Backgrounds

Information regarding each samples site will be detailed below. This information includes information regarding excavations that have been undertaken, details of archaeological finds and subsequent/previous analyses that have been performed.

Norton Priory

Norton Priory is a site located 2.5 miles east of Runcorn and less than a mile from the village of Norton in Northern Cheshire (see Figures 1, 2 and 3). The Augustinian priory was initially founded at Runcorn in 1115 by the second baron of Halton, William Fitz Nigel. It was dedicated to the Saxon St. Bertelin, a saint who has connections to the Mercian heartland of Staffordshire. The fact that Runcorn had existed as a burgh established by Aethelflaed, Queen of the Mercians, in 915 suggests that it was likely based on an existing church (Greene, 2004).

From the early 13th century, the barons become more remote and the Dutton family became the primary benefactors for the priory (Smith, 2012). This association led to the extension of the north and southern transepts (Brown, Howard-Davis et al., 2008) and the bestowing other endowments specifically for the construction for the North-Eastern Chapel that served as their family burial chamber until 1536 (Smith, 2012).

In the 1970s, the Runcorn Development Corporation commissioned Patrick Greene to undertake a series of community excavations to provide residents with a sense of history and place and currently the site exists as the Norton

Priory Museum Trust, a museum that houses the large archaeological collection and is curated by the Trust and the Barons of Halton (Smith, 2012).

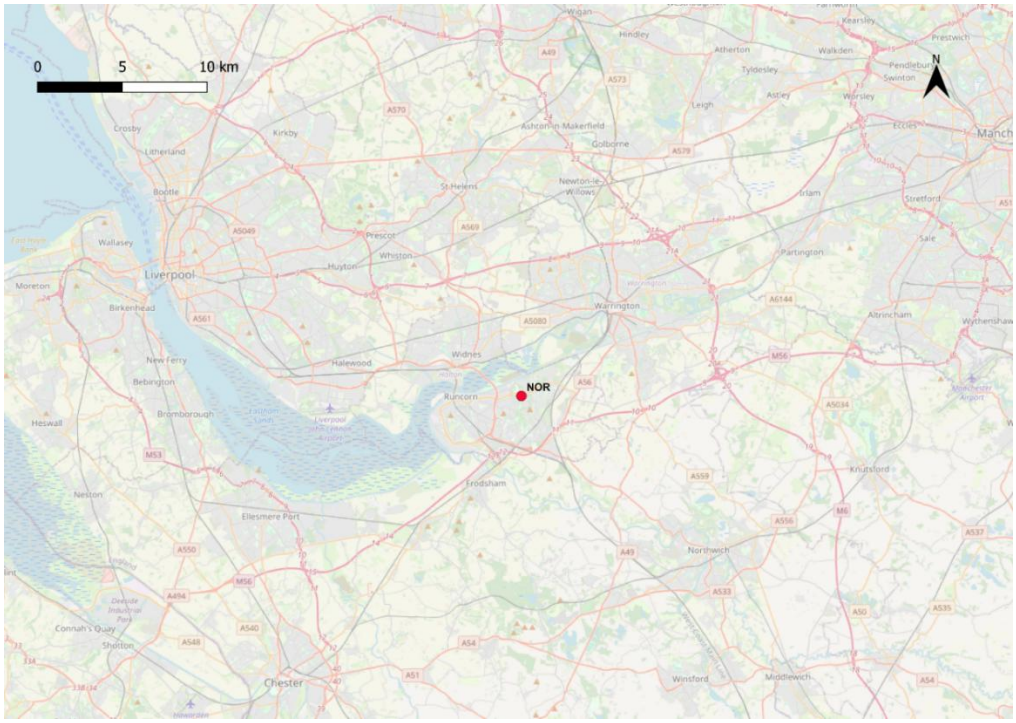

Figure 2: Map showing regional location of Norton Priory

Figure 3: Map detail showing the location of Norton Priory

There are 128 burials that were excavated as part of the series of excavations in the 1970s and these are housed on site by the Norton Priory Museum Trust. Historical evidence suggests that these burials began in the late 12th century until 1536, which includes three wills – Lawrence de Dutton's made in 1392, Sir Geoffrey Warbuton's made on 1st September 1448, and Sir Lawrence de Dutton's made on 4th October 1527 – and it has been hypothesised that the wills suggest that it is likely that the majority of the burials excavated do not belong to the canons but their lay benefactors instead (Greene, 2004).

Furthermore, in 2016 14C analysis conducted on three individuals from the collection confirmed they are Medieval in origin, dating from AD1150-1390; in 2018 14C analysis on 12 individuals covered ca. 400 years (1020-1479), while stable isotope analysis in both suggested a marine based diet consistent with monastic life (Burrell et al., 2016; Burrell et al., 2018).

Recent research on the remains at Norton Priory has identified the occurrence of what is likely an ancient form of Paget's Disease of Bone, a chronic metabolic disease that affects the normal turnover of bone (Burrell et al., 2016; Burrell et al., 2018). This disease is highly influenced by genes that likely pass through family lineages and the rates of occurrence are higher in the UK than other countries with a concentration in the North-West of England (Burrell et al., 2016; Burrell et al., 2018).

Chapel House Farm, Poulton, Cheshire

Chapel House Farm, Poulton is a multi-period site that is located six miles south of Chester in West Cheshire. The archaeological site overlooks the old

Pulford Brook, a stream that runs into the River Dee and marks the border between England and Wales (see Figures 1,4 and 5).

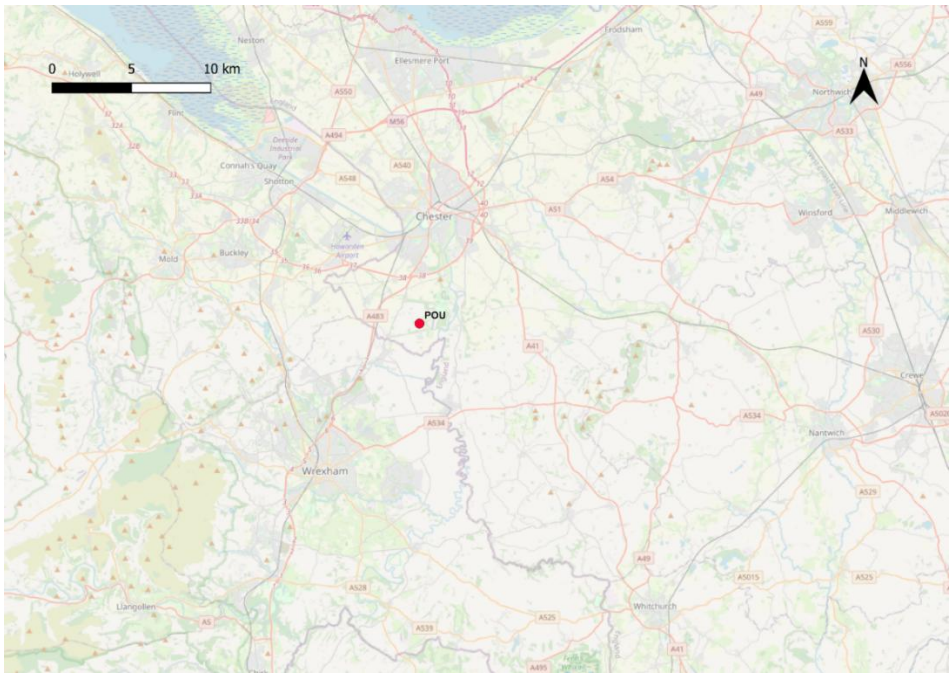

Figure 4: Map showing the regional location of Chapel House Farm, Poulton

This site is currently overseen by the Poulton Research Project, whose initial primary aim was to identify the site of the lost medieval Cistercian abbey. This abbey was short-lived, being founded in 1153-1158 until being moved to Dieulacres in Staffordshire in 1214 (Wessex Archaeology, 2007).

Following this, the site became a grange, a monastic farming estate, in 1453 the abbot at Dieulacres leased the land and buildings at Poulton to the Manleys, and after the dissolution of the monasteries in 1544, parts of the estate were granted to Sir George Cotton although the Manleys remained leaseholders until the last Manley died childless in 1601 (Emery et al., 1995).

The first archaeological evidence at the site was discovered by a farmer, R.G Williams, who uncovered stones and skeletal remains in 1892 in the

southern area of Chapel Field (Emery et al., 1995). Subsequently in the late 1960s, Mr Gerry Fair, the landowner and farmer, discovered a decorated medieval floor tile and human mandible also at Chapel Field which provided a probable location for the abbey (Cootes et al., 2016) and further investigations were undertaken by archaeologist Michael Emery with University of Liverpool and Chester City Council.

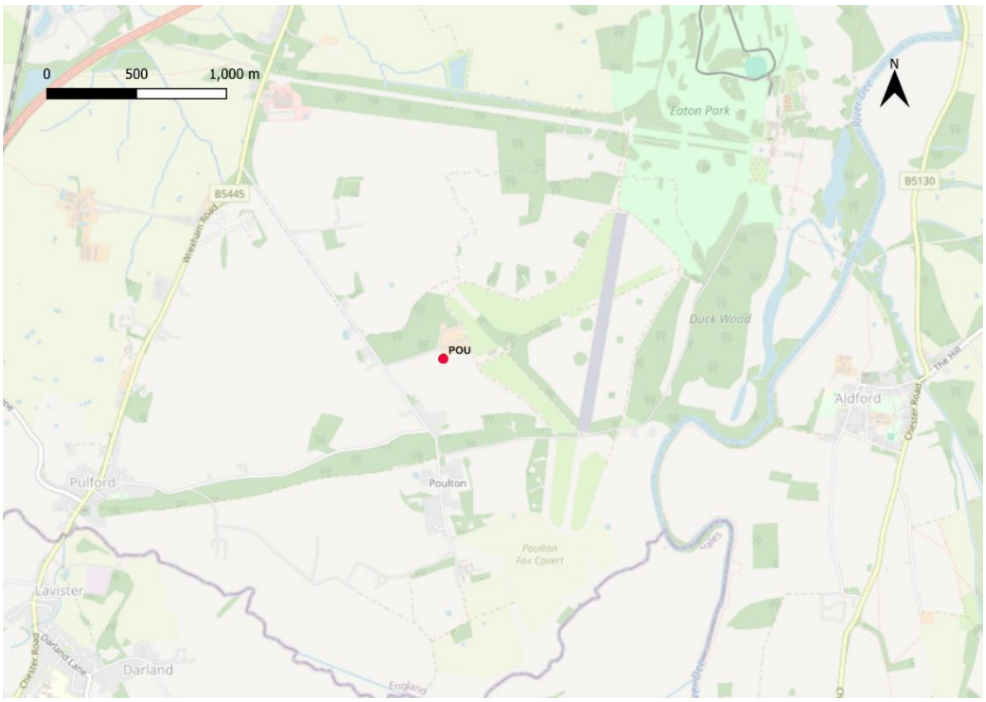

Figure 5: Map detail showing the location of Chapel House Farm, Poulton

The excavations in the late 1990s were unsuccessful in finding the location of the abbey; however, they did reveal a small chapel with a secular graveyard (Emery, 2000). This chapel consists of a nave contemporaneous with the foundation of the abbey and the chancel and tower added in later periods (Wessex Archaeology, 2007). The graveyard is suggested to have been in use for around 400 years (Emery et al., 1995; Emery, 2000) and since excavations began over 700 human skeletons and a large amount of disarticulated material have been found (Burrel, 2018).

There is evidence that the site was in use prior to the chapel as significant amounts of tenth- century Chester Ware pottery have been discovered at the site indicating early medieval use, and in trench 1 the remains of the medieval chapel were underlain by Roman deposits and ditches and the interments and other features of the graveyard contained residual finds from the Mesolithic, Neolithic, Bronze Age, Iron Age, Roman and Saxon periods (Cootes et al., 2016).

As well as this, approximately 80m North of the Chapel, middle-late iron age roundhouses, Roman field boundaries and features related to industry were found in trenches 16 and 50 (Cootes et al., 2016) and Romano-British finds have been found through field walking including tiles stamped "LEG XX" which show material was produced by the 20th Legion based at Holt to the South-West (Wessex Archaeology 2007).

As previously noted, these finds indicate a long term and intense activity at the site (Cootes, et al., 2016) which would suggest that there is a increased likelihood of population continuity and as there appears to be similarity in the material culture from even the Mesolithic period to other sites across the region (Cootes et al., 2016), it is possible there is an increased likelihood that the dental affinities from the chapel's graveyard will be greater with other populations from North West England than other regions.

St Owen's church, Gloucester

St Owen's church, located on Southgate but outside of the walls of Gloucester city, was a parish in the Diocese of Gloucester, founded in 1100 and was subsequently acquired by Llanthony Priory in 1137 (Atkin and Garrod 1990;

Fullbrook-Leggatt, 1945). The Church remained in use until 1643 before it was damaged during a siege (Burrel, 2018) and was finally demolished in 1847 during the extension of the docks (Atkin and Garrod, 1990). Demolition material from the church has been found to be built into the foundations of an 18th century house that is built into the Southgate frontage and so it has been suggested that study of these could be used to build a broad picture of the building sequence of the church (Atkin and Garrod, 1990).

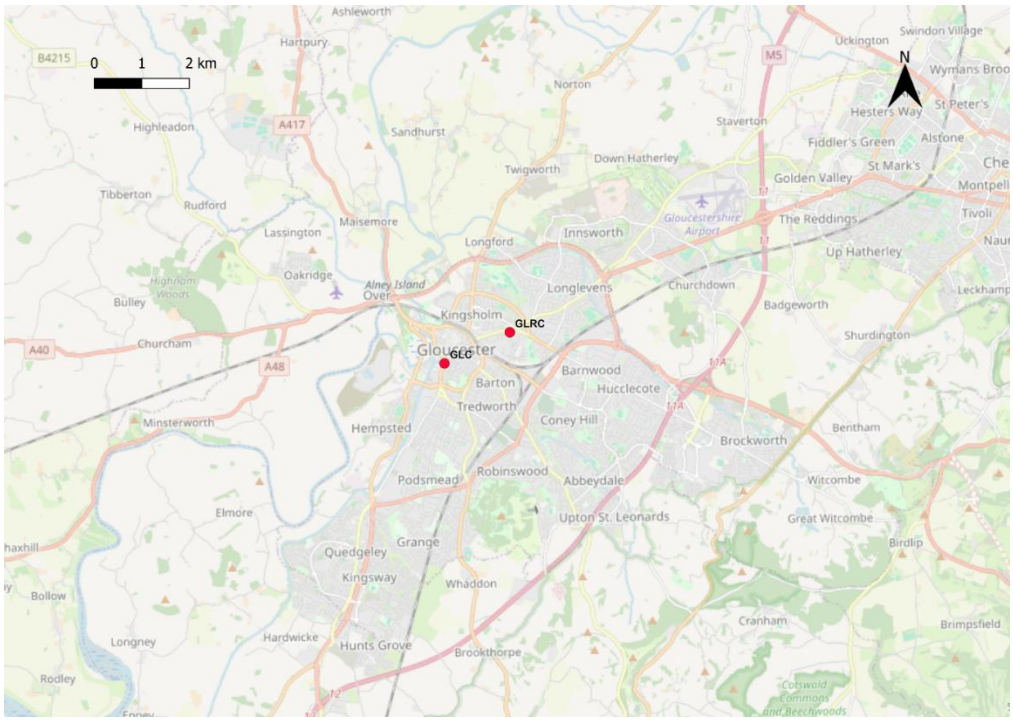

Figure 6: Map showing regional locations of sites from Gloucester. GLC= St Owen's church, GLRC= London Road

Two excavations were held at this site; firstly, an area in the north part of the site was excavated in 1983 by C.J Guy on behalf of the Western Archaeological Trust (Rawes, 1984) which was named "site 13/83", and, secondly, a nine-month excavation by the Bristol and Gloucester Archaeological Society (Atkin, Garrod, 1990) named "site 3/89" (see Figures 1,6 and 7).

In the excavations at site 3/89 evidence for several periods of use was found. Firstly, evidence from the Roman period consists a row of timber buildings date to the late 1st/2nd century with associated ironworks was found in the west margins of the site, although this was abandoned until a serious of courtyard and linear-plan masonry buildings were constructed in the 3rd century and it is suggested the suburb was re-abandoned in the 4th century (Atkin, 1990).

Subsequently, evidence from the Saxon period suggests re-occupation of the site in the 10th/11th century with the construction of a row of timber buildings as evidence was found for three post-hole constructed buildings that are divided by metalled yards (Atkin, 1990). It has also been hypothesised that the off-street location of St. Owen's Church suggests a pre-Norman foundation with a Late Saxon church set behind the housing along Southgate Street (Atkin, 1990).

Figure 7: Map detail showing the location of site 3/89, St Owen's church

Finally, the first evidence of the medieval period is a series of tenements of stone-built houses after being acquired by Llanthony Priory. Three of which were excavated and show evidence of an interruption of the building sequence in the late-medieval that suggests they were abandoned until the 15th century (Atkin and Garrod, 1990).

There were also over 300 burials excavated from the churchyard with later burials from the Independent Chapel and Royal Infirmary, with an increased density of burials that is contemporaneous to the disruption in the building sequence (Atkin and Garrod, 1990). Therefore, it has been suggested that the area suffered a localised epidemic or was abandoned during the time of the Black Death (Atkin and Garrod, 1990).

Overall, the site appears to show pattern of occupation then abandonment that occurs within and between different periods. This would seem to suggest that is more likely that the population would have weaker affinities with other local populations as there appears to be a discontinuation in population and subsequent repopulation from different areas and/or cultures.

London Road, Gloucester

London Road is located 1.2km east of the city centre of Gloucester in the suburb of Wooton, which is situated on the north-western part of the gravel ridge that is part of the fourth terrace of the River Severn. London Road itself lies on a Roman road that exited the former north gate of the Roman city and

joined Ermin Street in Wooton, which is now the junction of Barnwood Road and Denmark Road (Simmonds et al., 2008).

Figure 8: Map detail showing the location of London Road site

The area of Gloucester during the Roman invasion in AD 43 is believed to have been in the territory of a group called the Dobunni and came under Roman rule peacefully and it is suggested that parts of the southern Cotswolds and Upper Thames lay within a locally governed client kingdom (Simmonds et al., 2008; Miles et al., 2007). While the first Roman intervention in the area was the founding of the fortress at Kingsholm in what is now the northern part of the city and this was likely due to the presence of a native centre with some importance (Simmonds et al., 2008; Hurst 1999).

This fortress was abandoned in the 60s and a new fortress built on the site of the modern city (Simmonds et al., 2008). This fortress was then

subsequently converted into a *colonia*, the date of which could either be during the reign of Nerva (AD96-98) due to a tombstone indicating the name '*Colonia Nerva Glevensium*' (Wacher, 1995) or shortly after AD 86 based on rebuilding identified in excavations in numerous locations (Hurst, 1972; 1974).

Between August 2004 and January 2006, a programme of archaeological excavation commissioned by CgMS Consulting on behalf of McCarthy and Stone (Developments) Ltd was carried out by Oxford Archaeology at 120-122 London Road, Gloucester in order to mitigate the effects of the construction of sheltered apartments (Simmonds et al., 2008).

The site is located on the South side of London Road and is c. 80m from the Barnwood Road and Denmark Road junction, NGR SO 8432 1893, and consisted of an area c. 0.17ha with a level of c. 23m OD (see Figures 1,6 and 8) (Simmonds et al., 2008).

The site lies within the Wotton Cemetery that is known to have extended at least 500m on the road that connected the colonia to Ermin Street with cremation burials concentrated on the east end and inhumations extending along the south-west suggesting that it began as a cremation cemetery in the 1st century AD and was expand in the later Roman period (Simmonds et al., 2008). It is also likely that the majority of burials from Roman period of Gloucester are dated to after the 2nd century AD due to the majority of them being inhumations (Simmonds et al., 2008).

Previous excavation consisted of three trenches during an archaeological field evaluation carried out by Gloucester Archaeological Unit in 2004

which found a sequence of deposits that dated from the Roman, Medieval and Post-medieval periods in the southern and eastern areas with an urned cremation burial in the south-east corner (Simmonds et al., 2008). The north-western area of the site, however, had been disturbed by the construction of the former service station so no archaeological remains survived (Simmonds et al., 2008).

The earliest archaeological material found from the site were the remains of an adult hippopotamus, and probable bison and elephant that dated to the Pleistocene found in the north central part of the site (Simmonds et al., 2008). Evidence of human activity that pre-dates the cemetery comes from plough scars observed in the eastern part of the site, although no dateable material from these features was able to be recovered and they are suggested to represent prehistoric or early Roman cultivation of the area (Simmonds et al., 2008).

Excavations revealed part of the cemetery that dated from the 1st – 4th centuries that was sealed by a soil layer containing an assemblage of pottery dating between the 11th and 15th centuries (Simmonds et al., 2008). There was also a ditch through the middle of the site that cut through several graves and the north-western edge of the mass grave that contained pottery suggesting 16-17th century in date, a ditch on the southern edge of the site that is suggesting to be post-roman due to relationship with the burials and a ditch terminus on the eastern edge that contained two sherds of pottery from the 12th- 13th century (Simmonds et al., 2008).

The site contained nine cremation burials, 64 inhumation burials, a mass grave containing at least 91 individuals and 3 probable graves with no skeletons (Simmonds et al., 2008). Dating via ceramic, stratigraphy or radiocarbon dating was possible for a minority of these burials. Four urned cremation burials, at least one unurned cremation burial, four crouched inhumations and a possible inhumation were dated to the late 1st/early 2nd century based on graves goods. Radiocarbon dating from burials 1243 and 1334 yielded dates of AD 1-130 and AD 50- 230 respectively (Simmonds et al., 2008).

Several burials were able to be dated using radiocarbon dating and produced results suggestive of the 2nd/early 3rd century: skeleton 1286 yielded the date AD 60-240, and its grave (1288) was later in sequence than grave 1243 which it intercut, skeleton 1184 from yielded a date of AD 70-240 and its grave (1228) was cut by grave 1229 which was then cut by grave 1230 which contained a late 3rd century coin and skeleton 1277 yielded a date of AD 50-220 (Simmonds et al., 2008). 2nd century pottery from the back-fills of graves 1388, 1403 and 1720 and a fragment of 2nd/3rd century glass from grave 1144 were used as a *terminus post quem* (Simmonds et al., 2008). The mass grave is also dated to the later 2nd century (Simmonds et al., 2008).

Five of the graves contained material dating to the 3rd-4th century and several other were suggested to be a similar date due to their relationships with these graves (Simmonds et al., 2008). These graves were located one two clusters, one consisting of seven graves cutting the back-fill of the mass grave and the other along the western edge of the grave distribution (Simmonds et al., 2008).

A single molar was taken from 21 individuals (10 discrete inhumations and 11 mass grave) to be used in isotope analysis (Simmonds et al., 2008). The results showed two different groups. The first, consisting of 8 discrete skeletons and six mass grave skeletons, had wide ranging $^{87}Sr/^{86}Sr$ values but most referred to the geology in a 20km radius of Gloucester and oxygen values suggesting water zones through the UK (Simmonds et al., 2008). The second, consisting of two discrete skeletons and three mass grave skeletons, had strontium values that tended to cluster suggesting a common origin with geology that is different to Gloucester and oxygen values suggesting water zones on the extreme Western or Southern Europe, North Africa or arid locations, although similar values might be found in Cornwall, Ireland and the East Coast of Italy (Simmonds et al., 2008).

Overall, this site shows continuous use throughout a range of centuries and between periods which might give an indication that there is at least some degree of population continuity. Analyses that have been performed on the individuals from this Roman cemetery, on the other hand, suggest that the inhabitants of Gloucester within the Roman period alone were of diverse origin.

Great House Farm, Llandough

The Village of Llandough in South Wales is situated north of Penarth and 3.5km from the centre of Cardiff and overlooks estuary of the River Ely. Located in the town is the present church of St. Dochdwy that dates to the mid-19th century, although this church was considered to overlie a major medieval monastery of Glamorgan that is recorded in the Llandaff charters

and a late 10th/early 11th century cross on the grounds provided evidence of the age of the site's usage (Holbrook and Thomas, 2005).

The first excavation at Llandough was in an area south of the church by Barry and Vale in 1963 (Holbrook and Thomas, 2005) (see Figures 1, 9 and 10). Following this, Glamorgan-Gwent Archaeological Trust conducted further investigations to this area in 1979 which found a possible late Iron-age roundhouse that may have been part of a farmstead, a Roman villa that was constructed in the 2nd century A.D., expanded in the early 3rd century and occupied until the early 4th century and evidence that the some of the villa's walls were used as foundations for a 12th or 13th century barn (Owen-John, 1988).

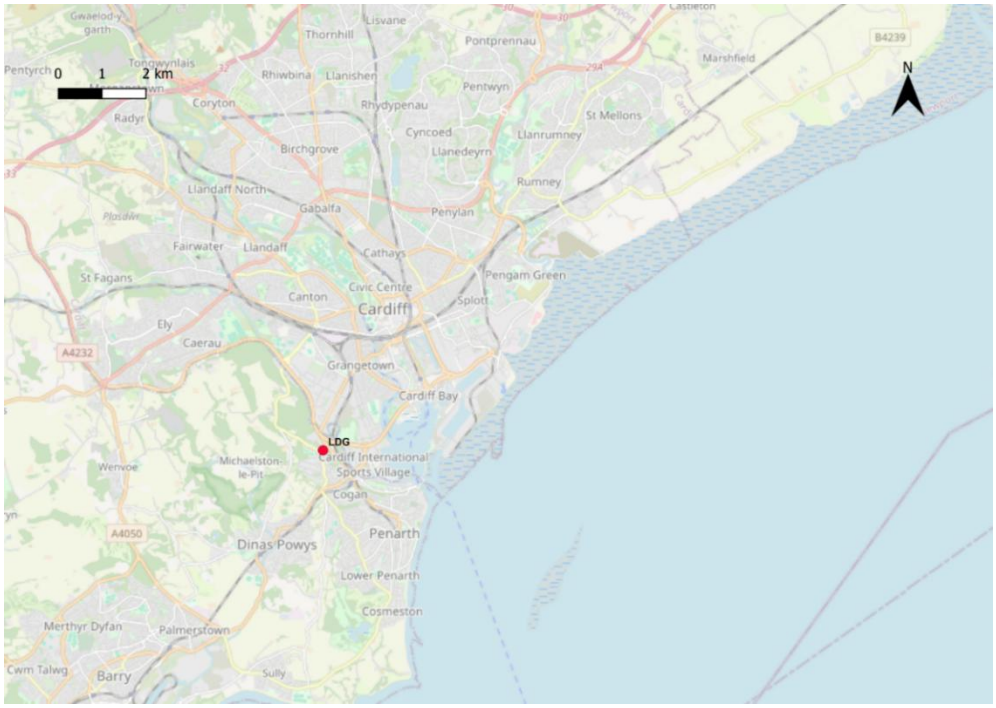

Figure 9*:* Map showing the regional location of Great House Farm, Llandough

In 1990, after proposal for residential development, Glamorgan-Gwent Archaeological Trust excavated eight trial trenches across the development

area and results suggested large parts of the site had seen disturbance caused by post-medieval quarrying and levelling and that closer to the churchyard wall disarticulated human remains had been disturbed from their original contexts (Holbrook and Thomas, 2005). As a result, Glamorgan-Gwent Archaeological Trust designated this part of the site as having a medium-high archaeological importance (Holbrook and Thomas, 2005).

Figure 10: Map detail showing the location of Great House Farm, Llandough

In 1992, full planning permission was obtained for residential development with no need for further archaeological excavation. The developers, Ideal Homes Wales Ltd., voluntarily sponsored an archaeological investigation into the medium-high archaeological importance area and, in 1994, Cotswold Archaeological Trust (now Cotswold Archaeology) was commissioned to excavate a 0.1 ha area, although in the early stages it became clear that this area would need to be expanded (Holbrook and

Thomas, 2005). The excavation ended in September 1994 with an area of 0.22ha comprising a total of 1066 burials (Holbrook and Thomas, 2005).

The site was divided into three areas based on spatial distribution of the burials. Area I was defined by burials within a suspected curvilinear boundary based on a concentration of graves in a NE-SW alignment, Area II in the west of the site was defined by rows of occasionally intercutting burials, and Area III were further burials to the north of Area I which may extend to the south-west to cut the original burials of area II (Holbrook and Thomas, 2005)

All burials at the site were inhumations and almost all were single burials with individual grave cuts with the exceptions of a single adult male directly on top of a child, two instances, one in Area I and one in Area III, in which two male adults and two children were placed side-by-side and in Area II were an adult and a foetus/new-born were buried together (Holbrook, Thomas, 2005). Of the burials, 30% were male or probably male, 25% were female or probably female and 26% were sub-adult and, while no groupings could be observed for age and sex of adult burials, there was a distinct concentration of child and young-child burials in Area III (Holbrook and Thomas, 2005).

Dating evidence for burials came from stratigraphic relationship to other burials, radiocarbon dating or finds used as *terminus post quem* or *terminus ante quem* with later medieval, post-medieval pottery finds in grave fills being considered intrusive and incidental Roman pottery finds being considered residual (Holbrook and Thomas, 2005). The dating for the

cemetery covers a wide span of time from the 4th Century A.D. (e.g. C^{14} for B2 gives the dates 370-640 cal A.D. with a roman pot as a dateable find) to the 11th century AD (e.g. C^{14} for B228 gives the dates 885-1035 cal A.D.) (Holbrook and Thomas, 2005).

One artefact of particular interest was a girdle found as corroded iron banding that lay above and in front of the pelvis in B631 (Holbrook and Thomas, 2005). Upon analysis, the girdle appeared to be constructed on two iron bands (upper and lower) the ends of both met and closed at the vertebral column with mineral-replaced wood with the wood rays aligning parallel to the vertebral column.

One interpretation for this artefact is that it could be a penitential belt worn as a form of penance for sins which is possible as the writings of John Cassian, a practitioner of austere auscetic traditions of the East was active in Gaul in 415 A.D and his writings were known in Anglo-Saxon England (Holbrook and Thomas, 2005). Although, this type of spirituality is thought to grown in popularity around the 12th century and most cases of this type of belt post-date the 6th century (Holbrook and Thomas, 2005).

The other interpretation is the artefact is a hernia girdle as iron banding found around the pelvis have been identified as such in Merovingian graves in France and Germany (Holkbrook and Thomas, 2005). There is no evidence of such medical injury that required treatment on the skeleton, however, it is noted that hernias would not leave any evidence on the skeleton (Holbrook and Thomas, 2005).

There have been several discussions into understanding the Early Medieval cemetery at Llandough, mostly pertaining to the nature of the site itself and that of the grave goods found. It has been recognised that the use of Roman villa sites for cemeteries in the Early Medieval is known to occur in Western Europe, being particularly characteristic of south-west Gaul but found across Gaul and northern Spain (Knight, 2005). This phenomenon, however, is rare in Britain with fewer closely paralleling Llandough, for example, post-Roman burials are known from villa sites in Wessex but the number of burials is too limited to constitute cemeteries such as at Thruxton (Knight, 2005). The closest parallels are Llantwit and two cemeteries at Caerwent, and so it has been posited that this may relate to local conditions in the former tribal territory of the Silures (Knight, 2005).

A number of graves contained what have been understood to have been deliberate grave goods rather than incidental finds. These finds include iron knives, Roman coins and beads (Holbrook and Thomas, 2005). Iron knives are one of the few grave goods commonly found in post-Roman cemeteries and those found at Llandough have parallels in sites such as monastic graves in Whithorn, Dumfries (Holbrook and Thomas, 2005). The placing of coins into graves is common in Late-Roman burials, however, Roman coins are also known to be found in Anglo-Saxon graves and to be found in burials that have been radiocarbon dated to the $6^{th}/7^{th}$ century suggesting that practice survive until well into the post-Roman period (Holbrook and Thomas, 2005).

There were also 122 pebbles of quartz and other non-local stone associated with the burials and disarticulated remains with three burials using a

terminus post quem for the late 5th century and radiocarbon dating giving the date 361-662 cal A.D. and another burial having radiocarbon dating as 885-1035 cal A.D. which suggests that the practice was well established before the 7th century and persisted until at least the 9th century (Holbrook and Thomas, 2005). The practice of burial pebbles has not only been found at other Early-Christian Welsh contexts such Capel Maelog but also at sites in Ireland, Scotland, the Isle of Man and Cornwall with the largest assemblage being found from the monastic graveyards Whithorn (Holbrook and Thomas, 2005).

Site 92, Atlantic Trading Estate, Barry

The Atlantic Trading Estate is an industrial estate that is located in the town of Barry in the Vale of Glamorgan in South Wales, with the industrial estate itself being located east of the Barry Docks and close to the mouth of Cadoxton River which lets out into the Bristol Channel (see Figures 1, 11 and 12)

During the 1980s, there were a series of excavations undertaken at the Atlantic Trading Estate which revealed a cemetery containing 45 burials, arranged in rows (Price 1996; Evans, 2003). The cemetery was bounded by a stone revetment to the south that provides a *terminus post quem* of the 3rd century AD and by a fence to the north represented by a shallow trench with stakeholes that was 7m the revetement and parallel with it (Evans, 2003). Radiocarbon determinations suggest that two of the burials were Roman, dating to the mid-3rd to early 5th centuries AD, while the remaining

determinations were between the 5th and early 8th centuries AD with the majority being 5th-6th century AD (Evans, 2003).

Other excavations between 1987-1990 in the Atlantic Trading Estate revealed a Bronze Age settlement (Sell, 1999). Evidence of the settlement included a round, a four-posted building and assemblages of flint and bronze age pottery; the pottery assemblage was used to date the site to 2400-1200BC. Further archaeological watching briefs in the Atlantic Trading Estate area only revealed modern foundation of brick and concrete that was possibly related to World War II period structures and a post-medieval field drain (Stafford, 2016; Thomas, 2017; O'Connell, Moore and Muller, 2018)

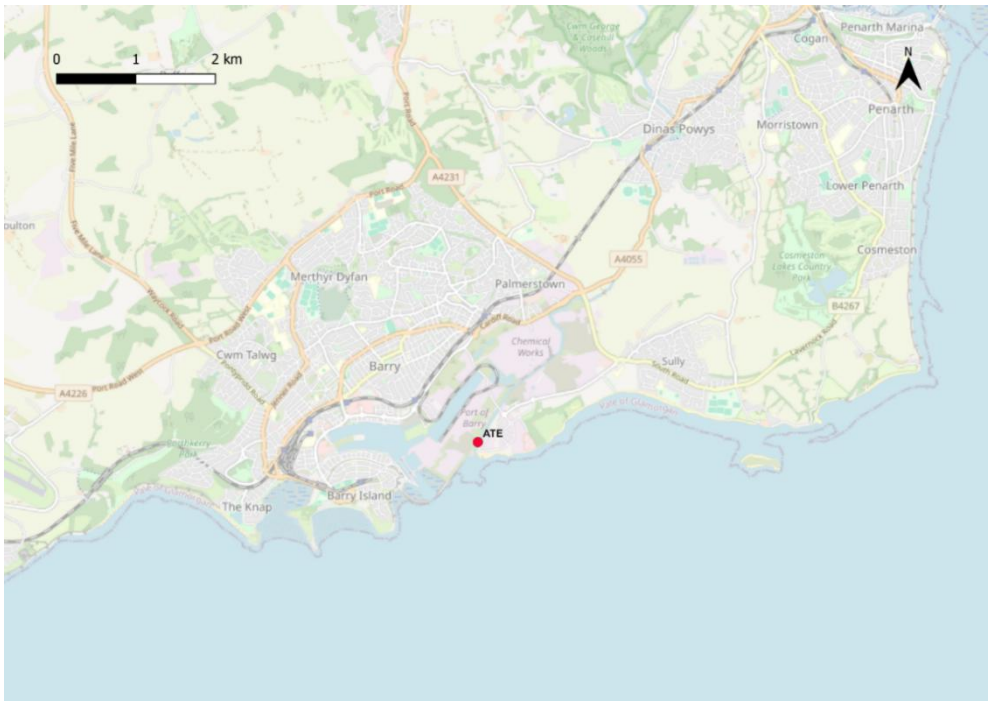

Figure 11: map showing the regional location of site 92, Atlantic Trading Estate, Barry (ATE)

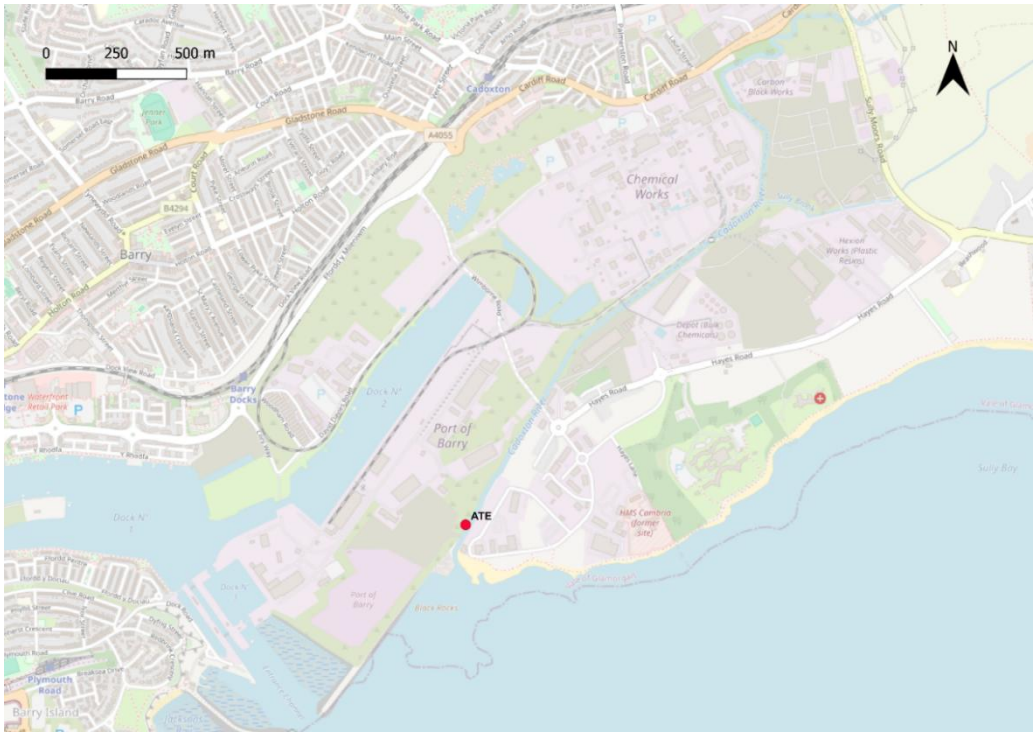

***Figure 12**: map detail showing the location of site 92, Atlantic Trading Estate, Barry (ATE)*

Brownslade Barrow, Castlemartin

Brownslade Barrow is situated in the Castlemartin parish near the western tip of the Castlemartin peninsula, Pembrokeshire in an area requisitioned by the Ministry of Defence in 1938 for live firing and dry training (Groom et al., 2011) (see Figures 1, 13 and 14). This area is a plateau of carboniferous limestone overlain by loess deposits and the barrow is situated towards the western end, 700m inland from the dune systems of Brownslade but still in an area of blown sand 1600m from the sea (Groom et al., 2011).

The date of the barrow is unknown; however, excavations were undertaken by Edward Laws in the 1880s, which found a stone lined cist 1m beneath the summit of the barrow that contained a human skeleton, charred bones and animal bones, and a sherd of wheel turned pottery (Groom et al., 2011). None of these are characteristic of bronze age or early medieval burials since wheel turned pottery is not prehistoric and grave goods are not known

in early medieval burial in west Wales and so it is hypothesised that this burial could potentially be Romano-British (Groom et al., 2011).

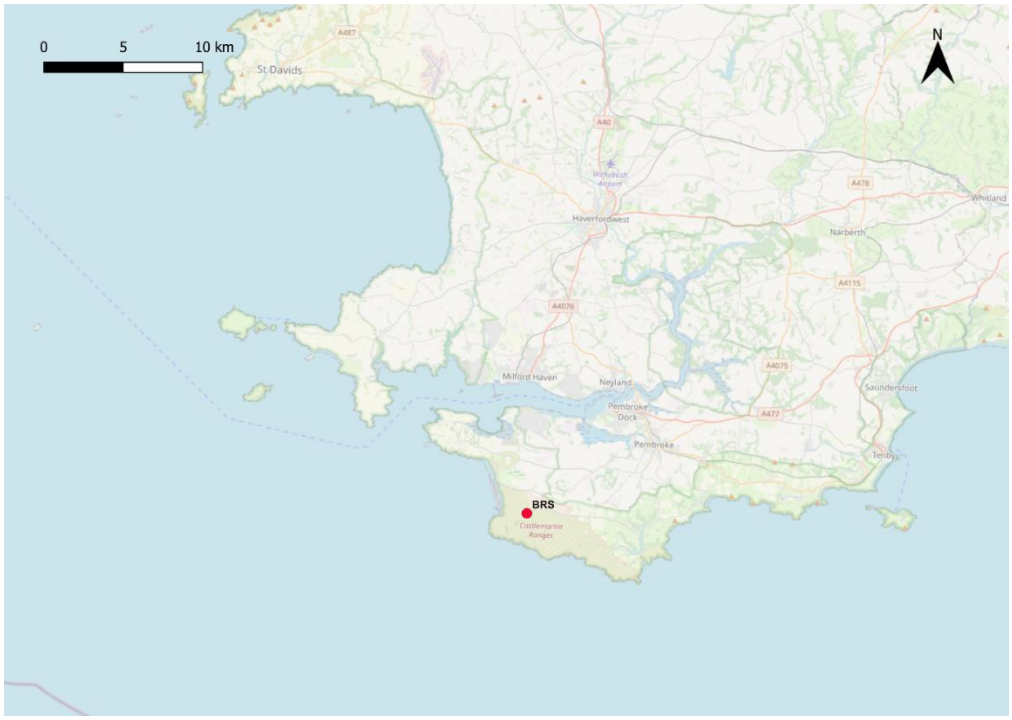

Figure 13: map showing the regional location of Brownslade Barrow (BRS)

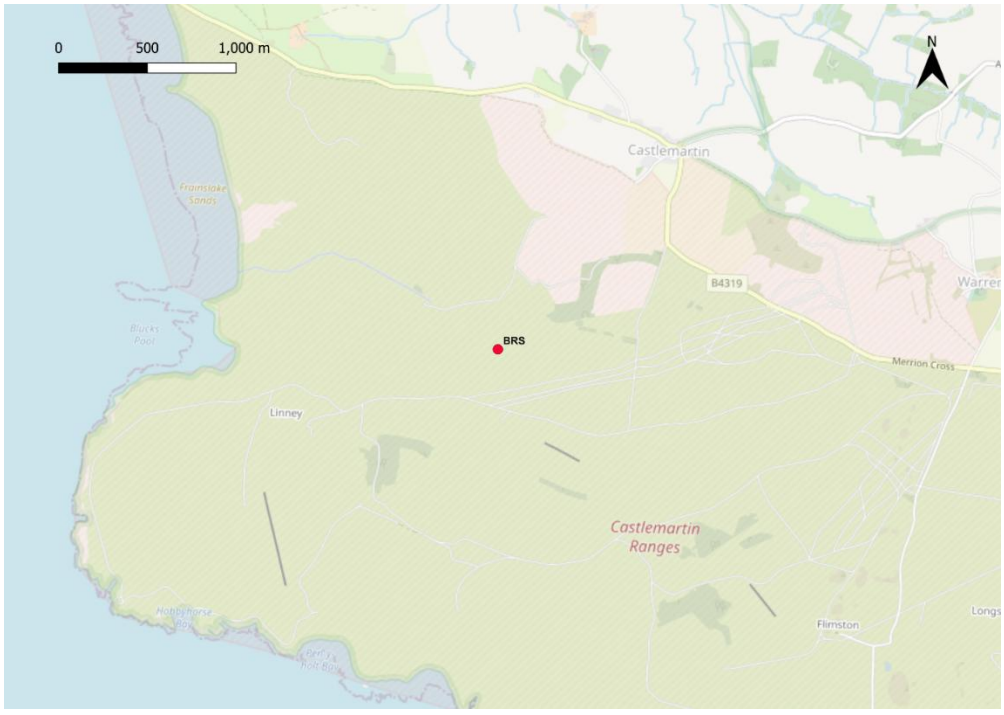

Figure 14: map detail showing the location of Brownslade Barrow (BRS)

The 1880's excavations also found a fragmentary group II early medieval inscribed stone, and revealed a large number of burials, some of which were in cist graves without lintel slabs which were presumed Christian, although there was no dating evidence, due to being extended and oriented (Groom et al., 2011). The precise location of the burials is not known; however, Laws describes his excavations as being on the south-eastern side of the barrow (Groom et al., 2011).

In 2002, due to damage by badger disturbance, the Defence Estates commissioned a topographic and geophysical survey followed by a small-scale excavation of the small stone building to the north of the quarry (Groom et al., 2011). Three radiocarbon dates collected from human bones provided dates from cal. AD 430 to cal. AD 940 and 2 sigma range which demonstrated the archaeological significance of the area and barrow and so the Defence Estates relocated the badger sett, erected badger proof fencing and commissioned full excavation of those areas most severely affected (Groom et al., 2011).

This excavation was in two stages: Stage 1 consisted of two trenches to the north of the barrow in May 2006 and Stage 2 the excavation of the badger sett to the south of the barrow (Groom et al., 2011). Apart from Trench 3 all trenches were hand excavated, however, Trench 3 had limited time for excavation and badgers had severely disturbed the upper archaeological deposits (Groom et al., 2011).

In Trench 3, an early medieval cemetery was discovered with a total of 32 burials cut into the wind-blown sand (Groom et al., 2011). Although bone

preservation at the site was excellent, the survival of the burials was highly variable due to the badger activity having affected all of them to some degree and, in addition to the remains found in the graves, over 1000 pieces of disarticulated human bone were found in badger disturbed topsoil (Groom et al., 2011). Twelve of the burials were associated with stone cists, 14 with simple dug graves and six were disarticulated remains and between them the 32 burials contained 52 individuals (Groom et al., 2011).

Three radiocarbon determinations from loose bones collected during the evaluation and seven from the cist and simple dug graves provided the only reliable dating for the cemetery (Groom et al., 2011). The overall date range is from cal. AD 430 to cal. AD 1020; it is argued seven radiocarbon dates shown that the main use of the cemetery was from the mid-seventh through to the end of the ninth century while two dates (Cal. AD 430-650 and Cal. AD 440-650) indicate burial may have started from the mid-fifth century and the latest date (cal. AD. 830-1020) could belong to the main period of burial and that the cemetery did not continue into the eleventh century (Groom et al., 2011).

All strontium isotope values are argued to be accommodated with the biosphere of Wales with a majority of concentrations between 40ppm and 111ppm with two outliers above 150ppm (Groom et al., 2011). It is suggested that these outliers could be caused by the use of seaweed as fertiliser or the consumption of seaweed-based produce (Groom et al., 2011).

On the other hand, there were a significant number of individuals who had elevated levels in phosphate oxygen analysis (Groom et al., 2011). Several hypotheses have been suggested; it could be the result of consumption of beer or the 'potage' method of cooking or, alternatively, the values are known to be compatible with the extreme west coast of Ireland and north-west of Scotland, as well as the coastal regions of the Mediterranean Basin and so these individuals may originate from one of these areas (Groom et al., 2011).

Culver Hole

Culver Hole is a semi-tidal cave that is situated to the north-west of the community of Llangennith in the county of Swansea and once considered part of the old county of Glamorgan (see Figures 1, 15 and 16). The cave itself is located at the base of a cliff, 3.7 metres from the current shoreline, and floods during high tide (Wilford, 2016). A narrow entrance leads into a chamber that is 7 metres wide and 9 metres high with two passages that lead 5.2 metres further into the cave creating a total length of 11 metres (Wilford, 2016).

The cave saw a series of excavations from 1861-1932 (Wilford, 2016; Penniman, 1932). During the excavations between 1924 and 1931 human remains belonging to a total of at least 41 individuals were found (Wilford, 2016). At least 30 individuals were found in contexts containing Wessex type bi-conical urns dating to the middle bronze age (Wilford 2016).

Many of the finds from the site has consisted of Bronze Age pottery (Penniman, 1932) such as a bucket or barrel-shaped urns with perforated

rims and diagonal slashing to the upper part of the jars suggested as a local development of Late Bronze Age II-III (Savory 1958). The association between the human remains with Bronze Age pottery finds forms the basis of the dating of the human remains.

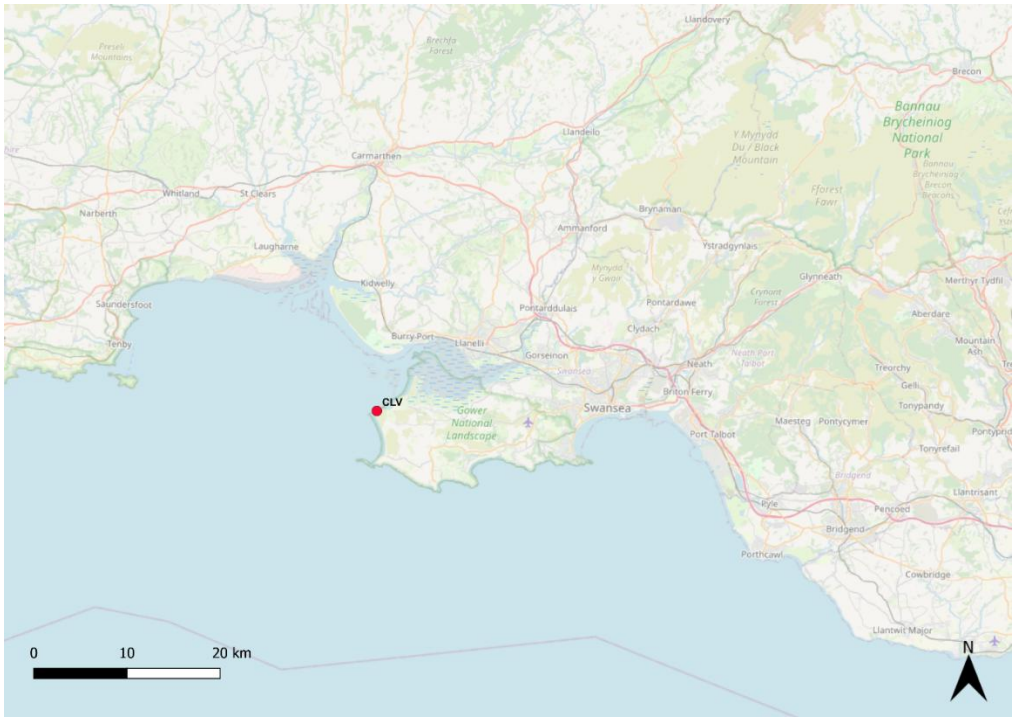

Figure 15: map showing the regional location of Culver Hole (CLV)

Buxton (1932) performed an analysis of the human material and stated that there were 8 skulls, 6 male and 2 female, alongside ‘a number of thigh bones’ suggesting there were at least 30 individuals. The remainder of the analysis focuses on reconstruction and measurement of the skulls’ cephalic index and came to the conclusion that they were dolichocephalic and so were more closely related to the Neolithic population rather than ‘Romano-British’ or ‘Beaker Folk’ types which tended to be mesocephalic (Buxton, 1932).

Many Roman finds were discovered in the cave, the majority of which came from the base of a sediment layer of small pool located to the left of the entrance (Branigan et al., 1991). The Several Roman Iron Age brooches were found including one damaged and two complete Headstud fibula dating to the late 2nd Century AD and a Fowler D5 type penannular brooch (Branigan et al., 1991). There is also Roman coinage found including sestertius of Hardian, a denarius of Marcus Aurelius, a coin of Antoninus and 11 Constantianian nummi (Branigan et al., 1991).

Figure 16: map detail showing the location of Culver Hole (CLV)

Other metalwork found in the cave include a late-Celtic style bronze statuette of a naked female with hands clasped in front found on the surface of the cave (Taylor, 1935), a bronze strip bracelet, an iron rod and a Holdfast (Branigan et al., 1991), a ring of sheet brass and a 9th century AD brooch (RCAHMW, 1976).

There was also the finds of a small flat spindle whorl and boar's tusk that may be Iron Age in date (Branigan et al., 1991) and a ring-shaped colourless glass bead with an opaque yellow central core dating to the 1st century BC-1st century AD (Savory, 1958).

This site shows signs that it may have been a place for burial within the Bronze Age, however, usage of the site continued through the Iron Age with usage ending in the 1st century AD.

Tinkinswood, St. Nicholas

Tinkinswood is a Neolithic burial chamber in South Wales located near to the village of St.Nicholas in the Vale of Glamorgan which lies west-southwest of Cardiff (Ward, 1916) (see Figures 1, 17 and 18). The site is 6.6km north of the modern coastline and situated on sloped south-facing ground with the surrounding landscape made up of pasture and woodlands (Reynolds, 2014). Enclosed by a revetment wall, the cairn would have originally capped with an earthen stone mound (Thompson, 2019). There is a paved forecourt and short passage on the eastern side that open to the small burial chamber that is constructed with six large stone orthostats and a slab line cist is situated within the cairn to the North (Thompson, 2019).

The site first gained antiquarian interest in the mid-1800s when Rev. H. Loungeville Jones found a human mandible and then antiquarian J.K. Lukis performed further exploration of the tomb, finding fragments of human teeth, unburnt bone and pottery sherds in the outside debris (Thompson, 2019). Following on from this, John Ward, the first keeper of archaeology at the National Museum of Wales undertook excavation and reconstruction of

Tinkinswood: in the forecourt human remains alongside 100 sherds of black course pottery were found, within the chamber commingled human and animal remains were excavated from a 60cm-deep deposit, and the slab lined cist at the North of the cairn was discovered containing and surrounded by fragments of human and animal bone (Ward, 1916; Thompson, 2019).

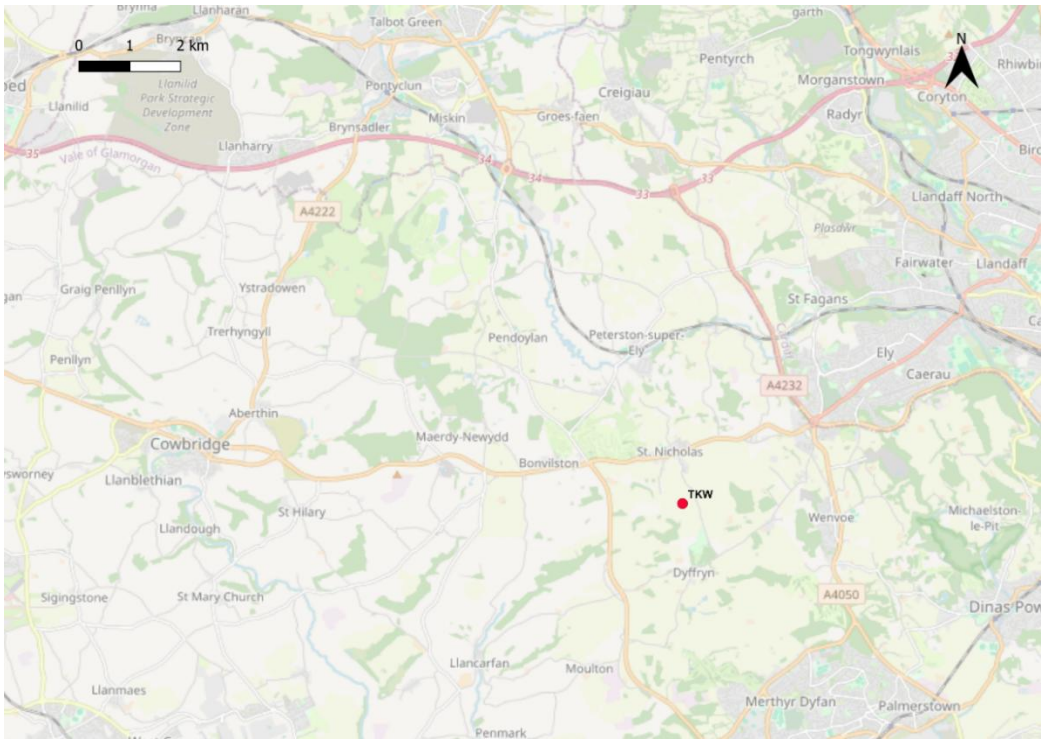

Figure 17: map showing the regional location of Tinkinswood burial chamber (TKW)

Analysis of the human remains was performed by Keith (1916). From 920 fragments he estimated 40-50 individuals of a wide range of age and both sexes had been deposited, he attributed sex to fragments based on robusticity and assigned small shaft fragments to sides (Keith, 1916; Thompson, 2019). Keith also described taphonomic alterations to the bone: there were eight small cremated cranial fragments alongside two fragments

of bone that had been charred post-skeletonization, no evidence of cut and scrape marks, few signs of rodent gnawing and fractures were noted.

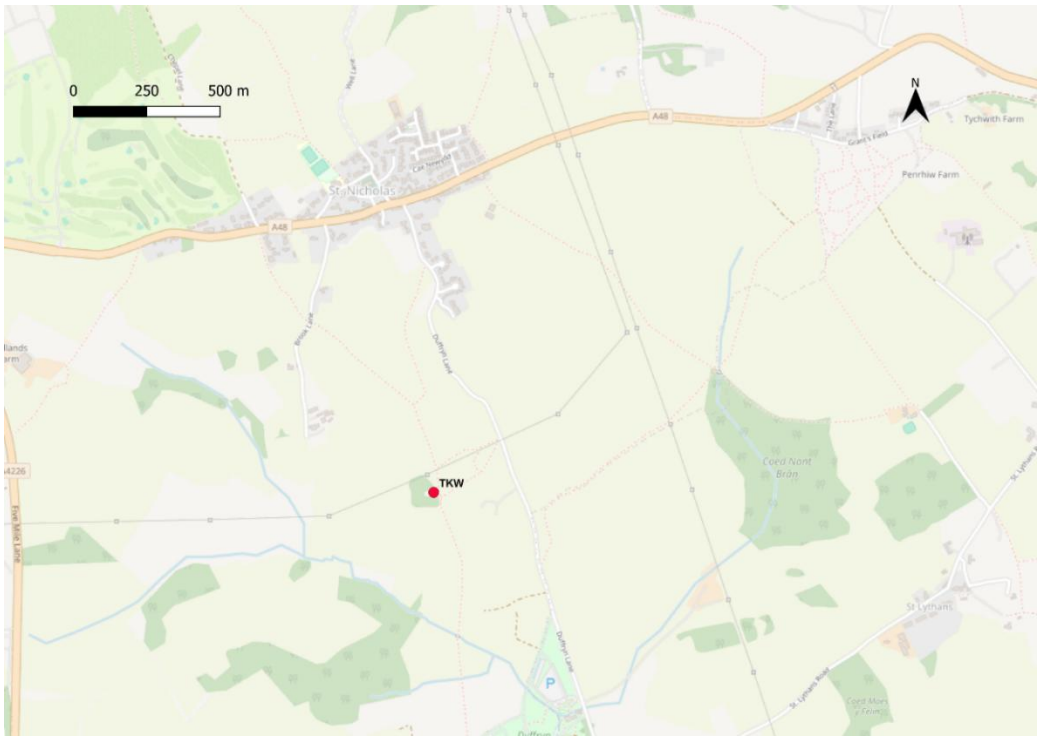

Figure 18: map detail showing location of Tinkinswood burial chamber (TKW)

However, more recently, Thompson (2019) has performed a re-analysis of the human remains. Each bone fragment was identified, when possible, to skeletal element and side, as well as macroscopically examined for taphonomic processes such as weathering, root damage, gnawing, cutmarks and breakage, and each fragment was quantified to assess the extent of fragmentation, and the colour of charred and cremated remains was described. This re-analysis found Keith's analysis for the minimum number of individuals (MNI) was erroneous due to inaccurate methods and identified that the MNI for the site was 20 individuals. It also found that peri-mortem breaks were rarely noted in contrary to Keith's findings (Keith, 1916; Thompson, 2019) and it is postulated that with minimal evidence of weathering may be congruent with secondary deposition of a small number

of curated elements, however, due to lack of excavation records, movement and rearrangement could not be fully assessed and that the practices at contemporary nearby monuments of Ty Isaf and Pipton may be comparable to Tinkinswood (Thompson, 2019).

Tinkinswood has also been recently analysed as part of a large-scale study of Neolithic assemblages in southern Britain in which location of entheseal changes were found to differ between females from Tinkinswood and West Kennet and between males from Tinkinswood and Parc le Breos Cwm (Wysocki and Whittle, 2000). It was also included in a study analysing aDNA of the ancestry of early Neolithic British populations which found that Welsh populations had the lowest levels of western hunter gatherer admixture followed by South-West and Central English populations, and posits that the British cline in the western hunter gatherer ancestry may be due to a single population moved across Britain from a western entry point and progressively admixed with local hunters (Brace et al. 2018).

Strath Glebe Farm, Isle of Skye

The farm of Strath Glebe is located within Strath Suardal, south of the Red Cuillen on the Isle of Skye (Wildgoose, Kozikowski, 2018) (see Figures 1, 19 and 20). An archaeological survey of the farm recorded a setting of rectangular limestone and granite slabs protruding on the summit of an outcrop at NG 6199 2038 and at the request of the owner subsequent excavations were undertaken by Phoenix Archaeology between 2015-2018 (Wildgoose, Kozikowski, 2018).

The setting was divided into quadrants and excavated NW, SE, and NE, SW as Trench 1 followed by 4 subsequent one-meter-wide trenches (Trench 2-5) based on the extended quadrant lines to define the extent of the site (Wildgoose, Kozikowski, 2018). The results of which demonstrated it was a denuded burial cairn (Wildgoose, Kozikowski, 2018).

Figure 19: map showing the regional location of Strath Glebe chambered cairn (STG)

The cairn and chamber are a Neolithic style with the forecourt resembling Rubh an Dunain on Skye and Dyffryn Ardudwy's early phase (Wildgoose, Kozikowski, 2018; Scott, 1932; Powel, 1973). The construction appears to mirror the surrounding landscape with west side mainly consisting of granite boulders and stones reflecting the granite hills to the west and limestone boulders and stones on the east reflecting the limestone hills to the east (Wildgoose, Kozikowski, 2018).

Similarly, all trenches contained white quartz pebbles (26 in total) and red/brown quartzite (11 in total) (Wildgoose, Kozikowski, 2018). White

quartz is not found locally and will have been brought to the site from elsewhere whereas red/brown quartzite is found on local beaches (Wildgoose, Kozikowski, 2018).

Figure 20: map detail showing location of Strath Glebe chambered cairn (STG)

Trenches 1 and 2 demonstrated that the site had been previously excavated in the early 20th century, with a stratified 1897 penny in Trench 2 provided a terminus post quem, and a backfill layer consisting of human bone, stone and soil with an earthen-ware glaze teapot and iron wire being found (Wildgoose, Kozikowski, 2018).

A number of human remains were found at the site: a pit named “Feature B” that predates the structure contained a single tibia and 15 human teeth, a selected bone deposit named SBD2 was located at two long stones in the forecourt boundary with smaller fragmentary bones included in a brown soil layer that covers the forecourt, and finally a second selected bone deposit (SBD1) that appears to date to final construction or the construction of a

nearby enclosure was found in a pit cut into the body of the cairn (Wildgoose, Kozikowski, 2018). Radiocarbon dates that have been obtained from the human remains place the use of the monument at 4569±35 BP (3494-3104 cal BC) (Sheridan et al., 2019).

Finds that characterised the site as Neolithic included four leaf-shaped flint arrowheads (two in the south-east of the chamber, one 200mm away from the first two in the south-west of the chamber and one in the forecourt area), carinated style pottery from the hearth area and a jet bead included with SBD1 (Wildgoose, Kozikowski, 2018). Other finds were also made such as a marine ivory bead, a flint scraper and a limpet shell necklet deposited with SBD2 and a small mudstone/tuff blade deposited with SBD1 (Wildgoose, Kozikowski, 2018).

Distillery Cave, Oban

Distillery Cave was a rock cave located in Oban, Argyll and Bute behind the Oban Distillery buildings (National Grid Reference: approximately NM 8598 3015) (Canmore.org.uk, No Date A) (see Figures 1, 21 and 22). The cave was discovered in 1890, when it was exposed due to excavation and rock blasting by workmen. Construction was part of a new warehouse in connection with the Oban Distillery and after excavation the building was built on top of the site (Canmore.org.uk, No Date A; Turner, 1895). Situated 40ft above sea level, the mouth of the cave was 9ft wide and 10ft high and facing North-North-West, while the depth of the cave was 12ft and the height at the back was 4ft (Turner, 1895).

Figure 21: map showing the regional location of Oban cave sites. DIS= Distillery Cave and RAS= Raschoille Cave

Figure 22: map detail showing the location of Distillery Cave, Oban (DIS)

A large quantity of shells was found and removed, along with a number of bones which were located either in the shell-beds or at the bottom end of the cave, (Turner, 1895). As a result of the actions by the workmen in exposing the cave, however, it was not possible to recognise any stratification in the soil or shell deposits, nor was it possible to ascertain the position of most of the bone prior to disturbance (Turner, 1895).

The shells were identified as belonging to several species including oyster, limpet, common whelk, patella, solen and *Venus Verrucosa* (Turner, 1895). Some of the limpet shells had been reduced to ring-like bases with a large part of the body removed, although it was unclear whether this was through taphonomic processes or deliberate alteration for ornament (Turner, 1895).

The human remains from the cave indicated an NMI of eight, consisting of four adults and four juveniles based on eight mandibles that were found (Canmore.org.uk, No Date A; Turner, 1895). Most of the bones were in a fractured condition, particularly skull material, of which it was noted that reconstruction was not possible (Turner, 1895).

Post-cranial skeletal elements were also identifiable as belonging to juveniles. Juvenile bones included four femora of different epiphyseal fusion stages, the youngest estimated at 1-2 years old, as well as tibiae, clavicles, innominate bones, scapulae and vertebrae (Turner, 1895).

Adult post-cranial bones were noted to include long bones such as a left tibia, four humeri, complete left ulna and radius from the same individual, and another left radius (Turner, 1895). The four humeri exhibited marked

muscular ridges, and two tali exhibited changes to the morphology associated with acute flexure such as squatting. (Turner, 1895).

There was very little animal bone recovered from the cave. The animal bones from the site represented a number of species including a fragmented mandible of a young harbour seal (*Phoca Vitulina*), a pig tooth, and mandible of a ruminant, as well as fish and bird bones (Turner, 1895).

Several tools were also found at the site. Two of these tools were made using animal bone: a spatula made from deer antler with signs of attrition on the ends that is suggested to have been used for moulding clay and a borer that shows signs of polish and marking near the point suggested to have been used for boring holes into hides (Turner, 1895). The other tools were stone: a nodule of cherty flint with a naturally round surface on one side and split surface with a bulb of percussion on the other and showing no sign of secondary working; a small flake of flint approx. 28.58 mm in length with no secondary working; three irregular pieces of flint ranging from approx. 12.7mm to 19.05mm that show no working on the edges (Turner, 1895).

A radiocarbon determination was obtained from the antler spatula (OxA-4509) which provided a Mesolithic date of 3780 ± 60 BP 2460- 2030 cal. BC (Canmore.org.uk, No Date A). Three determinations were obtained from human bone samples as part of the GENSCOT ancient DNA project and yielded Neolithic dates of 4914 ± 27 BP 3762-3644 cal. BC (SUERC-68702), 4631 ± 29 BP 3514-3353 cal. BC (SUERC-68703) and 4881 ± 25 BP 3701-3640 cal. BC (SUERC-68704) (Armit et al., 2016; Sheridan et al., 2019). This shows that the site saw an extended period of use.

Raschoille Cave

Raschoille Cave is located by Glenshellach Road in Oban, Argyll and Bute, (National Grid Reference: NM 8550 2890) (see Figures 1, 21 and 23). Situated on the North-West side of Glen Shellach, the cave would have been on the edge of a sea inlet in prehistoric times and is considered a natural sea cave caused by erosion in the Easdale Slate series at 8 metres, the level of the lowest raised beach (Connock, 1985).

Figure 23: map detail showing the location of Raschoille Cave, Oban (RAS)

In May 1984, the previously unknown cave was revealed by mechanical digger operations removing material from below the cliff face to increase the area of ground around a house and three human cranial vaults were observed by the operator who subsequently informed the police (Connock, 1984; Connock, 1985). Following this, excavations sponsored by the Lorn Archaeological and Historical Society and the Ancient Monuments Division

of the Scottish Development Department took place for 26 days in June and July 1984 (Connock, 1985).

A total of 109 separate deposits of material (some later amalgamated) were recorded within the cave were assigned a unique identification number and closely associated material given the same number with datums marked on the cave wall for vertical and horizontal relationships (Connock, 1985). These were also assigned to one of ten layers, labelled in Roman numerals 0-X (no layer was labelled IX and Layer 0 represented unstratified material), however, due to lack of defined archaeological these layers were relatively arbitrary (Connock, 1985).

As a result of excavations, a total of c.2000 pieces of bone, weighing c.17kg, was recovered (Connock, 1985). None of the bones were in articulation and large amounts were in a fragmentary condition and mostly represented human skull and long bones, with mandibles, teeth and small bones such as that of the hands and feet being low in number (Connock, 1985). There was an abundance of smaller animals including rodents, amphibians, birds and fish represented within these samples, however, very few of the larger bones were non-human (Connock, 1984; Connock, 1985).

Additionally, a total of c.11kg of shells were recovered from the site (Connock, 1985). These were identified as belonging to a range of marine molluscs such as edible periwinkle, flat periwinkle, mussel, oyster, limpet, whelk, cockle, and pullet carpet shell (Connock, 1985).

Provisionally, the site was considered potentially Bronze Age in date due to the presence of a flint arrowhead as the only artefact found and the

disarticulation of human remains matching the practices of excarnation and redeposition that was practiced in the Neolithic and Bronze Ages (Connock, 1985). Subsequent radiocarbon dating, however, revealed the earliest remains came from a red deer bone were Mesolithic in date (OxA-8396 7469 ± 80 BP) and the latest were humans remains that were Neolithic in date (OxA-8537 4535 ± 50 BP) (Bronk Ramsey et al. 2002; Canmore.org.uk, No Date B).

Recently, Bownes (2018) obtained radiocarbon dates for nine human samples from the site which had been recalibrated to adjust for the marine resource consumption with the earliest individual dating to 4738 ± 31 BP 3633-3372 cal. BC and the latest dating to 4432 ± 31 BP 3310-2891 cal. BC. In this study, reconstruction of the diet of the population using stable isotope analysis and modelling (FRUITS) showed that the diet of the population was comparable to other Neolithic populations from across Scotland including Carding Mill Bay, Embo, the Holm of Westray, Loch Barralie and 3 tombs at Caithness (Bownes, 2018).

Whithorn Priory

Whithorn is located in the historic county of Wigtownshire in Dumfries and Galloway, Scotland and is approximately 10 miles south of Wigtown (see Figures 1, 24 and 25). The area has long been considered an important Christian site in Scotland due to having been associated to St. Ninian, who founded a church dedicated to St. Martin, referred to by Bede as Candida Casa, and spread Christianity through Southern Scotland (Broun, 2000).

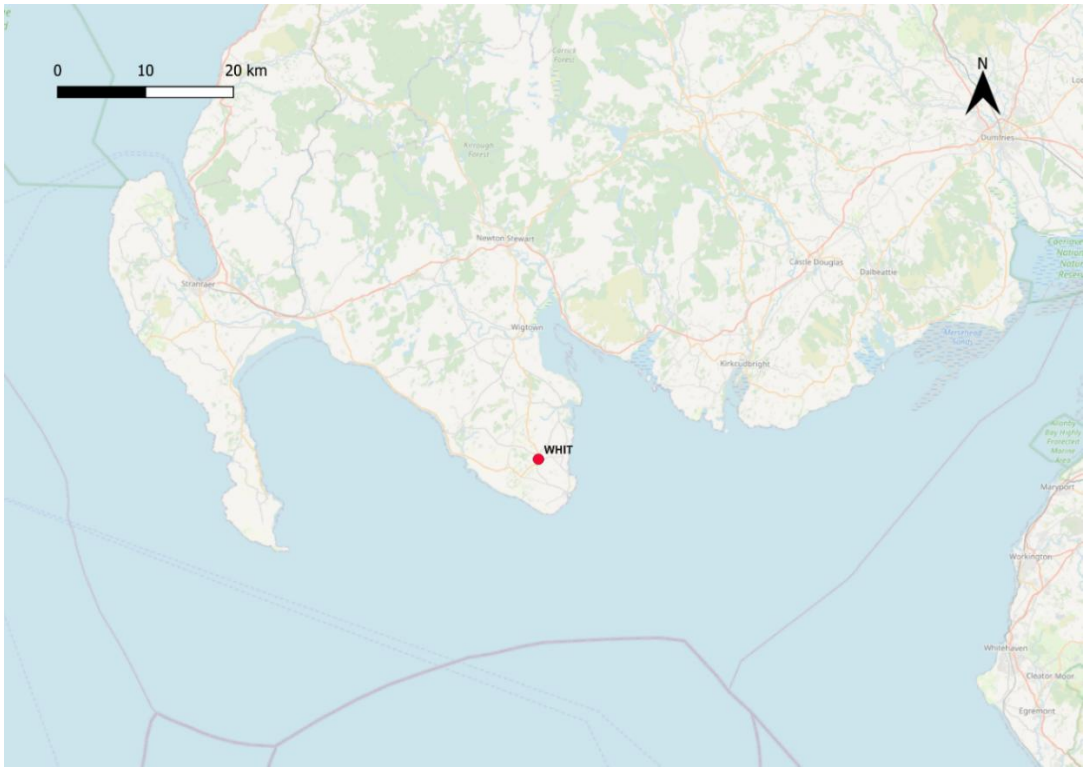

***Figure 24**: Map showing the regional location of Whithorn Priory (WHIT)*

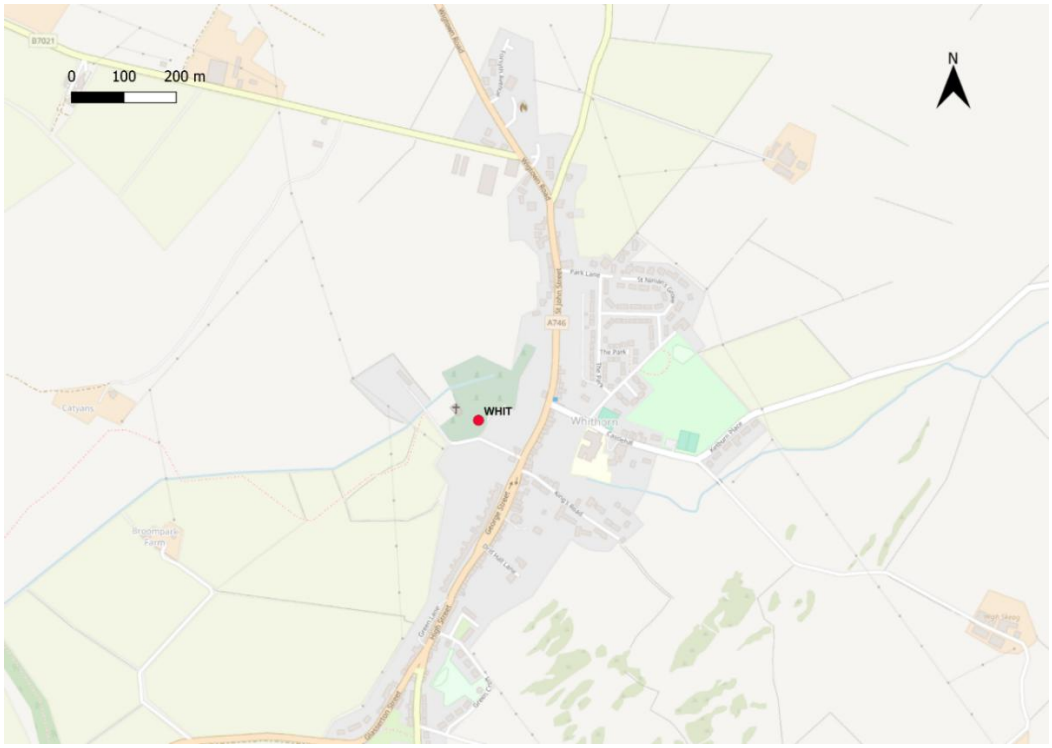

***Figure 25**: Map detail showing the location of Whithorn Priory (WHIT) within Whithorn*

Between 1957 and 1967 a series excavations took place at the Eastern end of the priory church under the direction of P.R. Ritchie. A large quantity of

human bone was discovered during Ritchie's excavations, and it is this collection that is used in this study. The absolute minimum number of individuals was 41 adults and 9 sub-adults (Henderson, 2009). 18 of these individuals were *in situ* and articulated while some intact burials were not recorded, the excavated skeletons were not stored as discrete entities and other material that was disarticulated and disturbed by other groundwork activities were labels as charnel (Henderson, 2009). The skeletal assemblage was assessed to be composed of 21 males and 13 females and comprised of all ages from perinatal to elderly (e.g. 70+) (Henderson, 2009).

Radiocarbon dates for skeletons within this sample have returned dates between 11th century AD and the late 14th century AD (Lowe, 2009). Carbon and Nitrogen isotope analyses on individuals from the collection suggest that there were distinctions in diet between social classes with bishops eating significantly more fish than lay individuals and oxygen and strontium isotopes suggest a distinction in mobility between social classes as a majority of high-ranking clerics were not local to Whithorn, unlike the lay individuals (Müldner, Montgomery et al., 2009).

Between 1984-1991, a series of excavations were undertaken in an area known as Glebe Field (Hill, 1997). Hill identified a number of phases of activity: the first is up to 730AD evidenced by undated features and some Roman finds, the second phase is c.730-845AD in which the site is occupied by a minster church and its community and related to Northumbrian rule, the third phase is from 845AD to 1000-1050AD, the fourth phase consists of an expansion of the monastery between c.1000-1050 and 1250-1300 and,

finally, the fifth phase is in the 16th century (Hill, 1997; McComish and Petts, 2008).

Excavations in Fey Field, Whithorn in 1992 and 1993 directed by David Pollock and in 1995-1996 directed by Amanda Clarke provided evidence of multi-period settlement (McComish and Petts, 2008). This settlement had seven periods: Period 1 was naturally occurring deposits, Period 2 was pre-6th century undated features directly above the natural deposits, Period 3 was a 6th-early 8th century AD settlement and burial ground, Period 4 was a c.730-845 AD settlement and burial ground related to the Northumbrian monastery, Period 5 was a c.845-c.1250-1230 AD settlement and burial ground, Period 6 was a c.1250-1230 AD-16th century AD medieval priory and quarry and Period 7 was horticultural deposits (McCormish and Petts, 2008).

A total of 156 articulated inhumations were recovered (26 from 1993, 56 from 1995 and 74 from 1996) and a large amount of disarticulate remains was recovered from 85 contexts (10 from 1992,10 from 1993, 28 from 1995 and 37 from 1996) (McCormish and Petts, 2008).

These excavations also recovered pottery such as late Roman amphorae and E ware from the Early Medieval period and 503 small finds recorded as medieval pottery and 345 small finds recorded as Post-Medieval pottery (McCormish and Petts, 2008). There were also small finds such as 25 sherds of early medieval imported glass and a large amount of metalworking waste, stone objects and 44 coins (McCormish and Petts, 2008).

Southgreen, Kildare, Co. Kildare

Southgreen Townland is situated in Kildare, County Kildare (see Figures 1, 26, and 27). In February 2019, archaeological investigations were conducted under the supervision of Donald Murphy of Archaeological Consultancy Services Unit (ACSU) under license 19E0009 at the site of proposed new link road in the townland after human remains were discovered during construction works (Murphy, Gibney, 2021). These excavations failed to reveal any archaeological deposits or features, although some areas of the sites were unavailable to test due to overhead cables (Murphy, Gibney, 2021).

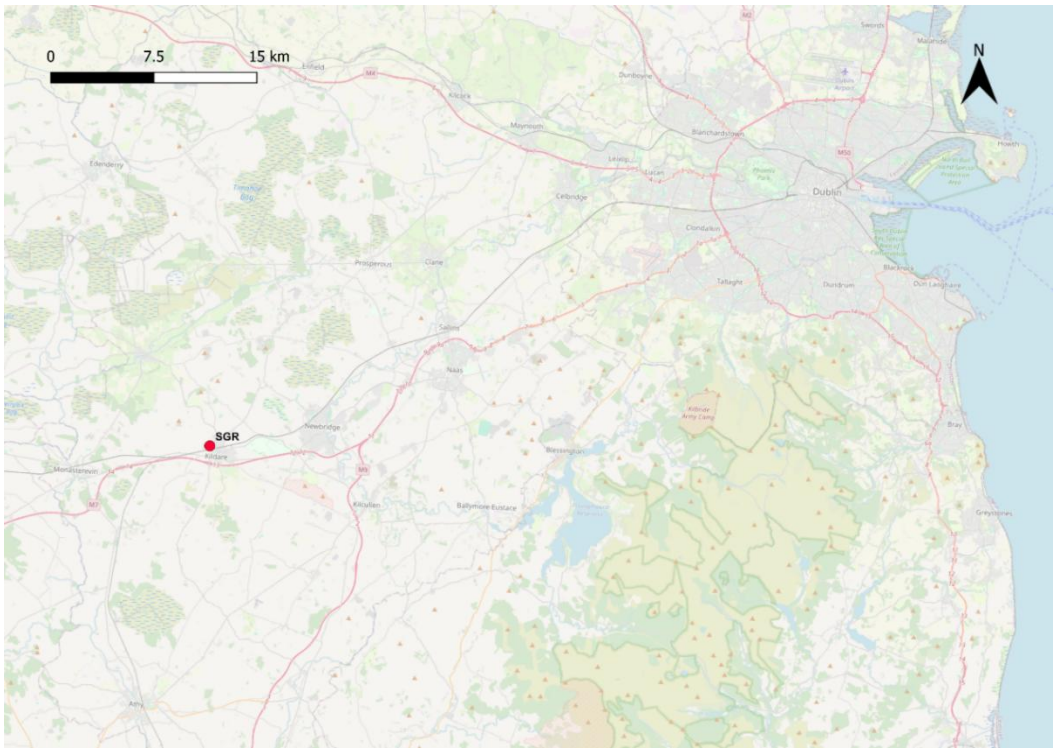

Figure 26: map showing the regional location of Southgreen site (SGR)

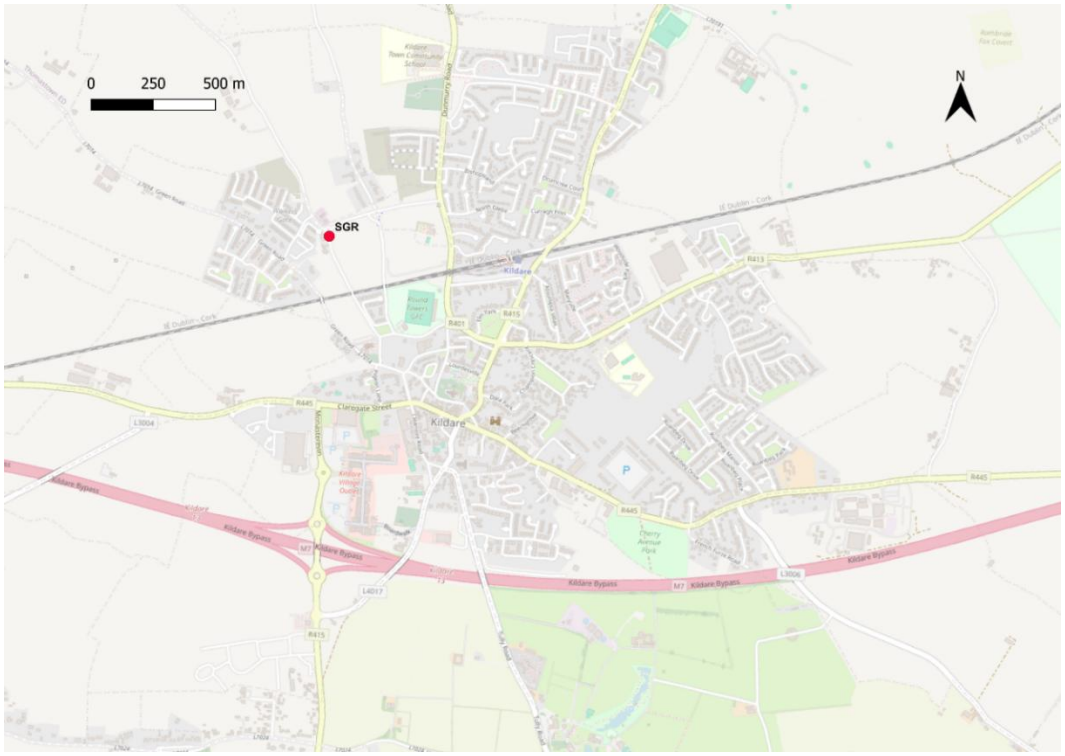

Figure 27: map detail showing the location of Southgreen site (SGR)

Human remains were again found in the townland by contractors constructing a tie between the new Southgreen Link Road and existing Southgreen Road on 26th February 2019 (ITM 672254, 713081) (Murphy, Gibney, 2021). This was in the area previously inaccessible to the excavations in February 2019 (Murphy, Gibney, 2021).

Following inspections by the Gardai, ACSU were requested to determine if the remains were archaeological in nature (Murphy, Gibney, 2021). The remains were determined to be archaeological and represented more than one individual and therefore National Museum of Ireland and the Coroner were notified, and subsequently a new license and extension to license 19E0009 were granted (Murphy, Gibney, 2021).

Excavations of the human remains and archaeological features and monitoring of the works during the construction of the link road were

undertaken between 8th October 2019 and 15th March 2020 but works were temporarily suspended on site due to the Covid19 pandemic and all archaeological samples were removed to the ACSU head office in Drogheda, Co. Louth. (Murphy, Gibney, 2021). The Site re-opened and monitoring of all works continued on 5th May 2020 (Murphy, Gibney, 2021).

This investigation uncovered 35 burials containing 36 skeletons in a mix of simple and stone-lined graves (Murphy, Gibney, 2021). All of the burials were in an east-west orientation and were excavated under the direct supervision of osteoarchaeologist Glenn Gibney from ACSU (Murphy, Gibney, 2021). In addition to these, 504 fragments of disarticulated bone were found, 18 of which were complete, and 2 individuals could be identified within these disarticulated remains (one adult and one juvenile) (Murphy, Gibney, 2021). Therefore, the total number of individuals at the site was counted as 38 and comprised of 5 males, 14 females, 3 individuals on indeterminate sex, 1 adolescent, 2 juveniles and 4 infants (Murphy, Gibney, 2021).

Four individuals were selected for radiocarbon dating (SK3, SK10, SK17 and SK30); one skeleton (SK3) returned results that showed dates between the 2nd-5th centuries (Cal. AD. 263-275, 347-422) while the other three skeletons returned results that showed dates between the 5th-6th centuries (SK10: Cal. AD 425-542, SK17: Cal. AD 427-551, SK30: Cal. AD 425-546) (Murphy, Gibney, 2021). From this it has been suggested the SK3 was a foundational burial for the cemetery and part of a transitional period between iron age and Christian practices due to being the only burial

containing a grave good of a worked stone with a flat base and conical tip that is similar offer artefacts found from other iron age sites and believed to be gaming pieces (Murphy, Gibney, 2021; Johnson, 2012; Rafferty, 1969), while the later dates suggest the cemetery was abandoned by the middle of the 6th century AD.

There were also the remnants of three ring-ditches (Ring-ditch #1, #2, #3) contained within the site and recorded as C07, C11 and C72 (Murphy, Gibney, 2021). Only one ring-ditch (Ring-ditch #2, C11) was complete (Murphy, Gibney, 2021). The site also a contained number of other archaeological features such as 11 pits (C34, C41, C52, C53, C54, C55, C61, C67, C69, C144), 3 Kilns (C30, C60, 71) and 3 post holes (C31, C43, C45) (Murphy, Gibney 2021). Most of these features were situated in an area approximately measuring 14m east-west and 8m north-south at the Northern side of the site and therefore it is proposed that they are likely to represent a different phase of activity on the site than that of the burials (Murphy, Gibney, 2021).

Parknahown 5, Co. Laois

Parknahown 5, Contract 1, Co. Laois was a site excavated as part of the M7 Portlaoise-Castletown/M8 Portlaoise-Cullahill Motorway Scheme. The site was situated south-west of Cullahill village, south of the River Goul and north of Cullahill Lane and is located between Chainage 11500 and 12100 of the proposed scheme in the townland of Parknahown within the Parish of Aghmacart (Irish National Grid Co-ordinates 234225, 174183) (see Figures 1, 28, and 29) (O'Neill, 2009).

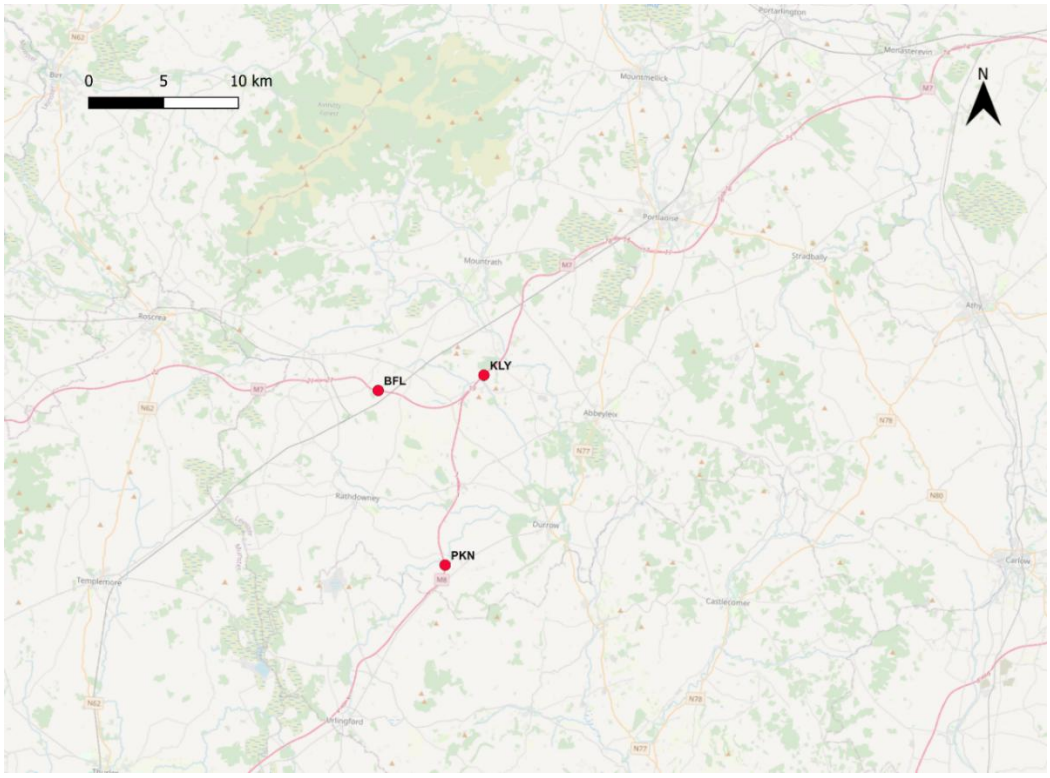

Figure 28: map showing the regional location of the sites from Co. Laois used in the study. PKN= Parknahown 5, KLY= Killieany 1, BFL= Bushfield/Lismore

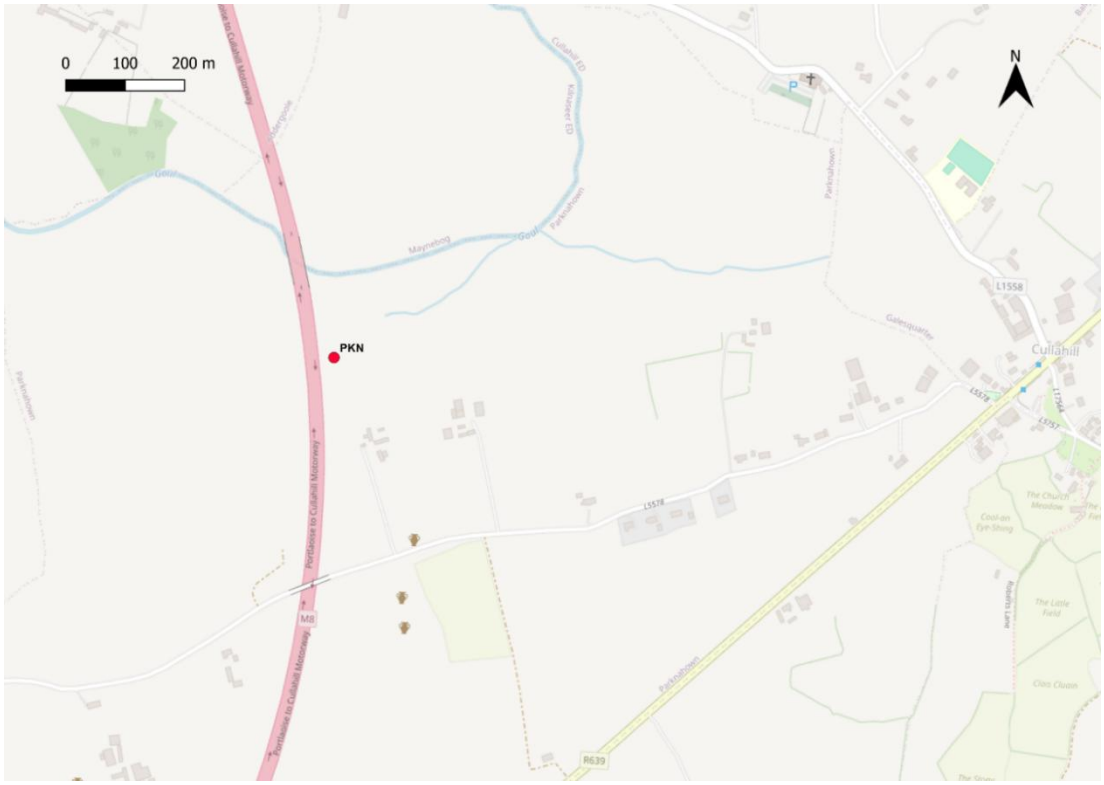

Figure 29: map detail showing the location of Parknahown 5 (PKN)

The Townland of Parknahown is located on low ground that slopes up towards Cullahill Mountain which is south-east, and it is c.1km north of the boundary between co. Laois and co. Kilkenny (O'Neill, 2009). The site, although originally in the Barony of Upper Ossory, is located in the Barony of Clarmallagh and would have been in the north of Osraige Territory (O'Neill, 2009).

The site stratigraphically had two periods, Period I had two phases and Period II had three phases (O'Neill, 2009). Period I was Bronze Age with phases as follows: Phase 1 consisted of the Early Bronze Age initial clearance of the site and cutting of the Trough (F007, F362), related pits and appearance of burnt spreads (F005, F361) and Early Bronze Age Pits and Post-holes in the south-eastern extent of Field 32; Phase 2 consisted of Late Bronze Age pits at the southern extent of Field 32 (O'Neill, 2009). Period II was Early Medieval with phases as follows: Phase 1 was initial Early Medieval activity; enclosures F106 and F156 with re-cut F1452, ditch cuts (F264, F134 and F160), deposit F257, Boundary F902 and initial cemetery activity and burials in 400-650 AD; Phase 2 consisted of burials and double ditch (F29, F24), the use of the enclosure F156, a horse burial, circular structure and its internal features from 650-850AD; Phase 3 consisted of burials and re-cut F391 in ditch F156 with industrial activity, and outer cemetery enclosure F1384 in 850-1300AD (O'Neill, 2009).

Finds associated with the Early Bronze Age include animal bone in upper fill F009 of trough F007 with the fill radiocarbon dated to 2470-2270BC, animal bone and a flint scraper found in a fulacht spread F005 and on the southern extent of the site one post-hole (F1357) had a fill (F1356) that

contained two shards of Neolithic Grooved Ware and a flint blade while another post-hole (F1359) had a fill (F1358) which contained a flint scraper (O'Neill, 2009).

Excavation of the Early Medieval cemetery uncovered 425 individuals and 800 litres of disarticulated human bone (O'Neill, 2009). The individuals buried at Parknahown 5 consisted of 57 males, 96 Females, 61 unsexed adults and 211 non-adults (O'Neill, 2009; Keating, 2008). The earliest inhumations were dated to the fifth and sixth centuries AD while the most recent of the burials dated was a male who had been buried east-west rather than west-east in accordance with Christian practice dated to cal. 1020-1210 AD (O'Neill, 2009).

Due to the prolonged use and small size of the cemetery there was a great deal of disturbance between burials with later burials truncating earlier ones and as such a full matrix across the cemetery was not possible, instead the cemetery was divided into quadrants A-D and phased in levels according to burials relationships to each other and other depositional events (O'Neill, 2009). Eight phases were identified in this manner and the topsoil above the burial ground F001 contained a number of finds including large number of Neolithic flint finds, iron nails and tools, corroded iron fragments, whetstones, a blue glass bead, quartz stones and sherds of medieval pottery which were presumed to come from disturbed deposits (O'Neill, 2009). This also suggests the burial area had previously seen Neolithic activity due to the flint finds (O'Neill, 2009).

There was a lack of settlement except for remains of a structure represented by two curvilinear slot ditches F282-F283 dated to Cal. 660-870 AD and three associated post-holes (O'Neill, 2009). It is unlikely this was used for domestic dwelling but rather food preparation or hide skinning (O'Neill, 2009).

Animal bone found on the sites comprised of cattle (58%), pig (14.2%), sheep (14.1%) horse (4.8%), dog (3.7%), cat (1.1%) and domestic fowl and wild birds (0.6%) (O'Neill, 2009; Tommasino, 2008). It is suggested that the high proportion of cattle means the site was high status (O'Neill, 2009).

A number of finds that could be considered high status were found at the site. The most significant of these was a zoomorphic copper-alloy Anglo-Saxon pen-annular brooch that is similar to a brooch found with moulds at Clogh, Co. Antrim, and it is unknown whether this was imported or produced in Ireland (O'Neill, 2009). Other finds included a decorated antler comb that is dated to the sixth century and has significant characteristics seen in combs from Lagore, Cloghmore Cave in Co. Kerry and Rathinaun crannog in Co. Sligo, a highly decorated cylindrical bronze bead with decoration being similar to a Sutton Hoo hanging bowl escutcheon from the later sixth century AD and a similar object being found in Ballinderry crannog and a copper-alloy enamelled mount (O'Neill, 2009).

Killeany 1, Co. Laois

Killeany 1, Contract 3, Co. Laois was a site excavated as part of the M7 Portlaoise-Castletown/M8 Portlaoise-Cullahill Motorway Scheme and located in the townland of Killeany and in the parish of Clonenagh and

Clonagheen that is between Chainage 21960 and 23230 of the proposed scheme (Irish National Grid Co-ordinates 235926, 187024) (Wiggins and Kane, 2009) (see Figures 1, 28 and 30). The site is around a low hill approximately 150m north-east of the river Gully and north of Gorthnacleae (Wiggins and Kane, 2009). The land immediately north and north-east was poor drained bogland and forestland while the land in the north-west, west and south was bounded by a section of the river Gully that is prone to flooding and the floodplain visible as a yellow marshy grassland pasture (Wiggans and Kane, 2009).

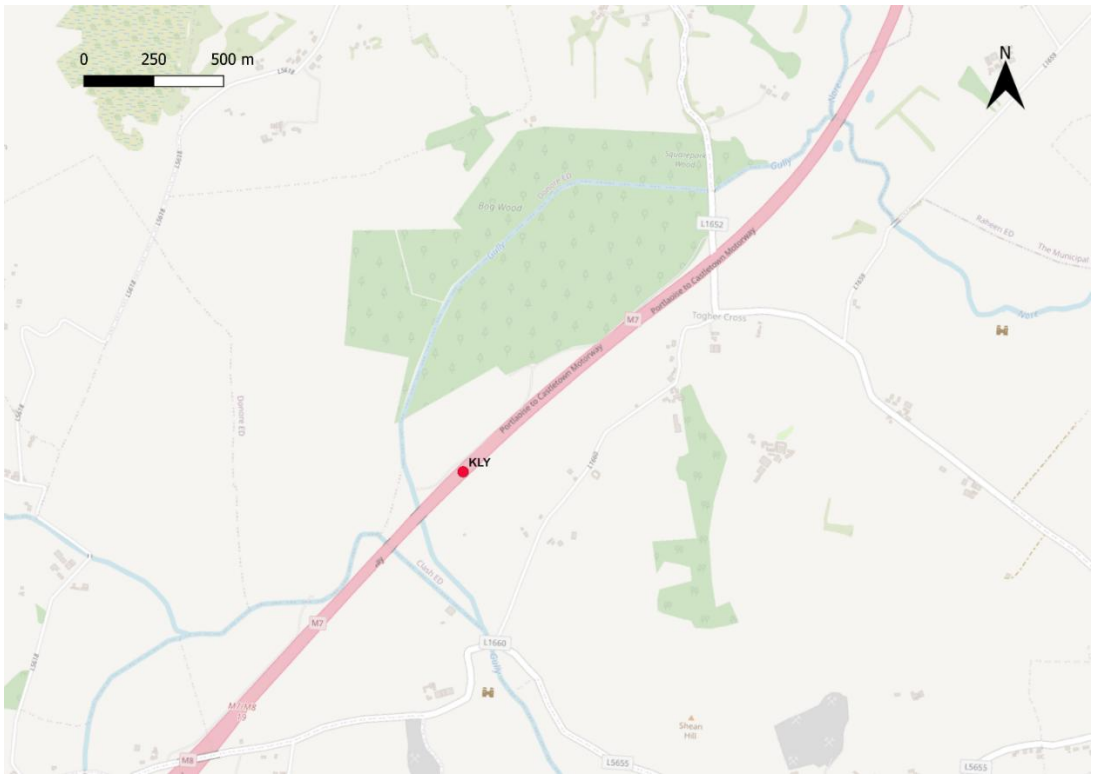

Figure 30: map detail showing the location of Killeany 1 (KLY)

The site was divided into eight zones, zones A-H, and all but two of these (zones C and F) were traversed by the outer ditch of the enclosure which was the largest individual feature of the site (Wiggins and Kane, 2009). This outer ditch was curvilinear in plan with an overall excavated length of 180m

with a width of typically 3m and a depth of typically 1.5m and contained a total of 97 separate deposits (20 primary fills, 62 middle fills and 15 upper fills) (Wiggins and Kane 2009).

Overall, the site was split stratigraphically into three periods each separated into two phases (Wiggins and Kane, 2009) Period I was Prehistoric with Phase 1 being the cutting of the original features, and Phase 2 the abandonment of the site; Period II was Early Medieval with Phase 1 was the reoccupation of the site and recutting of new features, and Phase 2 the abandonment of the site; Period III was post-medieval with Phase 1 being digging of agricultural features and Phase 2 being the formation of topsoil (Wiggins and Kane, 2009)

Phase 1 is represented by two ditches (Ditches 3 and 4) and two slot trenches (structures 1 and 2) with their associated post-holes and other features (Wiggins, Kane, 2009). A number of features produced radiocarbon dates that were from the mid-late Bronze Age including charcoal from the fill of Ditch 3 was dated to cal. 1130-910 BC and charcoal from the fill of post-hole F1020 dated to cal. 1220-990 BC and fill of pit F079 associated with Structure dated to 1380-1120 BC (Wiggins and Kane, 2009).

Part of the site was a cemetery with 67 burials discovered within the limits of the inner enclosure in Zone C a further burial (Burial 68) discovered in the north-east terminal of the outer ditch in zone D, and 92 separate amounts of disarticulated human bone (Wiggins and Kane, 2009). These burials were divided into four levels (Levels 1 -4): Level 1 (Burials 1-45 consisted of burials that either had no stratigraphic relationship to other burials, were

truncated by a level 2 burial or impacted Ditch 2; Level 2 burials (Burials 46-64) truncated Level 1 burials; Level 3 (Burials 65 and 66) truncated Level 2 burials: Level 4 consisted of a single burial (Burial 67) that truncates one Level 3 burial (Wiggins and Kane, 2009).

Radiocarbon dates were obtained for eleven of the Level 1 burials, one Level 2 burial and the Level 4 burial (Wiggins and Kane, 2009). Burial 36/SK094 was the earliest dated individual on the site and the earliest of four stratigraphically related skeletons (Level 2 Burial 54/SK088, Level 3 Burial 65/SK051 and Level 4 Burial 67/SK042) with a date of cal. 420-590AD, Burial 1/SK001 was the most recent dated Level 1 burial with a date of cal. 800-1000 AD, Burial 64/SK163 was dated to cal. 550-660AD which was earlier than most Level 1 burials and Burial 67/SK042 was dated to cal. 680-880AD (Wiggins and Kane, 2009).

Burials were in extended supine position in shallow earth-cut graves that were generally east-west alignment with the head orientated at the south-west end (Wiggins and Kane, 2009). Three of the burials included grave goods: a forty-four-piece, polished bone disc paternoster was found with Burial 1/ SK001, a bead- like component of an antler gaming piece was found with Burial 19/SK098 and unidentified corroded metal disc was found with Burial 64/SK193 (Wiggins and Kane, 2009). The presence of grave goods and a double burial (Burials 56 and 57/SK 101 and SK125) are suggested to imply pagan practices are still included and not all burial practices were strictly Christian practices at Killeany 1 (Wiggins and Kane, 2009).

Killeany 1 also shows evidence of agricultural use through the finds of an iron ploughshare, 6 corn drying kilns, charred grain remains in soil samples from kilns and pits and animal bone (Wiggins and Kane, 2009). Macrofossil evidence shows that Barley was the pre-eminent crop, although wheat was recorded frequently in low proportions, both cultivated and wild oats were found and rye species were present but in very low numbers which is in keeping with early medieval sites in Ireland (Wiggins and Kane, 2009). Radiocarbon dates for features that contained grains include Pit F296 dated to cal.530-650 AD and Pit F201 dated to cal. 430-620 AD (Wiggins and Kane, 2009).

Cattle was the most common species found at the site, representing over 60% of the identified specimens and 37.5% of the minimum number of individuals, followed by sheep representing 13.2% of identified specimens and 9.4% of the minimum number of individuals and third being horse representing 12.4% of identified specimens and 9.4% of the minimum number of individuals (Wiggins and Kane, 2009). It has been suggested sheep and cattle were bred, slaughtered, consumed and disposed of at the site whereas horses were used as work animals and died of natural causes (Wiggins, Kane, 2009). One cattle metacarpal was dated to cal. 970-1160AD (Wiggins and Kane, 2009).

There were also signs of metalworking on the site. Ferrous metal objects were the most presence type of object in the finds assemblage and included iron knives, iron nails, two curved iron objects and iron fragments (Wiggins, and Kane, 2009). It is suggested that these items were likely for agricultural use and may have utilised the iron-rich bogland as a resource (Wiggins and

Kane, 2009). While there was no *in situ* evidence of smithing there was indirect evidence of small-scale smithing from furnace bottom slag pieces and there is iron slag is well represented across the site (Wiggins and Kane, 2009).

It is suggested that the early Medieval abandonment of the site could potentially be due to political unrest (Wiggins and Kane, 2009). The region saw political unrest in the Early Medieval with the decline of the ruling Laígis in West Laois alongside the rise of the Osraige and Viking raids into Laois that started in 831 AD and intensified in the 850s and 860s AD under a Viking leader named Rudolph (Wiggins and Kane, 2009). This is significant as Killeany 1's cemetery being close to a territorial boundary may have been used as a territorial marker as in pre-Christian practice (Wiggins and Kane, 2009).

Bushfield/Lismore 1, Co. Laois

Bushfield/Lismore, Contract 2, Co. Laois was a site excavated as part of the M7 Portlaoise-Castletown/M8 Portlaoise-Cullahill Motorway Scheme and located West of the townland of Kilcotton, c.4km south-east of Borris-in-Ossory and c. 11km south-west of Mountrath, Co. Laois between the Chainage 13500 and 13460 of the proposed scheme in the townland of Bushfield or Maghernaskeagh and Lismore within the Parish of Agherboe (Irish National Grid Co-ordinates 228765, 185508)(Wiggins and Kane, 2009B) (see Figures 1, 28 and 31). The site enclosure is located on low-lying land and it not located near to any major rivers or lakes therefore the location does not seem to be dictated by a need for a wide view, a prominent

position or proximity to a water source with the nearest part of the River Nore is c.3.5km to the north-west and some n arrow tributaries of the River Quinn to the south-west and prominent ground at Knockseera Hill to the east or a Knockaroe to the north (Wiggins and Kane, 2009B).

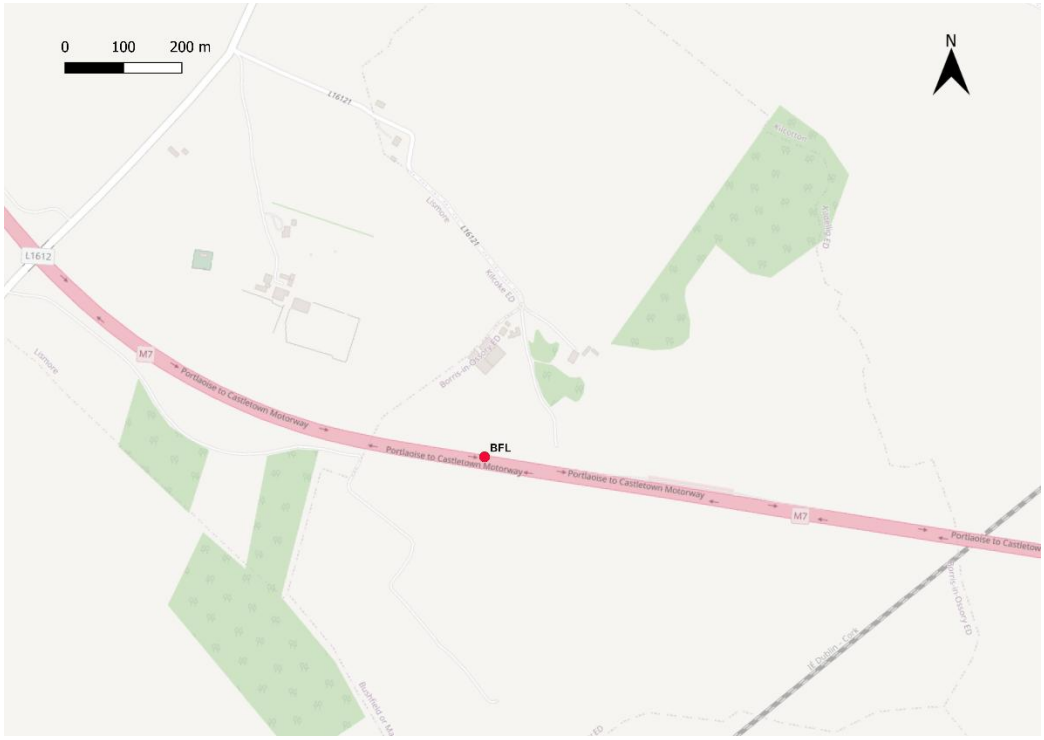

Figure 31: map detail showing the location of the Bushfield/Lismore site (BFL)

The site stratigraphically had four periods, the first two of which were single phased and the second two of which were divided into two phases each (Wiggins and Kane, 2009B). The periods and phases are as follows: Period I was Early Bronze Age with Phase 1 consisting of burnt spreads; Period II was Iron Age with Phase 1 consisting of metalworking activity; Period III was Early Medieval with Phase 1 being the enclosed settlement, metalworking and burials and Phase 2 is the development of the south-quadrant; Period IV is Post-Medieval with Phase 1 being the pre-levelling of the monument and Phase 2 being the post-levelling of the monument (Wiggins and Kane, 2009B).

The Early Bronze Age activity at the site is limited to Zone F located c.60m north-west of the enclosure (Wiggins and Kane, 2009B). Three burnt spreads were recorded (F854, F856/859 and F858) each was a single deposit with cuts (F854, F853, and F857) measuring between 7.05-13m x 0.07-0.15m (Wiggins and Kane, 2009B). Below the burnt spreads were three sub-rectangular unlined troughs (F860, F853, and F854) and other troughs were discovered in the zone (F862 and F864) (Wiggins and Kane, 2009B). A sample of hazel charcoal from fill F865 of trough F864 was radiocarbon dated to cal. 2350-2130 BC (Wiggins and Kane, 2009B).

Iron Age activity was evidenced by the presence of five 'slagpit' furnaces (F086, F088, F090, F092, F095) in 3 x 3m area in Zone A and Pit F195 in Zone C (Wiggins and Kane, 2009B). Fill F194 of Pit F195 was radiocarbon dated to cal. 260-50 BC with 69.8% probability and fill F091 of slagpit furnace F090 was radiocarbon dated to cal. 90 BC – 80 AD (95.4% probability) (Wiggins and Kane, 2009B)

A cemetery was one of the most significant elements of the archaeology at the site, which located in the north-east quadrant, Zone C, with graves contained in an area measuring c.27m east-west by 17m north-south (Wiggins and Kane, 2009B). The cemetery contained 60 burials, 57 of which were adult and 3 were non-adult, that were mainly laid in an extended position and orientated east-west with skulls placed on the west side facing east in simple earth-cut, unlined graves that tapered at the end (Wiggins and Kane, 2009B). Radiocarbon dates were obtained from four individuals and all returned dates from the 6th-7th centuries (Group 1 burial SK 77 dated to cal. 550-650 AD, Level 2 Group 1 burial SK65 dated to cal. 550-670 AD,

Group 2 burial SK07 dated to cal. 580-660 AD and Group 4 burial SK79 dated to cal. 540-645 AD) (Wiggins and Kane, 2009B).

Other than the cemetery, the Early Medieval Phase 1 was evidenced by the F003 ovoid ditch that was continuous within the excavation limits except for a 5m north-facing entrance (Wiggins and Kane, 2009B). The ditch on the Lismore side (Zones A and B) had a length of 78m west of the entrance and 5m east of the entrance while the Bushfield side (Zones C,D and E) had a length of 67m and there was 31m outside the northern CPO fence and 87m outside the southern CPO fence (Wiggins, Kane, 2009B). Due to this ditch, the enclosure can be considered a univallate ringfort which is typical of the Early Medieval (Wiggins and Kane, 2009B).

There are also a number of pits and post-holes associated with the Early Medieval activity (Wiggins and Kane, 2009B). Radiocarbon dates from the site included animal bone from one the eight fills (F072) from pit F050 dated to cal. 590-720AD, hazel charcoal from fill F174 of pit F175 was dated to cal. 420-590AD, ash charcoal from fill F186 of pit F187 was dated to cal. 570-665 and ash charcoal from fill F164 from a ring-gully feature in Zone D dated to cal. 420-600 AD (Wiggins and Kane, 2009B).

The finds assemblage from the site was poor which is typical of ringforts (Wiggins and Kane, 2009B). Some notable items include a fine glass ring from a fill of the enclosure ditch in Zone B, iron shank of a ringed pin that is early medieval in date found in a fill of a pit in Zone D, two sharpening stones from the large pit F050 in Zone B and an iron knife from the fill of a pit in Zone C (Wiggins and Kane, 2009B).

Summary

Data were collected in a total of 570 individuals from 17 collections. These collections were from four regions: four were from England; five were from Wales; four were from Scotland; four were from Ireland. These collections were from a range of periods between the Neolithic and Medieval periods: four were from the Medieval; seven were from the Early Medieval; one was from the Roman period; one was from the Bronze Age; four were from the Neolithic.

Chapter 5: Methods

This chapter describes the methods that were used in this study for the data collection and statistical analyses, as well as the rationale for their use.

Data Collection

Individuals from each sample site were examined for observable non-metric crown and root traits (see Table 1 for total individuals scored in each sample). The standardised ASUDAS system was used to collect the data. Thirty-six traits, based on Irish (1993) (see Appendix I for trait descriptions) were used in this analysis and have been successfully used to compare the biological affinities between populations in previous studies (Anctil 2016, 2020; Coppa et al., 1998, 2007; Cucina et al., 1999; Hanihara, 2008; Irish, 1993, 1997, 2006, 2008, 2010, 2016; Irish and Guatelli-Steinberg, 2003 among others).

The non-metric traits were scored using the ASUDAS scoring procedures and trait breakpoints that were established in Turner et al. (1991) and expanded in Scott and Irish (2017) (Appendix I). The scores for the occurrences of each crown and root trait were recorded on ASUDAS scoring sheets (Appendix II).

As traits can have varying degrees of expression ‘breakpoints’ are used to dichotomise the data. The term ‘breakpoint’ denotes the grade at or above which a trait can be confidently defined as being expressed in a percentage of a sample’s individual, e.g. 2+ for shovelling (see Appendix I) (Scott, Maier and Heim, 2015).

The traits used in the analysis are either not or minimally sexually dimorphic, so the sexes were pooled according to standard procedure (Scott and Irish, 2017; Turner et al., 1991). As the ASUDAS system and breakpoints outlined by Turner et al. (1991) were based on permanent dentition, only individuals for which permanent teeth were present were recorded in this analysis, including sub-adults with mixed and/or visible unerupted permanent teeth. As a result, samples were not composed of individuals with complete dentitions and traits were scored and recorded based on the dentition available.

Individuals with fewer teeth were included as the number of observable traits that could be recorded were similar individuals with more teeth due to differences in tooth preservation, wear and pathologies. When only one side was present, it was recorded and assumed to be the highest degree of expression to maximise sample size; when present both antimeres were recorded and the side with the highest degree expression was counted to allow for maximum genetic potential (Scott and Irish, 2017; Turner et al., 1991). Traits were re-scored under the same conditions on non-adjacent days and analysed using Fisher's exact test to assess intra-observer error.

Crown wear can result in a sampling bias in which teeth subjectively deemed too worn are not recorded with the observer assuming the missing data are missing completely at random (MCAR) (Burnett, 2016). Due to this, a tooth with heavy wear may be excluded and recorded as no data when, in some cases, the trait was absent and should have been recorded as a Grade 0 (Burnett, 2016). To help account for the MCAR assumption, any

major differences in wear among samples were acknowledged (Scott and Irish, 2017).

It was determined whether the wear level allowed for trait scoring or if the wear was considered too great. Individuals with severe wear across the majority of the dentition were excluded from the analysis and for those with moderate to severe wear on specific teeth, such as molars, the antimere was scored if it was available.

Quantitative Analysis

The 36 traits were entered into the Statistical Package for Social Sciences, version 29.0.1.0. They were then dichotomised into the categories of present and absent based on each traits' expression threshold according to standard procedure (Scott, 1973; Nichol, 1990; Turner et al. 1991; Irish, 1993). Dichotomised data makes it possible to observe trait frequency differences, removing the issue of different sample sizes (Irish, 2005). It is necessary for this dichotomisation to calculate the inter-phenetic distances using the mean measure of divergence (MMD) distance statistic (Sjøvold, 1977). Dichotomisation can also, beneficially, increase heritability (Stanjowski, et al., 2019).

Principal Components Analysis

Principal components analysis (PCA) is used to edit and remove traits that are problematic before MMD analysis (Irish, 2010). Traits with little or no difference in frequency among the samples, e.g. 0% or 100%, are removed as this can result in negative MMD which provides no discriminatory value (Harris and Sjøvold, 2004). Furthermore, traits that are based on a small

number of observations (<3) are also removed as they are not likely to be representative. The remaining traits were then submitted to PCA to determine which are least and most likely to drive inter-sample variation (Irish, 2010). Any trait that did not receive a loading of at least |0.500| on any component was removed from further analysis.

In PCA, the original correlated variables are linearly transformed into a smaller set of uncorrelated compound variables (Abdi and Williams, 2010; Jackson, 2005). Reducing the dimensionality produces fewer linearly uncorrelated variables or principal components (Joliffe and Cadima, 2016). The first component explains the greatest variability, then the second component etc., to retain most information while remaining mutually uncorrelated and orthogonal (Joliffe and Cadima, 2010; Rasmus and Smilde, 2014)

Correlations (loadings) between original and principal components are calculated (Abdi and Williams, 2010; Rasmus and Smilde, 2014). Samples are plotted to visualise the data for interpretation of their differences and similarities and assess whether they can be grouped (Abdi and Williams, 2010; Irish, 2010; Rasmus and Smilde, 2014).

PCA was selected because specific dental traits responsible for inter-sample variation can be identified. Inter-sample distances should be based on as many traits as possible, however, these traits should not be highly correlated with each other or they may lead to erroneous results (Irish, 2010; Sjøvold, 1977). Undichotomised ASUDAS data were submitted to Kendall's tau-b correlation coefficient to determine inter-trait correlation. Kendall’s tau-b

was selected because it is more conservative than other tests such as a chi-square test of proportions, and rank grades more likely to identify inter-trait correlations, where more traits may be removed (Irish, 2010). Traits that are strongly correlated (Kendall's tau-b value (tb) ≥0.5) were removed from further analysis.

Mean Measure of Divergence (MMD)

The MMD, derived by CAB Smith, is a distance statistic used in many biological affinity studies (Anctil, 2016; 2020; Berry and Berry, 1967; Irish, 1993; 2005; 2006; 2008; Irish and Guatelli-Steinberg, 2003). It is a dissimilarity measure in which high values equal greater phenetic difference and low values greater affinity.

Based on the assumption that phenetic similarity equals genetic affinity, CAB Smith MMD distance statistic with Freeman-Tukey angular transformation was used. This corrects for low (<0.05) and high (more than 0.95) trait frequencies and low samples (Freeman and Tukey 1950; Irish 2010). The MMD formula from Harris and Sjøvold (2004) with Freeman and Tukey angular transformation (1950) incorporated is:

$$MMD = \frac{\sum_{i=1}^{r} (\theta_{1i} - \theta_{2i}) - \left(1 / \left(n_{1i} + {}^{1}/_{2}\right) + 1 / \left(n_{2i} + {}^{1}/_{2}\right)\right)}{r}$$

The parameters for this formula are as follows:

r is the number of uncorrelated traits

θ is the angular transformation and, here, $\theta = ½ \sin^{-1}(1-(2m)/(n+1)) + ½ \sin^{-1}(1-2(m+1)/(n+1))$

m is the number of positive observations of trait "*i*"

n is the number of individuals score for trait "*i"*

There are several benefits to using MMD instead of using other statistics to justify its use in this study. Firstly, as it uses group level trait frequencies, traits with missing data can be used without adverse effects unlike other statistics like Mahalanobis D^2 (Irish, 2010). Secondly, traits with little or no contributory information can be removed without biasing MMD values (Irish, 2010). Lastly, it has been shown to produce strong correlations to geographical data (Irish, 2010).

The MMD statistic was run in R, version 4.4.0, using the script written by Sołtysiak (2011); it produces a distance matrix that identifies if two groups are phenetically similar (Harris and Sjøvold, 2004). The script uses two Z scores, counted as MMD/SD, to calculate the statistical significance for each MMD value (Sołtysiak, 2011). The significance was set at the 0.025 alpha level (Sjøvold, 1977).

Multidimensional Scaling

The relationships between the samples identified by the MMD were illustrated using multidimensional scaling (MDS). This method replicates the relationship between samples in the fewest dimensions while optimising goodness of fit and is considered largely unbiased (Cox and Cox, 2001;

Irish, 2010; Kruskal and Wish, 1978) The spatial representation of the sample distribution was created by SPSS 29.0.1.0 procedure Alscal.

Isolation By Distance

Isolation by distance is a model commonly used to substantiate genetic and ethnic relationships within and among population. (Kimura and Weiss, 1964; Wright, 1943). In this model, limited dispersal results in genetic differences which are proportional to the geographical distance between populations, assuming genetic affinity is inverse to spatial distance (Kimura and Weiss, 1964; Relethford, 2004; Wright 1943). Migration rate is highest with adjacent population and declines as the distance between populations increase (Kimura and Weiss, 1864; Relethford, 2004).

Correlation in gene frequencies decreases exponentially as a function of the number of geographic steps, referred to as 'stepping stone model' (Kimura and Weiss, 1964). There are three variants: a one, two and three-dimensional models. In the first, each generation can only migrate one step meaning that individuals are only exchanged with an adjacent population (Kimura and Weiss, 1964).

According to Kimura and Weiss (1964) a population exchanges migrants with four surrounding populations in the two-dimensional model. Furthermore, they also state that the number of individuals in the population stays the same in each, but the rate of migration may vary on the x- and y-axes.

Additionally, Kimura and Weiss (1964) state that in three-dimensional model, a cubic array of populations extends to infinity in all directions, and

each population has 6 adjacent populations that they exchange migrants with each generation. They also note that genetic variation drops off more quickly with increasing geographical distance in the three-dimensional model than the other models.

As migration routes are generally not known, inter-population straight-line distances are commonly used (Irish et al., 2018; Relethford, 2004). These are approximations and do not reflect reality on the landscape. Due to the use of straight-line distances in this study, the linear one-dimensional stepping stone model is used. The geographic distance matrix was produced using The Geographic Distance Matrix Generator (Ersts, 2014).

Mantel Test

One common method of assessing the relationship between a phenetic or genetic distance and a geographical matrix is the Mantel's permutation test (Dutilleul et al., 2000; Guillot and Rousset, 2013; Smouse et al, 1986). This test makes two assumptions: firstly, the relationships between the distance are linear; secondly, the small values in the of the first set of distances correspond to the small values of the second set, while the large values of the first set correspond to the large values of the second set (Legendre, Fortin and Borcard, 2015). The resulting values that are close to 1 indicate that as the geographical distance between samples increases so do the genetic distances, values close to -1 indicate the opposite pattern and values close to 0 indicate no relationship between geographical and genetic distances (Diniz-Filho et al., 2013).

The correlations were performed on Past 4.17. The standardised Mantel test formula (Mantel, 1967; Diniz-Filho, 2013) is as follows:

$$Z_N = \frac{\sum_{i=1}^{n}\sum_{j=1}^{n}\left(g_{ij} - \overline{\mathbf{G}}\right) \times \left(d_{ij} \times \overline{\mathbf{D}}\right)}{\mathrm{var}(\mathbf{G})^{1/2} \times \mathrm{var}(\mathbf{D})^{1/2}}$$

In this formula, Z_N is the Pearson correlation *r* between the standardised elements of the genetic and distances matrices (Diniz-Filho et al., 2013) The parameters are as follows:

i= population 1

j= population 2

g_{ij}= the genetic distance between populations *i* and *j*

d_{ij}= the geographical distance between populations *i* and *j*

$\overline{\boldsymbol{G}}$= the mean of the genetic distance matrix

$\overline{\mathbf{D}}$= the mean of the geographic distance matrix

var (**G**) is the variance of the genetic distance matrix

var (**D**) is the variance of the geographic distance matrix (Diniz-Filho et al., 2013).

The test has been criticised regarding its power and Type I error rate (Guillot and Rousset, 2013; Legendre, Fortin and Borcard, 2015). Despite this, the test has been showed to yield results that are comparable to alternative methods (Diniz-Filho, 2013).

Additional Analyses

Finally, the samples from this study will be compared with data from global populations for 22 traits (16 crown and 6 root). These global population trait data have been used in previous analyses and can be found in Appendix A of Scott and Turner (1997).

First, the relationships between the study samples and global populations will be analysed by generating an MMD matrix in R and visualised using the MDS SPSS procedure ALSCAL, following the approach used in earlier analyses described in this chapter.

Second, a series of hi–lo charts were produced, in which trait frequency is represented by a vertical bar, with horizontal bars extending ±2 standard errors. These graphs are similar to those created for Scott and Turner's (1997) analysis of global populations. To facilitate comparison, some traits have been converted from absence frequencies to presence frequencies by subtracting the absence frequency from 1.000, as described in the prior study. These traits include the 3-cusped molar, 4-cusped molar, and 1-rooted molar. Where possible, trait names have been standardised to match those used in this study; for example, the 3-cusped molar is referred to as hypocone UM2, the 4-cusped molar as cusp number LM2, and the 1-rooted molar as root number LM2.

Summary

PCA, MMD, MDS and IBD will be used to investigate the relationships between the samples. These methods have been in previous biological

affinities studies using dental non-metric data and so shall be comparable to other works.

Chapter 6: Results

The results reported in this chapter were produced using the methods outlined in the previous chapter. Firstly, results of the intra-observer tests shall be reported, followed by those of the biodistance study (trait frequencies, PCA, Kendall's tau-b, MMD and MDS results) and, finally, the Mantel tests.

Observer Error

The results of the Fisher's exact tests found no statistically significant differences for any trait (p=0.05). The p values ranged between 0.6699-1.00 with majority of the traits (out of 36) producing a p value of 1.00 (see Appendix III). This indicates that the ASUDAS system is being applied consistently by the author.

Additionally, the author was provided training in the ASUDAS scoring procedure by Prof. Irish. During this training, inter-observer error was assessed and found to be random and non-directional.

Trait Numbers and Frequencies

Traits were dichotomised into "present" and "absent" using predefined breakpoints. The percentages of individuals exhibiting each trait, along with the total number of individuals scored, are presented in Table 2.

Several traits display comparable frequencies across samples, suggesting a degree of homogeneity. Notable trends include a complete absence of the 3-rooted LM1 and similarly for winging UI1, root number LM2, and lingual cusp LP2.

St. Owen’s Church, Gloucester (GLC) exhibits a low frequency of palatine torus. While this frequency is low overall, it is notably higher relative to other samples, where the trait is entirely absent.

Similarly, double shovelling of UI1 is absent in most samples (15 out of 17), but appears at low frequencies in Chapel House Farm, Poulton (POU), and St. Owen’s Church, Gloucester (GLC)—both medieval English sites. This trend is mirrored for odontome P1–P2 and deflecting wrinkle LM1.

Figure 32: Palatine Torus present in an individual (GLC-0173) from St Owen's Church, Gloucester

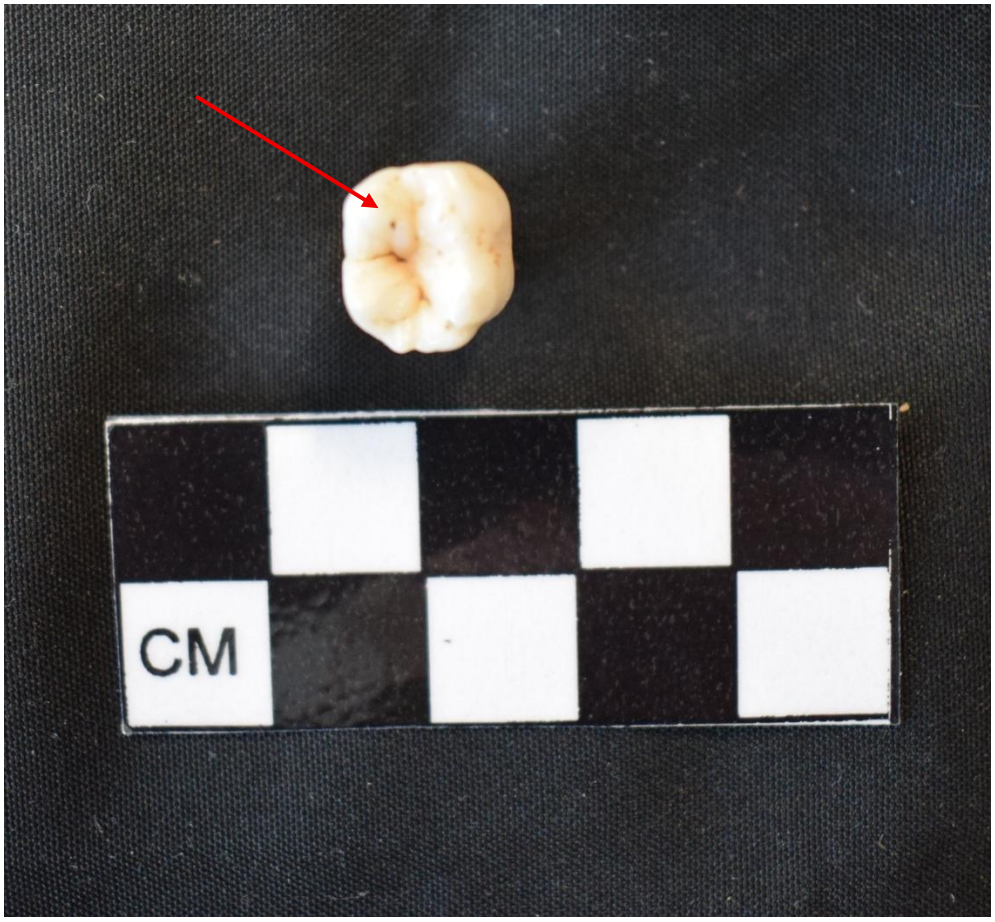

Figure 33: Deflecting Wrinkle (Grade 3) expressed on the lower first molar of an individual from St Owen's Church, Gloucester (GLC-0097)

Samples from Scotland—Strath Glebe (STG), Distillery Cave (DIS), Raschoille Cave (RAS), and Whithorn Priory (WHIT)—show relatively higher frequencies of shovelling UI1 compared to other regions, which have comparable lower frequencies. However, the small number of individuals scored in these samples may exaggerate the observed frequencies.

The Irish populations—Southgreen (SGR), Parknahown 5 (PKN), Killeany 1 (KLY), and Bushfield/Lismore (BFL)—are notable for high frequencies of mandibular torus, which is otherwise absent across other populations except for a low occurrence at Norton Priory (NOR). Additionally, Irish populations show distinctively low frequencies of certain traits: labial curvature UI1 is low in Killeany 1 (KLY) and absent in both Southgreen

(SGR) and Bushfield/Lismore (BFL); hypocone UM2 appears at lower frequencies in Southgreen (SGR) and Bushfield/Lismore (BFL); and mid-line diastema frequencies are comparatively low across all Irish samples except Bushfield (BFL).

Figure 34: Shovelling (Grade 2) expressed on both central incisors from an individual from Poulton, Cheshire (POU-617)

Carabelli's cusp UM1 generally occurs at higher frequencies in British samples than in Irish ones, though exceptions include low frequencies at London Road, Gloucester (GLRC) and Tinkinswood (TKW). Conversely, cusp 7 is mostly absent in British samples except for GLC and TKW, where the frequencies are comparable to those in Irish samples such as Southgreen (SGR) and Parknahown 5 (PKN).

Figure 35: Bilateral expression of Carabelli's cusp on the upper first molars of an individual from St. Owen's Church, Gloucester (GLC-0053)

Figure 36: Bilateral expression of cusp 7 on the first lower molars of an individual from St Owen's Gloucester (GLC-0107)

Figure 37: bilateral expression of torsomolar angle of the lower third molars of an individual from St. Owen's Church, Gloucester (GLC-0028). Both rotated lingually.

Culver Hole (CLV), Tinkinswood (TKW), Distillery Cave (DIS), and Raschoille Cave (RAS) frequently exhibit extreme trait frequencies (0% or 100%). As noted with shovelling UI1, these values may be skewed due to small sample sizes. Torsomolar angle LM3 exemplifies this, with samples based on small counts showing complete absence, while those with larger samples have more moderate frequencies.

Overall, the samples trend towards dentitions that are morphologically simple and mass-reduced—for example, low frequencies of cusp number LM1. Mass-additive traits that do occur at high frequencies in some samples, such as Carabelli's cusp UM1 and mandibular torus, are generally associated with European and high-latitude populations (Scott and Irish, 2017).

Principal Components Analysis (PCA)

As previously mentioned, samples that have low sizes were removed from any further analysis. These samples were Culver Hole (CLV), Tinkinswood (TKW), Distillery Cave (DIS) and Raschoille Cave (RAS).

Prior to MMD analysis, traits were edited to increase statistical power by removal of non-contributary traits. In the first stage of the trait editing, those traits with little to no difference among samples (traits at/near 100% or 0% across samples) were identified and removed from further analysis. These traits included Winging UI1, palatine torus, double shovelling UI1, odontome P1-P2, mid-line diastema UI1, and root number LM1. This reduced the number of traits to 30.

Table 2: Trait percentages of numbers of individuals scored by sample. NOR= Norton Priory, Runcorn, POU= Chapel House Farm, Poulton, GLC= St. Owen's Church Gloucester, GLRC= London Road, Gloucester, LDG= Great House Farm, Llandough, ATE= site 92, Atlantic Trading Estate, Barry, BRS= Brownslade Barrow, Castlemartin, CLV= Culver Hole, Llangennith, TKW= Tinkinswood Burial Chamber, St. Nicholas, STG= Strath Glebe chambered cairn, Skye, DIS= Distillery Cave, Oban, RAS= Raschoille Cave, Oban, WHIT= Whithorn Priory, Dumfries and Galloway, SGR= Southgreen, Kildare, PKN= Parknahown 5, Co. Laois, KLY= Killeany 1, Co. Laois, BFL= Bushfield/Lismore, Co. Laois.

TRAIT		NOR	POU	GLC	GLRC	LDG	ATE	BRS	CLV	TKW	STG	DIS	RAS	WHIT	SGR	PKN	KLY	BFL
WINGING UI1 (+= ASU 1)	**%**	9.09	13.33	11.76	0.00	0.00	7.69	0.00	0.00	0.00	0.00	0.00	0.00	0.00	0.00	0.00	14.29	0.00
	n	44	60	34	7	12	13	14	4	3	1	3	2	8	10	12	7	1
LABIAL CURVATURE UI1 (+=ASU 2-4)	**%**	25.00	20.41	16.67	13.79	35.29	26.67	50	-	-	0	100	0	33.33	0	30	7.69	0
	n	28	49	30	29	17	15	8	0	0	9	1	2	9	12	20	13	9
PALATINE TORUS (+= ASU 2-3)	**%**	0.00	0.00	3.23	0.00	0.00	0.00	0.00	0.00	0.00	0.00	0.00	0.00	0.00	0.00	0.00	0.00	0.00
	n	36	49	31	5	11	15	10	3	5	1	2	4	8	12	12	7	4
SHOVELLING UI1 (+= ASU 2-6)	**%**	5.26	9.52	25.00	0.00	7.69	8.33	16.67	-	-	44.44	100	50	33.33	12.50	25.00	0.00	0.00
	n	19	42	28	16	13	12	6	0	0	9	1	2	9	8	12	4	3
DOUBLE SHOVELLING UI1(+= ASU 2-6)	**%**	0.00	2	3.13	0.00	0.00	0.00	0.00	-	-	0.00	0.00	0.00	0.00	0.00	0.00	0.00	0.00
	n	23	50	32	28	18	15	7	0	0	9	1	2	9	8	14	5	5
INTERRUPTION GROOVE UI2 (+=ASU +)	**%**	23.08	33.33	34.78	31.03	23.53	23.81	52.86	-	0.00	14.29	100	100	36.36	7.69	20	18.18	33.33
	n	26	45	23	29	17	21	7	0	3	7	1	1	11	13	15	11	9
TUBERCULUM DENTALE UI2 (+= ASU 2-6)	**%**	36.00	32.50	8.00	0.00	0.00	19.05	28.57	-	33.33	0.00	0.00	0.00	18.18	23.08	33.33	27.27	25.00
	n	25	40	25	31	17	21	7	0	3	7	1	1	11	13	15	11	8
BUSHMAN CANINE UC (+= ASU 1-3)	**%**	0.00	0.00	3.13	9.68	0.00	0.00	0.00	-	0.00	10.00	0.00	0.00	0.00	0.00	5.26	8.33	0.00
	n	31	47	32	31	21	18	12	0	1	10	1	1	12	16	19	12	11
DISTAL ACCESSORY RIDGE UC (+= ASU 2-5)	**%**	16.67	15.38	36.84	42.86	17.65	15.38	11.11	-	0.00	25.00	0.00	100	37.5	22.22	16.67	20.00	11.11
	n	12	26	19	14	17	13	9	0	1	8	1	1	8	9	12	5	9

HYPOCONE UM2 (+= ASU 3-6)	**%**	60.61	52.08	70.59	55.56	66.67	73.68	100	75.00	75.00	100	100	80.00	75.00	36.36	55.00	55.56	40.00
	n	33	48	34	27	21	19	10	4	4	9	3	5	12	11	20	9	20
CUSP 5 UM1 (+= ASU 2-5)	**%**	8.00	10.53	20.00	13.64	0	36.36	12.5	25	25	20	25	16.67	0	28.57	42.86	37.5	21.43
	n	25	38	30	22	12	11	8	4	4	5	4	6	9	7	14	8	14
CARABELLI'S CUSP UM1 (+= ASU 2-7)	**%**	55.56	36.36	54.17	5.26	30.00	62.5	60	50	0.00	40	66.67	50	28.57	25	25	0.00	0.00
	n	18	22	24	19	10	8	5	4	4	5	3	4	7	4	8	1	6
PARASTYLE UM3 (+= ASU 1-5)	**%**	0.00	11.54	0.00	10.53	5.26	0.00	0.00	0.00	0.00	0.00	0.00	0.00	0.00	0.00	5.00	0.00	0.00
	n	13	26	15	19	19	17	7	1	1	1	0	4	10	10	20	9	17
ENAMEL EXTENSION UM1 (+= ASU 1-3)	**%**	2.86	5.13	12.5	3.85	9.09	22.22	0.00	0.00	0.00	0.00	100	16.67	6.25	0.00	0.00	0.00	8.70
	n	35	39	32	26	22	18	10	4	4	5	2	6	16	8	15	7	23
ROOT NUMBER UP1 (+= ASU 2+)	**%**	23.53	34.48	31.25	30.77	28.57	50.00	75.00	50.00	20.00	16.67	0.00	50.00	46.67	12.50	52.63	50.00	30.77
	n	34	29	32	26	21	22	12	2	5	6	1	4	15	8	19	14	13
ROOT NUMBER UM2 (+= ASU 3+)	**%**	65.79	58.33	70.59	69.23	54.17	75.00	62.5	66.67	100	90.00	50.00	100	69.23	54.55	74.07	35.29	40.91
	n	38	36	34	26	24	20	8	3	2	10	2	7	13	11	27	17	22
PEG-REDUCED UI2 (+= ASU P OR R)	**%**	6.90	4.92	6.67	0..00	0.00	0.00	0.00	0.00	0.00	0.00	0.00	0.00	0.00	7.69	0.00	0.00	0.00
	n	29	61	30	26	17	23	11	1	3	4	1	1	12	13	16	15	10
ODONTOME P1-P2 (+= ASU +)	**%**	0.00	1.89	2.00	0.00	0.00	0.00	0.00	0.00	0.00	0.00	0.00	0.00	0.00	0.00	0.00	0.00	0.00
	n	61	53	50	37	36	28	26	13	7	14	4	5	17	16	25	16	24
CONGENITAL ABSENCE UM3 (+= ASU -)	**%**	27.78	27.08	20.00	8.00	0.00	14.29	8.33	0.00	0.00	0.00	-	0.00	8.33	20.00	12.50	18.75	4.76
	n	36	48	30	25	24	21	12	3	3	2	0	6	12	15	24	16	21
MIDLINE DIASTEMA UI1 (+= ASU +≥ 0.5MM)	**%**	52.63	28.81	50.00	40.00	71.43	50.00	71.43	25.00	100	100	100	100	63.64	20.00	20.00	0.00	-
	n	38	59	34	5	7	10	7	4	1	2	2	2	11	10	5	3	0
LINGUAL CUSP LP2 (+= ASU 2-9)	**%**	92.68	60.00	93.94	100	93.55	85.71	87.5	100	80.00	100	100	50.00	80.00	100	87.50	100	86.67
	n	41	40	33	31	31	21	16	7	5	6	1	4	10	14	16	9	15
ANTERIOR FOVEA LM1 (+= ASU 2-4)	**%**	18.18	35.71	25	44.44	16.67	0.00	20.00	25.00	0.00	75.00	50.00	100	0.00	0.00	40.00	0.00	0.00
	n	11	14	20	9	6	3	5	4	1	4	2	2	2	2	5	1	4
MANDIBULAR TORUS (+= ASU 2-3)	**%**	1.54	0.00	0.00	0.00	0.00	0.00	0.00	0.00	0.00	0.00	0.00	0.00	0.00	31.58	11.54	12.50	50.00
	n	65	53	48	20	27	21	16	14	6	8	4	1	13	19	26	16	8
GROOVE PATTERN LM2 (+= ASU Y)	**%**	13.33	28.21	25.00	14.29	12.50	11.76	7.69	12.50	42.86	50.00	25.00	0.00	0.00	44.44	12.50	0.00	20.00
	n	45	39	32	28	24	17	13	8	7	6	4	3	9	9	16	10	20

ROCKER JAW (+= ASU 2-3)	**%**	10.94	5.77	6.38	5.26	3.45	9.09	13.33	30.77	0.00	14.29	0.00	0.00	18.18	0.00	0.00	0.00	0.00
	n	64	52	47	19	29	22	15	13	5	7	4	1	11	11	13	5	1
CUSP NUMBER LM1 (+= ASU 6+)	**%**	4.17	8.57	16.13	22.73	0.00	16.67	11.11	0.00	20.00	0.00	0.00	0.00	33.33	25.00	14.29	0.00	10.00
	n	24	35	31	22	12	6	9	3	5	10	6	2	3	4	7	2	10
CUSP NUMBER LM2 (+= ASU 5+)	**%**	16.13	22.22	45.16	18.18	10.00	20.00	0.00	25.00	20.00	33.33	25.00	0.00	0.000	33.33	27.27	0.00	21.43
	n	31	45	31	22	20	10	9	4	5	6	4	3	5	6	11	8	14
DEFLECTING WRINKLE LM1 (+= ASU 2-3)	**%**	28.57	55.56	71.43	14.29	33.33	25	33.33	0.00	0.00	11.11	0.00	50.00	0.00	40.00	0.00	0.00	0.00
	n	7	9	14	7	9	4	3	3	3	9	4	2	3	5	3	1	6
C1-C2 CREST LM1 (+= ASU +)	**%**	0.00	0.00	0.00	0.00	6.67	10.00	0.00	16.67	0.00	0.00	0.00	0.00	33.33	0.00	0.00	0.00	0.00
	n	16	17	31	18	15	10	8	6	4	9	6	2	3	5	8	4	9
PROTOSTYLID LM1 (+= ASU 1-6)	**%**	63.33	72.41	58.82	54.17	27.78	41.67	0.00	25.00	40.00	9.09	60.00	100	40.00	40.00	37.50	75.00	33.33
	n	30	29	34	24	18	12	9	8	5	11	5	2	5	5	8	4	6
CUSP 7 LM1 (+= ASU 2-4)	**%**	0.00	0.00	8.11	0.00	0.00	0.00	0.00	0.00	16.67	0.00	0.00	0.00	0.00	16.67	14.29	0.00	0.00
	n	32	34	37	22	18	12	14	10	6	11	6	3	6	6	14	8	17
TOME'S ROOT LP1 (+= ASU 3-5)	**%**	2.44	3.45	5.71	14.81	0.00	8.33	8.33	0.00	0.00	0.00	0.00	0.00	20.00	0.00	0.00	6.25	0.00
	n	41	29	35	27	23	24	12	1	4	4	1	3	10	15	24	16	18
ROOT NUMBER LC (+= ASU 2+)	**%**	2.17	2.38	8.57	9.68	7.41	14.81	7.69	0.00	50.00	0.00	0.00	0.00	0.00	14.29	4.17	0.00	0.00
	n	46	42	35	31	27	27	13	10	2	11	3	2	14	14	24	17	19
ROOT NUMBER LM1 (+= ASU 3+)	**%**	0.00	0.00	0.00	0.00	0.00	0.00	0.00	0.00	0.00	0.00	0.00	0.00	0.00	0.00	0.00	0.00	0.00
	n	49	36	44	26	29	27	20	14	11	9	7	3	14	13	29	18	21
ROOT NUMBER LM2 (+= ASU 2+)	**%**	72.55	81.82	77.5	71.43	79.31	85.71	88.89	100	87.50	88.89	100	100	75.00	83.33	75.86	68.42	73.68
	n	51	33	40	28	29	28	18	9	8	9	2	3	16	12	29	19	19
TORSOMOLAR ANGLE LM3 (+= ASU +)	**%**	26.47	43.59	41.18	36.36	52.17	40.00	33.33	22.22	0.00	0.00	0.00	0.00	36.36	18.18	31.58	30.77	30.00
	n	34	39	17	11	23	20	15	9	1	4	2	1	11	11	19	13	10

Secondly, traits with < 3 observations were identified removed from further analysis. These included Carabelli's cusp UM1, parastyle UM1, anterior fovea LM1, rocker jaw, cusp number LM1 and deflecting wrinkle LM1, to the number to 24.

The percentage data for these were then submitted to principal components analysis (PCA) in order to identify any additional traits that contribute little to across-sample variation. The PCA results can be seen in Table 3.

Eight of these components have eigenvalues > 1.00 and account for 91% of the variance. According to procedure, however, it is the first three components that will be used in this analysis. These components have eigenvalues > 2.0 and account for 55% of the variance. A three-dimensional scatterplot (Figure 32) was used to represent how the first three components were distributed among the samples.

Traits with strong positive and negative loadings (>|0.500|) are the ones responsible for most intersample variation (Irish, 2010). For component 1, the x-axis, strong positive loadings (> 5.0) were found for C1 – C2 crest LM1, Tome's root LP1 and torsomolar angle LM3 and very strong loadings (>0.7) for labial curvature UI1, interruption groove UI2 and root number UP1.These very strong loadings move samples with high frequencies further towards to positive end of the x-axis. Strong negative loadings (< -0.5) were found for peg-reduced UI2 and cusp 7 LM1 and very strong negative loadings (< -0.7) were found for groove pattern LM2 and cusp number LM2. Similar to the very strong positive

loadings, very strong negative loadings move samples with high frequencies of these traits towards the negative end of the x-axis.

For component 2, y-axis, a strong positive loading (>0.5) was found for root number LC and very strong positive loadings (>0.7 for shoveling UI1, hypocone UM2 and root number UM2. Samples with high frequencies of these are found towards the positive end of the y-axis. Conversely, negative loadings (<-0.5) are found for tuberculum dentale UI2, congenital absence UM3 and root number UM2; no very strong loadings (<-0.7) are found.

For component 3, the z-axis, a very strong positive loading (>0.7) is found for root number LM2. Samples with high frequencies of this trait will be moved towards the positive end of the z-axis. Strong negative loadings (<-0.5) are found for Bushman canine UC and distal accessory ridge UC.

Traits with loadings of < |0.500| across all three components are considered non-contributory and removed from further analysis. These traits included cusp 5 UM1, enamel extension UM1, lingual cusp LP2, mandibular torus and root number LC. This reduced the number of traits to 19.

The stress value is a measure of goodness-of- fit of the scaled data compared to the unscaled data with a stress level below 0.15 representing good fit (Dugard, Todman and Staines, 2010). The stress for the three-dimensional MDS graph for the 36-trait MMD values stress was calculated at 0.132 and is, therefore, low. This means that this graph is a good representation of the MMD-based relationships. Stress for the two-dimensional MDS graph for the 36-trait MMD

values was calculated at 0.229. This is a high stress and means that the graph may not be an accurate representation of the MMD-based relationships.

Kendall's Tau-b Correlation Coefficient

Results from Kendall's tau-b correlation coefficient show high correlations between interruption groove UI2 and tuberculum dentale UI2 (tb= 0.803) and between C1-C2 crest LM1 and protostylid LM1 (tb= 0.703). Due to this, tuberculum dentale UI2 and C1-C2 crest LM1 were removed from further analysis. This reduced the final number of traits to 17.

Mean Measurement of Divergence (MMD)

After the removal of Culver Hole (CLV), Tinkinswood (TKW), Distillery Cave (DIS) and Raschoille Cave (RAS), the remaining 13 samples were compared using the initial 36 traits and then the final 17 traits.

The MMD distance matrix for the 13 samples using 36 traits is presented in Table 4. Overall, the low MMD values indicate that there is a high level of affinity among the samples. Twenty of the sample pairings showed no biological distance. Furthermore, this lack of phenetic diversity is indicated by only a minority of sample pairings (six out of 78) being significantly different from each other at the 0.025 alpha level.

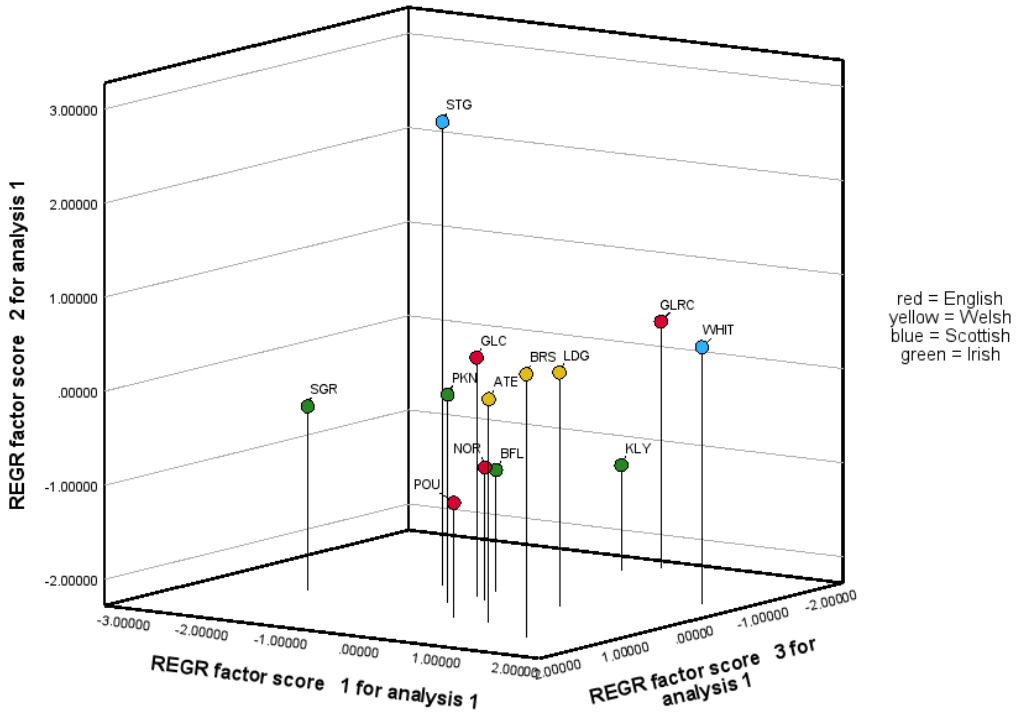

Figure 38: three-dimensional representation of the PCA loadings. NOR= Norton Priory, Runcorn, POU= Chapel House Farm, Poulton, GLC= St. Owen's Church Gloucester, GLRC= London Road, Gloucester, LDG= Great House Farm, Llandough, ATE= site 92, Atlantic Trading Estate, Barry, BRS= Brownslade Barrow, Castlemartin, CLV= Culver Hole, Llangennith, TKW= Tinkinswood Burial Chamber, St. Nicholas, STG= Strath Glebe chambered cairn, Skye, DIS= Distillery Cave, Oban, RAS= Raschoille Cave, Oban, WHIT= Whithorn Priory, Dumfries and Galloway, SGR= Southgreen, Kildare, PKN= Parknahown 5, Co. Laois, KLY= Killeany 1, Co. Laois, BFL= Bushfield/Lismore, Co. Laois.

Table 3: Principal Components Analysis loadings, Eigenvalues and variance explained for 24 traits.

	Principal component		
	1	2	3
Labial Curvature UI1	.791	.023	.403
Shoveling UI1	-.018	.776	.179
Interruption Groove UI2	.748	-.096	.096
Tuberculum Dentale UI2	.015	-.667	.407
Bushman Canine UC	-.275	.418	-.665
Distal Accessory Ridge UC	.056	.349	-.623

Hypocone UM2	.448	.758	.202
Cusp 5 UM1	-.475	-.139	.041
Enamel Extension UM1	.275	-.071	.192
Root Number UP1	.707	-.106	.209
Root Number UM2	.016	.774	.202
Peg-Reduced UI2	-.505	-.312	.300
Congenital Absence UM3	-.219	-.629	.216
Lingual Cusp LP2	-.421	.326	-.472
Mandibular Torus	-.496	-.410	-.036
Groove Pattern LM2	-.776	.407	.254
Cusp Number LM2	-.737	.226	.206
C1 - C2 Crest LM1	.612	.151	-.124
Protostylid LM1	-.126	-.681	-.359
Cusp 7 LM1	-.610	-.059	.248
Tomes' Root LP1	.687	.097	-.388
Root Number LC	-.141	.045	.339
Root Number LM2	-.042	.578	.731
Torsomolar Angle LM3	.595	-.473	.073
Eigenvalue	5.749	4.606	2.843
Variance (%)	23.956	19.193	11.846
Total Variance	23.956	43.149	54.499

The most distinct of the samples are Brownslade Barrow (BRS), Poulton, Cheshire (POU) and London road, Gloucester (GLRC) which are each significantly different from three samples: they are significantly different from each other; London road, Gloucester (GLRC) is significantly different from St. Owen's church, Gloucester (GLC); Poulton, Cheshire (POU) is significantly different from Great House Farm, Llandough (LDG); Brownslade Barrow (BRS) is significantly different from South Green, Kildare (SGR). There were

no significantly different pairings that involve the following seven samples: Atlantic Trading Estate, Barry (ATE); Bushfield/Lismore, co. Laois (BFL); Killeany, co. Laois (KLY); Norton Priory, Runcorn (NOR); Parknahown (PKN) Strath Glebe, Skye (STG) and Whithorn Priory, Dumfries and Galloway (WHIT).

These patterns indicated for 36 traits include the non-contributory traits identified by PCA and Kendall's tau-b correlation coefficient and, therefore, subsequent inter-sample affinities were determined by a 17-trait MMD analysis after trait editing. Those retained included included the following: labial curvature UI1; shovelling UI1; interruption groove UI2; bushman Canine UC; distal accessory ridge UC; hypocone UM2; root number UP1, root number UM2; peg-reduced UI2; congenital absence UM3; groove pattern LM2: cusp number LM2; protostylid LM1; cusp 7 LM1; Tome's root LP1; root number LM2; torsomolar angle LM3.

The resulting matrix for the MMD analysis is presented in Table 5. Overall, this analysis finds close affinities as with the previous 36-trait analysis as MMD values remain low. Twenty-six of the sample pairings showed no biological distance i.e MMD=0.0. This is reflected by the number of samples statistically different to each remaining the minority of sample pairings (10 of 78). However, while these are the minority, it is evident that diversity among samples is evident in this analysis compared to the previous; the number of significantly different samples has increased and MMD values for many

pairings are greater, e.g. the value for BRS – BFL increases from 0.052 to 0.205.

Similar to last time, Brownslade Barrow (BRS) is the most distinct among the samples as it is significantly different from seven other: Bushfield/Lismore, co. Laois (BFL); Killeany, co. Laois (KLY); Southgreen, Kildare (SGR); St. Owen's church, Gloucester (GLC); London Road, Gloucester (GLRC); Norton Priory (NOR); Poulton, Cheshire (POU). Following this, St. Owen's Gloucester (GLC), Killeany, co.Laois (KLY), Poulton, Cheshire (POU) and Strath Glebe, Skye (STG) are each included in two significantly different pairings while Bushfield/Lismore, co. Laois, London Road, Gloucester (GLRC), Great House Farm, Llandough (LDG) and Southgreen (SGR) are each included in only one significantly different pairing each. There were no significantly different pairings including Atlantic Trading Estate, Barry (ATE), Parknahown, co. Laois (PKN) or Whithorn Priory, Dumfries and Galloway (WHIT).

Multidimensional Scaling

The MDS ALSCAL procedure was used to produce a graphical representation of the MMD values in which each value is treated as a Euclidean distance. Within the MDS representation, the samples with closer proximity to each other have higher MMD values and the samples that are further apart have lower ones Three-dimensional and two-dimensional MDS ALSCAL graphs for 36-trait MMD values are presented in Figures 33 and 34 respectively and three-dimensional and two-dimensional MDS ALSCAL graphs for 17-trait MMD values are presented in Figures 35 and 36 respectively.

The stress value is a measure of goodness-of- fit of the scaled data compared to the unscaled data with a stress level below 0.15 representing good fit (Dugard, Todman and Staines, 2010). The stress for the three-dimensional MDS graph for the 36-trait MMD values stress was calculated at 0.132 and is, therefore, low. This means that this graph is a good representation of the MMD-based relationships. Stress for the two-dimensional MDS graph for the 36-trait MMD values was calculated at 0.229. This is a high stress and means that the graph may not be an accurate representation of the MMD-based relationship

Similarly, stress for the three-dimensional MDS graph for the 17-trait MMD values was calculated at 0.111 which is low, reflecting a good representation of the MMD-based relationships. Stress for the two-dimensional model, however, was calculated at 0.159 which is slightly high and, therefore, may not be an optimal representation of the relationships.

The r^2 value is a measure of the proportion of variance of the scaled data that can be explained by the MDS procedure and the correlation coefficient, r, between the MDS and MMD distances is calculated by finding the square root of this value (Kruskal and Wish, 1978). The r^2 value for the three-dimensional MDS graph for the 36 traits MMD values is 0.830 and the r value is 0.911. This indicates a high correlation between the two matrices with 91.1% of the variance explained by the distance values. The r^2 matrix for the two-dimensional MDS graph for the 36-trait MMD values is 0.685 and the r value is 0.828, therefore, 82.8% of the variance is explained.

Similarly, the r^2 value for the three-dimensional MDS graph for the 17-trait MMD values is 0.912 and the r value is 0.955, therefore, this is a high correlation between the matrices with 95.5% of the variance explained by the distances. The r^2 value for the two-dimensional MDS for the 17-trait MMD values is 0.884 and the r value is 0.940, meaning 94.0% of the variance is explained by the distances.

Overall, the three-dimensional MDS provide more accurate representations of the MMD-based relationships than the two-dimensional MDS graphs. The stress and r^2 values improved in the two-dimensional graph for the 17-trait MMD values compared to those for the two-dimensional graph for the 36-trait MMD values, however, the stress remained slightly high and so both must be considered with caution.

Both the three-dimensional and two-dimensional MDS graphs for the 36-trait MMD values (Figures 39 and 40) show high relatedness between the samples. Two clusters are evident in both these three-dimensional and two-dimensional MDS graphs: English and Irish samples are grouped together on the left side of dimension 1 whereas Welsh and Scottish samples are both grouped towards the right side of dimension 1.

The regional grouping is more distinct in the three-dimensional plot, showing that English samples, except for GLRC, are grouped closely together, as is the case with the Welsh and the Irish; however, the Scottish samples are not as closely grouped. This patterning is not visible in the two-dimensional MDS graph.

The three-dimensional and two-dimensional MDS graphs for the 17-trait MMD values (Figures 41 and 42) show similar patterning as those found for the 36-trait MMD values. Compared to the MDS graph for 36-trait MMD values the overall relationships have gotten closer; the regional grouping between English samples became closer while the grouping between the Welsh samples became more distant to each other. The Welsh and Scottish cluster has moved closer to the Irish and English. Furthermore, English samples in the two-dimensional MDS graph for the 17-trait MMD values (Figure 42) displayed grouping together that was not visible in the two-dimensional dimensional graph for the 36-trait MMD values (Figure 34).

Mantel tests

The geographical distance matrix based on the straight-line distances in kilometres (Table 6) was compared to the 36-trait and the 17- trait MMD distance matrices (Tables 4 and 5) using Mantel tests. As mentioned, the use of straight-line distances may be problematic as the topography of the landscape will influence the ways in which people move and influence biological and cultural isolation. Correlations are statistically significant at the 0.05 alpha level.

Firstly, the geographic distance data were compared against the 36-trait MMD data. The Mantel test found that there was a weak positive correlation, which is not statistically significant ($r= 0.09561$, $p= 0.2861$).

Table 4: 36-trait MMD Values. Red = significant at the p ≤ 0.025 level. NOR= Norton Priory, Runcorn, POU= Chapel House Farm, Poulton, GLC= St. Owen's Church Gloucester, GLRC= London Road, Gloucester, LDG= Great House Farm, Llandough, ATE= site 92, Atlantic Trading Estate, Barry, BRS= Brownslade Barrow, Castlemartin, CLV= Culver Hole, Llangennith, TKW= Tinkinswood Burial Chamber, St. Nicholas, STG= Strath Glebe chambered cairn, Skye, DIS= Distillery Cave, Oban, RAS= Raschoille Cave, Oban, WHIT= Whithorn Priory, Dumfries and Galloway, SGR= Southgreen, Kildare, PKN= Parknahown 5, Co. Laois, KLY= Killeany 1, Co. Laois, BFL= Bushfield/Lismore, Co. Laois.

	ATE	BFL	BRS	GLC	GLRC	KLY	LDG	NOR	PKN	POU	SGR	STG	WHIT
ATE	0.000	0.000	0.000	0.000	0.040	0.000	0.000	0.000	0.000	0.020	0.001	0.033	0.000
BFL	0.000	0.000	0.052	0.053	0.000	0.000	0.000	0.000	0.000	0.012	0.000	0.000	0.000
BRS	0.000	0.052	0.000	0.080	0.118	0.047	0.000	0.041	0.027	0.108	0.148	0.000	0.000
GLC	0.000	0.053	0.080	0.000	0.056	0.029	0.050	0.020	0.053	0.028	0.006	0.016	0.064
GLRC	0.040	0.000	0.118	0.056	0.000	0.000	0.007	0.054	0.015	0.081	0.035	0.020	0.017
KLY	0.000	0.000	0.047	0.029	0.000	0.000	0.015	0.000	0.000	0.000	0.000	0.100	0.000
LDG	0.000	0.000	0.000	0.050	0.007	0.015	0.000	0.018	0.052	0.069	0.077	0.013	0.000
NOR	0.000	0.000	0.041	0.020	0.054	0.000	0.018	0.000	0.015	0.000	0.012	0.049	0.002
PKN	0.000	0.000	0.027	0.053	0.015	0.000	0.052	0.015	0.000	0.038	0.000	0.016	0.000
POU	0.020	0.012	0.108	0.028	0.081	0.000	0.069	0.000	0.038	0.000	0.049	0.127	0.069
SGR	0.001	0.000	0.148	0.006	0.035	0.000	0.077	0.012	0.000	0.049	0.000	0.053	0.080
STG	0.033	0.000	0.000	0.016	0.020	0.100	0.013	0.049	0.016	0.127	0.053	0.000	0.041
WHIT	0.000	0.000	0.000	0.064	0.017	0.000	0.000	0.002	0.000	0.069	0.080	0.041	0.000

Table 5: 17-trait MMD values. Red = significant at the p ≤ 0.025 level. . NOR= Norton Priory, Runcorn, POU= Chapel House Farm, Poulton, GLC= St. Owen's Church Gloucester, GLRC= London Road, Gloucester, LDG= Great House Farm, Llandough, ATE= site 92, Atlantic Trading Estate, Barry, BRS= Brownslade Barrow, Castlemartin, CLV= Culver Hole, Llangennith, TKW= Tinkinswood Burial Chamber, St. Nicholas, STG= Strath Glebe chambered cairn, Skye, DIS= Distillery Cave, Oban, RAS= Raschoille Cave, Oban, WHIT= Whithorn Priory, Dumfries and Galloway, SGR= Southgreen, Kildare, PKN= Parknahown 5, Co. Laois, KLY= Killeany 1, Co. Laois, BFL= Bushfield/Lismore, Co. Laois.

	ATE	BFL	BRS	GLC	GLRC	KLY	LDG	NOR	PKN	POU	SGR	STG	WHIT
ATE	0.000	0.000	0.029	0.000	0.000	0.000	0.000	0.000	0.000	0.000	0.063	0.080	0.000
BFL	0.000	0.000	0.205	0.029	0.000	0.000	0.000	0.000	0.000	0.000	0.000	0.111	0.043
BRS	0.029	0.205	0.000	0.239	0.226	0.193	0.064	0.220	0.110	0.265	0.390	0.145	0.000
GLC	0.000	0.029	0.239	0.000	0.027	0.074	0.079	0.022	0.000	0.014	0.003	0.063	0.013
GLRC	0.000	0.000	0.226	0.027	0.000	0.000	0.028	0.008	0.036	0.028	0.070	0.167	0.000
KLY	0.000	0.000	0.193	0.074	0.000	0.000	0.028	0.000	0.016	0.003	0.078	0.281	0.000
LDG	0.000	0.000	0.064	0.079	0.028	0.028	0.000	0.031	0.000	0.056	0.103	0.164	0.000
NOR	0.000	0.000	0.220	0.022	0.008	0.000	0.031	0.000	0.017	0.000	0.027	0.169	0.010
PKN	0.000	0.000	0.110	0.000	0.036	0.016	0.000	0.017	0.000	0.035	0.005	0.081	0.000
POU	0.000	0.000	0.265	0.014	0.028	0.003	0.056	0.000	0.035	0.000	0.032	0.224	0.049
SGR	0.063	0.000	0.390	0.003	0.070	0.078	0.103	0.027	0.005	0.032	0.000	0.038	0.155
STG	0.080	0.111	0.145	0.063	0.167	0.281	0.164	0.169	0.081	0.224	0.038	0.000	0.124
WHIT	0.000	0.043	0.000	0.013	0.000	0.000	0.000	0.010	0.000	0.049	0.155	0.124	0.000

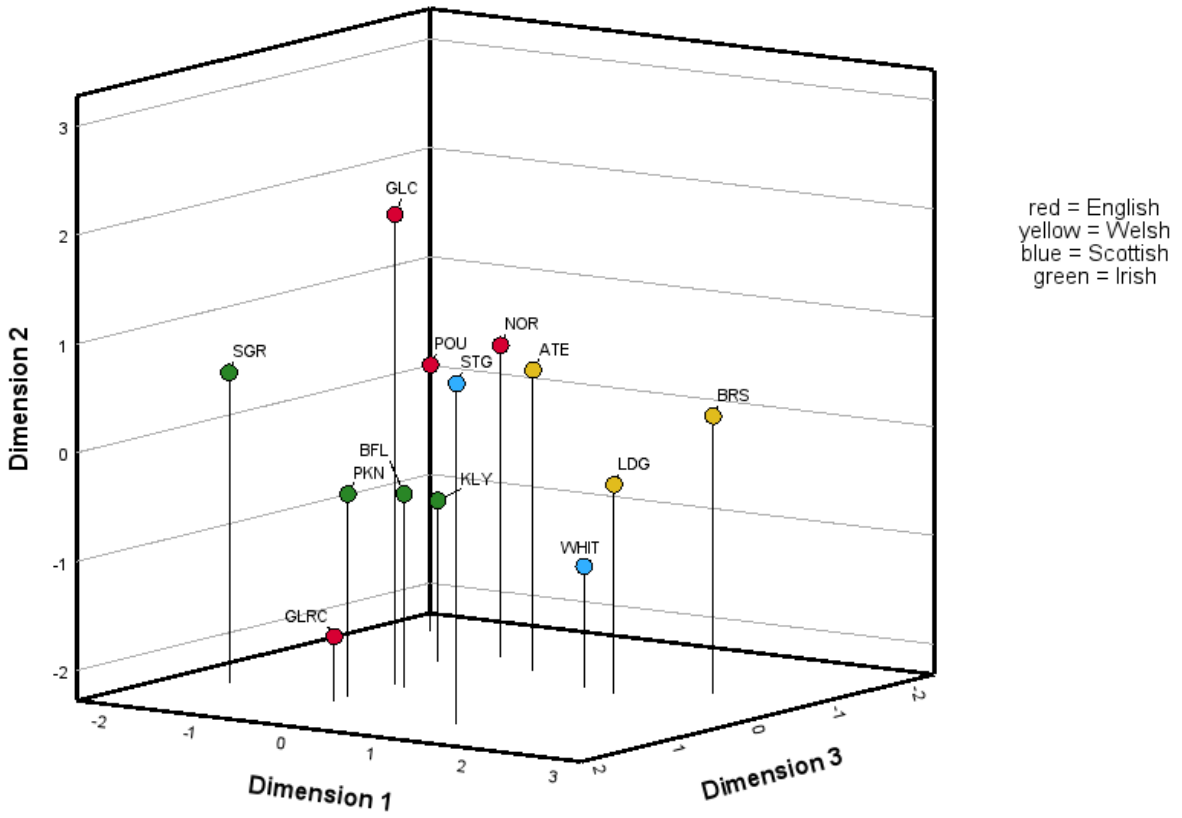

Figure 39: Three-dimensional MDS graph of 36-trait MMD values. NOR= Norton Priory, Runcorn, POU= Chapel House Farm, Poulton, GLC= St. Owen's Church Gloucester, GLRC= London Road, Gloucester, LDG= Great House Farm, Llandough, ATE= site 92, Atlantic Trading Estate, Barry, BRS= Brownslade Barrow, Castlemartin, CLV= Culver Hole, Llangennith, TKW= Tinkinswood Burial Chamber, St. Nicholas, STG= Strath Glebe chambered cairn, Skye, DIS= Distillery Cave, Oban, RAS= Raschoille Cave, Oban, WHIT= Whithorn Priory, Dumfries and Galloway, SGR= Southgreen, Kildare, PKN= Parknahown 5, Co Laois, KLY= Killeany 1, Co. Laois, BFL= Bushfield/Lismore, Co. Laois

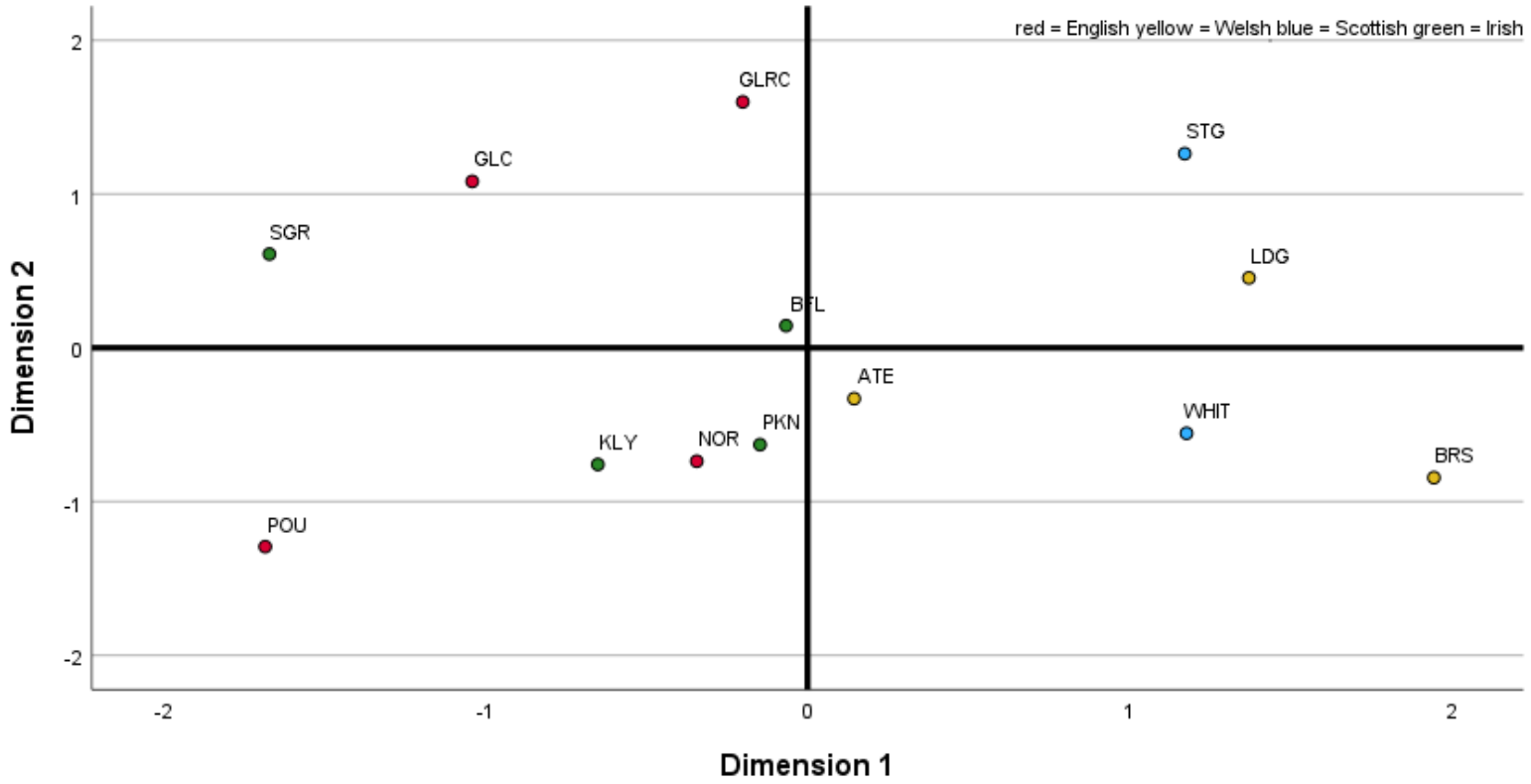

Figure 40: Two-dimensional MDS graph of MMD values for the 36 traits. NOR= Norton Priory, Runcorn, POU= Chapel House Farm, Poulton, GLC= St. Owen's Church Gloucester, GLRC= London Road, Gloucester, LDG= Great House Farm, Llandough, ATE= site 92, Atlantic Trading Estate, Barry, BRS= Brownslade Barrow, Castlemartin, CLV= Culver Hole, Llangennith, TKW= Tinkinswood Burial Chamber, St. Nicholas, STG= Strath Glebe chambered cairn, Skye, DIS= Distillery Cave, Oban, RAS= Raschoille Cave, Oban, WHIT= Whithorn Priory, Dumfries and Galloway, SGR= Southgreen, Kildare, PKN= Parknahown 5, Co. Laois, KLY= Killeany 1, Co. Laois, BFL= Bushfield/Lismore, Co. Laois.

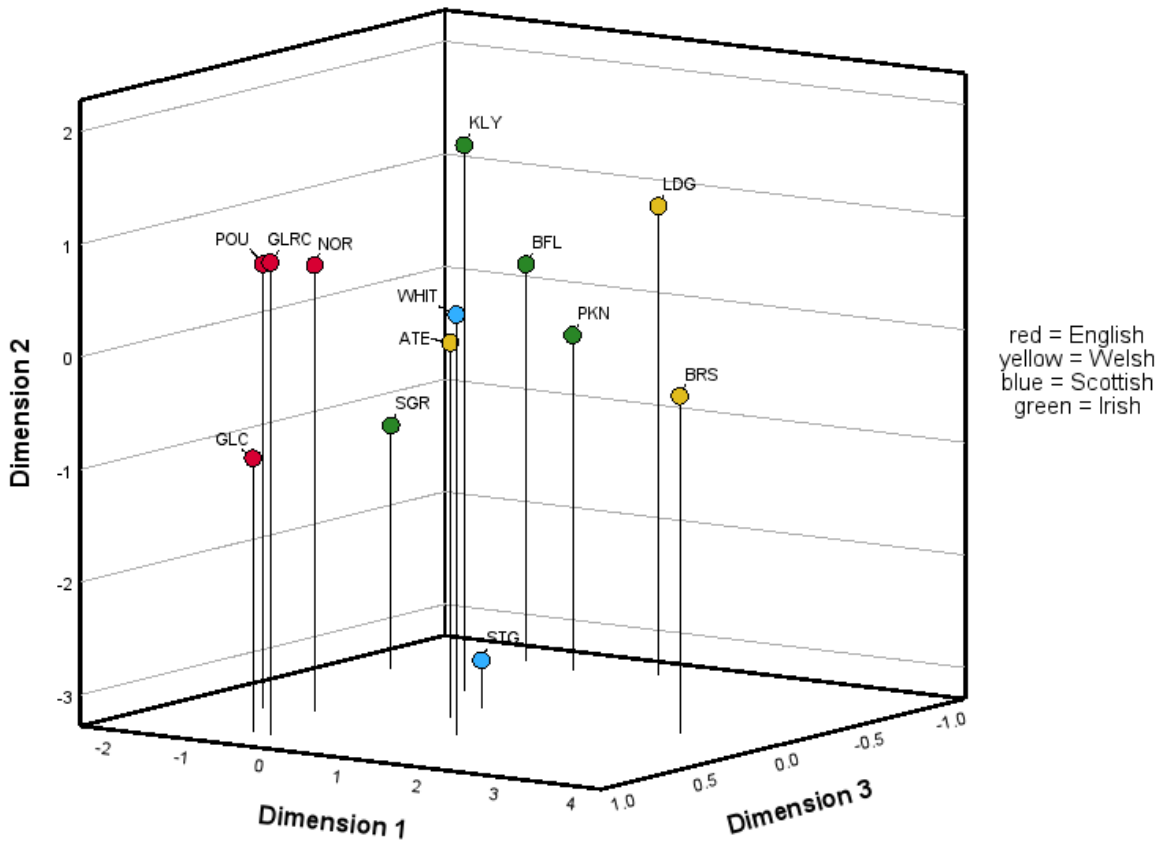

Figure 41: three-dimensional MDS graph of 17-trait MMD values. NOR= Norton Priory, Runcorn, POU= Chapel House Farm, Poulton, GLC= St. Owen's Church Gloucester, GLRC= London Road, Gloucester, LDG= Great House Farm, Llandough, ATE= site 92, Atlantic Trading Estate, Barry, BRS= Brownslade Barrow, Castlemartin, CLV= Culver Hole, Llangennith, TKW= Tinkinswood Burial Chamber, St. Nicholas, STG= Strath Glebe chambered cairn, Skye, DIS= Distillery Cave, Oban, RAS= Raschoille Cave, Oban, WHIT= Whithorn Priory, Dumfries and Galloway, SGR= Southgreen, Kildare, PKN= Parknahown 5, Co. Laois, KLY= Killeany 1, Co. Laois, BFL= Bushfield/Lismore, Co. Laois

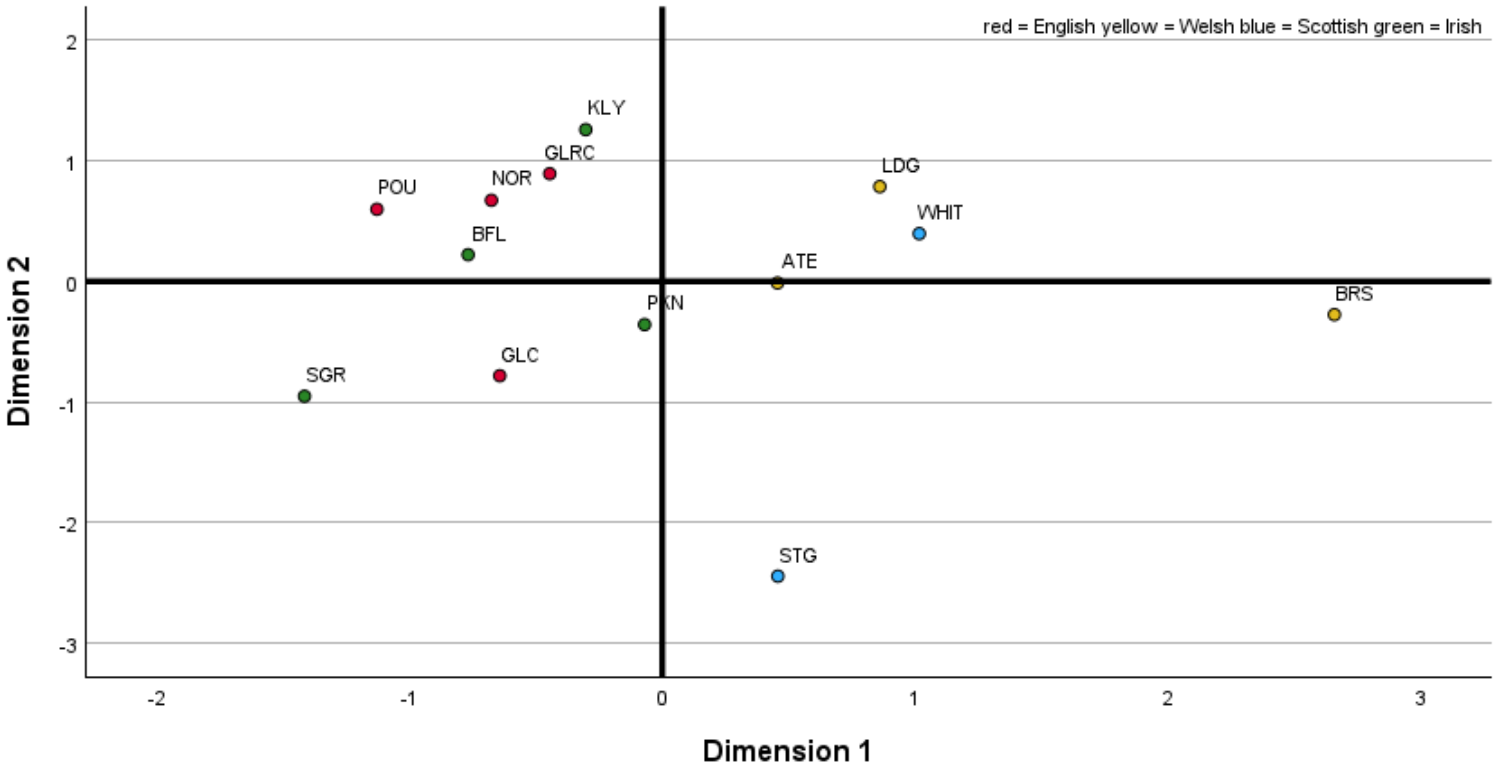

Figure 42: two-dimensional MDS graph of 17-trait MMD values. NOR= Norton Priory, Runcorn, POU= Chapel House Farm, Poulton, GLC= St. Owen's Church Gloucester, GLRC= London Road, Gloucester, LDG= Great House Farm, Llandough, ATE= site 92, Atlantic Trading Estate, Barry, BRS= Brownslade Barrow, Castlemartin, CLV= Culver Hole, Llangennith, TKW= Tinkinswood Burial Chamber, St. Nicholas, STG= Strath Glebe chambered cairn, Skye, DIS= Distillery Cave, Oban, RAS= Raschoille Cave, Oban, WHIT= Whithorn Priory, Dumfries and Galloway, SGR= Southgreen, Kildare, PKN= Parknahown 5, Co. Laois, KLY= Killeany 1, Co. Laois, BFL= Bushfield/Lismore, Co. Laois.

The geographical distance data were then compared against the 17-trait MMD data. The Mantel test found the correlation to still be positive and slightly stronger than the previous; however, the correlation is still weak and is not statistically significant (r= 0.2197, p= 0.1074).

Additional Analyses

The trait number of observations and frequencies can be found in Appendix V. Similarly, the hi-lo charts illustrating trait frequencies (Figures 62-83) can be found in Appendix VI. Many of the traits, e.g., deflecting wrinkle LM1 and root number UP1 (Figures 77 and 78), exhibit large ±2 standard errors due low sample sizes for British and Irish samples.

All British and Irish samples were included in the 22-trait MMD analysis except for Tinkinswood and Culverhole Cave which were excluded due to missing trait data. The 22-trait MMD values ranged from 0.000-0.751 and p-values ranged from 0.000-1.000. Between the British and Irish samples and the global populations, a majority of sample pairings had a statistically significant difference (217 of 315) (see Table 7).

Regarding the MDS graph, stress for the two-dimensional model for the 22-trait MMD values was calculated at 0.139 which reflects a good representation of the relationships. The r^2 value for the two-dimensional MDS for the 22-trait MMD values is 0.923 and the r value is 0.961, meaning 96.1% of the variance is explained by the distances.

Summary

The 36-trait MMD values ranged from between 0.00 to 0.127 and p-values ranged from 0.003-1.000. The 17-trait MMD values ranged from 0.000-0.390 and p-values ranged from 0.000-1.000.

The MDS showed that samples exhibited regional grouping, for example English samples were grouped together. Furthermore, English and Irish samples were grouped closer to each other while Scottish and Welsh were closer together.

The Mantel tests comparing geographic distance data against the 36-trait MMD data and the 17-trait MMD data both produced weak positive correlations that are not statistically significant. Results from this chapter will be used for the discussion in Chapter 7.

Table 6: Geographic Distance Matrix (km). NOR= Norton Priory, Runcorn, POU= Chapel House Farm, Poulton, GLC= St. Owen's Church Gloucester, GLRC= London Road, Gloucester, LDG= Great House Farm, Llandough, ATE= site 92, Atlantic Trading Estate, Barry, BRS= Brownslade Barrow, Castlemartin, CLV= Culver Hole, Llangennith, TKW= Tinkinswood Burial Chamber, St. Nicholas, STG= Strath Glebe chambered cairn, Skye, DIS= Distillery Cave, Oban, RAS= Raschoille Cave, Oban, WHIT= Whithorn Priory, Dumfries and Galloway, SGR= Southgreen, Kildare, PKN= Parknahown 5, Co. Laois, KLY= Killeany 1, Co. Laois, BFL= Bushfield/Lismore, Co. Laois.

	ATE	BFL	BRS	GLC	GLRC	KLY	LDG	NOR	PKN	POU	SGR	STG	WHIT
ATE	0.00	340.16	126.01	86.34	194.24	334.74	7.06	87.83	330.30	219.88	317.87	670.41	379.44
BFL	340.16	0.00	224.56	380.03	313.18	7.12	340.06	381.11	12.49	329.94	51.30	488.84	289.24
BRS	126.01	224.56	0.00	193.21	220.29	220.10	128.31	194.65	213.49	247.95	213.19	623.74	347.40
GLC	86.34	380.03	193.21	0.00	147.90	373.75	79.87	1.52	372.04	167.25	347.84	641.39	350.58
GLRC	194.24	313.18	220.29	147.90	0.00	306.10	187.78	147.70	309.46	28.00	268.02	493.78	204.18
KLY	334.74	7.12	220.10	373.75	306.10	0.00	334.55	374.82	12.96	322.82	44.68	486.04	283.33
LDG	7.06	340.06	128.31	79.87	187.78	334.55	0.00	81.37	330.37	213.28	316.79	665.38	374.20
NOR	87.83	381.11	194.65	1.52	147.70	374.82	81.37	0.00	373.14	166.86	348.80	641.27	350.54
PKN	330.30	12.49	213.49	372.04	309.46	12.96	330.37	373.14	0.00	327.05	54.37	498.98	293.94
POU	219.88	329.94	247.95	167.25	28.00	322.82	213.28	166.86	327.05	0.00	283.03	477.92	192.05
SGR	317.87	51.30	213.19	347.84	268.02	44.68	316.79	348.80	54.37	283.03	0.00	454.91	239.63
STG	670.41	488.84	623.74	641.39	493.78	486.04	665.38	641.27	498.98	477.92	454.91	0.00	291.91
WHIT	379.44	289.24	347.40	350.58	204.18	283.33	374.20	350.54	293.94	192.05	239.63	291.91	0.00

Table 7: 22-trait MMD Matrix. Red = significant at the p ≤ 0.025 level. WE= Western Europe, NoE= Northern Europe, NA= North Africa, WA= West Africa, SA= South Africa, KH=Khoisan, CM= China-Mongolia, Jo= Jomon, RJ= Recent Japan, NES= Northeast Siberia, SS= South Siberia, AA= American Arctic, NWA= Northwest America, NSAI= N. & S. American Indian, SEE= Southeast Asia (Early), SER=Southeast Asia (Recent), PO= Polynesia, MI= Micronesia, AU= Australia, NG= New Guinea, ML= Melanesia, NOR= Norton Priory, Runcorn, POU= Chapel House Farm, Poulton, GLC= St. Owen's Church Gloucester, GLRC= London Road, Gloucester, LDG= Great House Farm, Llandough, ATE= site 92, Atlantic Trading Estate, Barry, BRS= Brownslade Barrow, Castlemartin, STG= Strath Glebe chambered cairn, Skye, DIS= Distillery Cave, Oban, RAS= Raschoille Cave, Oban, SGR= Southgreen, Kildare, PKN= Parknahown 5, Co. Laois, KLY= Killeany 1, Co. Laois, BFL= Bushfield/Lismore, Co. Laois

	WE	***NoE***	***NA***	***WA***	***SA***	***KH***	***CM***	***JO***	***RJ***	***NES***	***SS***	***AA***	***NWA***	***NSAI***	***SEE***	***SER***	***PO***	***MI***	***AU***	***NG***	***ML***
WE	0.000	0.025	0.037	0.369	0.191	0.248	0.411	0.183	0.379	0.485	0.123	0.550	0.654	0.699	0.195	0.208	0.178	0.208	0.334	0.072	0.209
NoE	0.025	0.000	0.041	0.351	0.185	0.316	0.442	0.204	0.418	0.525	0.148	0.589	0.685	0.710	0.194	0.221	0.174	0.207	0.288	0.059	0.156
NA	0.037	0.041	0.000	0.249	0.089	0.209	0.362	0.191	0.337	0.469	0.131	0.552	0.628	0.636	0.139	0.153	0.168	0.154	0.243	0.064	0.127
WA	0.369	0.351	0.249	0.000	0.096	0.174	0.452	0.319	0.425	0.538	0.328	0.653	0.701	0.675	0.178	0.210	0.199	0.137	0.113	0.231	0.156
SA	0.191	0.185	0.089	0.096	0.000	0.130	0.402	0.229	0.359	0.469	0.231	0.573	0.658	0.647	0.152	0.164	0.189	0.130	0.154	0.116	0.143
KH	0.248	0.316	0.209	0.174	0.130	0.000	0.446	0.243	0.389	0.443	0.253	0.529	0.623	0.672	0.237	0.244	0.240	0.206	0.284	0.159	0.294
CM	0.411	0.442	0.362	0.452	0.402	0.446	0.000	0.238	0.008	0.062	0.127	0.102	0.091	0.118	0.092	0.069	0.140	0.173	0.260	0.438	0.289
JO	0.183	0.204	0.191	0.319	0.229	0.243	0.238	0.000	0.186	0.230	0.120	0.237	0.329	0.397	0.113	0.143	0.082	0.120	0.182	0.162	0.201
RJ	0.379	0.418	0.337	0.425	0.359	0.389	0.008	0.186	0.000	0.046	0.126	0.084	0.097	0.135	0.081	0.057	0.121	0.146	0.227	0.404	0.282
NES	0.485	0.525	0.469	0.538	0.469	0.443	0.062	0.230	0.046	0.000	0.179	0.018	0.031	0.077	0.151	0.145	0.191	0.211	0.331	0.515	0.350
SS	0.123	0.148	0.131	0.328	0.231	0.253	0.127	0.120	0.126	0.179	0.000	0.238	0.257	0.284	0.056	0.066	0.068	0.117	0.248	0.176	0.178
AA	0.550	0.589	0.552	0.653	0.573	0.529	0.102	0.237	0.084	0.018	0.238	0.000	0.036	0.119	0.231	0.225	0.249	0.303	0.407	0.586	0.428
NWA	0.654	0.685	0.628	0.701	0.658	0.623	0.091	0.329	0.097	0.031	0.257	0.036	0.000	0.033	0.241	0.249	0.293	0.326	0.440	0.687	0.451
NSAI	0.699	0.710	0.636	0.675	0.647	0.672	0.118	0.397	0.135	0.077	0.284	0.119	0.033	0.000	0.243	0.260	0.338	0.305	0.450	0.739	0.423
SEE	0.195	0.194	0.139	0.178	0.152	0.237	0.092	0.113	0.081	0.151	0.056	0.231	0.241	0.243	0.000	0.007	0.028	0.021	0.089	0.181	0.082
SER	0.208	0.221	0.153	0.210	0.164	0.244	0.069	0.143	0.057	0.145	0.066	0.225	0.249	0.260	0.007	0.000	0.043	0.047	0.109	0.197	0.126
PO	0.178	0.174	0.168	0.199	0.189	0.240	0.140	0.082	0.121	0.191	0.068	0.249	0.293	0.338	0.028	0.043	0.000	0.056	0.085	0.128	0.116
MI	0.208	0.207	0.154	0.137	0.130	0.206	0.173	0.120	0.146	0.211	0.117	0.303	0.326	0.305	0.021	0.047	0.056	0.000	0.079	0.188	0.092
AU	0.334	0.288	0.243	0.113	0.154	0.284	0.260	0.182	0.227	0.331	0.248	0.407	0.440	0.450	0.089	0.109	0.085	0.079	0.000	0.198	0.116
NG	0.072	0.059	0.064	0.231	0.116	0.159	0.438	0.162	0.404	0.515	0.176	0.586	0.687	0.739	0.181	0.197	0.128	0.188	0.198	0.000	0.146
ML	0.209	0.156	0.127	0.156	0.143	0.294	0.289	0.201	0.282	0.350	0.178	0.428	0.451	0.423	0.082	0.126	0.116	0.092	0.116	0.146	0.000

Table 7 (cont.)

	WE	*NoE*	*NA*	*WA*	*SA*	*KH*	*CM*	*JO*	*RJ*	*NES*	*SS*	*AA*	*NWA*	*NSAI*	*SEE*	*SER*	*PO*	*MI*	*AU*	*NG*	*ML*
ATE	0.073	0.048	0.095	0.386	0.247	0.389	0.382	0.279	0.348	0.481	0.165	0.567	0.655	0.676	0.181	0.172	0.179	0.181	0.282	0.160	0.214
BFL	0.000	0.000	0.000	0.321	0.141	0.189	0.262	0.044	0.244	0.337	0.018	0.388	0.467	0.522	0.088	0.109	0.047	0.134	0.216	0.000	0.109
BRS	0.040	0.002	0.056	0.417	0.238	0.455	0.435	0.293	0.428	0.583	0.158	0.663	0.730	0.726	0.203	0.231	0.220	0.211	0.345	0.173	0.209
DIS	0.152	0.239	0.152	0.555	0.330	0.377	0.000	0.132	0.000	0.110	0.000	0.133	0.133	0.188	0.065	0.015	0.113	0.200	0.341	0.281	0.300
GLC	0.150	0.144	0.166	0.358	0.229	0.266	0.305	0.254	0.274	0.314	0.134	0.400	0.458	0.479	0.144	0.158	0.177	0.140	0.284	0.234	0.225
GLRC	0.015	0.008	0.065	0.363	0.191	0.305	0.425	0.185	0.383	0.462	0.129	0.542	0.667	0.703	0.190	0.200	0.173	0.208	0.303	0.097	0.212
KLY	0.000	0.000	0.000	0.297	0.178	0.292	0.327	0.151	0.341	0.445	0.024	0.520	0.601	0.622	0.111	0.132	0.081	0.133	0.264	0.000	0.104
LDG	0.031	0.035	0.093	0.577	0.283	0.377	0.454	0.298	0.424	0.502	0.177	0.572	0.693	0.743	0.282	0.277	0.279	0.300	0.464	0.166	0.324
NOR	0.042	0.048	0.110	0.508	0.295	0.356	0.463	0.308	0.438	0.520	0.195	0.609	0.710	0.751	0.262	0.263	0.250	0.258	0.405	0.151	0.287
PKN	0.024	0.012	0.030	0.231	0.127	0.197	0.321	0.150	0.298	0.448	0.105	0.488	0.595	0.617	0.137	0.139	0.125	0.124	0.208	0.068	0.143
POU	0.058	0.040	0.083	0.411	0.210	0.286	0.374	0.218	0.348	0.399	0.131	0.485	0.561	0.593	0.165	0.192	0.174	0.169	0.311	0.123	0.199
RAS	0.011	0.010	0.000	0.366	0.189	0.353	0.156	0.160	0.146	0.279	0.001	0.345	0.388	0.388	0.038	0.045	0.143	0.096	0.273	0.225	0.145
SGR	0.053	0.004	0.043	0.192	0.077	0.084	0.308	0.135	0.270	0.333	0.087	0.397	0.488	0.524	0.102	0.122	0.065	0.112	0.149	0.000	0.079
STG	0.000	0.028	0.000	0.212	0.050	0.026	0.207	0.106	0.179	0.290	0.038	0.374	0.448	0.453	0.052	0.039	0.093	0.045	0.175	0.022	0.103
WHIT	0.001	0.000	0.021	0.443	0.212	0.414	0.274	0.164	0.262	0.408	0.086	0.466	0.548	0.556	0.143	0.147	0.148	0.168	0.300	0.131	0.184

Table 7 (cont.)

	ATE	BFL	BRS	DIS	GLC	GLRC	KLY	LDG	NOR	PKN	POU	RAS	SGR	STG	WHIT
ATE	0.000	0.110	0.000	0.018	0.010	0.022	0.000	0.008	0.000	0.000	0.028	0.000	0.061	0.000	0.000
BFL	0.110	0.000	0.065	0.107	0.188	0.000	0.000	0.020	0.061	0.018	0.019	0.077	0.000	0.000	0.000
BRS	0.000	0.065	0.000	0.074	0.029	0.031	0.000	0.000	0.000	0.000	0.000	0.000	0.037	0.000	0.000
DIS	0.018	0.107	0.074	0.000	0.046	0.216	0.113	0.111	0.158	0.099	0.132	0.000	0.167	0.000	0.000
GLC	0.010	0.188	0.029	0.046	0.000	0.121	0.068	0.064	0.053	0.067	0.009	0.000	0.018	0.000	0.092
GLRC	0.022	0.000	0.031	0.216	0.121	0.000	0.000	0.004	0.029	0.006	0.051	0.000	0.052	0.020	0.000
KLY	0.000	0.000	0.000	0.113	0.068	0.000	0.000	0.000	0.000	0.000	0.000	0.000	-0.007	0.000	0.000
LDG	0.008	0.020	0.000	0.111	0.064	0.004	0.000	0.000	0.000	0.041	0.000	0.000	0.034	0.000	0.000
NOR	0.000	0.061	0.000	0.158	0.053	0.029	0.000	0.000	0.000	0.036	0.000	0.000	0.054	0.000	0.000
PKN	0.000	0.018	0.000	0.099	0.067	0.006	0.000	0.041	0.036	0.000	0.074	0.000	0.000	0.000	0.000
POU	0.028	0.019	0.000	0.132	0.009	0.051	0.000	0.000	0.000	0.074	0.000	0.000	0.000	0.000	0.008
RAS	0.000	0.077	0.000	0.000	0.000	0.000	0.000	0.000	0.000	0.000	0.000	0.000	0.056	0.000	0.000
SGR	0.061	0.000	0.037	0.167	0.018	0.052	0.000	0.034	0.054	0.000	0.000	0.056	0.000	0.000	0.037
STG	0.000	0.000	0.000	0.000	0.000	0.020	0.000	0.000	0.000	0.000	0.000	0.000	0.000	0.000	0.000
WHIT	0.000	0.000	0.000	0.000	0.092	0.000	0.000	0.000	0.000	0.000	0.008	0.000	0.037	0.000	0.000

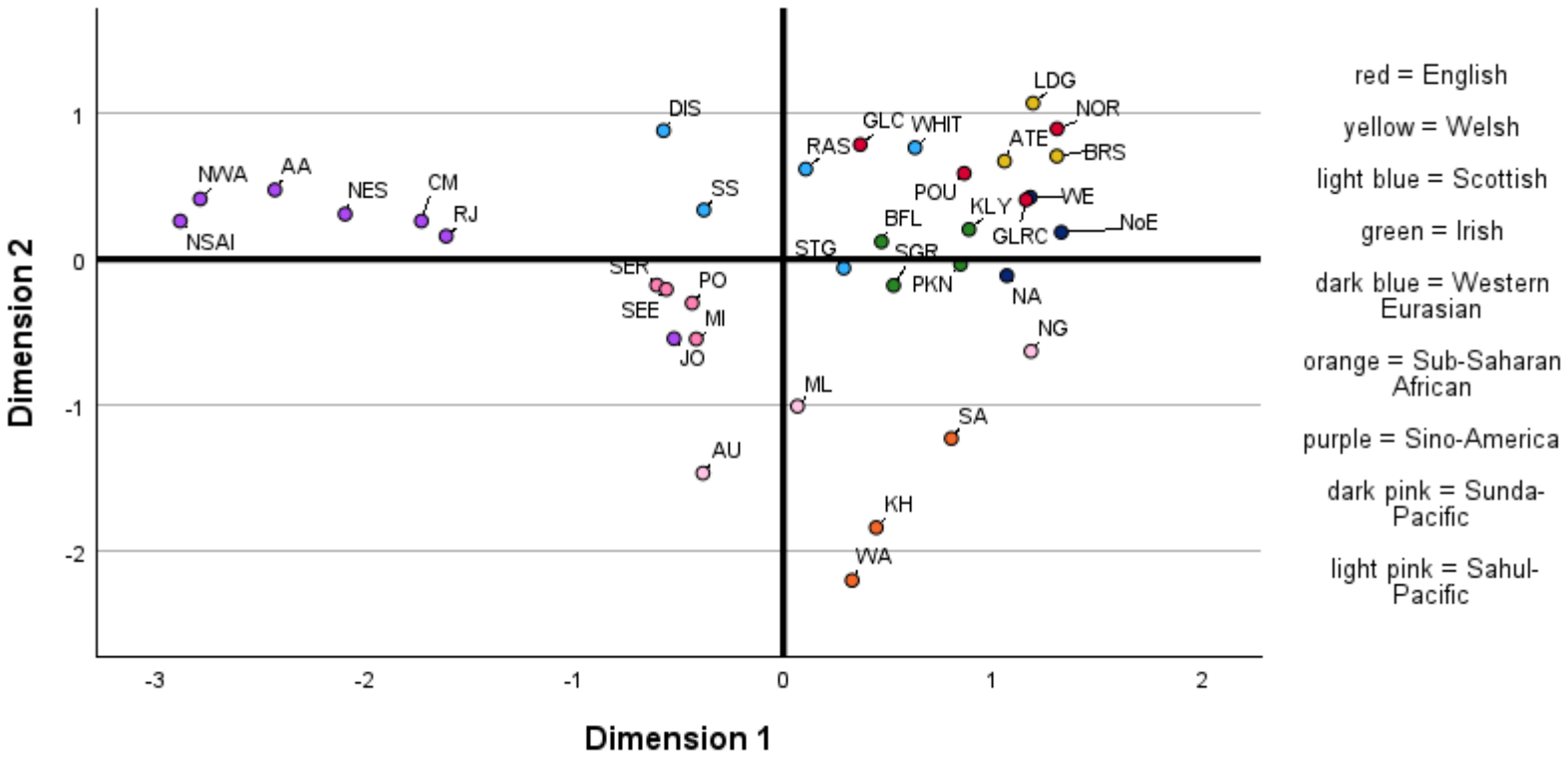

Figure 43: Two-dimensional MDS graph of 22-trait MMD values WE= Western Europe, NoE= Northern Europe, NA= North Africa, WA= West Africa, SA= South Africa, KH=Khoisan, CM= China-Mongolia, Jo= Jomon, RJ= Recent Japan, NES= Northeast Siberia, SS= South Siberia, AA= American Arctic, NWA= Northwest America, NSAI= N. & S. American Indian, SEE= Southeast Asia (Early), SER=Southeast Asia (Recent), PO= Polynesia, MI= Micronesia, AU= Australia, NG= New Guinea, ML= Melanesia, NOR= Norton Priory, Runcorn, POU= Chapel House Farm, Poulton, GLC= St. Owen's Church Gloucester, GLRC= London Road, Gloucester, LDG= Great House Farm, Llandough, ATE= site 92, Atlantic Trading Estate, Barry, BRS= Brownslade Barrow, Castlemartin, CLV= Culver Hole, Llangennith, TKW= Tinkinswood Burial Chamber, St. Nicholas, STG= Strath Glebe chambered cairn, Skye, DIS= Distillery Cave, Oban, RAS= Raschoille Cave, Oban, WHIT= Whithorn Priory, Dumfries and Galloway, SGR= Southgreen, Kildare, PKN= Parknahown 5, Co. Laois, KLY= Killeany 1, Co. Laois, BFL= Bushfield/Lismore, Co. Laois

Chapter 7: Discussion

In this chapter, the archaeological evidence and previous research (see Chapters 2 and 4) are used to contextualise the results of this study (see Chapter 5). The research questions and hypotheses outlined in Chapter 1 are addressed sequentially.

Do British and Irish populations exhibit phenetic variation patterns that support the concept of the Irish Sea Province?

This question explores whether the inter-sample phenetic variation aligns with the patterns seen in the archaeological record. The intent is to establish whether a biological mechanism such as migration is an underlying cause in the patterns seen. Findings suggest that there is gene flow among populations which broadly agrees with the patterns in the archaeological material.

The Irish Sea Province, as defined in Chapter 3, comprises areas of Britain and Ireland that share cultural elements evidenced by patterns in archaeological material. This thesis examines whether these patterns result from mechanisms lacking a biological component—such as cultural diffusion or trade—or whether a biological component, such as population admixture or replacement, is involved.

As noted previously (Chapter 5), only a minority of sample pairings showed significant differences. The majority did not, in both the MMD analysis of 36 traits (72 out of 78 pairings) and the MMD analysis of 17 traits (68 out of 78 pairings) (see Tables 4 and 5). Consequently, the null hypothesis—that

there is no significant difference in non-metric trait frequencies between British and Irish populations—cannot be rejected.

Given that most pairings are not significantly different and that MMD values are generally low (36-trait MMD: 0–0.127; 17-trait MMD: 0–0.169) (Tables 4 and 5), the results suggest close affinities within and among British and Irish populations. This pattern does not support Sheridan's (2004) model of "relatively long-distance and exclusive connections," as such a model would predict a higher number of significant differences. However, the data may still align with Sheridan's "commonality of origins" or "regular and sporadic contact" models (see relevant discussion).

The group clusters observed in the MDS graphs for both the 36- and 17-trait MMD analyses (Figures 39–42) show parallels with some archaeological evidence. Firstly, Irish samples are clustered with English ones. For instance, Anglo-Saxon archaeological material has been found at Parknahown 5 (see page 112), mirroring finds of Anglo-Saxon objects at other Irish sites (see page 112). This may indicate gene flow from Anglo-Saxon groups in England into Ireland.

Secondly, Scottish samples are clustered with Welsh samples. Early Medieval cemeteries at Llandough and Whithorn Priory exhibit similar burial practices, such as the inclusion of iron knives as grave goods and the use of burial pebbles (see pages 79 and 80). Furthermore, isotopic analyses have shown that the Whithorn Priory sample includes non-local individuals (Müldner, Montgomery et al., 2009; Montgomery, Müldner, and Cook,

2009), which may explain the close affinities between the Llandough (LDG) and Whithorn (WHIT) samples.

Conversely, some clusters are inconsistent with patterns found in archaeological, linguistic, and historical evidence. For example, the similarities between megalithic monuments in Wales and Scotland and those in Ireland (see page 34), as well as evidence of Irish presence in Wales and Scotland—such as ogham stones and the formation of the Dál Riata and Dyfed kingdoms (see pages 41 and 42)—suggest contact based more on trade and cultural diffusion than on significant population movement. This supports Alcock's (1970) argument that a lack of material transfer indicates superficial contact. The divergence between dental data and other evidence may be due to sampling limitations, as the Irish dataset is restricted to a narrow area (three samples from County Laois and one from County Kildare). Therefore, the relationships of Irish groups in contact with Wales and Scotland may not be fully represented.

The Brownslade Barrow (BRS) sample is particularly distinct, with seven out of 13 pairings in the 17-trait MMD analysis showing significant differences. Its closest affinities are to other Welsh samples (see Tables 4 and 5), suggesting limited contact with populations from other regions. However, pairings with Irish (Parknahown 5, PKN) and Scottish (Strath Glebe, STG; Whithorn Priory, WHIT) samples are not significantly different. These findings are consistent with isotopic analyses indicating that most individuals were local to Wales, though some may have originated from western Ireland or north-western Scotland (Groom et al., 2011; see page 77). This suggests that certain populations within the Irish Sea

Province experienced more localized interactions rather than widespread regional contact, contrary to what the concept generally implies.

Whithorn Priory (WHIT), in contrast, shows no significant differences from any other sample in either MMD analysis (see Tables 4 and 5). These results align with Adler's (2005) findings of close affinities between Whithorn and Irish samples. The similarities to English samples are consistent with Whithorn's historical association with Northumbria (Hill, 1997). Furthermore, isotopic data suggest that some individuals buried at Whithorn were non-local. Given that these individuals were identified as bishops rather than laypeople (see page 103) and considering the site's ecclesiastical significance, it is plausible that religious factors influenced patterns of population movement in the Irish Sea Zone. This interpretation is supported by the Norton Priory sample, another ecclesiastical site, which showed no significant differences in the 36-trait analysis and only one in the 17-trait analysis (with Brownslade Barrow), alongside overall low MMD values (see Tables 4 and 5).

In summary, the phenetic variation observed in the samples supports the hypothesis that gene flow occurred among populations in the Irish Sea Zone, alongside trade and cultural diffusion. Overall, there is broad agreement between the dental data and the archaeological record, although some discrepancies exist. These may be attributed to sampling limitations—particularly the lack of representation from Northern Ireland—or to differing patterns of contact across specific regions.

Were Scottish populations genetically influenced by Irish populations in the Early Medieval period?

This question explores whether the MMD distances suggest that Scottish populations were genetically influenced by the Irish populations in the Early Medieval. This improves the understanding of the nature of Irish activity in Scotland in the Early Medieval, e.g. whether the establishment of the kingdom of Dál Riata and the introduction of Gaelic into Scotland involved migration of Irish into Scotland. Findings suggest that Irish populations did genetically influence Scottish populations, however, it is similar to or less than the influence by Welsh or English populations.

Connections between Scotland and Ireland had a noticeable impact during the Early Medieval period, particularly with the establishment of the kingdom of Dál Riata between north-eastern Ireland and western Scotland (Alcock, 1970), and the introduction of Gaelic into Scotland around 500 AD (Gillies, 2009).

Due to limitations in sample availability, this study includes no Irish samples from before or after the Early Medieval period, and no Scottish samples specifically from the Early Medieval period. Therefore, inferences must be drawn using MMD values from the Irish Early Medieval samples (BFL, KLY, PKN, and SGR), the Scottish Medieval sample (WHIT), and the Neolithic Scottish sample (STG) (see Tables 4 and 5), alongside trait frequencies from the Neolithic samples at Distillery Cave, Oban (DIS) and Raschoille Cave, Oban (RAS) (see Table 2).

In the 36-trait MMD analysis, none of the Irish samples show significant differences from Strath Glebe (STG) or Whithorn Priory (WHIT) (see Table 4). In the 17-trait MMD analysis, only a minority of pairings (two out of eight) exhibit significant differences (see Table 5). As such, the null hypothesis—that there are no differences in non-metric trait frequencies between Early Medieval Irish populations and Scottish populations—cannot be rejected.

From the 17-trait MMD data (Table 5), several observations can be made. First, Whithorn Priory (WHIT) shows closer affinities to Irish samples than Strath Glebe (STG) does, with the exception of Southgreen (SGR). This suggests Irish genetic influence in Scotland between the Neolithic and Medieval periods. The presence of Irish activity in the area is further supported by the discovery of a Hiberno-Norse settlement near Whithorn Priory, dated from 850 AD to the mid-12th century (Hill, 1991).

Second, Whithorn Priory shows no significant biological differences from any Welsh sites (ATE, BRS, and LDG). This is supported by previously discussed archaeological parallels, such as the use of iron knives and burial pebbles at both Great House Farm, Llandough, and Early Medieval burials at Whithorn Priory (Holbrook and Thomas, 2005). Additionally, long cist burials—found at Brownslade (BRS)—were also the predominant form of burial in Early Medieval Scotland (Groom et al., 2011; Maldonado, 2013).

Third, Whithorn Priory has closer affinities to all English samples (NOR, GLRC, GLC, and POU) than Strath Glebe does. This aligns with findings from Adler (2005), who observed that Whithorn displayed more similarity

to English samples than to other Scottish ones. This may suggest that parts of Scotland were influenced or even partially peopled by individuals from England.

The three-dimensional MDS graph from the 17-trait MMD analysis (Figure 41) supports the conclusion of widespread affinities, as Whithorn is positioned centrally. The two-dimensional MDS graph (Figure 42) places Whithorn among Welsh samples on the right side, suggesting a particularly close relationship with Welsh populations.

In contrast, the 36-trait MMD values (Figures 39 and 40) show Strath Glebe (STG) as more closely related to other samples than suggested by the 17-trait MMD data, with no significant differences from Killeany (KLY) and Poulton (POU). In the three-dimensional MDS graph for the 36-trait MMD analysis (Figure 39), Scottish samples remain close to other regions, but the positions of Whithorn and Strath Glebe are reversed compared to the 17-trait graph (Figure 41), with Strath Glebe now centrally located. The two-dimensional model for the 36-trait MMD (Figure 40) shows similar shifts. Despite these changes, all graphs consistently indicate a close affinity between Scotland, Ireland, and Wales in the medieval period, thereby supporting the presence of gene flow either in the Early Medieval or earlier.

By calculating the mean 17-trait MMD values for sample pairings with Strath Glebe and comparing them to those with Whithorn (see Table 5), regional changes in affinity to Scotland from the Neolithic to the Medieval can be evaluated. The mean MMD values are as follows:

- Ireland–STG: 0.128; Ireland–WHIT: 0.039
- Wales–STG: 0.130; Wales–WHIT: 0.000
- England–STG: 0.156; England–WHIT: 0.018

These results show noticeable reductions in mean MMD values for all regions when compared to Whithorn. Ireland shows the smallest change, suggesting consistent affinity over time. Wales has the lowest mean MMD with Whithorn, indicating particularly strong ties, while England shows the greatest increase in affinity between the Neolithic and Medieval periods. Overall, the very low MMD values for all regions relative to Whithorn suggest gene flow from, or to, Scotland from all these regions. However, the pattern indicates that Ireland may have exerted the least genetic influence, with Wales and England having a greater impact.

There are ten traits are consistently high-frequency across all regions, and five traits are consistently low-frequency (see Table 2), further supporting the interpretation of widespread gene flow between Scotland and surrounding regions. The trait frequencies from Distillery Cave (DIS) and Raschoille Cave (RAS) differ noticeably from those in other regions (see Table 2), suggesting regional variation or earlier population differentiation.

In conclusion, dental data—when considered alongside archaeological and historical evidence—suggest that Irish populations had contact with, and exerted some genetic influence on, Scottish populations between the Neolithic and Medieval periods. However, the degree of this genetic influence appears to be similar to, or possibly less than, that from Wales and England. Thus, the cultural impact of Irish groups on Scottish populations

likely occurred through a combination of trade, cultural diffusion, and gene flow.

Were English populations genetically affected by Viking and Anglo-Saxon activity in the Early Medieval period?

This question explores whether the MMD distances suggest that the English populations saw genetic influence as a result of the Anglo-Saxon or Viking activity in the Early Medieval period. This improves the understanding of the nature of Anglo-Saxon and Viking activity in England during the Early Medieval and the effect that they had on English populations. Findings suggest Anglo-Saxon activity may have genetically influenced English populations, although this is not conclusive, and there was no evidence of Viking activity genetically affecting the samples.

As noted by Gretzinger et al. (2022), the Anglo-Saxon settlement remains one of the most intensely debated subjects in British history. Similarly, Robinson (2003) highlights that the processes by which Viking populations merged with local British communities are only beginning to be properly explored. This thesis investigates whether English populations included in this study experienced phenetic changes potentially attributable to Anglo-Saxon or Viking migrations.

Unfortunately, this study does not include any Early Medieval samples from England. As such, the impacts of these migrations must be inferred through a comparison of Medieval samples (GLC, NOR, and POU) and a Roman-period sample (GLRC). In the 17-trait MMD analysis, none of the Medieval

English samples show significant differences from the Roman Gloucester sample (GLRC), and the vast majority of pairings with other regional samples are also not statistically significant (see Table 5). Consequently, the null hypothesis—that there is no difference between English and other populations—cannot be rejected.

Although no significant differences were found, the 17-trait MMD analysis reveals that Norton Priory (NOR) shows greater affinity with Roman Gloucester (GLRC) than with Medieval Gloucester (GLC) (Table 5). St. Owen's Church, Gloucester (GLC), exhibits elevated frequencies of traits such as cusp number LM2, hypocone UM2, and UI1 shovelling relative to both NOR and GLRC (see Table 2). Two interpretations are possible:
A) The population at Norton Priory, contemporary with that of Roman Gloucester, retained common origins into the Medieval period, while Medieval Gloucester received gene flow from a distinct population, possibly of Anglo-Saxon origin.
B) Norton Priory and Poulton (POU) may have continued receiving gene flow from Roman Gloucester populations, while Medieval Gloucester diverged due to gene flow from other groups.

The former explanation appears more plausible, given the strong evidence of Roman activity in Cheshire. Chester, for example, was established and controlled by the Romans from AD 49 to AD 400 (Rudlin, Thompson, and Jarvis, 2016). Numerous Roman artefacts—including amphorae sherds and metalwork such as a buckle loop and plate—have been recovered from Chester (O'Leary, 2018). Furthermore, excavations at Poulton, Cheshire,

uncovered Roman tiles stamped with "LEG XX," indicating manufacture by the 20th Legion (Wessex, 2007). Gloucester's Roman origins similarly support this view, with the fortress at Kingsholm established in the AD 40s and later relocated to modern Gloucester (Simmonds et al., 2008; Hurst, 1972, 1974).

In addition, the 17-trait MMD analysis (Table 5) shows that St. Owen's Church, Gloucester (GLC), has its closest affinities with Southgreen, Kildare (SGR) and Whithorn Priory (WHIT). Whithorn's association with Northumbria (Hill, 1997) suggests a possible Anglo-Saxon influence. Southgreen's connection to Britain is less direct; however, a gaming piece found as a grave good—similar to those in Scotland and featuring Sutton Hoo-style helmets—indicates cultural exchange. While the Scottish gaming pieces date from the 5th to 7th centuries AD, the Southgreen burial dates to 263–422 AD (Murphy and Gibney, 2021), which predates the Anglo-Saxon period. These inhumation burials, novel in Ireland at the time, have been interpreted as signs of British contact in the Late Iron Age.

Moreover, St. Owen's Church (GLC) shows closer affinities to most Irish samples—excluding Bushfield/Lismore (BFL)—compared to Roman Gloucester (GLRC) (Table 5). Similarly, Parknahown (PKN) provides archaeological evidence of Anglo-Saxon connections, including a zoomorphic copper-alloy penannular brooch and a cylindrical bronze bead with decoration resembling Sutton Hoo artefacts (O'Neill, 2009).

Further comparisons between the two Gloucester samples reveal that St. Owen's Church (GLC) is significantly different from Great House Farm,

Llandough (LDG), whereas Roman Gloucester (GLRC) is not. Additionally, GLC displays closer affinities to Strath Glebe (STG) and Poulton (POU) (Table 5). These findings suggest that Medieval Gloucester received gene flow from more geographically distant populations than Roman Gloucester, although this does not conclusively indicate an Anglo-Saxon source, as such gene flow could also originate from native British groups.

Regarding other English samples, Norton Priory (NOR) is significantly different only from Brownslade Barrow (BRS), and Poulton (POU) differs only from BRS and Strath Glebe (STG). As discussed elsewhere, BRS is the most phenetically distinct sample in both the 36- and 17-trait MMD analyses, and STG is the earliest dated sample in the study. These differences are likely due to temporal, geographical, or cultural isolation rather than gene flow into the English samples.

Despite the MMD values suggesting that St. Owen's Church (GLC) may have greater affinities with non-local populations than Roman Gloucester (GLRC), the two-dimensional and three-dimensional MDS plots from the 17-trait analysis (Figures 35 and 36) show that GLC is more loosely grouped with other English samples than is GLRC. This would argue against strong Anglo-Saxon genetic influence. Conversely, the three-dimensional MDS graph from the 36-trait MMD analysis (Figure 33) shows the opposite: GLC appears more closely grouped with other English samples than GLRC, potentially supporting a greater Anglo-Saxon genetic impact.

In summary, while the affinities among English samples suggest that Anglo-Saxon activity may have influenced the genetics of the populations represented, the evidence is not statistically significant. The patterns observed could equally reflect continuity from Roman populations or gene flow from other British regions. Importantly, no evidence was found for Viking influence on the sampled populations, as none of the sites involved revealed material connections to Viking activity. Thus, while Anglo-Saxon influence cannot be entirely ruled out, its genetic impact appears to have been limited or at least indistinct based on the current data.

Are the morphological differences between the samples explained by the isolation-by-distance model?

This question explores whether phenetic differences observed in the samples can be explained by the isolation-by-distance model by comparing the MMD distance and geographic distance matrices. This is to improve understanding of the factors driving the phenetic differences seen in the samples. Findings suggest that the isolation-by-distance model may contribute marginally to the observed phenetic differences, but contributory factors are more complex.

As discussed in Chapter 5, both Mantel tests comparing the 36-trait and 17-trait MMD values to geographical distances reveal a weak positive relationship between morphological and spatial distance. However, neither result reached statistical significance; thus, the null hypothesis, that there is no correlation between morphological and geographical distance, cannot be rejected.

Contrary to what would be expected under the isolation-by-distance (IBD) model, the sample pairing with the greatest geographical distance (ATE–STG; 670.41 km) exhibits relatively small MMD values (36-trait MMD: 0.033; 17-trait MMD: 0.080). In contrast, the pairing of BRS–STG, which covers a shorter geographical distance, produced the highest MMD values (36-trait MMD: 0.148; 17-trait MMD: 0.390). This anomaly suggests that isolation by distance may not be the primary factor explaining phenetic variation between samples. Furthermore, it is possible that isolation-by distance is not a factor due to the small overall distances and low divergence between samples. Typically, isolation-by-distance model is more appropriate for larger geographic distances such as on a continental or global scale.

Dental data show that, while overall affinities are relatively close, some regional clustering is evident. This supports the notion of frequent small-scale migrations between nearby populations. This is consistent with findings from previous stable isotope studies, which have revealed individual and small-group migrations within Britain and also from continental Europe and Scandinavia (Budd et al., 2004; Müldner, Montgomery et al., 2009; Montgomery, Müldner and Cook, 2009; Shaw et al., 2016).

Moreover, major historical migrations—such as those of the Anglo-Saxons and Vikings—are well attested (see Chapter 2). While the source populations for these migrations lie outside the scope of this dataset, their gene flow may have affected the included regions contemporaneously. This

could result in lower MMD values between samples that did not exchange genes directly but were both influenced by similar external sources. Although speculative due to the absence of comparative extra-regional samples, previous research has found morphological and genetic similarities between Scotland, England, and Northern Europe (Adler, 2005).

One notable outlier is Brownslade Barrow (BRS), which is significantly different from more samples than any other in the study. In the 17-trait MMD analysis (Table 5), BRS is not significantly different from the other Welsh samples (ATE and LDG), the Scottish samples (STG and WHIT), or half of the Irish samples (BFL and SGR). However, it is significantly different from all English samples (GLRC, GLC, POU, and NOR) and the remaining Irish samples (KLY and PKN). This pattern could be explained by limited gene flow between the English and Irish samples, or by separate extra-regional gene flow into certain areas that did not affect others. Martiniano et al. (2016) also found that Welsh populations diverge phenetically and genetically from eastern English groups.

The distinctiveness of the Brownslade Barrow sample is further supported by trait frequencies. BRS exhibits elevated frequencies of labial curvature in UI1, incisal grooving in UI2, and additional roots in UM2, along with low frequencies of LM2 groove patterns compared to the other samples. These could result from gene flow from a different source not represented in this dataset, or from genetic drift acting on a relatively isolated population.

Another factor potentially influencing the results is the use of straight-line (Euclidean) distances to estimate spatial relationships. Migration routes are

often shaped by topography and accessibility rather than direct distance. Several topographical barriers exist between British and Irish regions, including the Irish Sea—a body of water with tidal-driven currents that could influence travel routes and timing (Robinson, 1979). In Scotland, major physical barriers include the Grampian Mountains and the Southern Uplands (e.g., Galloway Hills, Lowther Hills, and Merrick). Similarly, Welsh topography includes ranges such as the Bannau Brycheiniog (Brecon Beacons), Cambrian Mountains, Black Mountains, and Preseli Hills. Such terrain may make it more feasible to migrate to geographically farther locations if they are more accessible by natural corridors like rivers. Konigsberg (1990) notes that riverine routes can facilitate movement better than uplands, and Buikstra (1977) demonstrated that river distances often correlate more strongly with biological variation than straight-line distances.

In sum, although isolation by distance may contribute marginally to observed phenetic differences, it does not appear to be a dominant explanatory model for this dataset. Instead, the data suggest a complex interplay of factors, including small-scale mobility, cultural and geographical isolation, gene flow from external populations, and topographic constraints on migration. These findings underscore the importance of considering both biological and environmental variables when interpreting population structure in archaeological contexts

Comparisons to Global Populations

In this section, the similarities and dissimilarities between the British and Irish samples and other global populations are discussed. The findings

suggest that the British and Irish samples are concordant with other Western Eurasian groups, and that British and Irish MMD distances can be compared with broader groups to infer patterns of gene flow.

As discussed in Chapter 6, the samples tend towards simpler, mass-reduced dentitions, a pattern described by the term 'Eurodont', which has been proposed for Western Eurasian dental morphological variation exhibiting this trend. The Eurodont pattern is characterised by low frequencies of winging UI1, shovelling UI1, double shovelling UI1, Bushman canine UC, enamel extensions UM1, Y pattern LM2, cusp 6 LM1, cusp 7 LM1, protostylid LM1, deflecting wrinkle LM1, and three-rooted molar LM1, alongside high frequencies of Carabelli's cusp UM1, two or more lingual cusps LP1, three-cusped UM2, four-cusped LM1 and LM2, and two-rooted canines LC (Scott et al., 2013).

The mean frequencies for the British and Irish samples broadly conform to this pattern, with some exceptions. Notably, there is a high mean frequency of protostylid LM1 (45.77%), which is typically rare in Western Eurasians (Scott and Irish, 2017), and a mean frequency of the deflecting wrinkle (21.33%), which falls within Scott and Turner's (1997) intermediate category (20–35%). The elevated frequency of protostylid LM1 is consistent with previously reported rates for Irish and Scottish populations. Other traits, such as Carabelli's cusp UM1, cusp 7 LM1, and hypocone UM2, are comparable to those reported for England, Scotland, and Ireland, although some variation exists, for example in shovelling UI1 (Adler, 2005).

When comparing the frequencies of the 22 traits between the British and Irish samples and global groups, the majority of traits (14 out of 22) show greater similarity to Western Eurasian groups (see Figures 62, 64, 66, 67, 68, 69, 70, 72, 73, 75, 76, 80,81 and 82), while a minority (8 out of 22) differ and appear more similar to groups from other regions (see Figures 63, 65, 71, 74, 77,78, 79, and 83). As noted previously (see Chapter 6), some trait frequencies, particularly those from Tinkinswood, are affected by small sample sizes and may therefore not provide an accurate representation.

The British and Irish samples show the closest affinities to Western Eurasian groups. For Western Europe, the mean MMD value is 0.043 (lowest: STG–WE = 0.000; highest: DIS–WE = 0.152; second highest: GLC–WE = 0.150). For Northern Europe, the mean MMD value is 0.041 (lowest: BFL–NoE = 0.000; KLY–NoE = 0.000; WHIT = 0.000; highest: DIS–NoE = 0.239; second highest: GLC–NoE = 0.144). For North Africa, the mean MMD value is 0.061 (lowest: BFL–NA = 0.000; KLY–NA = 0.000; RAS–NA = 0.000; STG–NA = 0.000; highest: GLC–NA = 0.166). In contrast, the most distant group is North and South American Indians (mean MMD value: 0.564; highest: NOR–NSAI = 0.751; lowest: DIS–NSAI = 0.188) (see Table 7). Other mean MMD values range from low to high (0.061–0.543) (see Table 7).

Given the geographical location of Britain and Ireland in northwestern Europe, these close affinities with Western and Northern Europe are expected. The slightly closer similarity to Northern Europe compared to

Western Europe may reflect Viking activity in these regions during the early medieval period.

These relationships are also reflected in the MDS plot for the 22-trait MMD analysis, where most British and Irish samples cluster in the upper right of the graph alongside Western and Northern European groups (see Figure 43). An exception is Distillery Cave, Oban (DIS), which is positioned further towards Sino-American and Sunda-Pacific groups on dimension 1, although it remains similar to other British and Irish samples on dimension 2. This deviation is likely due to the small sample size for this site.

Previous research has suggested that a cline of primitive-to-derived trait frequencies parallels migration pathways, supporting an out-of-Africa model, with increasing derived trait frequencies observed in North Africa, Europe, Asia, the Americas, and Oceania (Irish et al., 2014). This pattern is reflected in the grouping of Sino-American populations, where the Jomon are closest to Sub-Saharan African groups on dimension 1, and populations progressively shift along migration routes, culminating in North and South American Indians being the most distant (see Figure 43).

A similar pattern is broadly visible among Western Eurasian groups, with North African samples closest to Sub-Saharan African groups on dimension 2 and British samples the most distant. However, this pattern is less clear than in Sino-American groups and does not fully match expectations. Irish samples often appear closer to Sub-Saharan African groups than many British samples, and some northern samples (e.g., NOR) are closer than more southerly ones (e.g., LDG) (see Figure 43). This suggests that

migration patterns in Britain, Ireland, and Europe are complex, supporting the findings of the IBD analysis.

The 36-trait and 17-trait MMD values show parallels with those reported for Native American populations by Scott and Dahlberg (1973). Among Native American groups, the Zuni exhibited the highest mean MMD value (0.108), reflecting their linguistic and archaeological distinctiveness, while their closest affinity was with the geographically proximate Hopi (MMD = 0.064). Similarly, among the British and Irish samples, Brownslade Barrow (BRS) shows the highest mean MMD values (36-trait: 0.052; 17-trait: 0.174), consistent with archaeological evidence indicating distinctiveness from other groups in west Wales (Groom et al., 2011). Its closest affinities are also with nearby Welsh sites (e.g., ATE and LDG).

This suggests that similar processes—such as localised gene flow between geographically proximate groups—may influence morphological variation without necessarily affecting cultural distinctiveness. Linguistic barriers, for example, have been shown to restrict cultural transmission more than gene flow (Ross, Greenhill and Atkinson, 2013), which may explain such patterns.

The Navajo, identified as a composite population, show relatively low differentiation from other Native American groups (mean MMD = 0.062). A comparable pattern is observed at Site 91, Atlantic Trading Estate, Barry (ATE), which shows the lowest mean MMD among the British and Irish samples (0.014). Although there is no direct archaeological evidence of

migration, the site's multi-period use and coastal location suggest it may have facilitated gene flow, resulting in a composite population.

Similarly, Parknahown 5 (PKN) and Whithorn Priory (WHIT) display close affinities with multiple samples (PKN mean MMD: 0.025; WHIT: 0.033). Archaeological and historical evidence indicates these were high-status sites with evidence of cultural exchange or migration (e.g., Broun, 2000; McCormick and Petts, 2008; Müldner et al., 2009; O'Neill, 2009), suggesting sustained gene flow and population mixing.

Unexpected similarities, such as between the Navajo and Hopi, have been attributed to gene flow during periods of small population size. A comparable case may be seen between London Road, Gloucester (GLRC) and Whithorn Priory (WHIT), which show close similarity despite geographical and temporal separation. This may reflect earlier gene flow, potentially supported by archaeological evidence from Whithorn, such as late Roman amphorae, indicating long-distance contacts.

Overall, the British and Irish MMD values and trait frequencies show strong affinities with Western Eurasian populations and align with patterns expected under a primitive-to-derived trait cline consistent with the out-of-Africa model. At a finer scale, comparisons with Native American populations suggest that similar processes—such as gene flow, population structure, and local interaction—may underlie patterns of morphological variation across different global regions.

Chapter 8: Summary and Conclusions

This study was conducted with the aim of contributing a biological perspective to the understanding of migrations in Britain and Ireland. The goal was to help clarify population processes that remain uncertain due to conflicting historical narratives and archaeological evidence, which can be challenging to interpret. A further objective was to address gaps in knowledge concerning regional variability in dental non-metric traits across Europe.

These goals were achieved by characterising the frequencies of dental non-metric traits across 17 sites in western Britain and Ireland. Data were collected from a substantial number of 570 individuals. Notably, most of these sites—excluding a few, such as Whithorn Priory—had not been previously included in dental affinity studies. As such, this research presents the first detailed analysis of their dental non-metric trait variation and their phenetic relationships with other sites in the region.

Overall, the observed trait frequencies display a pattern of reduced dentition and mass additive traits, consistent with patterns typically seen in European and high-latitude populations. Of the 36 traits examined, 15 displayed similar frequencies across all regions, while the remaining traits exhibited regional variation in high and low frequencies (see pages 133–139 and see Table 2 for full trait distribution).

The dental affinities identified in this study were used to address the research questions and test the hypotheses presented in Chapter 1:

Do British and Irish populations exhibit phenetic variation patterns that support the concept of the Irish Sea Province?

The null hypothesis—that there is no significant difference in non-metric trait frequencies based on MMD distances between British and Irish populations—could not be rejected. The dental data indicate strong affinities among the majority of populations in western Britain and Ireland, supporting the concept of an "Irish Sea Zone." However, the phenetic patterns observed may differ from those suggested by the archaeological record, implying that the nature of contact across the region was complex and multi-faceted.

Were Scottish populations genetically influenced by Irish populations in the Early Medieval period?

The null hypothesis—that there is no significant difference in non-metric trait frequencies based on MMD distances between Early Medieval Irish and Scottish populations—could not be rejected. The dental data support the idea that Irish populations contributed genetically to Scottish groups, with stronger affinities observed between Irish and Scottish samples than between Scottish samples and those from England or Wales. These findings align with previous dental affinity studies (Adler, 2005) and archaeological research (Groom et al., 2011; Hill, 1991; Holbrook and Thomas, 2005; Maldonado, 2013) and suggest more substantial interaction than the superficial contact proposed by Alcock (1970).

Were English populations genetically affected by Viking and Anglo-Saxon activity in the Early Medieval period?

The null hypothesis—that there is no significant phenetic difference within English populations or between English and other regional groups—could not be rejected. While the dental data suggest that Anglo-Saxon migration contributed to the English Medieval gene pool, it does not indicate large-scale population replacement. Instead, the results are consistent with a model of population continuity, as previously observed in other dental affinity studies (Lloyd-Jones, 1995, 1999). Moreover, similar migratory influences may be detected in Irish and Scottish samples as well.

Are the morphological differences between the samples explained by the isolation-by-distance model?

The null hypothesis—that non-metric trait variation is not significantly associated with geographic distance—could not be rejected. The data suggest that patterns of gene flow and migration in the region are more complex than those predicted by the simple, linear "stepping-stone" model. Straight-line distances likely do not capture the true nature of historical migration pathways, which would have been shaped by topography, waterways, and socio-political factors. These findings indicate that the dynamics influencing western Britain may differ from those observed elsewhere on the island, such as in Barkmeier's (2020) study of cranial non-metric traits, which did detect isolation-by-distance effects.

In conclusion, this study reveals close and intricate relationships in population movements across western Britain and Ireland during the Early

Medieval period. While the research does not pinpoint specific migration pathways, it challenges previously suggested models such as Sheridan's (2004) concept of "relatively long-distance and exclusive connections" and the invasion model often invoked in the context of Anglo-Saxon England (Lloyd-Jones, 1999). The findings advocate instead for a model of frequent, small-scale mobility and complex regional interactions.

Research Limitations

Although this study includes dental data from a relatively large number of individuals (570), several limitations affected the scope and representativeness of the analysis. The primary constraint was the uneven geographic distribution of sites across Britain and Ireland. In particular, poor skeletal preservation in regions such as Wales and Scotland—largely due to acidic soil conditions (Hemer et al., 2013; Maldonado, 2013)—resulted in a limited number of suitable samples from these areas. Secondly, the number of individuals included in the study does not fully represent the number of observations for any given trait as some traits may not be observable in an individual due to factors such as tooth loss and wear, e.g. traits such as shovelling UI1 or deflecting wrinkle LM1 are susceptible to wear.

Burial and funerary practices also significantly impacted the availability and condition of skeletal remains. In the Neolithic period, collective primary deposition, as well as secondary and tertiary deposition, were common (Fowler, 2010). These practices often led to disturbed remains, and intentional selection of certain skeletal elements further affected the

representation of anatomical features. Additionally, cremation, which was a prevalent burial practice across different periods, posed a major limitation for this study. In Britain, cremation was dominant during the Bronze Age (from the early second millennium BC to c. 1100 BC), and again in the 2nd and 1st centuries BC, before being replaced by inhumation in the 2nd/3rd centuries AD. In Ireland, cremation remained common from 1000 BC until the increased prevalence of extended inhumation between c. 1–400 AD (Brück, 2006; McGarry, 2007). The challenge with cremated remains lies in the fragmentation of tooth enamel during the process (McKinley, 2000), which renders dental trait analysis largely impossible. As a result, some chronological periods are underrepresented or entirely absent from the dataset.

Access to skeletal collections also posed logistical limitations. These collections are typically housed in museums or universities and are subject to institutional policies and availability. During the data collection phase, access was further restricted by the COVID-19 pandemic. Lockdowns temporarily suspended access, and even after restrictions were lifted, delays persisted. Furthermore, access to relevant collections in the Republic of Ireland was not possible during the research period, which limited the inclusion of additional Irish material.

Future Research

This study focused on sites located in the western regions of Britain and Ireland, subdivided into England, Wales, Scotland, and Ireland. However, several geographic gaps remain. Notably, there are no samples from North

Wales or Northern Ireland. Expanding future studies to include these underrepresented areas would provide a more comprehensive view of regional variation.

With respect to Ireland, this study only incorporated sites from County Laois and County Kildare. The inclusion of additional sites—particularly from Northern Ireland and coastal areas in the south such as County Dublin and County Wexford—would offer a broader understanding of Irish population history and help to refine current interpretations.

There are also temporal limitations in the present dataset. Only one Bronze Age sample was available, all Irish samples date to the Early Medieval period, and nearly all English samples are from the medieval period. Future research would benefit from incorporating samples spanning a wider range of time periods. This would improve our understanding of population continuity and change in response to historical events such as the Norman invasion of England and Ireland or the formation of Dál Riata and, later, the Kingdom of Alba in Scotland.

In some cases, it is possible to compare samples from different periods within the same localised area. For instance, both Early Medieval and Medieval burials are associated with Whithorn Priory (see Chapter 4). Including Early Medieval material from Whithorn alongside the Medieval sample already analysed would offer valuable insight into the population history of that community across time.

As this study was centred on the Irish Sea Province, it focused on western Britain. However, incorporating comparative material from eastern regions—such as Eastern Scotland and Eastern England—would provide important context and allow for evaluation of east-west differences and connections with Ireland. Similarly, as Viking activity was a widespread feature of the Early Medieval period across Britain and Ireland, the inclusion of samples from Scandinavia would allow for a more nuanced exploration of the Viking genetic impact and the extent to which it may explain affinities observed among British and Irish populations.

This study analysed dental non-metric traits exclusively. However, many of the skeletal collections examined also include cranial and post-cranial material that has not yet been assessed. Including these non-dental traits in future research would facilitate comparative analyses and may address some of the limitations encountered in this study—particularly the challenges related to preservation. Cranial or post-cranial traits, which may survive better in some contexts, could expand the sample size and temporal coverage.

Finally, while this study incorporated archaeological evidence in a descriptive capacity, future research could benefit from a more quantitative approach to integrating bioarchaeological and archaeological data. Methods such as multivariate analysis and spatial visualisation of archaeological assemblages could allow for more direct and meaningful comparisons with the dental data, deepening the interpretation of population movement and interaction patterns.

References

Abdi, H. and Williams, L.J., 2010. Principal component analysis. *Wiley interdisciplinary reviews: computational statistics*, *2*(4), pp.433-459.

Adler, A.J., 2005. *Dental anthropology in Scotland: morphological comparisons of Whithorn, St. Andrews and the Carmelite Friaries*. Arizona State University.

Alcock, L., 1970. Was there an Irish sea culture-province in the dark ages?'. *The Irish Sea Province in archaeology and history*, pp.55-65.

Alt, K.W., Loring Brace, C. And Türp, J.C., 1998. The history of dental anthropology. In *Dental Anthropology: Fundamentals, Limits and Prospects* (pp. 15-39). Vienna: Springer Vienna.

Anctil, M.J., 2016. *Ancient Celts: Myth, invention or reality? Dental affinities among continental and non-continental Celtic groups*. University of Alaska Fairbanks.

Anctil, M.J., 2020. *Ancient celts: A reconsideration of Celtic identity through dental nonmetric trait analysis*. Liverpool John Moores University (United Kingdom).

Armelagos, G.J. and Gerven, D.P.V., 2003. A century of skeletal biology and paleopathology: Contrasts, contradictions, and conflicts. *American anthropologist*, *105*(1), pp.53-64.

Armit, I., Sheridan, J.A., Reich, D., Cook, G., Tripney, B. and Naysmith, P., 2016. Radiocarbon dates obtained for the GENSCOT ancient DNA project, 2016. *"Discovery and excavation: Scotland"*, *17*.

Atkin, M. 1990. 'Excavations in Gloucester, 1989' in Rawes , B. (ed) *Glevensis 24: The Gloucester and District Archaeological Research Group Review.*

Atkin, M., and Garrod, A.P. 1990. Archaeology in Gloucester, 1989. *Transactions of the Bristol and Gloucester Archaeology Society*. Vol . 108, pp. 185-192.

Barkmeier, J.H., 2020. *The effects of feudalism on Medieval English mobility: A biological distance study using nonmetric cranial traits*. University of South Florida.

Bang, G. and Hasund, A., 1971. Morphologic characteristics of the Alaskan Eskimo dentition. I. Shovel-shape of incisors. *American Journal of Physical Anthropology*, *35*(1), pp.43-47.

Bateson, J.D., 1973. Roman material from Ireland: a re-consideration. *Proceedings of the Royal Irish Academy. Section C: Archaeology, Celtic Studies, History, Linguistics*, Literature, pp.21-97.

Berry, R.J., 1969. History in the evolution of Apodemus sylvaticus (Mammalia) at one edge of its range. *Journal of Zoology*, *159*(3), pp.311-328.

Berry, A .C., and Berry, R.J. 1967. Epigenetic variation in the human cranium. *Journal of Anatomy*, 101, pp.361-379.

Bittles, A.H. and Smith, M.T., 1991. ABO and Rh (D) blood group frequencies in the Ards Peninsula, northeastern Ireland: Evidence for the continuing existence of a major politico-religious boundary. *Annals of human biology*, *18*(3), pp.253-258.

Bownes, J., 2018. *Reassessing the Scottish Mesolithic-Neolithic transition: questions of diet and chronology*. Doctoral dissertation, University of Glasgow

Brace, S., Diekmann, Y., Booth, T.J., Faltyskova, Z., Rohland, N., Mallick, S., Ferry, M., Michel, M., Oppenheimer, J., Broomandkhoshbacht, N. and Stewardson, K., 2018. Population replacement in early Neolithic Britain. *Biorxiv*, p.267443.

Branigan, K. and Dearne, M.J., 1991. *A gazetteer of Romano-British cave sites and their finds*. University of Sheffield, Department of Prehistory and Archaeology.

Bronk Ramsey, C. *et al.* (2002) Radiocarbon dates from the Oxford AMS system: Archaeometry datelist 31. *Archaeometry* 44, Supplement 1, pp. 1-149.

Broun, C., 2000. St Ninian: Bishop of Candida Casa. *The Month*, *33*(11), p.440.

Brown, F., Howard-Davis, C., Bowden, A. and Carter, E., 2008. *Norton Priory: Monastery to Museum: Excavations 1970-87*. Oxford Archaeology North.

Brück, J., 2006. Death, exchange and reproduction in the British Bronze Age. *European Journal of Archaeology*, *9*(1), pp.73-101.

Bryk, J., Hardouin, E., Pugach, I., Hughes, D., Strotmann, R., Stoneking, M. and Myles, S., 2008. Positive selection in East Asians for an EDAR allele that enhances NF-κB activation. *PloS one*, *3*(5), p.e2209.

Budd, P., Millard, A., Chenery, C., Lucy, S. and Roberts, C., 2004. Investigating population movement by stable isotope analysis: a report from Britain. *Antiquity*, *78*(299), pp.127-141.

Buikstra, J.E., Frankenberg, S.R. and Konigsberg, L.W., 1990. Skeletal biological distance studies in American physical anthropology: recent trends. *American Journal of Physical Anthropology*, 82(1), pp.1-7.

Burnaby, T.P., 1966. Growth-invariant discriminant functions and generalized distances. *Biometrics*, pp.96-110.

Burnett, S.E., 2016. Crown wear: Identification and categorization. *A companion to dental anthropology*, pp.413-432.

Burrell, C.L., Gonzalez, S., Smith, L., Emery, M.M. and Irish, J.D., 2016. More than meets the eye: Paget's disease within archaeological remains. *American. Journal of Physical Anthropol*ology, *159*, pp.105-106.

Burrell, C.L., 2018. *Skeletal variation as a possible reflection of relatedness within three medieval British populations* (Doctoral dissertation, Liverpool John Moores University).

Burrell, C.L., Gonzalez, S., Layfield, R., Smith, L. and Irish, J.D., 2018, April. An ancient form of Paget's Disease at Norton Priory, UK. In *AMERICAN JOURNAL OF PHYSICAL ANTHROPOLOGY* 165, pp. 38-38). 111 RIVER ST, HOBOKEN 07030-5774, NJ USA: WILEY.

Buxton, L.H.D. 1932. Report on the human remains from Culver Hole. *Bulletin of the Board of Celtic Studies* 6 (2), pp. 198-200.

Campbell, E., 2001. Were the Scots Irish. *Antiquity*, *75*(288), pp.285-292.

Canmore.org.uk. No Date A. *Oban, Distillery Cave*

Canmore.org.uk, No Date B. *C14 Radiocarbon Dating - Index - Oban, Glenshellach Road*

Carabelli, G., 1842. *Anatomie des mundes*. Braumüller und Seidel.

Case, H., 1976. Acculturation and the earlier Neolithic in western Europe. *Acculturation and continuity in Atlantic Europe*, pp.45-58.

Champion, T. 2009. 'The Later Bronze Age" in Hunter, J. and Ralston, I. (eds) *The Archaeology of Britain: An Introduction from the Earliest Times to the Twenty-First Century*. 2nd ed. Abingdon: Routledge, pp. 126-148.

Colquhoun, I. and Burgess, C., 1988. *The swords of Britain* (Vol. 5). CH Beck.

Connelly, C., 2015. A partial reading of the Stones: a comparative analysis of Irish and Scottish Ogham pillar stones (Master's thesis, The University of Wisconsin-Milwaukee).

Connock, K. (1984) Oban, Glenshellach (Kilmore and Kilbride parish) ossuary cave. *Discovery and Excavation in Scotland 1984*, 24.

Connock, K.D., 1985. *Rescue excavation of the ossuary remains at Raschoille Cave, Oban: an interim report*. Lorn Archaeological and Historical Society.

Cooney, G., Mandal, S. and Byrnes, E., 1999. An Irish Stone Axe Project Report: Non-Porcellanite Stone Axes in Ulster. *Ulster Journal of Archaeology*, pp.17-31.

Cooney, G. and Mandal, S., 1998. *The Irish stone axe project* (Vol. 1). Wordwell.

Cooney, G., 2000. Genes and Irish origins. *Archaeology Ireland*, 14(2).

Cooney, G., 2001. Is it all in genes?. *Archaeology Ireland*, pp.34-35.

Cootes,K., Cowell, R. and Teather, A., 2016. III: Hunting for the gatherers and early farmers of Cheshire. *Journal of the Chester Archaeological Society 86*. Vol 86, pp. 11-31.

Coppa, A., Cucina, A., Mancinelli, D., Vargiu, R. and Calcagno, J.M., 1998. Dental anthropology of Central-Southern, Iron Age Italy: The evidence of metric versus nonmetric traits. *American Journal of Physical Anthropology: The Official Publication of the American Association of Physical Anthropologists*, *107,*4, pp.371-386.

Coppa, A., Cucina, A., Lucci, M., Mancinelli, D. and Vargiu, R., 2007. Origins and spread of agriculture in Italy: a nonmetric dental

analysis. *American Journal of Physical Anthropology: The Official Publication of the American Association of Physical Anthropologists*, *133*(3), pp.918-930.

Corcoran, J.X.W.P., 1972. 'Multi-period construction and the origins of the chambered long cairn in western Britain and Ireland' in Lynch, F.M. and Burgess, C. (eds) *Prehistoric Man in Wales and the West,* Bath: Adams and Dart, pp.31-63.

Cadien, J.D., 1972. Dental variation in man. *Perspectives on human evolution*, *2*, pp.199-222.

Corruccini, R.S., 1974. An examination of the meaning of cranial discrete traits for human skeletal biological studies. *American Journal of Physical Anthropology*, *40*(3), pp.425-445.

Cox, T.F. and Cox, M.A., 2000. *Multidimensional scaling*. CRC press.

Cronin, S., Berger, S., Ding, J., Schymick, J.C., Washecka, N., Hernandez, D.G., Greenway, M.J., Bradley, D.G., Traynor, B.J. and Hardiman, O., 2008. A genome-wide association study of sporadic ALS in a homogenous Irish population. *Human molecular genetics*, *17*(5), pp.768-774.

Cucina, A., Lucci, M., Vargiu, R. and Coppa, A., 1999. Dental evidence of biological affinity and environmental conditions in prehistoric Trentino (Italy) samples from the Neolithic to the Early Bronze Age. *International Journal of Osteoarchaeology*, *9*(6), pp.404-416.

Cummings, V., 2009. *A view from the west: the Neolithic of the Irish Sea zone*. Oxbow Books.

Dahlberg AA. 1956. Materials for the establishment of standards for classification of tooth characteristics, attributes and techniques in morphological studies of the dentition. *Zoller Laboratory of Dental Anthropology*. Chicago: University of Chicago Press.

Dahlberg, A.A., 1963. Dental evolution and culture. *Human biology*, *35*(3), pp.237-249.

Davies, M., 1946. The diffusion and distribution pattern of the megalithic monuments of the Irish Sea and North Channel coastlands. *The Antiquaries Journal*, *26*(1-2), pp.38-60.

De Souza, P. And Houghton, P., 1977. The mean measure of divergence and the use of non-metric data in the estimation of biological distances. *Journal of Archaeological Science*, 4(2), pp.163-169.

Delgado, M., Ramírez, L.M., Adhikari, K., Fuentes-Guajardo, M., Zanolli, C., Gonzalez-José, R., Canizales, S., Bortolini, M.C., Poletti, G., Gallo, C. and Rothhammer, F., 2019. Variation in dental morphology and inference of continental ancestry in admixed Latin Americans. *American Journal of Physical Anthropology*, *168*(3), pp.438-447.

Dempsey, P.A. and Townsend, G.C., 2001. Genetic and environmental contributions to variation in human tooth size. *Heredity*, *86*(6), pp.685-693.

Diniz-Filho, J.A.F., Soares, T.N., Lima, J.S., Dobrovolski, R., Landeiro, V.L., Telles, M.P.D.C., Rangel, T.F. and Bini, L.M., 2013. Mantel test in population genetics. *Genetics and molecular biology*, *36*, pp.475-485.

Dugard, P., Todman, J. and Staines, H., 2010. *Approaching multivariate analysis: A practical introduction*. Routledge.

Dutilleul, P., Stockwell, J.D., Frigon, D. and Legendre, P., 2000. The Mantel test versus Pearson's correlation analysis: Assessment of the differences for biological and environmental studies. *Journal of agricultural, biological, and environmental statistics*, pp.131-150.

Edgar, H.J.H., 2004. Dentitions, distance, and difficulty: a comparison of two statistical techniques for dental morphological data. *Dental Anthropology Journal*, 17(2), pp.55-62.

Edwards, N., 2001. Early-medieval inscribed stones and stone sculpture in Wales: context and function. *Medieval archaeology*, 45(1), pp.15-39.

Emery, M.M., Gibbins, D.J.L. and Matthews, K.J., 1995. The Archaeology of an Ecclesiastical Landscape. *Chapel House Farm, Poulton (Cheshire)*.

Emery, M.M., 2000. The Poulton Chronicles: Tales from a Medieval Chapel.

Eogan, G., 1969. 'Lock-Rings' of the Late Bronze Age. *Proceedings of the Royal Irish Academy. Section C: Archaeology, Celtic Studies, History, Linguistics, Literature*, 67, pp.93-148.

Ersts,P.J., 2014. Geographic Distance Matrix Generator (version 1.2.3*). American Museum of Natural History, Center for Biodiversity and Conservation. Available from http://biodiversityinformatics.amnh.org/open_source/gdmg*. Accessed on 10/12/2024

Evans, E. 2003. *Early medieval ecclesiastical sites in southeast Wales: Desk-based assessment*. Swansea: Glamorgan-Gwent Archaeological Trust Ltd.

Fisher, R.A., 1936. "The coefficient of racial likeness" and the future of craniometry. *The Journal of the Royal Anthropological Institute of Great Britain and Ireland*, 66, pp.57-63.

Forsyth, K.S., 1996. *The Ogham inscriptions of Scotland: an edited corpus*. Harvard University.

Fowler, C., 2010. Pattern and diversity in the Early Neolithic mortuary practices of Britain and Ireland: contextualising the treatment of the dead. *Documenta praehistorica*, *37*, pp.1-22.

Fox, C. 1947. *The Personality of Britain*. Cardiff: National Museum of Wales.

Freeman, M.F. and Tukey, J.W., 1950. Transformations related to the angular and the square root. *The annals of mathematical statistics*, pp.607-611.

Fullbrook-Leggatt, L.E.W.O., 1945. Medieval Gloucester I. *Transactions of the Bristol and Gloucestershire Archaeological Society*, *66*(1), pp.1-48.

Gilbert, E., O'Reilly, S., Merrigan, M., McGettigan, D., Molloy, A.M., Brody, L.C., Bodmer, W., Hutnik, K., Ennis, S., Lawson, D.J. and Wilson, J.F., 2017. The Irish DNA Atlas: revealing fine-scale population structure and history within Ireland. *Scientific reports*, *7*(1), p.17199.

Gillies, W., 2009. Scottish Gaelic. In *The Celtic Languages* (pp. 244-318). Routledge.

Goldstein, M.S., 1948. Dentition of Indian crania from Texas. *American Journal of Physical Anthropology*, *6*(1), pp.63-84.

Greene, J.P., 2004. *Norton Priory: the archaeology of a medieval religious house*. Cambridge University Press.

Greene, R. and Suchey, J., 1976. The use of inverse sine transformation in the analysis of non-metrical data. American *Journal of Physical Anthropology*, 45(1), pp.61-8.

Gretzinger, J., Sayer, D., Justeau, P., Altena, E., Pala, M., Dulias, K., Edwards, C.J., Jodoin, S., Lacher, L., Sabin, S. and Vågene, Å.J., 2022. The Anglo-Saxon migration and the formation of the early English gene pool. *Nature*, *610*(7930), pp.112-119.

Grewal, M.S., 1962. The rate of divergence of sublines in the C57BL strain of mice. *Genetical Research*, 3(2), pp.226-237.

Griffiths, D.W., 1991. *Anglo-Saxon England and the Irish Sea region AD 800-1100: an archaeological study of the Lower Dee and Mersey as a border area* (Doctoral dissertation, Durham University).

Griffiths, D., 2004. Settlement and acculturation in the Irish Sea region. In Hines, J., Lane, A., and Redknap, M. (eds), *Land, Sea and Home* (pp. 125-138). London: Routledge.

Groom, P., Schlee, D., Hughes, G., Crane, P., Ludlow, N. and Murphy, K., 2011. Two Early Medieval Cemeteries in Pembrokeshire: Brownslade Barrow and West Angle Bay. *Archaeologia Cambrensis*, *160*, pp.133-203.

Grüneberg, H., 1952. Genetical studies on the skeleton of the mouse: IV. Quasi-continuous variations. *Journal of Genetics*, *51*, pp.95-114.

Guillot, G. and Rousset, F., 2013. Dismantling the Mantel tests. *Methods in ecology and evolution*, *4*(4), pp.336-344.

Harvey, R.G., Smith, M.T., Sherren, S., Bailey, L. and Hyndman, S.J., 1986. How Celtic are the Cornish?: a study of biological affinities. *Man*, pp.177-201.

Hanihara, K., 1961. Criteria for classification of crown characters of the human deciduous dentition. *Journal of the Anthropological Society of Nippon*, 69(1), pp.27-45.

Hanihara, K., 1963. Crown characters of the deciduous dentition of the Japanese-American hybrids. *Dental anthropology*, pp.105-124

Hanihara, T., 2008. Morphological variation of major human populations based on nonmetric dental traits. *American Journal of Physical Anthropology: The Official Publication of the American Association of Physical Anthropologists*, *136*(2), pp.169-182.

Hanihara, T.,2013. 19 Geographical structure of dental variation in the major populations of the world. Anthropol. Perspect. Tooth Morphol. Genetic. Evil. Variation., 66 p.479

Harpending H, Jenkins T. 1973. Genetic distance among Southern African populations. In: Crawford M, Workman J, editors. *Methods and Theories in Anthropological Genetics.* Albuquerque: UNM Press. P 177-199

Harpending, H.C., Ward R. 1982. Chemical systematics and human evolution. In Nitecki, M (ed)., *Biochemical Aspects of Evolutionary Biology*. Chicago: University of Chicago Press

Harris, E.F. and Sjøvold, T., 2004. Calculation of Smith's mean measure of divergence for intergroup comparisons using nonmetric data. *Dental Anthropology Journal*, *17*(3), pp.83-93.

Harrison, S.H., 2015. 'Warrior graves'? The weapon burial rite in Viking Age Britain and Ireland. In Barrett, J.H., and Gibbon S.J., *Maritime Societies of the Viking and Medieval World*. Leeds: Maney Publishing. pp. 219-319

Hefner, J.T., Pilloud, M.A., Buikstra, J.E. and Vogelsberg, C.C., 2016. A brief history of biological distance analysis. In Pilloud, M.A., and Hefner, J.T., *Biological distance analysis: forensic and bio archaeological perspectives*. Academic Press. pp. 3-22

Hemer, K.A., Evans, J.A., Chenery, C.A. and Lamb, A.L., 2013. Evidence of early medieval trade and migration between Wales and the Mediterranean Sea region. *Journal of Archaeological Science*, *40*(5), pp.2352-2359.

Henderson, D. 2009. The Human Remains. In Lowe, C.E. *'Clothing for the Soul Divine': Burials at the Tomb of St Ninian: Excavations at Whithorn Priory, 1957-67*. Historic Environment Scotland.

Herity, M., 1982. Irish decorated Neolithic pottery. *Proceedings of the Royal Irish Academy. Section C: Archaeology, Celtic Studies, History, Linguistics, Literature*, pp.247-404.

Hill, E.W., Jobling, M.A. and Bradley, D.G., 2000. Y-chromosome variation and Irish origins. *Nature*, *404*(6776), pp.351-352.

Hill, P., 1991. Whithorn: the missing years. *Oram and Stell*, pp.27-44.

Hill, P., 1997. *Whithorn and St Ninian: the excavation of a monastic town, 1984-91*. Alan Sutton Publishing.

Hingley, R., Bonacchi, C. and Sharpe, K., 2018. 'Are you local?'Indigenous Iron Age and mobile Roman and post-Roman populations: then, now and in-between. *Britannia*, *49*, pp.283-302.

Holbrook, N. and Thomas, A., 2005. An early-medieval monastic cemetery at Llandough, Glamorgan: excavations in 1994. *Medieval Archaeology*, *49*(1), pp.1-92.

Hooton, E.A., 1940. Stature, head form, and pigmentation of adult male Irish. *American Journal of Physical Anthropology*, *26*(1), pp.229-249.

Hooton, E.A., Dupertuis, C.W. and Dawson, H.L. (1955) *The physical anthropology of Ireland. Cambridge, Mass.: Peabody Museum of Archaeology and* Ethnography, Harvard University (Papers of the Peabody Museum of Archaeology and Ethnology, Harvard University, Vol. 30, no. 1-2).

Hrdlička, A., 1920. Shovel-shaped teeth. *American Journal of Physical Anthropology*, 3(4), pp.429-465.

Hubbard, A.R., 2012. *An examination of population history, population structure, and biological distance among regional populations of the Kenyan coast using genetic and dental data* (Doctoral dissertation, The Ohio State University).

Hubbard, A.R., Guatelli-Steinberg, D. And Irish, J.D., 2015. Do nuclear DNA and dental nonmetric data produce similar reconstructions of regional population history? An example from modern coastal K enya. *American journal of physical anthropology*, 157(2), pp.295-304.

Hurst, H., 1972. Excavations at Gloucester, 1968–1971: first interim report. *The Antiquaries Journal*, *52*(1), pp.24-69.

Hurst, H., 1974. Excavations at Gloucester, 1971–1973: Second Interim Report1. *The Antiquaries Journal*, *54*(1), pp.8-52.

Hurst, H.R. ed., 1999. *The Coloniae of Roman Britain: New Studies and a Review: Papers of the Conference Held at Gloucester on 5-6 July, 1997*. Journal of Roman Archaeology.

Irish, J.D., 1993. *Biological affinities of late Pleistocene through modern African aboriginal populations: the dental evidence*. Arizona State University.

Irish, J.D., 1997. Characteristic high-and low-frequency dental traits in sub-Saharan African populations. *American Journal of Physical Anthropology: The Official Publication of the American Association of Physical Anthropologists*, *102*(4), pp.455-467.

Irish, J.D., 2005. Population continuity vs. discontinuity revisited: Dental affinities among late Paleolithic through Christian-era Nubians. *American Journal of Physical Anthropology: The Official Publication of the American Association of Physical Anthropologists*, *128*(3), pp.520-535.

Irish, J.D., 2006. Who were the ancient Egyptians? Dental affinities among Neolithic through postdynastic peoples. *American Journal of Physical Anthropology: The Official Publication of the American Association of Physical Anthropologists*, *129*(4), pp.529-543.

Irish, J.D., 2008. Dental morphometric analyses of the Neolithic human skeletal sample from R12: characterizations and contrasts. *A Neolithic cemetery in the Northern Dongola reach: excavations at site*, *12*, pp.105-112.

Irish, J.D., 2010. The mean measure of divergence: Its utility in model-free and model-bound analyses relative to the Mahalanobis D2 distance for nonmetric traits. *American Journal of Human Biology*, *22*(3), pp.378-395.

Irish, J.D. and Guatelli-Steinberg, D., 2003. Ancient teeth and modern human origins: an expanded comparison of African Plio-Pleistocene and recent world dental samples. *Journal of Human Evolution*, *45*(2), pp.113-144.

Irish, J.D., Guatelli-Steinberg, D., Legge, S.S., de Ruiter, D.J. and Berger, L.R., 2014. News and views: Response to 'Non-metric dental traits and hominin phylogeny'by Carter et al., with additional information on the Arizona State University Dental Anthropology System and phylogenetic

‘place’of Australopithecus sediba. *Journal of Human Evolution*, *69*, pp.129-134.

Irish, J.D., Lillios, K.T., Waterman, A.J. and Silva, A.M., 2017. “Other” possibilities? Assessing regional and extra-regional dental affinities of populations in the Portuguese Estremadura to explore the roots of Iberia's Late Neolithic-Copper Age. *Journal of Archaeological Science: Reports*, *11*, pp.224-236.

Irish, J.D., Morez, A., Girdland Flink, L., Phillips, E.L. and Scott, G.R., 2020. Do dental nonmetric traits actually work as proxies for neutral genomic data? Some answers from continental-and global-level analyses. *American Journal of Physical Anthropology*, *172*(3), pp.347-375.

Jackson, J.E., 2005. *A user's guide to principal components*. John Wiley and Sons.

Jensen, J.L., Bohonak, A.J. and Kelley, S.T., 2005. Isolation by distance, web service. *BMC genetics*, 6, pp.1-6.

Johnson, K. 2012. Gaming pieces, dices and counters from Late Iron Age burials. In Eagan, G,. *The Archaeology of Knowth in the first and second millenia AD. Excavations at Knowth*, 5, Dublin

Jolliffe, I.T. and Cadima, J., 2016. Principal component analysis: a review and recent developments. *Philosophical transactions of the royal society A: Mathematical, Physical and Engineering Sciences*, *374*(2065), p.20150202.

Kavanagh, R.M., 1976. Collared and cordoned cinerary urns in Ireland. *Proceedings of the Royal Irish Academy. Section C: Archaeology, Celtic Studies, History, Linguistics, Literature*, pp.293-403.

Keith, A., 1916. The human remains (St. Nicholas chambered tumulus). *Archaeologia Cambrensis (6th ser.)*, *16*, pp.268-93.

Kimura, M. and Weiss, G.H., 1964. The stepping stone model of population structure and the decrease of genetic correlation with distance. *Genetics*, *49*(4), p.561.

Kimura, R., Yamaguchi, T., Takeda, M., Kondo, O., Toma, T., Haneji, K., Hanihara, T., Matsukusa, H., Kawamura, S., Maki, K. and Osawa, M., 2009. A common variation in EDAR is a genetic determinant of shovel-shaped incisors. *The American Journal of Human Genetics*, *85*(4), pp.528-535.

Knight, J.K., 2005. From villa to monastery: Llandough in context. *Medieval Archaeology*, *49*(1), pp.93-107.

Konigsberg, L.W., 1990. Analysis of prehistoric biological variation under a model of isolation by geographic and temporal distance. *Human Biology*, pp.49-70.

Kruskal, J.B., and Wish, M., 1978. *Multidimensional scaling*. Beverly Hills, CA: Sage Publications.

Legendre, P., Fortin, M.J. and Borcard, D., 2015. Should the Mantel test be used in spatial analysis?. *Methods in Ecology and Evolution*, *6*(11), pp.1239-1247.

Leslie, S., Winney, B., Hellenthal, G., Davison, D., Boumertit, A., Day, T., Hutnik, K., Royrvik, E.C., Cunliffe, B., Wellcome Trust Case Control Consortium 2 and International Multiple Sclerosis Genetics Consortium, 2015. The fine-scale genetic structure of the British population. *Nature*, *519*(7543), pp.309-314.

Lilley, K., 2002. Imagined geographies of the 'celtic fringe'and the cultural construction of the 'other'in medieval Wales and Ireland. *Celtic geographies: old culture, new times*, pp.21-36.

Livingstone, F.B., 1991. Phylogenies and the forces of evolution. *American journal of human biology*, *3*(2), pp.83-89.

Lloyd-Jones, J., 1995. Measuring biological affinity among populations: a case study of Romano-British and Anglo-Saxon populations. In Huggett, J. and Ryan, N. (Eds.), *Computer Applications and Quantitative Methods in Archaeology 1994*, pp. 69-73. Oxford: British Archaeological Reports International Series 600.

Lloyd-Jones, J.L., 1999. *The biological affinities of several Romano-British and Anglo-Saxon populations as shown by dental morphology* (Doctoral dissertation, University of Glasgow).

Longworth, I.H., 1984. *Collared Urns of the Bronze Age in Great Britain and Ireland*. CUP Archive.

Lowe, C.E., 2009. *'Clothing for the Soul Divine': Burials at the Tomb of St Ninian: Excavations at Whithorn Priory, 1957-67*. Historic Environment Scotland.

Lynn, C.J., 1993. House-Urns in Ireland?. *Ulster Journal of Archaeology*, pp.70-77.

Mahalanobis, P.C., 1936. On the generalized distance in statistics. *Proceedings of the National Institute of Science, India*, 2 pp.49-55.

Maldonado, A., 2013. Burial in Early Medieval Scotland: New Questions: WINNER OF THE 2013 MARTYN JOPE AWARD. *Medieval Archaeology*, *57*(1), pp.001-034.

Martiniano, R., Caffell, A., Holst, M., Hunter-Mann, K., Montgomery, J., Müldner, G., McLaughlin, R.L., Teasdale, M.D., Van Rheenen, W., Veldink, J.H. and Van Den Berg, L.H., 2016. Genomic signals of migration and continuity in Britain before the Anglo-Saxons. *Nature communications*, *7*(1), p.10326.

McManus, D. 1991. *A Guide to Ogham*. An Sagart, Maynooth.

McComish, J.M. and Petts, D., 2008. *Archaeological excavations at Fey Field, Whithorn*.

McGarry, T., 2007. Irish late prehistoric burial practices: continuity, developments and influences. *Trowel*, *11*, pp.7-25.

Miles, D. and Allen, L., 2007. *Iron Age and Roman Settlement in the Upper Thames Valley: Excavations at Claydon Pike and Other Sites Within the Coltswold Water Park*. Oxford Archaeology.

Mizoguchi, Y., 1985. Shovelling: A statistical analysis of its morphology. *University Museum Bulletin*, *26*.

Mizoguchi, Y., 1993. Adaptive significance of Carabelli trait. *Bulletin of the National Science Museum, Tokyo, Series D*, *19*, pp.21-57.

Montgomery, J., Müldner, G., Cook, G., Gledhill, A. and Ellam, R., 1957. Isotope analysis of bone collagen and tooth enamel. *Clothing for the Soul Divine': Burials at the Tomb of St Ninian. Excavations at Whithorn Priory*, *67*, pp.63-80.

Müldner, G., Montgomery, J., Cook, G., Ellam, R., Gledhill, A. and Lowe, C., 2009. Isotopes and individuals: diet and mobility among the medieval Bishops of Whithorn. *Antiquity*, *83*(322), pp.1119-1133.

Murphy, D and Gibney, G. 2021. *Archaeological Excavation at Southgreen Link Road, Kildare, co. Kildare*. ACSU Report 1894.

Nash, C., 2006. Irish origins, celtic origins: population genetics, cultural politics. *Irish Studies Review*, *14*(1), pp.11-37.

Nelson, C.T., 1938. The teeth of the Indians of Pecos Pueblo. *American Journal of Physical Anthropology*, *23*(3), pp.261-293.

Nichol, C.R., 1990. *Dental genetics and biological relationships of the Pima Indians of Arizona*. Arizona State University.

Noble, G., Gondek, M., Campbell, E. and Cook, M., 2013. Between prehistory and history: the archaeological detection of social change among the Picts. *Antiquity*, *87*(338), pp.1136-1150.

O'Connell, K, Moore, D., and Muller, J. 2018. *Atlantic Trading Estate (Phase 3), Barry, Vale of Glamorgan: Archaeological Watching Brief*. AW Report 1664.

O'Dushlaine, C.T., Morris, D., Moskvina, V., Kirov, G., Gill, M., Corvin, A., Wilson, J.F., Cavalleri, G.L. and International Schizophrenia Consortium, 2010. Population structure and genome-wide patterns of variation in Ireland and Britain. *European Journal of Human Genetics*, *18*(11), pp.1248-1254.

O'Neill, T. 2009. *Report on the Archaeological Excavation of Parknahown 5, co. Laois*. Archaeological Consultancy Services Ltd. E2170.

Owen, R., 1840. *Odontography, or, a treatise on the comparative anatomy of the teeth, their physiological relations, mode of developement, and microscipic structure, in the vertebrate animals*. Bailliere.

Owen-John, H.S., 1988. Llandough: the rescue excavation of a multi-period site near Cardiff, South Glamorgan. *Biglis, Caldicot and Llandough: Three Late Iron Age and Romano-British Sites in South-East Wales, Excavations 1977-1979*, pp.123-177.

Park, J.H., Yamaguchi, T., Watanabe, C., Kawaguchi, A., Haneji, K., Takeda, M., Kim, Y.I., Tomoyasu, Y., Watanabe, M., Oota, H. and Hanihara, T., 2012. Effects of an Asian-specific nonsynonymous EDAR variant on multiple dental traits. *Journal of human genetics*, *57*(8), pp.508-514.

Pearson, K., 1926. On the coefficient of racial likeness. *Biometrika*, pp.105-117.

Peng, Q., Li, J., Tan, J., Yang, Y., Zhang, M., Wu, S., Liu, Y., Zhang, J., Qin, P., Guan, Y. and Jiao, Y., 2016. EDARV370A associated facial characteristics in Uyghur population revealing further pleiotropic effects. *Human genetics*, *135*(1), pp.99-108.

Penniman, T.K., 1932. Culver Hole Cave and vicinity, Llangennith and Llanmadoc, Gower. *Bulletin of the Board of Celtic Studies*, *6*, pp.196-200.

Penrose, L.S., 1952. Distance, size and shape. *Annals of Eugenics*, 17(1), pp.337-343.

Phythian-Adams, C., 1993. Introduction: an agenda for English local history. *Societies, cultures and kinship*, pp.1580-1850.

Powell, T.G.E., 1973. I.—Excavation of the Megalithic Chambered Cairn at Dyffryn Ardudwy, Merioneth, Wales. *Archaeologia*, *104*, pp.1-49.

Price, C. 1996. *Excavations at Atlantic Trading Estate, Barry, Site 92-Preliminary Report*. Glamorgon Gwent Archaeological Trust.

Rafferty, B. 1969. Freestone Hill, co. Kilkenny: An Iron Age Hillfort and Bronze Age Cairn: Excavation Gerhard Bersu, 1948-1949, *Proceedings of the Royal Irish Academy: Archaeology, Culture, History, Literature*, 68, pp. 1-108.

Rasmus, B. and Smilde, A.K., 2014. Principal component analysis. *Analytical methods*, *6*(9), pp.2812-2831.

Rathmann, H. and Reyes-Centeno, H., 2020. Testing the utility of dental morphological trait combinations for inferring human neutral genetic

variation. *Proceedings of the National Academy of Sciences*, *117*(20), pp.10769-10777.

Rawes, B. 1984 . Archaeology in Gloucestershire, 1976-1977. *Transactions of the Bristol and Gloucestershire Archaeological Society*. Vol: 96, pp. 83-90.

Relethford, J.H., 1983. Genetic structure and population history of Ireland: a comparison of blood group and anthropometric analyses. *Annals of Human Biology*, *10*(4), pp.321-333.

Relethford, J.H., 1988. Effects of English admixture and geographic distance on anthropometric variation and genetic structure in 19th-century Ireland. *American journal of physical anthropology*, *76*(1), pp.111-124.

Relethford, J.H., 1991. Genetic drift and anthropometric variation in Ireland. *Human Biology*, pp.155-165.

Relethford, J., 2004. Global patterns of isolation by distance based on genetic and morphological data. *Human biology*, *76*(4), pp.499-513.

Relethford, J.H. and Blangero, J., 1990. Detection of differential gene flow from patterns of quantitative variation. *Human Biology*, pp.5-25.

Relethford, J.H. and Lees, F.C., 1982. The use of quantitative traits in the study of human population structure. *American Journal of Physical Anthropology*, 25(S3), pp.113-132.

Relethford, J.H., Lees, F.C. and Crawford, M.H., 1980. Population structure and anthropometric variation in rural western Ireland: Migration and biological differentiation. Annals of Human Biology, 7(5), pp.411-428.

Relethford, J.H., Lees, F.C. and Crawford, M.H., 1981. Population structure and anthropometric variation in rural western Ireland: Isolation by distance and analysis of the residuals. American Journal of Physical Anthropology, 55(2), pp.233-245.

Reynolds, F., 2014. A site's history does not end: transforming place through community archaeology at Tinkinswood chambered tomb and surrounding landscape, Vale of Glamorgan. *Journal of Community Archaeology and Heritage*, *1*(2), pp.173-189.

Ricaut, F.X., Auriol, V., von Cramon-Taubadel, N., Keyser, C., Murail, P., Ludes, B. And Crubézy, E., 2010. Comparison between morphological and genetic data to estimate biological relationship: The case of the Egyin Gol necropolis (Mongolia). *American Journal of Physical Anthropology*, 143(3), pp.355-364.

Robinson, I.S., 1979. The tidal dynamics of the Irish and Celtic Seas. *Geophysical Journal International*, *56*(1), pp.159-197.

Rohlf, R. and Sokal, R., 1965. Coefficients of correlation and distance in numerical taxonomy. *University of Kansas Science Bulletin*, 45 (1).

Ross, R.M., Greenhill, S.J. and Atkinson, Q.D., 2013. Population structure and cultural geography of a folktale in Europe. *Proceedings of the Royal Society B: Biological Sciences*, *280*(1756).

Royal Commission on Ancient and Historical Monuments in Wales. 1976. An Inventory of the Ancient Monuments in Glamorgan. Volume I: Pre-Norman Part I. The Stone and Bronze Ages. HMSO, Cardiff.

Rudlin, D., Thompson, R. and Jarvis, S., 2016. Chester. In *Urbanism* (pp. 88-89). Routledge.

Ryan, M., 1973. Native pottery in early historic Ireland. *Proceedings of the Royal Irish Academy. Section C: Archaeology, Celtic Studies, History, Linguistics, Literature*, pp.619-645.

Saville, A., 1999. A cache of flint axeheads and other flint artefacts from Auchenhoan, near Campbeltown, Kintyre, Scotland. In *Proceedings of the Prehistoric Society*. 65, pp. 83-123). Cambridge University Press.

Savory, H.N., 1958. *The Late Bronze Age in Wales: some new discoveries and new interpretations*. Archaeologia Cambrensis 107, pp. 3-63.

Schiffels, S., Haak, W., Paajanen, P., Llamas, B., Popescu, E., Loe, L., Clarke, R., Lyons, A., Mortimer, R., Sayer, D. and Tyler-Smith, C., 2016. Iron age and Anglo-Saxon genomes from East England reveal British migration history. *Nature communications*, *7*(1), p.10408.

Scott, G.R., 1973. *Dental morphology: a genetic study of American white families and variation in living Southwest Indians*. Arizona State University.

Scott, G.R. and Irish, J.D., 2017. *Human tooth crown and root morphology*. Cambridge University Press.

Scott, G.R., Maier, C. and Heim, K., 2015. Identifying and recording key morphological (nonmetric) crown and root traits. *A companion to dental anthropology*, pp.245-264.

Scott, G.R., Schmitz, K., Heim, K.N., Paul, K.S., Schomberg, R. and Pilloud, M.A., 2018a. Sinodonty, Sundadonty, and the Beringian Standstill model: Issues of timing and migrations into the New World. *Quaternary International*, *466*, pp.233-246.

Scott, G.R., Pilloud, M.A., Navega, D., d'Oliveira, J., Cunha, E. and Irish, J.D., 2018b. rASUDAS: A new web-based application for estimating ancestry from tooth morphology. *Forensic Anthropology*, *1*(1), pp.18-31.

Scott, G.R. and Turner, C.G., 1988. Dental anthropology. *Annual review of Anthropology*, *17*, pp.99-126.

Scott, G.R. and Turner, C.G., 1997. *The anthropology of modern human teeth*. Cambridge: Cambridge University Press.

Scott, W.L., 1932, November. Rudh'an Dunain chambered cairn, Skye. In *Proceedings of the Society of Antiquaries of Scotland* (Vol. 66, pp. 183-213).

Sell, S. H. 1999. Excavations of a Bronze Age settlement at the Atlantic Trading Estate, Barry, South Glamorgan (ST 134 673). *Studia Celtica*. 32, pp. 1-26.

Seltzer, C.C., 1937. A critique of the coefficient of racial likeness. *American Journal of Physical Anthropology*, 23(1), pp.101-109.

Shaw, H., Montgomery, J., Redfern, R., Gowland, R. and Evans, J., 2016. Identifying migrants in Roman London using lead and strontium stable isotopes. *Journal of Archaeological Science*, *66*, pp.57-68.

Sheridan, J.A., 1986. Porcellanite artifacts: a new survey. *Ulster Journal of Archaeology*, *49*, pp.19-32.

Sheridan, A., Cooney, G. and Grogan, E., 1992. Stone axe studies in Ireland. *Journal of Social Archaeology*, *58*, pp.389-416.

Sheridan, J. A. 2000. Achnacreebeag and its French connections: vive the 'Auld Alliance'. *British Archaeological Reports, International Series 861*. pp.1-15.

Sheridan, A, 2004. Neolithic connections along and across the Irish Sea. *The Neolithic of the Irish Sea*, pp.9-21.

Sheridan, A., Armit, I., Reich, D., Booth, T., Bernardos, R., Barnes, I., Thomas, M., Charlton, S., Craig, O., Lawson, J. and Dulias, K., 2019. A summary round-up list of Scottish archaeological human remains that have been sampled/analysed for DNA as of January 2019. *Discov. Excav. Scotl.(Digit. Version)*, *19*, pp.227-250.

Simmonds, A., Márquez-Grant, N. and Loe, L., 2008. *Life and death in a Roman city: excavation of a Roman cemetery with a mass grave at 120–122 London Road, Gloucester*. Oxford Archaeological Unit Ltd.

Simpson, D.D.A., 1979. 'The Early Bronze Age' in Megaw, J.V.S. and Simpson, D.D.A. (eds) *Introduction the British Prehistory*. Leicester UP. pp. 178-241.

Simpson, D. and Meighan, I., 1999. Pitchstone: A New Trading Material in Neolithic Ireland. *Archaeology Ireland*, pp.26-30.

Smouse, P.E., Long, J.C. and Sokal, R.R., 1986. Multiple regression and correlation extensions of the Mantel test of matrix correspondence. *Systematic zoology*, *35*(4), pp.627-632.

Sjøvold, T., 1973. The occurrence of minor non-metrical variants in the skeleton and their quantitative treatment for population comparisons. *Homo*, 24, pp.204-233.

Sjøvold, T., 1977. Non-metrical divergence between skeletal populations: The theoretical foundation and biological importance of CA B. *Smith's mean measure of divergence*, *4*(1), pp.1-133.

Smith, C.A., 1972. Coefficients of biological distance. *Annals of human genetics*, 36, pp.241-245.

Smith, L., 2012. Norton Priory, Runcorn. *Archaeological Journal*, *169*(sup1), pp.23-29.

Sofaer, J.A., Niswander, J.D., MacLean, C.J. and Workman, P.L., 1972. Population studies on Southwestern Indian tribes V. Tooth morphology as an indicator of biological distance. American Journal of Physical Anthropology, 37(3), pp.357-366.

Sołtysiak, A., 2011. An R script for Smith's mean measure of divergence. *Bioarchaeology of the near East*, *5*, pp.41-44.

Sposato, P.W., 2009. The Perception of Anglo-Norman Modernity and the Conquest of Ireland. *Comitatus: A Journal of Medieval and Renaissance Studies*, *40*(1), pp.25-44.

Stafford, L, 2016. *Atlantic Trading Estate, Barry, Vale of Glamorgan: Archaeological Watching Brief*. AW Report 1481

Standish, C.D., Dhuime, B., Hawkesworth, C.J. and Pike, A.W., 2015, December. A non-local source of Irish Chalcolithic and Early Bronze Age gold. In *Proceedings of the Prehistoric Society* (Vol. 81, pp. 149-177). Cambridge University Press.

Stojanowski, C.M. and Hubbard, A.R., 2017. Sensitivity of dental phenotypic data for the identification of biological relatives. *International Journal of Osteoarchaeology*, 27(5), pp.813-827.

Stojanowski, C.M., Paul, K.S., Seidel, A.C., Duncan, W.N. and Guatelli-Steinberg, D., 2018. Heritability and genetic integration of anterior tooth crown variants in the South Carolina Gullah. *American Journal of Physical Anthropology*, *167*(1), pp.124-143.

Stojanowski, C.M., Paul, K.S., Seidel, A.C., Duncan, W.N. and Guatelli-Steinberg, D., 2019. Quantitative genetic analyses of postcanine morphological crown variation. *American Journal of Physical Anthropology*, *168*(3), pp.606-631.

Stojanowski, C.M. and Schillaci, M.A., 2006. Phenotypic approaches for understanding patterns of intracemetery biological variation. *American journal of physical anthropology*, 131(S43), pp.49-88.

Swallow, R., 2016. Cheshire castles of the Irish Sea cultural zone. *Archaeological Journal*, *173*(2), pp.288-341.

Tan, J., Peng, Q., Li, J., Guan, Y., Zhang, L., Jiao, Y., Yang, Y., Wang, S. and Jin, L., 2014. Characteristics of dental morphology in the Xinjiang Uyghurs and correlation with the EDARV370A variant. *Science China Life Sciences*, *57*(5), pp.510-518.

Taylor, M.V. 1935. Roman Britain in 1934. *Journal of Roman Studies,* 25, pp.201-202.

Thomas, A.C., 1968. Grassmarked Pottery in Cornwall. In Coles and Simpson (ed.), *Studies in Ancient Europe*. Leicester: Leicester University Press. pp.327.

Thomas, C., 1973. Irish colonists in south-west Britain. *World Archaeology*, 5(1), pp.5-13.

Thomas, S. 2017. *Atlantic Trading Estate (Phase 2), Barry, Vale of Glamorgan: Archaeological Watching Brief*. AW Report 1593

Thompson, J.E., 2019. 'Tinkering with the dead: taphanomic analysis of human remains from Tinkinswood chambered tomb, Wales', *Archaeologia Cambrensis*, Vol. 168, pp. 35-37.

Tomes, C.S., 1923. *A manual of dental anatomy: human and comparative*. Macmillan.

Turner, W., 1895. On human and animal remains found in caves at Oban, Argyllshire. In *Proceedings of the Society of Antiquaries of Scotland*, 29, pp. 410-438.

Turner CG II, Nichol CR, Scott GR. 1991. Scoring procedures for key morphological traits of the permanent dentition: the Arizona State University Dental Anthropology System. In Kelly MA, Larsen CS, editors. *Advances in dental anthropology*. New York: Wiley-Liss p 13-31.

Wacher, J. ed., 1995. *Towns of Roman Britain*. 2nd ed. Routledge.

Waddell, J., 1993. The Irish Sea in Prehistory, *The Journal of Irish Archaeology*, Vol. 6, pp. 29-40.

Ward, J., 1916. *The St. Nicholas Chambered Tumulus, Glamorgan*. National Museum of Wales.

Weets, J.D., 2004. *A dental anthropological approach to issues of migration and population continuity in ancient Ireland*. The Pennsylvania State University.

Weets, J.D., 2009. A promising mandibular molar trait in ancient populations of Ireland. *Dental Anthropology Journal*, *22*(3), pp.65-72.

Wessex Archaeology. 2007. *Poulton Hall, Pulford, Cheshire. Archaeological evaluation and assessment of the results.* Ref: 62506.01.

Wiggins, K and Kane. 2009. *Report on the Archaeological Excavtion of Killeany 1, co. Laois*. Archaeological Consultancy Services Ltd. E2171.

Wiggins, K and Kane. 2009B. *Report on the Archaeological Excavtion of Bushfield or Maghernaskeagh/Lismore 1, co. Laois*. Archaeological Consultancy Services Ltd. E2220.

Wildgoose, M and Kozikowski, G. 2018. *Strath Glebe: Isle of Skye: The Excavation of a Rectangular Stone Setting on Strath Glebe Farm 2015-18: Data Structure Report*. Phoenix Archaeology.

Wright, S., 1940. Breeding structure of populations in relation to speciation. *The American Naturalist*, 74(752), pp.232-248.

Wright, S., 1943. Isolation by distance. *Genetics*, 28(2), p.114.

Wysocki, M. and Whittle, A., 2000. Diversity, lifestyles and rites: new biological and archaeological evidence from British Earlier Neolithic mortuary assemblages. *Antiquity*, *74*(285), p.591.

Appendix I: ASUDAS trait descriptions

Winging UI1

A patterned rotation of the upper central incisors with marginal borders rotated outwards

Breakpoint: Grade 1

Grade 0 (absence): if the line parallel to the labial surface or if the distal margins fall below the line. Angle is ≥180°

Grade 1: mesial margins of the upper incisors fall slightly below the line. The angle is 160-180°

Grade 2: mesial margins further removed from the line. Angle is 135-159°

Grade 3: there is a distinct distance between the line and the mesial margins. Angle is <135°

Labial Curvature UI1

Variation in the curvature of the labial surface of the upper incisors.

Breakpoint: Grade 2+

Grade 0: labial surface is flat

Grade 1: labial surface exhibits trace convexity

Grade 2: labial surface exhibits weak convexity

Grade 3: labial surface exhibits moderate convexity

Grade 4: labial surface exhibits pronounced convexity

Grade 5: pronounced convexity not observed in modern humans but present in earlier hominins (not shown on ASUDAS plaque)

Palatine Torus

A bony exostosis expressed on both sides of the midline on the hard palate.

Grade 0: absence

Grade 1: small (elevated 1-2mm)

Grade 2: moderate (elevated 2-5mm)

Grade 3: marked (covers more of the palate, 5-10mm relief)

Grade 4: very marked (>10mm high and broad)

Shoveling UI1

Development of the mesial and distal marginal ridges on the lingual surface.

Breakpoint: Grade 2+

Grade 0 (absence): it is rare for UI1 to expression the complete absence of marginal ridges. For this reason, grade 0 on the UI1 shoveling plaque shows very slight marginal ridge expression

Grade 1 (trace): marginal ridges can be discerned but expression is slight, with mesial ridge not extending to the basal eminence.

Grade 2 (low moderate): ridges more pronounced, with mesial ridge extending further down on the basal eminence.

Grade 3 (high moderate): ridges more pronounced, almost coalescing at the basal eminence.

Grade 4 (low pronounced): well-developed ridges that converge at the basal eminence.

Grade 5 (medium pronounced): more pronounced ridges meeting at the basal eminence.

Grade 6 (high pronounced): pronounced ridges that meet at the basal eminence, almost folding around on themselves.

Grade 7 (extreme pronounced): Any expression that exceeds grade 6 can be placed in grade 7. This grade would involve marginal ridges that folded around on themselves, similar to grade 6 on the UI2 shoveling plaque.

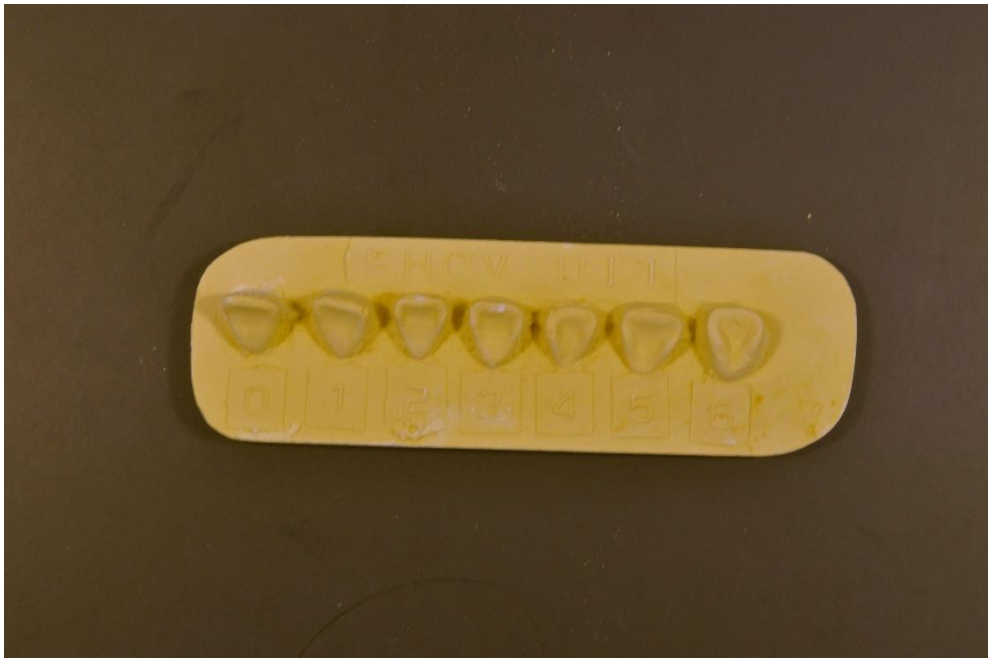

Figure 14: ASUDAS plaque for shovelling UI1

Double Shovelling UI1

Development of the mesial and distal marginal ridges on the labial surface.

Breakpoint: Grade 2

Grade 0 (absence): no labial marginal ridges present; surface is smooth

Grade 1 (faint): very faint labial ridging, more evident in mesial than distal marginal

Grade 2 (trace): ridge more distinct than faint expression of grade 1 but still slight

Grade 3 (slight): ridges distinct enough to be palpated

Grade 4 (moderate): ridging clearly evident along at least one half of crown height

Grade 5 (pronounced): very distinct ridging expressed from incisal edge to crown root junction

Grade 6: extreme double-shoveling with well-developed ridges along both the mesial and distal labial margins

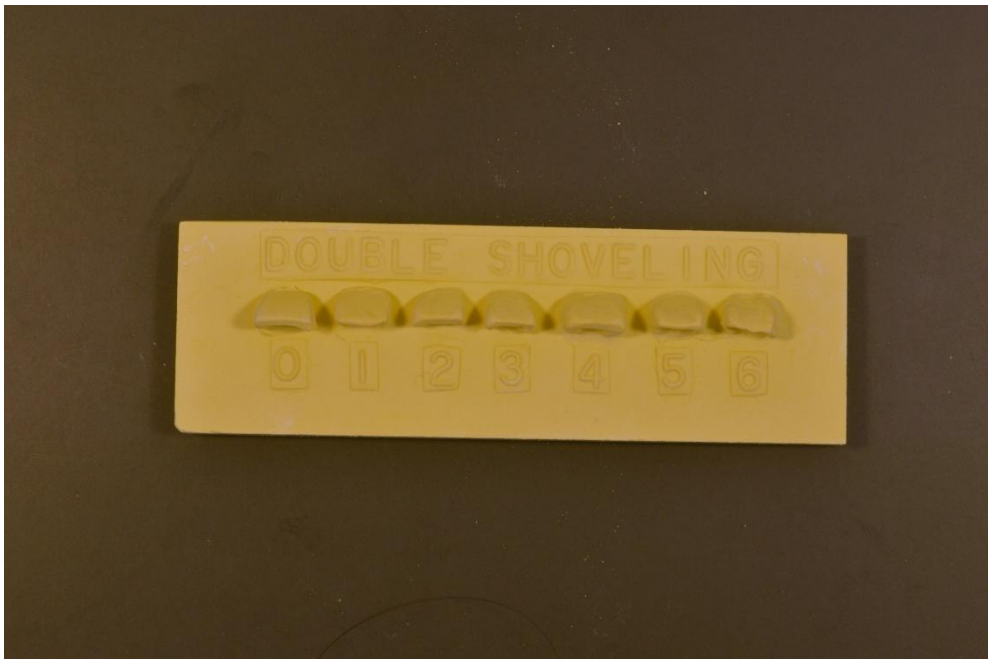

Figure 15: ASUDAS plaque for double shovelling UI1

Interruption Groove UI2

Distinct depressions or grooves that interrupt the normal course of the mesial or distal margins or the basal cingulum

Breakpoint: Any presence of a groove on any lingual marginal ridges or on the basal cingulum is treated as trait being present

Grade 0: absence of grooves in the lingual marginal ridges and basal cingula

M: groove on the mesiolingual marginal ridge

D: groove on the distolingual marginal ridge

MD: grooves on both the mesiolingual and distolingual marginal ridges

Med: groove on mesial aspect of the basal cingulum, sometimes extending onto root

Tuberculum Dentale UI2

Cingular projections on the lingual surface that typically takes the form of ridges and/or tubercles

Breakpoint: 2+

Grade 0: absence of ridge or tubercle formation

Grade 1: slight ridge

Grade 2: moderate ridge

Grade 3: small tubercle

Grade 4: moderate tubercle

Grade 5: large or double tubercle

Grade 6: welt on the basal cingulum (distinct from talon cusp)

Bushman Canine UC

Upper Canine expresses a hypertrophied mesial ridge and tubercle that coalesce to the point where the lingual sulcus is distal to the midline of the tooth

Breakpoint: Grade 1+

Grade 0: mesial and distal lingual ridges are the same size. Neither are attached to the *tuberculum dentale*.

Grade 1: Mesiolingual ridge is larger than the distolingual and is weakly attached to the *tuberculum dentale*, if present.

Grade 2: Mesiolingual is larger than distolingual and is moderately attached to the *tuberculum dentale*.

Grade 3: Morris's type form. Mesiolingual ridge is much larger than the distolingual and fully incorporated into the *tuberculum dentale*

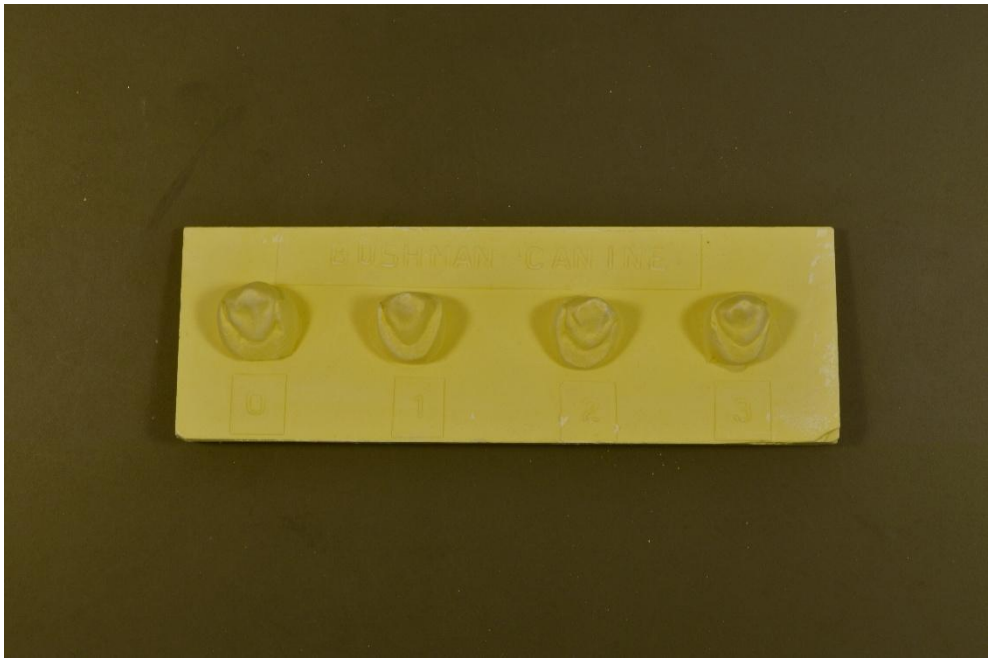

Figure 16: ASUDAS plaque for Bushman Canine UC

Distal Accessory Ridge UC

An additional ridge that manifests on the lingual aspect of the distal lobe segment of the canine

Breakpoint: 2+

Grade 0: trait absence

Grade 1: faint expression

Grade 2: slight expression

Grade 3: moderate development

Grade 4: strongly developed

Grade 5: pronounced expression

Figure 17: ASUDAS plaque for Distal Accessory Ridge UC

Hypocone UM2

The hypocone is the cusp attached to the distolingual surface of the trigon in the upper molars. Variation in the hypocone takes the form of reduction and loss.

Breakpoint: 2+

Grade 0: no hypocone expression of any form: a true three-cusped tooth

Grade 1: for this grade, there is a low-level expression of the hypocone, often expressed as no more than an outline on the distolingual aspect of the trigon. In Dahlberg's original classification, this would be scored as a three-cusped upper molar along with grade 0

Grade 2: In the Dahbrg classification, 3+ was equivalent to a small conical hypocone on the distolingual border of the trigon; grade 2 reflects this phenotype are there is basically a conical cusp, or tubercle, with a free apex

Grade 3: the hypocone is reduced in size but assumes a normal ovate shape along with a distinct free apex

Grade 4: this grade would be equivalent to 3.5 on the modified hypocone plaque; the hypocone is reduced in size but is moderate rather than slight in expression

Grade 5: hypocone is well-developed, a step beyond grade 4

Grade 6: pronounced expression of the hypocone, often equals or exceeds the size of the major cusps of the trigon

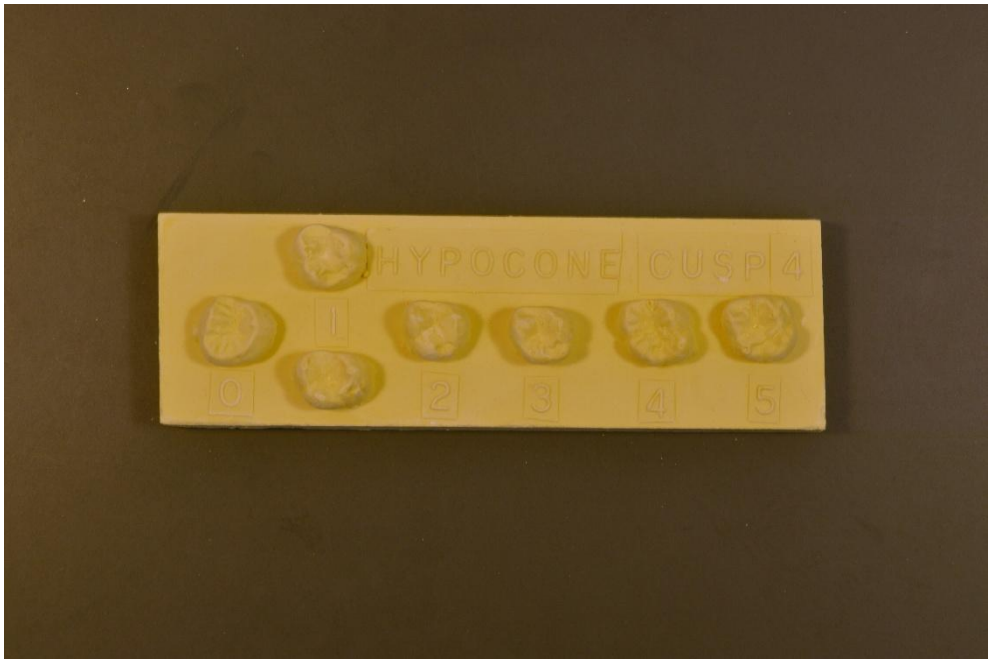

Figure 18: ASUDAS plaque for hypocone

Cusp 5 UM1

Cusp 5 takes the form of a couple that is expressed between the hypocone and metacone of the upper molars. To be scored as present, the cusp should show two vertical grooves that run in parallel on the distal marginal ridge complex.

Breakpoint: 1+

Grade 0: trait is absent, only one vertical grooves on distal surface of upper molar between hypocone and metacone

Grade 1: slight conule

Grade 2: trace conule

Grade 3: small cusp

Grade 5: medium cusp

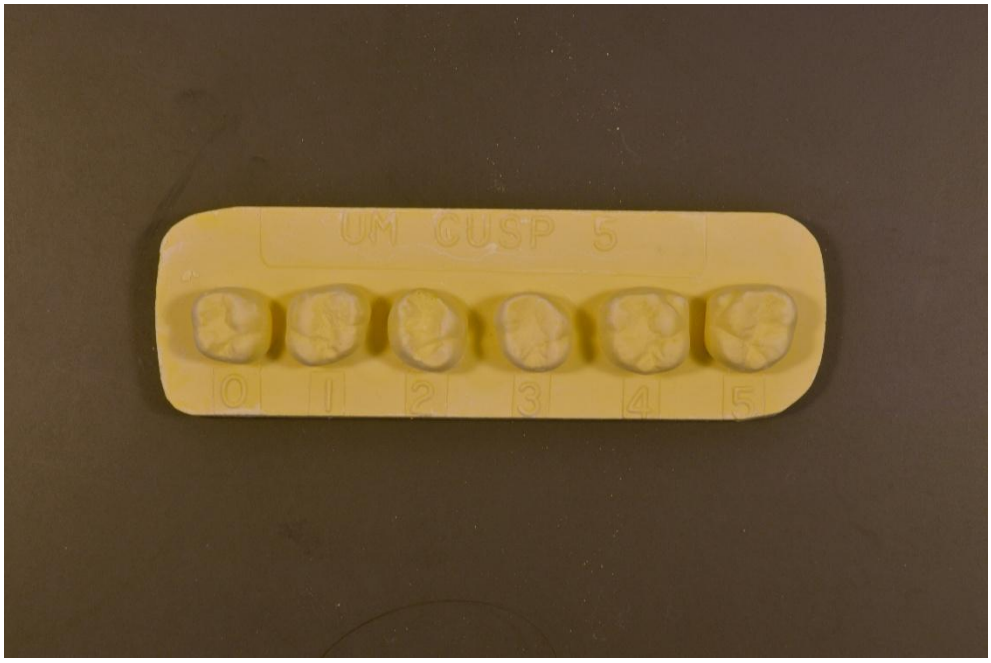

Figure 19: ASUDAS plaque for Cusp 5 UM

Carabelli's Cusp UM1

A Cingular derivative expressed on the lingual surface of the protocone. It shows a wide range of expression, from complete absence to a large free-standing tubercle that approximates the hypocone in size.

Breakpoint: Grade 2+

Grade 0: Mesiolingual cusp does not exhibit any grooves or pits on the lingual surface

Grade 1: a vertical groove separates the protocone from the mesial marginal ridge complex; grade 1 expression occurs when there is a slight eminence that reflects distally from this groove.

Grade 2: when expression goes beyond a slight groove or eminence and takes the form of a pit

Grade 3: expression is still slight but takes on a more distinct form than shown by grades 1 and 2

Grade 4: the most pronounced expression of Carabelli's trait that does not involve a tubercle with a free apex; grade 4 takes the classic bird-winf form

Grade 5: small tubercle with a free apex

Grade 6: moderate tubercle with a free apex

Grade 7 pronounced tubercle with a free apex

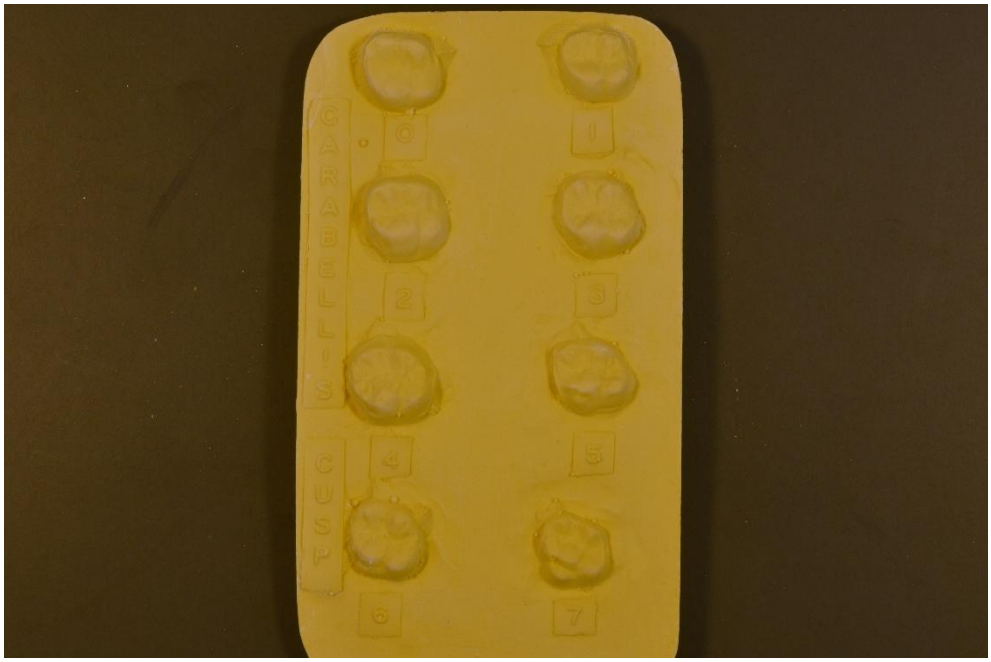

Figure 20: ASUDAS plaque for Carabelli's cusp

Parastyle UM3

Typcially, the parastyle is expressed on the paracone of the upper molars. It ranges in size from a pit to a large free-standing tubercle.

Breakpoint: Grade 2+

Grade 0: buccal surfaces of cusps 2 and 3 are smooth

Grade 1: a small pit near the buccal groove between cusps 2 and 3

Grade 2: small cusp but no free apex

Grade 3: medium cusp with free apex

Grade 4: large cusp with free apex

Grade 5: very large cusp with free apex that may extend onto the surfaces of both cusps 2 and 3

Grade 6: peg-shaped crown attached to root of second or third molar. This class form of Bolk's paramolar tubercle may represent a supernumerary tooth that is fused to the buccal surface of UM2 or UM3. Accessory cusps with all the characteristics of a paramolar tubercle have also been observed on LM2 and LM3, adding evidence to the possibility these are fused supernumerary teeth

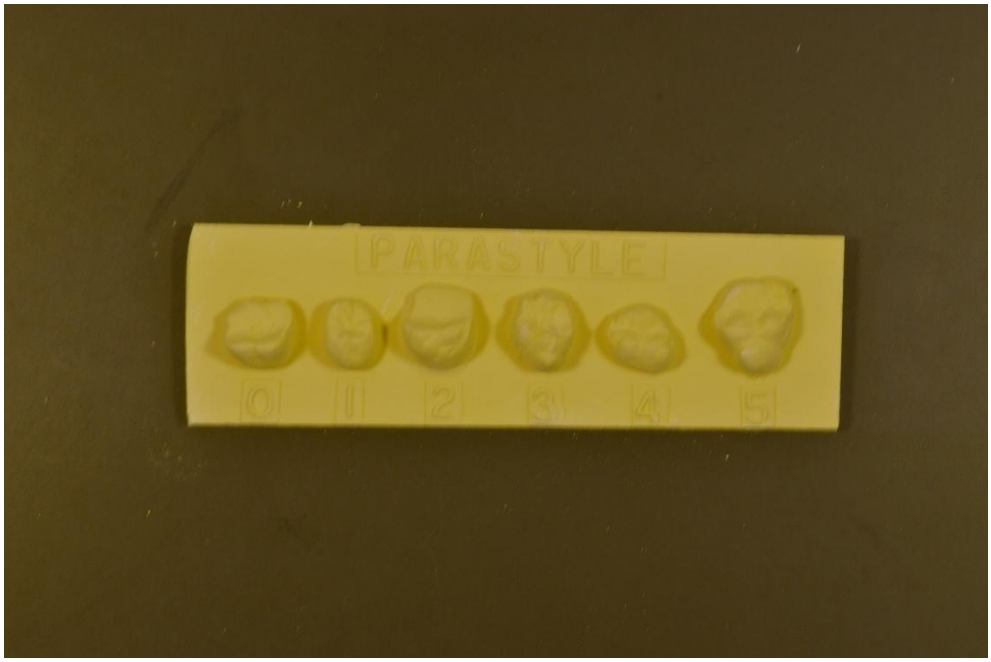

Figure 21: ASUDAS plaque for parastyle

Enamel Extension UM1

Variation in the course of the cervical enamel line. The enamel extends towards the apex of the root in the direction of the bifurcation of the two buccal aspects of the roots.

Breakpoint: Grade 2+

Grade 0: cervical enamel is horizontal

Grade 1: enamel line extends about 1mm toward root bifurcation

Grade 2: enamel line extends about 2mm towards root bifurcation

Grade 3: enamel line extends 4mm or more towards root bifurcation

Root Number UP1

Upper premolars have either Two or three root cones When there is no separation and you can only observe a vertical groove, the tooth is one-rooted. Bifurcation can result in a two or three-rooted tooth. Bifurcation must extend from ¼ to 1/3 of the total root length.

Breakpoint: Grade 2-3

Grade 1: one-rooted UP1 (root grooves separate cones but no inter-radicular projection)

Grade 2: two-rooted UP1 (inter-radicular projection separates buccal and lingual root cones for ¼ to 1/3 of total root length

Grade 3: three-rooted UP1 (there is an inter-radicular projection that separates the buccal root into two distinct roots, and another projection separating the two buccal roots from a single root)

Root Number UM2

Upper molars often have three separate roots. Sometimes, roots fuse resulting in a two-rooted or one-rooted tooth. Independent roots must show bifurcation of at least ¼ to 1/3 of total root length.

Breakpoint: Grade 3

Grade 1: one-rooted UM2 (root cones separated by grooves but there are no inter-radicular projections)

Grade 2: two-rooted UM2 (one inter-radicular projection separates one root from two fused roots)

Grade 3: three-rooted UM3 (three inter-radicular projections separate all three roots for at least ¼ to 1/3 of total root length)

Peg-Reduced UI2

Upper lateral incisors can assume a variety of forms and exhibit many unusual morphological features.

Breakpoint: Grade 1+

Grade 0: UI2 normal in form and size

Grade 1: UI2 normal in form but diminutive in size (less than ½ mesiodistal diameter of UI1)

Grade 2: congenital absence

Grade 3: peg-shaped UI2, conical in form, often with no morphological features

Grade 4: talon cusp (in same location but much more pronounced and distinctive than a *tuberculum dentale*)

Odontome P1-P2

The upper and lower premolars can both express odontomes in the central sulcus. Typically, odontomes are conical in shape.

Breakpoint: Grade 1

Grade 0: absence

Grade 1: odontome present in central sulcus (score all eight premolars)

Congenital Absence UM3

Loss and reduction are the elements of the same phenomenon; they are grouped together to form a single trait that involves pegged or reduced forms plus congenital absence.

Breakpoint: Grade 1

Grade 0: third molar present and normal

Grade 1: third molar significantly reduced in size (ca. ½ normal size, with two or more cusps)

Grade 2: third molar peg-shaped (only a single cusp evident)

Grade 3: third molar congenitally absent

Mid-line Diastema UI1

Presence of space between the upper central incisors midway between the base (or neck) of the tooth and the unworn incisal edge. The crown can be worn down approximately ¼ of it's original (estimated) height and still allow recording.

Breakpoint: Grade 1

Grade 0: no diastema (space < 0.5mm)

Grade 1: Diastema (space > 0.5mm)

Lingual Cusp LP2

Lower premolars can have one, two or three lingual cusps. Expanded classifications include absence and nine degrees of trait presence. Lower premoalrs have lingual cusps that are always smaller than the buccal cusps. Typically, the lingual cusp of the lower premolars has a mesial placement relative to the buccal cusp. When there are accessory cusps, they are usually smaller and distal to the larger mesial lingual cusp.

Breakpoint: Grade 2-9 on plaques

Grade 0: lingual cusp has no free apex

Grade 1: single lingual cusp (on plaque, grades 0-1)

Grade 2: two lingual cusps (on plaque, grades 2-7)

Grade 3: three lingual cusps (on plaque, grades 8-9)

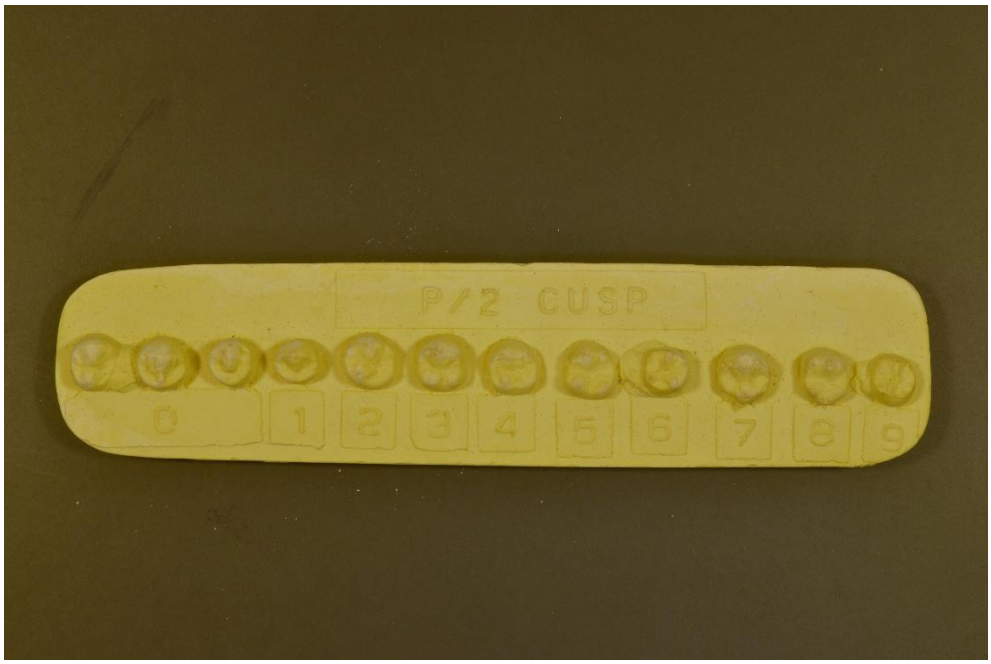

Figure 22: ASUDAS plaque for lingual cusp LP2

Anterior Fovea LM1

A polymorphic trait expressed on the mesial aspect of the trigonid of the lower molars. It involves three primary elements: distinct essential ridges on the protoconid and metaconid that meet close to the centre of the trigonid, and a mesial marginal ridges that is expressed to varying degrees. The conjoining of these three features produces a Fovea, or depression, on the mesial section of the trigonid.

Breakpoint:

Grade 0: absence

Grade 1: trace, with slight development of mesial marginal ridge

Grade 2: essential ridges on trigonid better developed, as is marginal ridge

Grade 3: essential ridges pronounced and marginal ridge well developed, producing a distinctive fovea on the anterior portion for the trigonid

Grade 4: pronounced essential ridges and marginal ridge produce a well-defined fovea

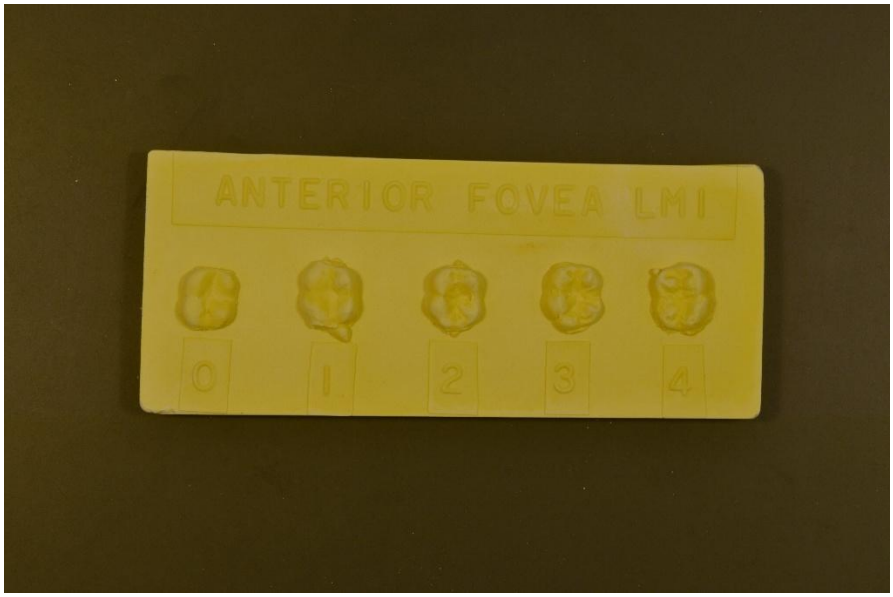

Figure 23: ASUDAS plaque for anterior fovea LM1

Mandibular Torus

This trait is expressed as one or two (or more) lobes that originate on the lingual surface of the mandible below the canine. The torus varies from a small elevation below the canine and first premolar to a multi-lobed exostosis that extends as far back as the second molar.

Breakpoint:

Grade 0: absence of torus (palpation required)

Grade 1: small (slight elevation below LC and LP1)

Grade 2: moderate (large elevation with more extended coverage, sometimes as two small lobes)

Grade 3: marked (more pronounced expression, extends from LC to LM1)

Grade 4: very marked (extends from LC to LM2, with very little separation of lobes across the mandible)

Groove Pattern LM2

Variation in the pattern of contact between the major cusps of the lower molars.

Breakpoint: Grade Y

Y pattern: contact between cusps 2 and 3

X pattern: contact between cusps 1 and 4

+ pattern: contact between cusps 1,2,3 and 4 at the central sulcus

Rocker Jaw

The left and right inferior horizontal rami of the mandible are convex which causes the mandible to rock back and forth when placed upon a flat surface and pushed.

Breakpoint: 1

Grade 0: no expression. Both inferior rami are flat or together are tripod-like in appearance; in the latter case, projections of the chin (i.e., gnathin craniometric measurement point) and the two distal-most points of the horizontal rami that transition into the vertical rami (goniom) form the base of the tripod.

Grade 1: near rocker. The inferior horizontal rami are convex enough that the mandible is unstable when laid on a flat surface. The mandible will "rock" for about a second when pushed.

Grade 3: rocker. The horizontal rami are so convex that the mandible will easily rock back and forth on a flat surface for more than a second.

Cusp Number LM1

This trait is based on the variation in the number of cusps present on the lower first molar. The lower first molar typically have 5 cusps (i.e. presence of the hypoconulid). Variations include four-cusped and six-cusped teeth. Cusp 5 must be present for cusp 6 to be scored. Details for scoring cusp 6 are presented below.

Breakpoint: 6 cusps +

Grade 0: absence of cusp 6

Grade 1: cusp 5 is more than twice the size of cusp 6

Grade 2: cusp 5 is about twice as large as cusp 6

Grade 3: cusp 5 and 6 are about equal in size

Grade 4: cusp 6 is slightly larger than cusp 5

Grade 5: cusp 6 is markedly larger than cusp 5

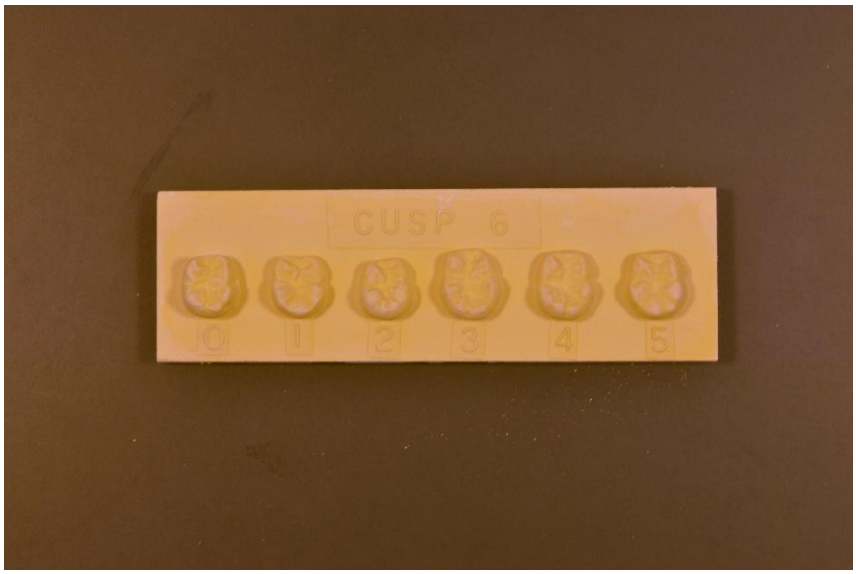

Figure 24: ASUDAS plaque for cusp 6

Cusp Number LM2

This trait is based on the variation in the number of cusps present on the lower second molar. Cusp 5 is highly variable in presence and size on the lower second molar. Variations can include four-cusped and six-cusped teeth. Cusp 5 must be present for cusp 6 to be scored. Details for scoring Cusp 5 are presented below.

Breakpoint: 5+

Grade 0: hypoconulid is absent (four-cusped tooth)

Grade 1: trace expression

Grade 2: slight

Grade 3: moderate

Grade 4: strong

Grade 5: pronounced

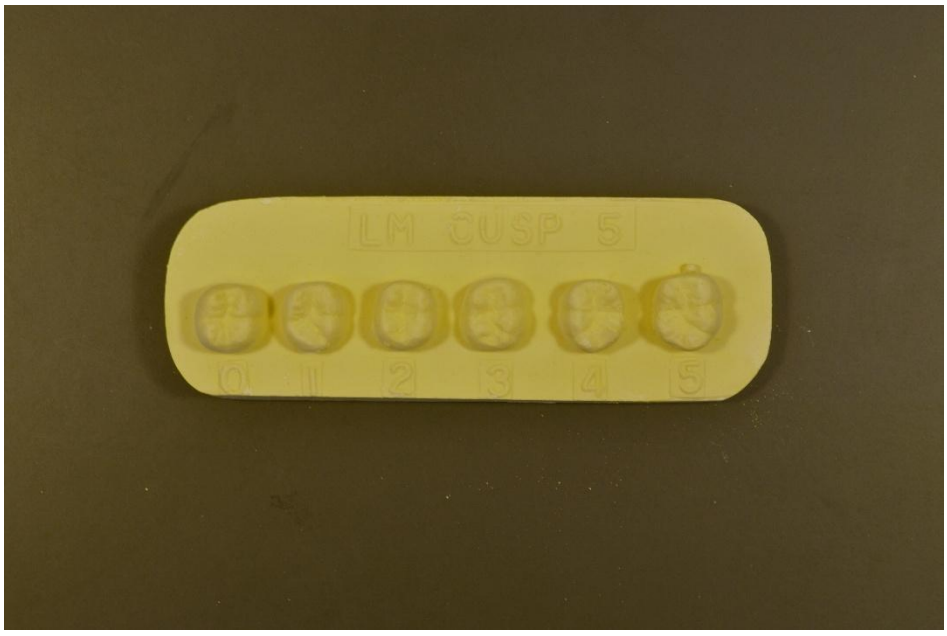

Figure 25: ASUDAS plaque for LM cusp 5

Deflecting Wrinkle LM1

The deflecting Wrinkle is expressed on the occlusal surface of the mesiolingual cusp (metaconid) of the lower molars. The trait is an unusual manifestation of the essential ridges of the metaconulid. The essential ridge runs a direct course from the cusp tip of the metaconulid to the central occlusal fossa. In some instances, the ridge changes course (or deflects) about halfway along its length before it terminates in the central sulcus.

Breakpoint: 2+

Grade 0: deflecting Wrinkle is absent; essential ridges of the metaconulid runs a straight course from cusp tip to central occlusal fossa

Grade 1: essential ridges is straight but with midpoint constriction

Grade 2: essential ridges deflects at the halfway point toward central occlusal fossa but does not contact the hypoconid.

Grade 3: essential ridges shows strong deflection at midpoint and does contact hypoconid

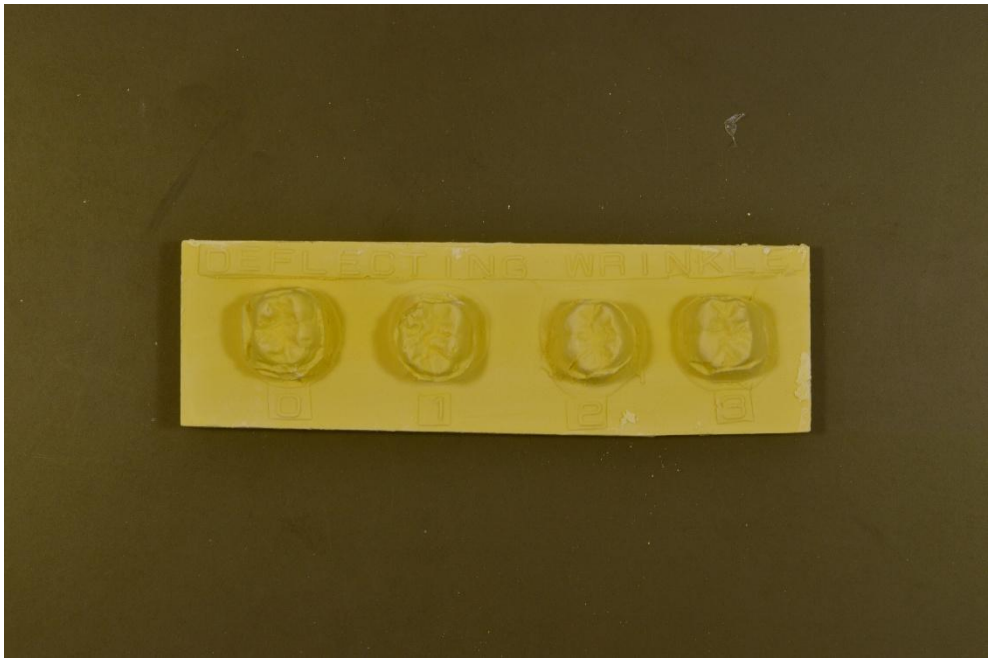

Figure 26: ASUDAS plaque for deflecting wrinkle

C1-C2 Crest LM1

The two major cusps of (protoconid and metaconid) can exhibit ridges that are connected. If the location of the ridge runs from one essential cusp to the other, the trait is referred to as a mid-trigonid crest. A distal trigonid crest is present when the distal accessory ridges run a direct course along the distal portion of the cusps and come in contact at a point close to the central occlusal sulcus. Both crests can be continuous or discontinuous.

Breakpoint: Grade 1

Grade 0: trigonid crest absent

Grade 1: trigonid crest present

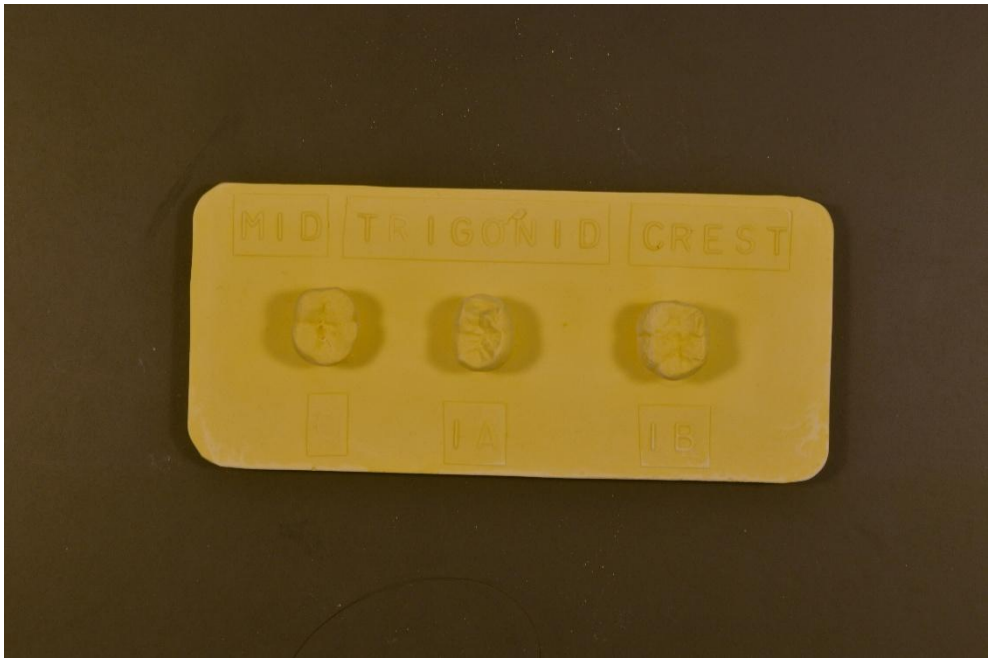

Figure 27: ASUDAS plaque for mid-trigonid crest

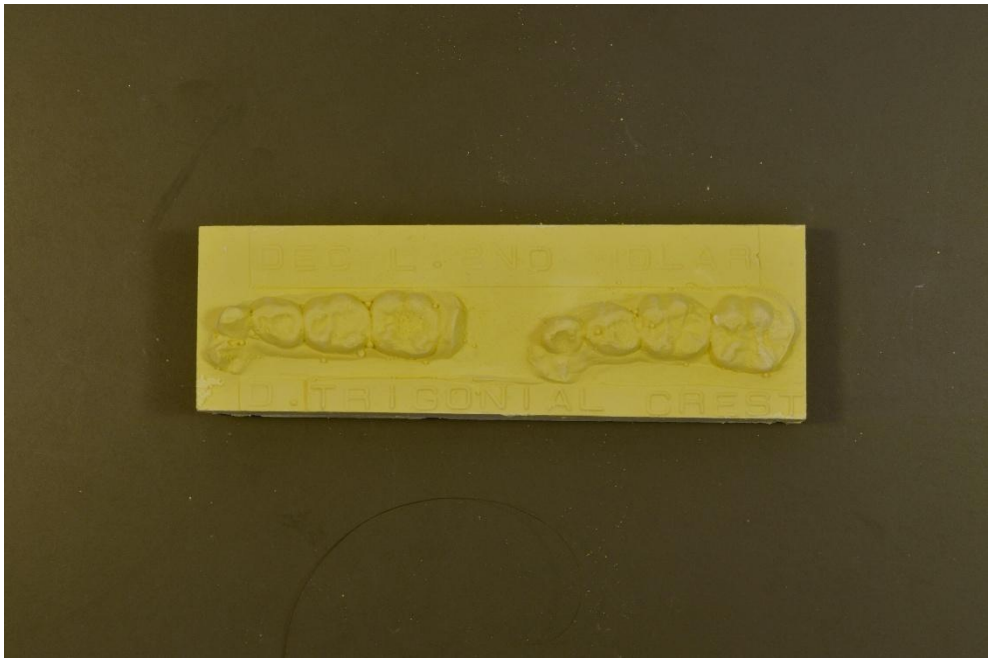

Figure 28: ASUDAS plaque for distal trigonid crest

Protostylid LM1

The protostylid is a cingular derivative. This trait is expressed on the mesiobuccal cusp of the lower molars. Expression ranges from a buccal pit to a tubercle.

Breakpoint:

Grade 0: no pit or positive expression on the buccal surface of lower molar

Grade 1: buccal pit(a pit of varying sizes, situated around the midpoint of the crown in the protoconid-hypoconid inter-lobal groove)

Grade 2: a very slight swelling and associated groove coursing mesially from buccal groove

Grade 3: slight positive expression on the mesiobuccal cusp

Grade 4: moderate positive expression

Grade 5: strong positive expression

Grade 6: pronounced positive expression

Grade 7: most distinctive form of protostylid, expressed as tubercle

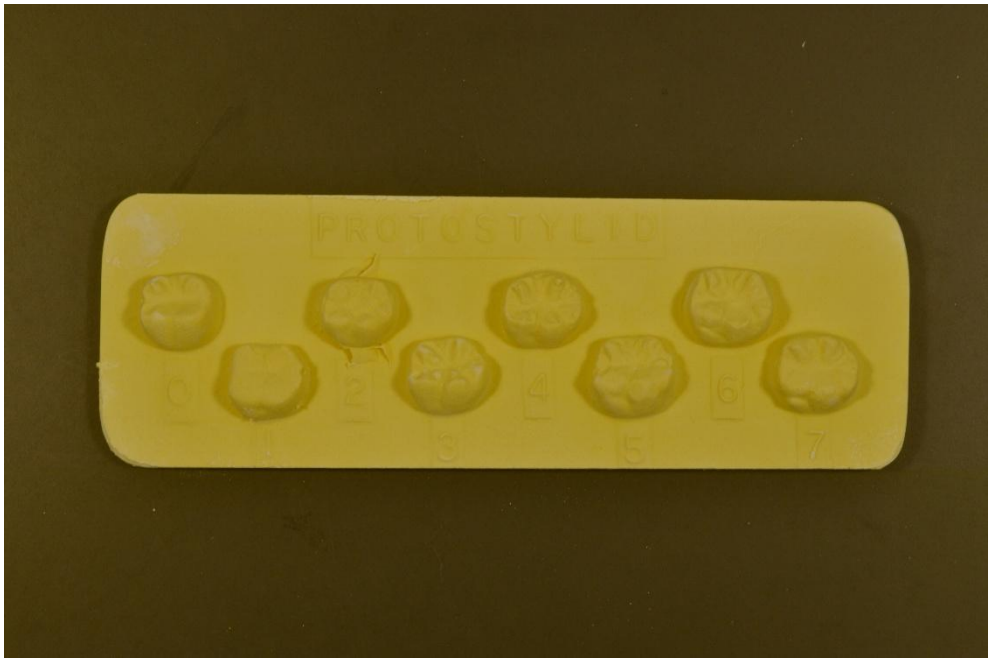

Figure 29: ASUDAS plaque for protostylid

Cusp 7 LM1

Cusp 7 is a wedge-shaped accessory cusp expressed between cusps 2 (metaconid) and cusp 4 (entoconid). Grade 1A obscures a distinctive pattern of geographic variation and, therefore, is not included in deriving the total frequency of cusp 7.

Breakpoint: 1+

Grade 0: no accessory cusp between cusps 2 and 4

Grade 1: small, wedge-shaped cusp between cusps 2 and 4

Grade 1A: this expression does not assume the typical wedge-shaped form of a cusp 7 but is marked by a groove on the lingual surface of the metaconid

Grade 2: distinct but small cusp

Grade 3: moderate cusp

Grade 4: large cusp

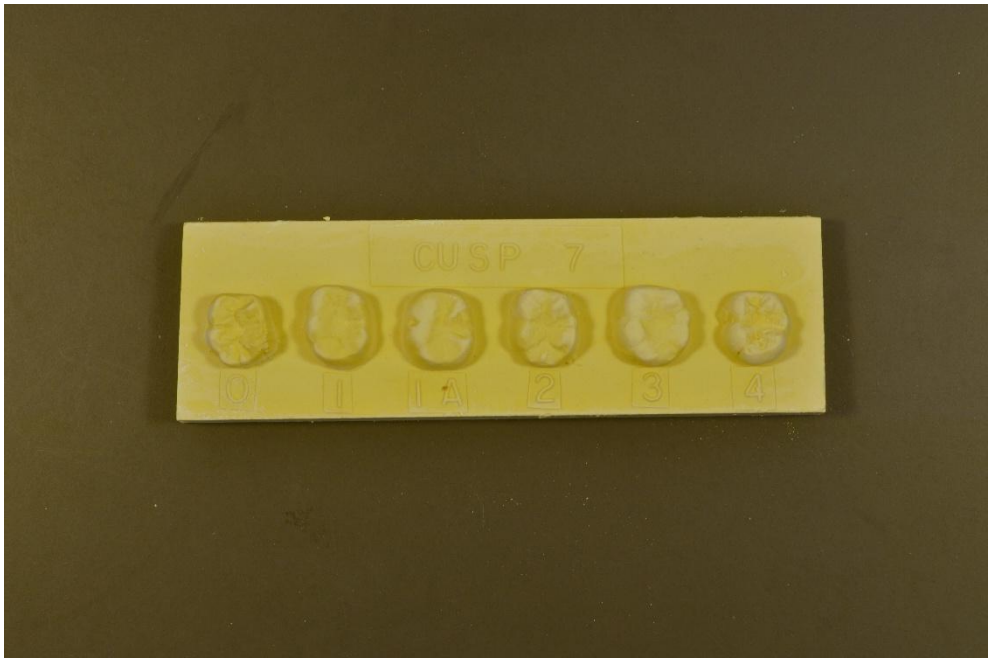

Figure 30: ASUDAS plaque for cusp 7

Tomes' Root LP1

Lower premolars have a buccal root cone and one or or more lingual cones, with the most prominent on the mesial boundary of the tooth. An LP1 may exhibit one, two, three or four root radicals. There may or may not be inter-radicular projections separating these radicals. Tomes' root constitutes that instance where a Mesiolingual root cone exhibits an inter-radicular projection, producing an independent root.

Breakpoint:

Grade 0: slight or no groove separating cones in mesial surface of LP1 root

Grade 1: slight V-shaped groove separating cones

Grade 2: depper V-shaped groove separating cones

Grade 3: deep developmental groove separating root cones along at least 1/3 of root

Grade 4: deep grooving in both mesial and distal surfaces of root

Grade 5: inter-radicular projection present so LP1 has two roots, a large buccal root and a smaller mesial/lingual root

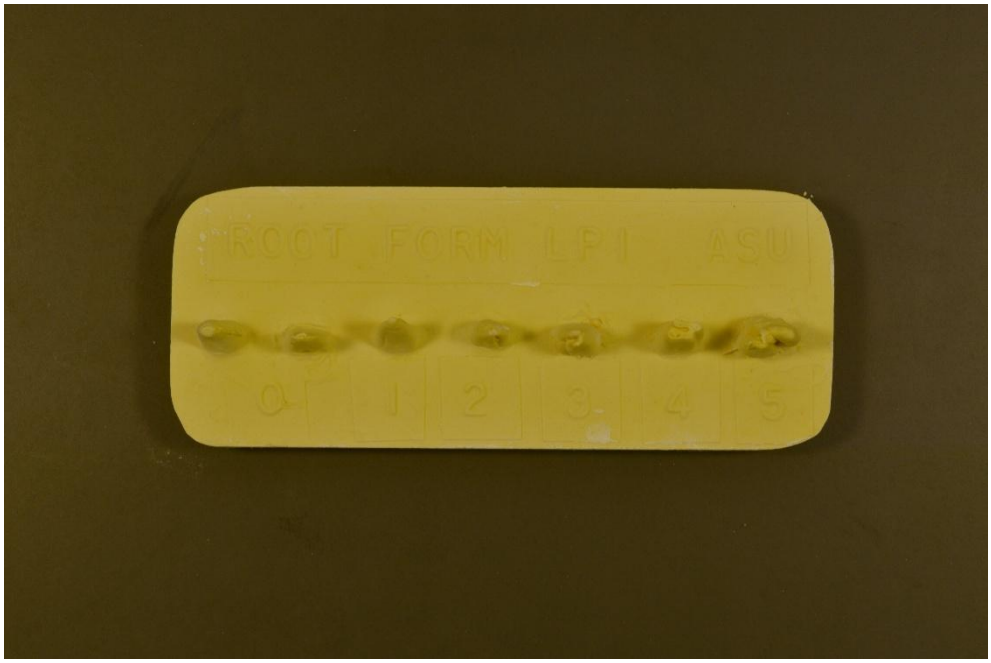

Figure 31: ASUDAS plaque for Tomes' Root LP1

Root Number LC

Upper and lower canines are typically single-rooted teeth. In some instances, however, the lower canines exhibit two roots. Although canines are single-cusped teeth, they are associated with two-root cones. The inter-radicular projection must separate the cones by at least ¼ to 1/3 of the total root length to be scored as independent roots.

Breakpoint: Grade 1

Grade 0: one-rooted LC, with or without root grooves separating the buccal and lingual cones

Grade 1: two-rooted LC, with inter-radicular projection separating buccal and lingual cones by at least ¼ to 1/3 of total root length

Root Number LM1

Lower molars generally have two roots, a mesial root associated with the trigonid and a distal root associated with the talonid. The lower first molar usually retains the two-rooted phenotype, however, sometimes these can be fused resulting in a one-rooted tooth or, additionally, a distolingual accessory root is present resulting in a three-rooted tooth.

Breakpoint: Grade 3

Grade 1: one-rooted lower first molar (no inter-radicular projection separating roots)

Grade 2: two-rooted lower first molar (distinct mesial and distal roots)

Grade 3: three-rooted lower first (3RM1) (distinct distolingual accessory root)

Root Number LM2

Lower molars generally have two roots, a mesial root associated with the trigonid and a distal root associated with the talonid. The lower second molar can exhibit two complete roots, or the two roots may be fused in one of three ways: the lingual aspect open; the buccal aspect open; or both the buccal and lingual aspects fuse. All three phetotypes constitute a one -rooted molar. Separation of the mesial and distal roots must be at least ¼ to 1/3 of the total root length to be considered independent.

Grade 1: one-rooted lower molar (mesial and distal roots of the lower molars can be fused on either buccal or lingual aspect or both)

Grade 2: inter-radicular structure produces clear separation of mesial and distal roots for at least ¼ to 1/3 of total root length

Torsomolar Angle LM3

The lower third molars may be rotated either buccally or lingually relative to a line running through the centre of the lower first and second molars. It is independent of dental crowding, if the latter is present in a dentition, torsomolar angle should not be scored.

Breakpoint: Grade 1

Grade 0: absent (torsomolar angle <10°)

Grade 1: present (torsomolar angle ≥10° in either buccal or lingual direction)

Appendix II: ASUDAS Data recording sheets

DATE:_____ FACILITY: _____
FILE NAME & NO : _____ AGE: _____ SEX: ____

MAXILLA	I1R	I1L	I2R	I2L	CR	CL	P1R	P1L	P2R	P2L	M1R	M1L	M2R	M2	M3R	M3L
STATUS/WEAR																
CARIES																
WINGING																
LABIAL CURVE																
SHOVEL																
DOUBLE SHOVEL																
INTER GROOVE																
I & C TD																
BUSHMAN C																
C DAR																
P M&D CUSPS																
METACONE					UA-P											M
HYPOCONE																H
CUSP 5																5
CARABELLI.																C
C2 PARASTYLE																P
ENAMEL EXT.																X
ROOT NO.																R
PEG/REDUCE																p
ODONTOME																O
CONG ABSENT																c
MLD																M

Extra Teeth: _____
Torus: None____Tr____Med____ Mark___
Abscess: _____
Perio: G1____ G2____ G3____ Pkts _____
Chipping: _____
Cult Treat: _____
TMJ Damage: R _____ L _____

COMMENTS:

MANDIBLE	I1L	I1R	I2L	I2R	CL	CR	P1L	P1R	P2L	P2R	M1L	M1R	M2L	M2	M3L	M3R	
STATUS/WEAR																	
CARIES																	
SHOVEL																	
C DAR																	
P LING CUSPS													← ANTERIOR FOVEA				
GROOVE PAT																	G
M CUSP NO																	C
DEF WRINKLE																	D
C1—C2 CREST																	T
PROTOSTYLID																	P
CUSP 5																	5
CUSP 6																	6
CUSP 7																	7
ENAMEL EXT.																	X
ROOT NO.																	R
ODONTOME																	
CONG ABS																	c

Torus: None_____ Tr_____ Med_____ Mark_____
Rocker: None_____ Near _____ Rocker _____
Gonial Eversion 0_____ 1_____ 2_____
Abscess: _____
Perio: G1_____ G2_____ G3_____ Pkts _____
Chipping: _____
Cult Treat: _____
Extra Teeth: _____

TOMES →

TORSOMOLAR ANG

COMMENTS:

Appendix III: Intra-observer error test

	PRESENT		ABSENT		FISHER'S
	First score	Re-score	First score	Re-score	
WNG	1	0	14	15	1.00
LC	1	0	16	17	1.00
TORU	0	0	10	10	1.00
SHV	3	4	15	14	1.00
DSH	0	0	18	18	1.00
IG	5	3	10	12	0.68
TD	2	2	12	12	1.00
BUS	0	0	16	16	1.00
CDAR	5	7	6	4	0.67
HYP	11	11	4	4	1.00
C5	14	14	2	2	1.00
CRB	5	7	10	8	0.71
PAR	1	1	10	10	1.00
X	1	1	16	16	1.00
ROUP	4	4	7	7	1.00
ROUM	11	11	2	2	1.00
PR	0	0	17	17	1.00
OD	0	0	17	17	1.00
CON	3	3	13	13	1.00
MLD	5	4	11	12	1.00
CP	11	12	5	4	1.00
ANT	3	3	9	9	1.00
TORL	0	0	15	15	1.00
PAT	5	4	10	11	1.00
ROC	0	0	16	16	1.00
MC1	2	3	17	16	1.00
MC2	7	5	10	12	0.72
DEF	2	2	14	14	1.00
C12	0	0	18	18	1.00
PRS	12	12	7	7	1.00
C7	1	1	18	18	1.00
TOM	3	3	10	10	1.00
ROLC	0	0	15	15	1.00
ROLM1	0	0	16	16	1.00
ROLM2	9	9	1	1	1.00
TMA	6	6	7	7	1.00

Appendix IV: Kendall's Tau-b results

		Winging UI1	Labial Curvature UI1	Palatine Torus	Shoveling UI1	Double Shoveling UI1	Interruption Groove UI2
Winging UI1	Correlation Coefficient	1.000	0.300	0.469	0.333	0.343	0.301
	Sig. (2-tailed)		0.000	0.000	0.000	0.000	0.000
Labial Curvature UI1	Correlation Coefficient	0.300	1.000	0.136	0.592	0.705	0.463
	Sig. (2-tailed)	0.000		0.000	0.000	0.000	0.000
Palatine Torus	Correlation Coefficient	0.469	0.136	1.000	0.146	0.145	0.153
	Sig. (2-tailed)	0.000	0.000		0.000	0.000	0.000
Shoveling UI1	Correlation Coefficient	0.333	0.592	0.146	1.000	0.774	0.428
	Sig. (2-tailed)	0.000	0.000	0.000		0.000	0.000
Double Shoveling UI1	Correlation Coefficient	0.343	0.705	0.145	0.774	1.000	0.459
	Sig. (2-tailed)	0.000	0.000	0.000	0.000		0.000
Interruption Groove UI2	Correlation Coefficient	0.301	0.463	0.153	0.428	0.459	1.000
	Sig. (2-tailed)	0.000	0.000	0.000	0.000	0.000	

		Winging UI1	Labial Curvature UI1	Palatine Torus	Shoveling UI1	Double Shoveling UI1	Interruption Groove UI2
Tuberculum Dentale UI2	Correlation Coefficient	0.274	0.466	0.127	0.450	0.479	0.803
	Sig. (2-tailed)	0.000	0.000	0.001	0.000	0.000	0.000
Bushman Canine UC	Correlation Coefficient	0.338	0.451	0.226	0.436	0.464	0.572
	Sig. (2-tailed)	0.000	0.000	0.000	0.000	0.000	0.000
Canine Distal Accessory Ridge UC	Correlation Coefficient	0.264	0.331	0.156	0.354	0.359	0.371
	Sig. (2-tailed)	0.000	0.000	0.000	0.000	0.000	0.000
Hypocone UM2	Correlation Coefficient	0.269	0.285	0.201	0.272	0.264	0.307
	Sig. (2-tailed)	0.000	0.000	0.000	0.000	0.000	0.000
Cusp 5 UM1	Correlation Coefficient	0.239	0.238	0.168	0.286	0.285	0.221
	Sig. (2-tailed)	0.000	0.000	0.000	0.000	0.000	0.000
Carabelli's Cusp UM1	Correlation Coefficient	0.151	0.171	0.094	0.277	0.247	0.188
	Sig. (2-tailed)	0.000	0.000	0.017	0.000	0.000	0.000

		Winging UI1	Labial Curvature UI1	Palatine Torus	Shoveling UI1	Double Shoveling UI1	Interruption Groove UI2
Parastyle UM3	Correlation Coefficient	0.142	0.260	0.122	0.237	0.265	0.287
	Sig. (2-tailed)	0.001	0.000	0.003	0.000	0.000	0.000
Enamel Extension UM1	Correlation Coefficient	0.219	0.270	0.190	0.331	0.321	0.296
	Sig. (2-tailed)	0.000	0.000	0.000	0.000	0.000	0.000
Root Number UP1	Correlation Coefficient	0.191	0.179	0.194	0.103	0.167	0.203
	Sig. (2-tailed)	0.000	0.000	0.000	0.007	0.000	0.000
Root number UM2	Correlation Coefficient	0.165	0.215	0.151	0.149	0.169	0.197
	Sig. (2-tailed)	0.000	0.000	0.000	0.000	0.000	0.000
Peg-Reduced UI2	Correlation Coefficient	0.386	0.453	0.248	0.368	0.439	0.584
	Sig. (2-tailed)	0.000	0.000	0.000	0.000	0.000	0.000
Odontome	Correlation Coefficient	0.184	0.219	0.163	0.208	0.242	0.247
	Sig. (2-tailed)	0.000	0.000	0.000	0.000	0.000	0.000

		Winging UI1	Labial Curvature UI1	Palatine Torus	Shoveling UI1	Double Shoveling UI1	Interruption Groove UI2
Congenital absence UM3	Correlation Coefficient	0.237	0.251	0.271	0.194	0.221	0.277
	Sig. (2-tailed)	0.000	0.000	0.000	0.000	0.000	0.000
Mid-line Diastema	Correlation Coefficient	0.629	0.275	0.467	0.306	0.337	0.280
	Sig. (2-tailed)	0.000	0.000	0.000	0.000	0.000	0.000
Cusp Number LP2	Correlation Coefficient	0.123	0.274	0.033	0.256	0.290	0.226
	Sig. (2-tailed)	0.002	0.000	0.405	0.000	0.000	0.000
Anterior Fovea LM1	Correlation Coefficient	0.037	0.136	0.008	0.189	0.162	0.108
	Sig. (2-tailed)	0.360	0.000	0.846	0.000	0.000	0.006
Mandibular Torus	Correlation Coefficient	0.152	0.041	0.101	0.073	0.081	0.074
	Sig. (2-tailed)	0.000	0.289	0.012	0.061	0.046	0.060
Groove Pattern LM2	Correlation Coefficient	0.079	0.174	0.035	0.173	0.171	0.182
	Sig. (2-tailed)	0.040	0.000	0.359	0.000	0.000	0.000

		Winging UI1	Labial Curvature UI1	Palatine Torus	Shoveling UI1	Double Shoveling UI1	Interruption Groove UI2
Rocker Jaw	Correlation Coefficient	0.109	0.032	0.078	0.085	0.100	0.079
	Sig. (2-tailed)	0.007	0.404	0.053	0.030	0.013	0.047
Cusp Number LM1	Correlation Coefficient	0.109	0.158	0.027	0.229	0.204	0.191
	Sig. (2-tailed)	0.007	0.000	0.495	0.000	0.000	0.000
Cusp Number LM2	Correlation Coefficient	0.141	0.208	0.070	0.236	0.202	0.210
	Sig. (2-tailed)	0.000	0.000	0.079	0.000	0.000	0.000
Deflecting Wrinkle LM1	Correlation Coefficient	-0.045	0.070	-0.030	0.121	0.075	0.068
	Sig. (2-tailed)	0.267	0.068	0.463	0.002	0.063	0.084
C1-C2 Crest LM1	Correlation Coefficient	-0.004	0.168	-0.041	0.260	0.219	0.150
	Sig. (2-tailed)	0.915	0.000	0.321	0.000	0.000	0.000
Protostylid LM1	Correlation Coefficient	0.050	0.162	-0.057	0.250	0.218	0.183
	Sig. (2-tailed)	0.209	0.000	0.151	0.000	0.000	0.000

		Winging UI1	Labial Curvature UI1	Palatine Torus	Shoveling UI1	Double Shoveling UI1	Interruption Groove UI2
Cusp 7 LM1	Correlation Coefficient	0.033	0.166	-0.014	0.212	0.196	0.190
	Sig. (2-tailed)	0.416	0.000	0.732	0.000	0.000	0.000
Tomes' Root LP1	Correlation Coefficient	0.079	0.124	0.034	0.089	0.097	0.150
	Sig. (2-tailed)	0.048	0.001	0.392	0.021	0.014	0.000
Root Number LC	Correlation Coefficient	0.015	0.128	-0.043	0.063	0.105	0.060
	Sig. (2-tailed)	0.721	0.001	0.291	0.109	0.010	0.132
Root Number LM1	Correlation Coefficient	-0.008	0.094	-0.036	0.073	0.079	0.111
	Sig. (2-tailed)	0.850	0.017	0.386	0.069	0.054	0.006
Root Number LM2	Correlation Coefficient	0.018	0.083	0.004	0.048	0.067	0.081
	Sig. (2-tailed)	0.657	0.027	0.913	0.214	0.092	0.036
Torsomolar Angle LM3	Correlation Coefficient	0.061	0.097	0.091	0.024	0.030	0.102
	Sig. (2-tailed)	0.122	0.010	0.021	0.532	0.447	0.008

		Tuberculum Dentale UI2	Bushman Canine UC	Canine Distal Accessory Ridge UC	Hypocone UM2	Cusp 5 UM1	Carabelli's Cusp UM1
Winging UI1	Correlation Coefficient	0.274	0.338	0.264	0.269	0.239	0.151
	Sig. (2-tailed)	0.000	0.000	0.000	0.000	0.000	0.000
Labial Curvature U1	Correlation Coefficient	0.466	0.451	0.331	0.285	0.238	0.171
	Sig. (2-tailed)	0.000	0.000	0.000	0.000	0.000	0.000
Palatine TORUS	Correlation Coefficient	0.127	0.226	0.156	0.201	0.168	0.094
	Sig. (2-tailed)	0.001	0.000	0.000	0.000	0.000	0.017
Shoveling UI1	Correlation Coefficient	0.450	0.436	0.354	0.272	0.286	0.277
	Sig. (2-tailed)	0.000	0.000	0.000	0.000	0.000	0.000
Double Shoveling UI1	Correlation Coefficient	0.479	0.464	0.359	0.264	0.285	0.247
	Sig. (2-tailed)	0.000	0.000	0.000	0.000	0.000	0.000
Interruption Groove UI2	Correlation Coefficient	0.803	0.572	0.371	0.307	0.221	0.188
	Sig. (2-tailed)	0.000	0.000	0.000	0.000	0.000	0.000

		Tuberculum Dentale UI2	Bushman Canine UC	Canine Distal Accessory Ridge UC	Hypocone UM2	Cusp 5 UM1	Carabelli's Cusp UM1
Tuberculum Dentale UI2	Correlation Coefficient	1.000	0.575	0.368	0.327	0.239	0.209
	Sig. (2-tailed)		0.000	0.000	0.000	0.000	0.000
Bushman Canine UC	Correlation Coefficient	0.575	1.000	0.584	0.391	0.339	0.203
	Sig. (2-tailed)	0.000		0.000	0.000	0.000	0.000
Canine Distal Accessory Ridge UC	Correlation Coefficient	0.368	0.584	1.000	0.296	0.363	0.312
	Sig. (2-tailed)	0.000	0.000		0.000	0.000	0.000
Hypocone UM2	Correlation Coefficient	0.327	0.391	0.296	1.000	0.435	0.315
	Sig. (2-tailed)	0.000	0.000	0.000		0.000	0.000
Cusp 5 UM1	Correlation Coefficient	0.239	0.339	0.363	0.435	1.000	0.635
	Sig. (2-tailed)	0.000	0.000	0.000	0.000		0.000
Carabelli's Cusp UM1	Correlation Coefficient	0.209	0.203	0.312	0.315	0.635	1.000
	Sig. (2-tailed)	0.000	0.000	0.000	0.000	0.000	

		Tuberculum Dentale UI2	Bushman Canine UC	Canine Distal Accessory Ridge UC	Hypocone UM2	Cusp 5 UM1	Carabelli's Cusp UM1
Parastyle UM3	Correlation Coefficient	0.296	0.370	0.315	0.410	0.279	0.173
	Sig. (2-tailed)	0.000	0.000	0.000	0.000	0.000	0.000
Enamel Extension UM1	Correlation Coefficient	0.347	0.401	0.334	0.441	0.542	0.423
	Sig. (2-tailed)	0.000	0.000	0.000	0.000	0.000	0.000
Root Number UP1	Correlation Coefficient	0.219	0.247	0.106	0.166	0.098	0.043
	Sig. (2-tailed)	0.000	0.000	0.006	0.000	0.011	0.260
Root Number UM2	Correlation Coefficient	0.183	0.306	0.138	0.438	0.181	0.077
	Sig. (2-tailed)	0.000	0.000	0.000	0.000	0.000	0.041
Peg-Reduced UI2	Correlation Coefficient	0.568	0.478	0.318	0.300	0.200	0.141
	Sig. (2-tailed)	0.000	0.000	0.000	0.000	0.000	0.000
Odontome	Correlation Coefficient	0.250	0.388	0.261	0.266	0.192	0.141
	Sig. (2-tailed)	0.000	0.000	0.000	0.000	0.000	0.000

		Tuberculum Dentale UI2	Bushman Canine UC	Canine Distal Accessory Ridge UC	Hypocone UM2	Cusp 5 UM1	Carabelli's Cusp UM1
Congenital Absence UM3	Correlation Coefficient	0.284	0.364	0.236	0.354	0.238	0.148
	Sig. (2-tailed)	0.000	0.000	0.000	0.000	0.000	0.000
Mid-line Diastema	Correlation Coefficient	0.246	0.304	0.210	0.259	0.192	0.165
	Sig. (2-tailed)	0.000	0.000	0.000	0.000	0.000	0.000
Cusp Number LP2	Correlation Coefficient	0.219	0.290	0.229	0.203	0.112	0.090
	Sig. (2-tailed)	0.000	0.000	0.000	0.000	0.004	0.020
Anterior Fovea LM1	Correlation Coefficient	0.126	0.081	0.157	0.106	0.207	0.324
	Sig. (2-tailed)	0.001	0.045	0.000	0.004	0.000	0.000
Mandibular Torus	Correlation Coefficient	0.072	0.059	0.022	0.020	-0.042	-0.077
	Sig. (2-tailed)	0.067	0.151	0.571	0.602	0.283	0.049
Groove Pattern LM2	Correlation Coefficient	0.178	0.165	0.191	0.196	0.161	0.166
	Sig. (2-tailed)	0.000	0.000	0.000	0.000	0.000	0.000

		Tuberculum Dentale UI2	Bushman Canine UC	Canine Distal Accessory Ridge UC	Hypocone UM2	Cusp 5 UM1	Carabelli's Cusp UM1
ROCKER	Correlation Coefficient	0.082	0.066	0.038	-0.004	-0.062	-0.093
	Sig. (2-tailed)	0.038	0.106	0.336	0.909	0.114	0.018
Cusp Number LM1	Correlation Coefficient	0.172	0.142	0.177	0.169	0.280	0.343
	Sig. (2-tailed)	0.000	0.001	0.000	0.000	0.000	0.000
Cusp Number LM2	Correlation Coefficient	0.194	0.186	0.188	0.236	0.241	0.250
	Sig. (2-tailed)	0.000	0.000	0.000	0.000	0.000	0.000
Deflecting Wrinkle LM1	Correlation Coefficient	0.067	-0.014	0.110	0.081	0.211	0.310
	Sig. (2-tailed)	0.088	0.731	0.006	0.032	0.000	0.000
C1-C2 Crest LM1	Correlation Coefficient	0.175	0.103	0.203	0.160	0.281	0.389
	Sig. (2-tailed)	0.000	0.014	0.000	0.000	0.000	0.000
Protostylid LM1	Correlation Coefficient	0.190	0.095	0.165	0.143	0.232	0.332
	Sig. (2-tailed)	0.000	0.018	0.000	0.000	0.000	0.000

		Tuberculum Dentale UI2		Canine Distal Accessory Ridge UC	Hypocone UM2	Cusp 5 UM1	Carabelli's Cusp UM1
Cusp 7 LM1	Correlation Coefficient	0.184	0.139	0.205	0.173	0.268	0.293
	Sig. (2-tailed)	0.000	0.001	0.000	0.000	0.000	0.000
Tomes' Root LP1	Correlation Coefficient	0.135	0.133	0.116	0.053	-0.022	-0.029
	Sig. (2-tailed)	0.000	0.001	0.003	0.153	0.563	0.450
Root |Number LC	Correlation Coefficient	0.037	0.071	0.097	0.004	-0.058	-0.057
	Sig. (2-tailed)	0.351	0.085	0.015	0.914	0.144	0.144
Root Number LM1	Correlation Coefficient	0.104	0.075	0.055	0.025	-0.032	-0.060
	Sig. (2-tailed)	0.010	0.071	0.175	0.517	0.418	0.133
Root Number LM2	Correlation Coefficient	0.077	0.103	0.038	0.053	-0.113	-0.096
	Sig. (2-tailed)	0.046	0.010	0.328	0.148	0.003	0.012
Torsomolar Angle LM3	Correlation Coefficient	0.068	0.139	0.092	0.031	-0.056	-0.136
	Sig. (2-tailed)	0.078	0.001	0.017	0.403	0.147	0.000

		Parastyle UM3	Enamel Extension UM1	Root Number UP1	Root Number UM2	Peg-Reduced UI2	Odontome
Winging UI1	Correlation Coefficient	0.142	0.219	0.191	0.165	0.386	0.184
	Sig. (2-tailed)	0.001	0.000	0.000	0.000	0.000	0.000
Labial Curvature U1	Correlation Coefficient	0.260	0.270	0.179	0.215	0.453	0.219
	Sig. (2-tailed)	0.000	0.000	0.000	0.000	0.000	0.000
Palatine Torus	Correlation Coefficient	0.122	0.190	0.194	0.151	0.248	0.163
	Sig. (2-tailed)	0.003	0.000	0.000	0.000	0.000	0.000
Shoveling UI1	Correlation Coefficient	0.237	0.331	0.103	0.149	0.368	0.208
	Sig. (2-tailed)	0.000	0.000	0.007	0.000	0.000	0.000
Double Shoveling UI1	Correlation Coefficient	0.265	0.321	0.167	0.169	0.439	0.242
	Sig. (2-tailed)	0.000	0.000	0.000	0.000	0.000	0.000
Interruption Groove UI2	Correlation Coefficient	0.287	0.296	0.203	0.197	0.584	0.247
	Sig. (2-tailed)	0.000	0.000	0.000	0.000	0.000	0.000

		Parastyle UM3	Enamel Extension UM1	Root Number UP1	Root Number UM2	Peg-Reduced UI2	Odontome
Tuberculum Dentale UI2	Correlation Coefficient	0.296	0.347	0.219	0.183	0.568	0.250
	Sig. (2-tailed)	0.000	0.000	0.000	0.000	0.000	0.000
Bushman Canine UC	Correlation Coefficient	0.370	0.401	0.247	0.306	0.478	0.388
	Sig. (2-tailed)	0.000	0.000	0.000	0.000	0.000	0.000
Canine Distal Accessory Ridge UC	Correlation Coefficient	0.315	0.334	0.106	0.138	0.318	0.261
	Sig. (2-tailed)	0.000	0.000	0.006	0.000	0.000	0.000
Hypocone UM2	Correlation Coefficient	0.410	0.441	0.166	0.438	0.300	0.266
	Sig. (2-tailed)	0.000	0.000	0.000	0.000	0.000	0.000
Cusp 5 UM1	Correlation Coefficient	0.279	0.542	0.098	0.181	0.200	0.192
	Sig. (2-tailed)	0.000	0.000	0.011	0.000	0.000	0.000
Carabelli's Cusp UM1	Correlation Coefficient	0.173	0.423	0.043	0.077	0.141	0.141
	Sig. (2-tailed)	0.000	0.000	0.260	0.041	0.000	0.000

		Parastyle UM3	Enamel Extension UM1	Root Number UP1	Root Number UM2	Peg-Reduced UI2	Odontome
Parastyle UM3	Correlation Coefficient	1.000	0.363	0.168	0.357	0.302	0.293
	Sig. (2-tailed)		0.000	0.000	0.000	0.000	0.000
Enamel Extension UM1	Correlation Coefficient	0.363	1.000	0.225	0.315	0.307	0.262
	Sig. (2-tailed)	0.000		0.000	0.000	0.000	0.000
Root Number UP1	Correlation Coefficient	0.168	0.225	1.000	0.247	0.316	0.203
	Sig. (2-tailed)	0.000	0.000		0.000	0.000	0.000
Root Number UM2	Correlation Coefficient	0.357	0.315	0.247	1.000	0.217	0.195
	Sig. (2-tailed)	0.000	0.000	0.000		0.000	0.000
Peg-Reduced UI2	Correlation Coefficient	0.302	0.307	0.316	0.217	1.000	0.236
	Sig. (2-tailed)	0.000	0.000	0.000	0.000		0.000
Odontome	Correlation Coefficient	0.293	0.262	0.203	0.195	0.236	1.000
	Sig. (2-tailed)	0.000	0.000	0.000	0.000	0.000	

		Parastyle UM3	Enamel Extension UM1	Root Number UP1	Root Number UM2	Peg-Reduced UI2	Odontome
Congenital	Correlation Coefficient	0.684	0.399	0.249	0.411	0.340	0.269
Absence UM3	Sig. (2-tailed)	0.000	0.000	0.000	0.000	0.000	0.000
Mid-line	Correlation Coefficient	0.134	0.233	0.173	0.132	0.407	0.140
Diastema	Sig. (2-tailed)	0.001	0.000	0.000	0.001	0.000	0.000
Cusp Number	Correlation Coefficient	0.233	0.137	0.070	0.098	0.208	0.475
LP2	Sig. (2-tailed)	0.000	0.001	0.072	0.010	0.000	0.000
Anterior Fovea	Correlation Coefficient	0.032	0.120	-0.041	-0.048	0.067	0.053
LM1	Sig. (2-tailed)	0.429	0.003	0.294	0.207	0.099	0.193
Mandibular	Correlation Coefficient	0.036	0.010	0.048	0.008	0.145	0.130
Torus	Sig. (2-tailed)	0.373	0.812	0.217	0.839	0.000	0.002
Groove Pattern	Correlation Coefficient	0.231	0.149	-0.012	0.043	0.138	0.194
LM2	Sig. (2-tailed)	0.000	0.000	0.749	0.243	0.000	0.000

		Parastyle UM3	Enamel Extension UM1	Root Number UP1	Root Number UM2	Peg-Reduced UI2	Odontome
Rocker Jaw	Correlation Coefficient	0.014	-0.013	0.004	0.004	0.122	0.125
	Sig. (2-tailed)	0.723	0.751	0.915	0.924	0.003	0.002
Cusp Number LM1	Correlation Coefficient	0.058	0.133	-0.052	-0.027	0.046	0.126
	Sig. (2-tailed)	0.152	0.001	0.187	0.481	0.254	0.002
Cusp Number LM2	Correlation Coefficient	0.152	0.189	0.015	0.028	0.163	0.202
	Sig. (2-tailed)	0.000	0.000	0.690	0.456	0.000	0.000
Deflecting Wrinkle LM1	Correlation Coefficient	-0.008	0.072	-0.093	-0.111	-0.024	-0.025
	Sig. (2-tailed)	0.842	0.074	0.017	0.004	0.555	0.542
C1-C2 Crest LM1	Correlation Coefficient	0.091	0.136	-0.052	-0.062	0.040	0.085
	Sig. (2-tailed)	0.029	0.001	0.196	0.113	0.331	0.041
Protostylid LM1	Correlation Coefficient	0.065	0.108	-0.056	-0.070	0.053	0.146
	Sig. (2-tailed)	0.105	0.006	0.142	0.065	0.183	0.000

		Parastyle UM3	Enamel Extension UM1	Root Number UP1	Root Number UM2	Peg-Reduced UI2	Odontome
Cusp 7 LM1	Correlation Coefficient	0.150	0.143	-0.055	-0.010	0.063	0.203
	Sig. (2-tailed)	0.000	0.000	0.166	0.792	0.128	0.000
Tomes' Root LP1	Correlation Coefficient	0.110	0.026	0.228	0.174	0.162	0.235
	Sig. (2-tailed)	0.006	0.511	0.000	0.000	0.000	0.000
Root |Number LC	Correlation Coefficient	0.107	0.008	0.180	0.138	0.129	0.141
	Sig. (2-tailed)	0.009	0.848	0.000	0.000	0.002	0.001
Root Number LM1	Correlation Coefficient	0.128	0.036	0.037	0.096	0.090	0.245
	Sig. (2-tailed)	0.002	0.388	0.353	0.015	0.030	0.000
Root Number LM2	Correlation Coefficient	0.131	0.006	0.129	0.229	0.100	0.196
	Sig. (2-tailed)	0.001	0.882	0.001	0.000	0.012	0.000
Torsomolar Angle LM3	Correlation Coefficient	0.203	0.034	0.011	0.069	0.153	0.204
	Sig. (2-tailed)	0.000	0.391	0.765	0.069	0.000	0.000

		Congenital Absence UM3	Mid-line Diastema	Cusp Number LP2	Anterior Fovea LM1	Mandibular Torus	Groove Pattern LM2
Winging UI1	Correlation Coefficient	0.237	0.629	0.123	0.037	0.152	0.079
	Sig. (2-tailed)	0.000	0.000	0.002	0.360	0.000	0.040
Labial Curvature U1	Correlation Coefficient	0.251	0.275	0.274	0.136	0.041	0.174
	Sig. (2-tailed)	0.000	0.000	0.000	0.000	0.289	0.000
Palatine Torus	Correlation Coefficient	0.271	0.467	0.033	0.008	0.101	0.035
	Sig. (2-tailed)	0.000	0.000	0.405	0.846	0.012	0.359
Shoveling UI1	Correlation Coefficient	0.194	0.306	0.256	0.189	0.073	0.173
	Sig. (2-tailed)	0.000	0.000	0.000	0.000	0.061	0.000
Double Shoveling UI1	Correlation Coefficient	0.221	0.337	0.290	0.162	0.081	0.171
	Sig. (2-tailed)	0.000	0.000	0.000	0.000	0.046	0.000
Interruption Groove UI2	Correlation Coefficient	0.277	0.280	0.226	0.108	0.074	0.182
	Sig. (2-tailed)	0.000	0.000	0.000	0.006	0.060	0.000

		Congenital Absence UM3	Mid-line Diastema	Cusp Number LP2	Anterior Fovea LM1	Mandibular Torus	Groove Pattern LM2
Tuberculum Dentale UI2	Correlation Coefficient	0.284	0.246	0.219	0.126	0.072	0.178
	Sig. (2-tailed)	0.000	0.000	0.000	0.001	0.067	0.000
Bushman Canine UC	Correlation Coefficient	0.364	0.304	0.290	0.081	0.059	0.165
	Sig. (2-tailed)	0.000	0.000	0.000	0.045	0.151	0.000
Canine Distal Accessory Ridge UC	Correlation Coefficient	0.236	0.210	0.229	0.157	0.022	0.191
	Sig. (2-tailed)	0.000	0.000	0.000	0.000	0.571	0.000
Hypocone UM2	Correlation Coefficient	0.354	0.259	0.203	0.106	0.020	0.196
	Sig. (2-tailed)	0.000	0.000	0.000	0.004	0.602	0.000
Cusp 5 UM1	Correlation Coefficient	0.238	0.192	0.112	0.207	-0.042	0.161
	Sig. (2-tailed)	0.000	0.000	0.004	0.000	0.283	0.000
Carabelli's Cusp UM1	Correlation Coefficient	0.148	0.165	0.090	0.324	-0.077	0.166
	Sig. (2-tailed)	0.000	0.000	0.020	0.000	0.049	0.000

		Congenital Absence UM3	Mid-line Diastema	Cusp Number LP2	Anterior Fovea LM1	Mandibular Torus	Groove Pattern LM2
Parastyle UM3	Correlation Coefficient	0.684	0.134	0.233	0.032	0.036	0.231
	Sig. (2-tailed)	0.000	0.001	0.000	0.429	0.373	0.000
Enamel	Correlation Coefficient	0.399	0.233	0.137	0.120	0.010	0.149
Extension UM1	Sig. (2-tailed)	0.000	0.000	0.001	0.003	0.812	0.000
Root Number	Correlation Coefficient	0.249	0.173	0.070	-0.041	0.048	-0.012
UP1	Sig. (2-tailed)	0.000	0.000	0.072	0.294	0.217	0.749
Root Number	Correlation Coefficient	0.411	0.132	0.098	-0.048	0.008	0.043
UM2	Sig. (2-tailed)	0.000	0.001	0.010	0.207	0.839	0.243
Peg-Reduced	Correlation Coefficient	0.340	0.407	0.208	0.067	0.145	0.138
UI2	Sig. (2-tailed)	0.000	0.000	0.000	0.099	0.000	0.000
Odontome	Correlation Coefficient	0.269	0.140	0.475	0.053	0.130	0.194
	Sig. (2-tailed)	0.000	0.000	0.000	0.193	0.002	0.000

		Congenital Absence UM3	Mid-line Diastema	Cusp Number LP2	Anterior Fovea LM1	Mandibular Torus	Groove Pattern LM2
Congenital Absence UM3	Correlation Coefficient	1.000	0.219	0.200	0.016	0.092	0.159
	Sig. (2-tailed)		0.000	0.000	0.684	0.021	0.000
Mid-line Diastema	Correlation Coefficient	0.219	1.000	0.121	0.056	0.155	0.083
	Sig. (2-tailed)	0.000		0.002	0.152	0.000	0.027
Cusp Number LP2	Correlation Coefficient	0.200	0.121	1.000	0.159	0.221	0.297
	Sig. (2-tailed)	0.000	0.002		0.000	0.000	0.000
Anterior Fovea LM1	Correlation Coefficient	0.016	0.056	0.159	1.000	0.052	0.236
	Sig. (2-tailed)	0.684	0.152	0.000		0.189	0.000
Mandibular Torus	Correlation Coefficient	0.092	0.155	0.221	0.052	1.000	0.119
	Sig. (2-tailed)	0.021	0.000	0.000	0.189		0.002
Groove Pattern LM2	Correlation Coefficient	0.159	0.083	0.297	0.236	0.119	1.000
	Sig. (2-tailed)	0.000	0.027	0.000	0.000	0.002	

		Congenital Absence UM3	Mid-line Diastema	Cusp Number LP2	Anterior Fovea LM1	Mandibular Torus	Groove Pattern LM2
Rocker Jaw	Correlation Coefficient	0.044	0.153	0.163	0.058	0.711	0.108
	Sig. (2-tailed)	0.270	0.000	0.000	0.147	0.000	0.005
Cusp Number LM1	Correlation Coefficient	0.024	0.094	0.232	0.565	0.011	0.337
	Sig. (2-tailed)	0.551	0.017	0.000	0.000	0.793	0.000
Cusp Number LM2	Correlation Coefficient	0.129	0.159	0.318	0.342	0.128	0.587
	Sig. (2-tailed)	0.001	0.000	0.000	0.000	0.001	0.000
Deflecting Wrinkle LM1	Correlation Coefficient	-0.088	-0.012	0.057	0.558	-0.064	0.135
	Sig. (2-tailed)	0.027	0.768	0.150	0.000	0.113	0.000
C1-C2 Crest LM1	Correlation Coefficient	0.000	0.020	0.175	0.634	0.021	0.332
	Sig. (2-tailed)	0.995	0.616	0.000	0.000	0.615	0.000
Protostylid LM1	Correlation Coefficient	-0.003	0.072	0.277	0.511	0.080	0.323
	Sig. (2-tailed)	0.938	0.061	0.000	0.000	0.042	0.000

		Congenital Absence UM3	Mid-line Diastema	Cusp Number LP2	Anterior Fovea LM1	Mandibular Torus	Groove Pattern LM2
Cusp 7 LM1	Correlation Coefficient	0.062	0.049	0.328	0.464	0.085	0.433
	Sig. (2-tailed)	0.124	0.217	0.000	0.000	0.036	0.000
Tomes' Root LP1	Correlation Coefficient	0.094	0.022	0.166	-0.004	0.243	0.100
	Sig. (2-tailed)	0.017	0.573	0.000	0.921	0.000	0.008
Root |Number LC	Correlation Coefficient	0.131	0.010	0.166	0.010	0.291	0.163
	Sig. (2-tailed)	0.001	0.791	0.000	0.796	0.000	0.000
Root Number LM1	Correlation Coefficient	0.108	-0.008	0.325	0.179	0.243	0.298
	Sig. (2-tailed)	0.008	0.843	0.000	0.000	0.000	0.000
Root Number LM2	Correlation Coefficient	0.127	-0.003	0.148	-0.056	0.242	0.239
	Sig. (2-tailed)	0.001	0.938	0.000	0.148	0.000	0.000
Torsomolar Angle LM3	Correlation Coefficient	0.238	0.082	0.266	-0.024	0.312	0.191
	Sig. (2-tailed)	0.000	0.033	0.000	0.544	0.000	0.000

		Rocker Jaw	Cusp Number LM1	Cusp Number LM2	Deflecting Wrinkle LM1	C1-C2 Crest LM1	Protostylid LM1
Winging UI1	Correlation Coefficient	0.109	0.109	0.141	-0.045	-0.004	0.050
	Sig. (2-tailed)	0.007	0.007	0.000	0.267	0.915	0.209
Labial Curvature U1	Correlation Coefficient	0.032	0.158	0.208	0.070	0.168	0.162
	Sig. (2-tailed)	0.404	0.000	0.000	0.068	0.000	0.000
Palatine Torus	Correlation Coefficient	0.078	0.027	0.070	-0.030	-0.041	-0.057
	Sig. (2-tailed)	0.053	0.495	0.079	0.463	0.321	0.151
Shoveling UI1	Correlation Coefficient	0.085	0.229	0.236	0.121	0.260	0.250
	Sig. (2-tailed)	0.030	0.000	0.000	0.002	0.000	0.000
Double Shoveling UI1	Correlation Coefficient	0.100	0.204	0.202	0.075	0.219	0.218
	Sig. (2-tailed)	0.013	0.000	0.000	0.063	0.000	0.000
Interruption Groove UI2	Correlation Coefficient	0.079	0.191	0.210	0.068	0.150	0.183
	Sig. (2-tailed)	0.047	0.000	0.000	0.084	0.000	0.000

		Rocker Jaw	Cusp Number LM1	Cusp Number LM2	Deflecting Wrinkle LM1	C1-C2 Crest LM1	Protostylid LM1
Tuberculum Dentale UI2	Correlation Coefficient	0.082	0.172	0.194	0.067	0.175	0.190
	Sig. (2-tailed)	0.038	0.000	0.000	0.088	0.000	0.000
Bushman Canine UC	Correlation Coefficient	0.066	0.142	0.186	-0.014	0.103	0.095
	Sig. (2-tailed)	0.106	0.001	0.000	0.731	0.014	0.018
Canine Distal Accessory Ridge UC	Correlation Coefficient	0.038	0.177	0.188	0.110	0.203	0.165
	Sig. (2-tailed)	0.336	0.000	0.000	0.006	0.000	0.000
Hypocone UM2	Correlation Coefficient	-0.004	0.169	0.236	0.081	0.160	0.143
	Sig. (2-tailed)	0.909	0.000	0.000	0.032	0.000	0.000
Cusp 5 UM1	Correlation Coefficient	-0.062	0.280	0.241	0.211	0.281	0.232
	Sig. (2-tailed)	0.114	0.000	0.000	0.000	0.000	0.000
Carabelli's Cusp UM1	Correlation Coefficient	-0.093	0.343	0.250	0.310	0.389	0.332
	Sig. (2-tailed)	0.018	0.000	0.000	0.000	0.000	0.000

		Rocker Jaw	Cusp Number LM1	Cusp Number LM2	Deflecting Wrinkle LM1	C1-C2 Crest LM1	Protostylid LM1
Parastyle UM3	Correlation Coefficient	0.014	0.058	0.152	-0.008	0.091	0.065
	Sig. (2-tailed)	0.723	0.152	0.000	0.842	0.029	0.105
Enamel Extension UM1	Correlation Coefficient	-0.013	0.133	0.189	0.072	0.136	0.108
	Sig. (2-tailed)	0.751	0.001	0.000	0.074	0.001	0.006
Root Number UP1	Correlation Coefficient	0.004	-0.052	0.015	-0.093	-0.052	-0.056
	Sig. (2-tailed)	0.915	0.187	0.690	0.017	0.196	0.142
Root Number UM2	Correlation Coefficient	0.004	-0.027	0.028	-0.111	-0.062	-0.070
	Sig. (2-tailed)	0.924	0.481	0.456	0.004	0.113	0.065
Peg-Reduced UI2	Correlation Coefficient	0.122	0.046	0.163	-0.024	0.040	0.053
	Sig. (2-tailed)	0.003	0.254	0.000	0.555	0.331	0.183
Odontome	Correlation Coefficient	0.125	0.126	0.202	-0.025	0.085	0.146
	Sig. (2-tailed)	0.002	0.002	0.000	0.542	0.041	0.000

		Rocker Jaw	Cusp Number LM1	Cusp Number LM2	Deflecting Wrinkle LM1	C1-C2 Crest LM1	Protostylid LM1
Congenital	Correlation Coefficient	0.044	0.024	0.129	-0.088	0.000	-0.003
Absence UM3	Sig. (2-tailed)	0.270	0.551	0.001	0.027	0.995	0.938
Mid-line	Correlation Coefficient	0.153	0.094	0.159	-0.012	0.020	0.072
Diastema	Sig. (2-tailed)	0.000	0.017	0.000	0.768	0.616	0.061
Cusp Number	Correlation Coefficient	0.163	0.232	0.318	0.057	0.175	0.277
LP2	Sig. (2-tailed)	0.000	0.000	0.000	0.150	0.000	0.000
Anterior Fovea	Correlation Coefficient	0.058	0.565	0.342	0.558	0.634	0.511
LM1	Sig. (2-tailed)	0.147	0.000	0.000	0.000	0.000	0.000
Mandibular	Correlation Coefficient	0.711	0.011	0.128	-0.064	0.021	0.080
Torus	Sig. (2-tailed)	0.000	0.793	0.001	0.113	0.615	0.042
Groove Pattern	Correlation Coefficient	0.108	0.337	0.587	0.135	0.332	0.323
LM2	Sig. (2-tailed)	0.005	0.000	0.000	0.000	0.000	0.000

		Rocker Jaw	Cusp Number LM1	Cusp Number LM2	Deflecting Wrinkle LM1	C1-C2 Crest LM1	Protostylid LM1
Rocker Jaw	Correlation Coefficient	1.000	0.066	0.114	-0.066	0.035	0.083
	Sig. (2-tailed)		0.103	0.004	0.102	0.388	0.036
Cusp Number LM1	Correlation Coefficient	0.066	1.000	0.505	0.538	0.746	0.659
	Sig. (2-tailed)	0.103		0.000	0.000	0.000	0.000
Cusp Number LM2	Correlation Coefficient	0.114	0.505	1.000	0.234	0.424	0.433
	Sig. (2-tailed)	0.004	0.000		0.000	0.000	0.000
Deflecting Wrinkle LM1	Correlation Coefficient	-0.066	0.538	0.234	1.000	0.629	0.499
	Sig. (2-tailed)	0.102	0.000	0.000		0.000	0.000
C1-C2 Crest LM1	Correlation Coefficient	0.035	0.746	0.424	0.629	1.000	0.703
	Sig. (2-tailed)	0.388	0.000	0.000	0.000		0.000
Protostylid LM1	Correlation Coefficient	0.083	0.659	0.433	0.499	0.703	1.000
	Sig. (2-tailed)	0.036	0.000	0.000	0.000	0.000	

		Rocker Jaw	Cusp Number LM1	Cusp Number LM2	Deflecting Wrinkle LM1	C1-C2 Crest LM1	Protostylid LM1
Cusp 7 LM1	Correlation Coefficient	0.068	0.719	0.482	0.472	0.696	0.689
	Sig. (2-tailed)	0.097	0.000	0.000	0.000	0.000	0.000
Tomes' Root LP1	Correlation Coefficient	0.223	-0.043	0.050	-0.115	-0.030	-0.008
	Sig. (2-tailed)	0.000	0.279	0.202	0.004	0.448	0.844
Root Number LC	Correlation Coefficient	0.219	-0.018	0.073	-0.136	-0.043	-0.008
	Sig. (2-tailed)	0.000	0.648	0.066	0.001	0.299	0.835
Root Number LM1	Correlation Coefficient	0.242	0.250	0.231	0.115	0.227	0.252
	Sig. (2-tailed)	0.000	0.000	0.000	0.005	0.000	0.000
Root Number LM2	Correlation Coefficient	0.208	-0.018	0.184	-0.106	-0.045	-0.001
	Sig. (2-tailed)	0.000	0.640	0.000	0.007	0.261	0.983
Torsomolar Angle LM3	Correlation Coefficient	0.274	-0.004	0.135	-0.144	-0.012	0.024
	Sig. (2-tailed)	0.000	0.924	0.001	0.000	0.769	0.538

		Cusp 7 LM1	Tomes' Root LP1	Root Number LC	Root Number LM1	Root Number LM2	Torsomolar Angle LM3
Winging UI1	Correlation Coefficient	0.033	0.079	0.015	-0.008	0.018	0.061
	Sig. (2-tailed)	0.416	0.048	0.721	0.850	0.657	0.122
Labial Curvature U1	Correlation Coefficient	0.166	0.124	0.128	0.094	0.083	0.097
	Sig. (2-tailed)	0.000	0.001	0.001	0.017	0.027	0.010
Palatine Torus	Correlation Coefficient	-0.014	0.034	-0.043	-0.036	0.004	0.091
	Sig. (2-tailed)	0.732	0.392	0.291	0.386	0.913	0.021
Shoveling UI1	Correlation Coefficient	0.212	0.089	0.063	0.073	0.048	0.024
	Sig. (2-tailed)	0.000	0.021	0.109	0.069	0.214	0.532
Double Shoveling UI1	Correlation Coefficient	0.196	0.097	0.105	0.079	0.067	0.030
	Sig. (2-tailed)	0.000	0.014	0.010	0.054	0.092	0.447
Interruption Groove UI2	Correlation Coefficient	0.190	0.150	0.060	0.111	0.081	0.102
	Sig. (2-tailed)	0.000	0.000	0.132	0.006	0.036	0.008

		Cusp 7 LM1	Tomes' Root LP1	Root Number LC	Root Number LM1	Root Number LM2	Torsomolar Angle LM3
Tuberculum Dentale UI2	Correlation Coefficient	0.184	0.135	0.037	0.104	0.077	0.068
	Sig. (2-tailed)	0.000	0.000	0.351	0.010	0.046	0.078
Bushman Canine UC	Correlation Coefficient	0.139	0.133	0.071	0.075	0.103	0.139
	Sig. (2-tailed)	0.001	0.001	0.085	0.071	0.010	0.001
Canine Distal Accessory Ridge UC	Correlation Coefficient	0.205	0.116	0.097	0.055	0.038	0.092
	Sig. (2-tailed)	0.000	0.003	0.015	0.175	0.328	0.017
Hypocone UM2	Correlation Coefficient	0.173	0.053	0.004	0.025	0.053	0.031
	Sig. (2-tailed)	0.000	0.153	0.914	0.517	0.148	0.403
Cusp 5 UM1	Correlation Coefficient	0.268	-0.022	-0.058	-0.032	-0.113	-0.056
	Sig. (2-tailed)	0.000	0.563	0.144	0.418	0.003	0.147
Carabelli's Cusp UM1	Correlation Coefficient	0.293	-0.029	-0.057	-0.060	-0.096	-0.136
	Sig. (2-tailed)	0.000	0.450	0.144	0.133	0.012	0.000

		Cusp 7 LM1	Tomes' Root LP1	Root Number LC	Root Number LM1	Root Number LM2	Torsomolar Angle LM3
Parastyle UM3	Correlation Coefficient	0.150	0.110	0.107	0.128	0.131	0.203
	Sig. (2-tailed)	0.000	0.006	0.009	0.002	0.001	0.000
Enamel Extension UM1	Correlation Coefficient	0.143	0.026	0.008	0.036	0.006	0.034
	Sig. (2-tailed)	0.000	0.511	0.848	0.388	0.882	0.391
Root Number UP1	Correlation Coefficient	-0.055	0.228	0.180	0.037	0.129	0.011
	Sig. (2-tailed)	0.166	0.000	0.000	0.353	0.001	0.765
Root Number UM2	Correlation Coefficient	-0.010	0.174	0.138	0.096	0.229	0.069
	Sig. (2-tailed)	0.792	0.000	0.000	0.015	0.000	0.069
Peg-Reduced UI2	Correlation Coefficient	0.063	0.162	0.129	0.090	0.100	0.153
	Sig. (2-tailed)	0.128	0.000	0.002	0.030	0.012	0.000
Odontome	Correlation Coefficient	0.203	0.235	0.141	0.245	0.196	0.204
	Sig. (2-tailed)	0.000	0.000	0.001	0.000	0.000	0.000

		Cusp 7 LM1	Tomes' Root LP1	Root Number LC	Root Number LM1	Root Number LM2	Torsomolar Angle LM3
Congenital Absence UM3	Correlation Coefficient	0.062	0.094	0.131	0.108	0.127	0.238
	Sig. (2-tailed)	0.124	0.017	0.001	0.008	0.001	0.000
Mid-line Diastema	Correlation Coefficient	0.049	0.022	0.010	-0.008	-0.003	0.082
	Sig. (2-tailed)	0.217	0.573	0.791	0.843	0.938	0.033
Cusp Number LP2	Correlation Coefficient	0.328	0.166	0.166	0.325	0.148	0.266
	Sig. (2-tailed)	0.000	0.000	0.000	0.000	0.000	0.000
Anterior Fovea LM1	Correlation Coefficient	0.464	-0.004	0.010	0.179	-0.056	-0.024
	Sig. (2-tailed)	0.000	0.921	0.796	0.000	0.148	0.544
Mandibular Torus	Correlation Coefficient	0.085	0.243	0.291	0.243	0.242	0.312
	Sig. (2-tailed)	0.036	0.000	0.000	0.000	0.000	0.000
Groove Pattern LM2	Correlation Coefficient	0.433	0.100	0.163	0.298	0.239	0.191
	Sig. (2-tailed)	0.000	0.008	0.000	0.000	0.000	0.000

		Cusp 7 LM1	Tomes' Root LP1	Root Number LC	Root Number LM1	Root Number LM2	Torsomolar Angle LM3
Rocker Jaw	Correlation Coefficient	0.068	0.223	0.219	0.242	0.208	0.274
	Sig. (2-tailed)	0.097	0.000	0.000	0.000	0.000	0.000
Cusp Number LM1	Correlation Coefficient	0.719	-0.043	-0.018	0.250	-0.018	-0.004
	Sig. (2-tailed)	0.000	0.279	0.648	0.000	0.640	0.924
Cusp Number LM2	Correlation Coefficient	0.482	0.050	0.073	0.231	0.184	0.135
	Sig. (2-tailed)	0.000	0.202	0.066	0.000	0.000	0.001
Deflecting Wrinkle LM1	Correlation Coefficient	0.472	-0.115	-0.136	0.115	-0.106	-0.144
	Sig. (2-tailed)	0.000	0.004	0.001	0.005	0.007	0.000
C1-C2 Crest LM1	Correlation Coefficient	0.696	-0.030	-0.043	0.227	-0.045	-0.012
	Sig. (2-tailed)	0.000	0.448	0.299	0.000	0.261	0.769
Protostylid LM1	Correlation Coefficient	0.689	-0.008	-0.008	0.252	-0.001	0.024
	Sig. (2-tailed)	0.000	0.844	0.835	0.000	0.983	0.538

		Cusp 7 LM1	Tomes' Root LP1	Root Number LC	Root Number LM1	Root Number LM2	Torsomolar Angle LM3
Cusp 7 LM1	Correlation Coefficient	1.000	0.011	0.013	0.351	0.050	0.068
	Sig. (2-tailed)		0.786	0.743	0.000	0.207	0.087
Tomes' Root LP1	Correlation Coefficient	0.011	1.000	0.430	0.269	0.324	0.137
	Sig. (2-tailed)	0.786		0.000	0.000	0.000	0.000
Root Number LC	Correlation Coefficient	0.013	0.430	1.000	0.270	0.318	0.269
	Sig. (2-tailed)	0.743	0.000		0.000	0.000	0.000
Root Number LM1	Correlation Coefficient	0.351	0.269	0.270	1.000	0.452	0.328
	Sig. (2-tailed)	0.000	0.000	0.000		0.000	0.000
Root Number LM2	Correlation Coefficient	0.050	0.324	0.318	0.452	1.000	0.256
	Sig. (2-tailed)	0.207	0.000	0.000	0.000		0.000
Torsomolar Angle LM3	Correlation Coefficient	0.068	0.137	0.269	0.328	0.256	1.000
	Sig. (2-tailed)	0.087	0.000	0.000	0.000	0.000	

Appendix V: 22-Trait Frequencies and Numbers

Table 8: Trait percentages of numbers of individuals scored for a sub-set of 22 traits by sample. NOR= Norton Priory, Runcorn, POU= Chapel House Farm, Poulton, GLC= St. Owen's Church Gloucester, GLRC= London Road, Gloucester, LDG= Great House Farm, Llandough, ATE= site 92, Atlantic Trading Estate, Barry, BRS= Brownslade Barrow, Castlemartin, CLV= Culver Hole, Llangennith, TKW= Tinkinswood Burial Chamber, St. Nicholas, STG= Strath Glebe chambered cairn, Skye, DIS= Distillery Cave, Oban, RAS= Raschoille Cave, Oban, WHIT= Whithorn Priory, Dumfries and Galloway, SGR= Southgreen, Kildare, PKN= Parknahown 5, Co. Laois, KLY= Killeany 1, Co. Laois, BFL= Bushfield/Lismore, Co. Laois.

TRAIT		NOR	POU	GLC	GLRC	LDG	ATE	BRS	CLV	TKW	STG	DIS	RAS	WHIT	SGR	PKN	KLY	BFL
WINGING UI1 (+= ASU 1)	**%**	9.09	13.33	11.76	0.00	0.00	7.69	0.00	0.00	0.00	0.00	0.00	0.00	0.00	0.00	0.00	14.29	0.00
	n	44	60	34	7	12	13	14	4	3	1	3	2	8	10	12	7	1
SHOVELLING UI1 (+= ASU 2-6)	**%**	5.26	9.52	25.00	0.00	7.69	8.33	16.67	-	-	44.44	100	50	33.33	12.50	25.00	0.00	0.00
	n	19	42	28	16	13	12	6	0	0	9	1	2	9	8	12	4	3
DOUBLE SHOVELLING UI1(+= ASU 2-6)	**%**	0.00	2	3.13	0.00	0.00	0.00	0.00	-	-	0.00	0.00	0.00	0.00	0.00	0.00	0.00	0.00
	n	23	50	32	28	18	15	7	0	0	9	1	2	9	8	14	5	5
INTERRUPTION GROOVE UI2 (+=ASU +)	**%**	23.08	33.33	34.78	31.03	23.53	23.81	52.86	-	0.00	14.29	100	100	36.36	7.69	20	18.18	33.33
	n	26	45	23	29	17	21	7	0	3	7	1	1	11	13	15	11	9
BUSHMAN CANINE UC (+= ASU 1-3)	**%**	0.00	0.00	3.13	9.68	0.00	0.00	0.00	-	0.00	10.00	0.00	0.00	0.00	0.00	5.26	8.33	0.00
	n	31	47	32	31	21	18	12	0	1	10	1	1	12	16	19	12	11
HYPOCONE UM2 (+= ASU 3-6)	**%**	60.61	52.08	70.59	55.56	66.67	73.68	100	75.00	75.00	100	100	80.00	75.00	36.36	55.00	55.56	40.00
	n	33	48	34	27	21	19	10	4	4	9	3	5	12	11	20	9	20
CUSP 5 UM1 (+= ASU 2-5)	**%**	8.00	10.53	20.00	13.64	0	36.36	12.5	25	25	20	25	16.67	0	28.57	42.86	37.5	21.43
	n	25	38	30	22	12	11	8	4	4	5	4	6	9	7	14	8	14
CARABELLI'S CUSP UM1 (+= ASU 2-7)	**%**	55.56	36.36	54.17	5.26	30.00	62.5	60	50	0.00	40	66.67	50	28.57	25	25	0.00	0.00
	n	18	22	24	19	10	8	5	4	4	5	3	4	7	4	8	1	6

ENAMEL EXTENSION UM1 (+= ASU 1-3)	**%**	2.86	5.13	12.5	3.85	9.09	22.22	0.00	0.00	0.00	0.00	100	16.67	6.25	0.00	0.00	0.00	8.70
	n	35	39	32	26	22	18	10	4	4	5	2	6	16	8	15	7	23
ROOT NUMBER UP1 (+= ASU 2+)	**%**	23.53	34.48	31.25	30.77	28.57	50.00	75.00	50.00	20.00	16.67	0.00	50.00	46.67	12.50	52.63	50.00	30.77
	n	34	29	32	26	21	22	12	2	5	6	1	4	15	8	19	14	13
ROOT NUMBER UM2 (+= ASU 3+)	**%**	65.79	58.33	70.59	69.23	54.17	75.00	62.5	66.67	100	90.00	50.00	100	69.23	54.55	74.07	35.29	40.91
	n	38	36	34	26	24	20	8	3	2	10	2	7	13	11	27	17	22
ODONTOME P1-P2 (+= ASU +)	**%**	0.00	1.89	2.00	0.00	0.00	0.00	0.00	0.00	0.00	0.00	0.00	0.00	0.00	0.00	0.00	0.00	0.00
	n	61	53	50	37	36	28	26	13	7	14	4	5	17	16	25	16	24
4-CUSPED LM1 (-= ASU 4-)	**%**	12.5	2.86	0	9.09	8.33	16.67	0	0	0	0	0	0	0	0	0	0	10
	n	24	35	31	22	12	6	9	3	5	10	6	2	3	4	7	2	10
GROOVE PATTERN LM2 (+= ASU Y)	**%**	13.33	28.21	25.00	14.29	12.50	11.76	7.69	12.50	42.86	50.00	25.00	0.00	0.00	44.44	12.50	0.00	20.00
	n	45	39	32	28	24	17	13	8	7	6	4	3	9	9	16	10	20
CUSP NUMBER LM1 (+= ASU 6+)	**%**	4.17	8.57	16.13	22.73	0.00	16.67	11.11	0.00	20.00	0.00	0.00	0.00	33.33	25.00	14.29	0.00	10.00
	n	24	35	31	22	12	6	9	3	5	10	6	2	3	4	7	2	10
CUSP NUMBER LM2 (+= ASU 5+)	**%**	16.13	22.22	45.16	18.18	10.00	20.00	0.00	25.00	20.00	33.33	25.00	0.00	0.00	33.33	27.27	0.00	21.43
	n	31	45	31	22	20	10	9	4	5	6	4	3	5	6	11	8	14
DEFLECTING WRINKLE LM1 (+= ASU 2-3)	**%**	28.57	55.56	71.43	14.29	33.33	25	33.33	0.00	0.00	11.11	0.00	50.00	0.00	40.00	0.00	0.00	0.00
	n	7	9	14	7	9	4	3	3	3	9	4	2	3	5	3	1	6
CUSP 7 LM1 (+= ASU 2-4)	**%**	0.00	0.00	8.11	0.00	0.00	0.00	0.00	0.00	16.67	0.00	0.00	0.00	0.00	16.67	14.29	0.00	0.00
	n	32	34	37	22	18	12	14	10	6	11	6	3	6	6	14	8	17
TOME'S ROOT LP1 (+= ASU 3-5)	**%**	2.44	3.45	5.71	14.81	0.00	8.33	8.33	0.00	0.00	0.00	0.00	0.00	20.00	0.00	0.00	6.25	0.00
	n	41	29	35	27	23	24	12	1	4	4	1	3	10	15	24	16	18
ROOT NUMBER LC (+= ASU 2+)	**%**	2.17	2.38	8.57	9.68	7.41	14.81	7.69	0.00	50.00	0.00	0.00	0.00	0.00	14.29	4.17	0.00	0.00
	n	46	42	35	31	27	27	13	10	2	11	3	2	14	14	24	17	19
ROOT NUMBER LM1 (+= ASU 3+)	**%**	0.00	0.00	0.00	0.00	0.00	0.00	0.00	0.00	0.00	0.00	0.00	0.00	0.00	0.00	0.00	0.00	0.00
	n	49	36	44	26	29	27	20	14	11	9	7	3	14	13	29	18	21
ROOT NUMBER LM2 (+= ASU 2+)	**%**	72.55	81.82	77.5	71.43	79.31	85.71	88.89	100	87.50	88.89	100	100	75.00	83.33	75.86	68.42	73.68
	n	51	33	40	28	29	28	18	9	8	9	2	3	16	12	29	19	19

Table 9: Trait percentages of numbers of individuals scored for sub-set of 22 traits by global population sample. WE= Western Europe, NoE= Northern Europe, NA= North Africa, WA= West Africa, SA= South Africa, KH=Khoisan, CM= China-Mongolia, Jo= Jomon, RJ= Recent Japan, NES= Northeast Siberia, SS= South Siberia, AA= American Arctic, NWA= Northwest America, NSAI= N. & S. American Indian, SEE= Southeast Asia (Early), SER=Southeast Asia (Recent), PO= Polynesia, MI= Micronesia, AU= Australia, NG= New Guinea, ML= Melanesia

TRAIT		WE	NOE	NA	WA	SA	KH	CM	JO	RJ	NES	SS	AA	NWA	NSAI	SEE	SER	PO	MI	AU	NG	ML
WINGING UI1 (+= ASU 1)	**%**	7.20	4.70	7.50	19.20	4.20	16.70	24.50	19.90	21.90	33.90	18.30	23.20	35.80	50.00	27.50	22.60	20.40	39.70	9.40	7.60	18.70
	n	180	150	460	52	496	90	591	166	265	112	109	220	226	1177	131	270	274	78	508	170	209
SHOVELLING UI1 (+= ASU 2-6)	**%**	2.70	2.20	7.50	7.30	9.30	13.30	72.00	25.70	66.00	62.00	36.70	69.20	83.10	91.90	30.50	34.90	20.70	31.30	20.10	0.00	8.90
	n	186	46	194	41	220	155	542	117	276	61	98	172	172	1368	184	261	275	83	274	30	135
DOUBLE SHOVELLING UI1(+= ASU 2-6)	**%**	3.80	5.00	8.60	2.60	1.80	0.00	28.80	1.40	19.50	32.50	15.20	34.90	56.70	70.50	15.90	12.00	4.50	8.20	4.20	0.00	4.50
	n	184	100	175	39	282	79	545	138	267	43	92	155	158	1231	182	199	287	85	261	32	134
INTERRUPTION GROOVE UI2 (+=ASU +)	**%**	42.00	30.00	32.40	10.40	12.00	15.70	43.00	64.60	44.50	46.30	54.50	59.60	65.00	51.00	38.50	29.00	35.30	24.50	18.20	16.10	18.80
	n	224	100	241	48	301	83	537	189	301	95	145	275	223	1405	200	272	329	102	357	56	165
BUSHMAN CANINE UC (+= ASU 1-3)	**%**	4.30	0.00	6.10	29.10	12.60	35.10	2.80	18.00	4.80	2.50	8.40	0.00	0.40	1.60	6.00	6.00	2.90	5.10	2.00	1.90	2.90
	n	230	125	261	55	398	77	615	136	365	119	115	339	268	1402	235	366	382	121	391	54	174
HYPOCONE UM2 (+= ASU 3-6)	**%**	75.30	80.80	89.40	96.40	92.80	93.80	89.20	82.00	86.50	78.20	85.80	69.40	85.80	88.50	91.50	88.50	92.30	84.90	96.70	95.30	92.50
	n	308	239	446	83	531	86	798	206	482	192	233	569	459	2381	368	730	632	186	643	191	295
CUSP 5 UM1 (+= ASU 2-5)	**%**	11.80	10.00	18.50	62.50	21.60	34.80	24.20	31.50	19.70	10.40	25.10	16.70	21.40	16.70	32.40	31.00	42.70	27.60	61.50	45.70	44.40
	n	238	140	357	48	439	66	633	146	390	106	191	418	378	1780	328	581	565	163	449	151	234
CARABELLI'S CUSP UM1 (+= ASU 2-7)	**%**	27.30	18.10	20.00	21.30	11.40	16.80	16.20	2.30	14.90	5.30	14.00	1.90	5.50	5.60	18.70	20.80	21.70	22.50	21.40	18.70	20.30
	n	249	138	200	61	246	155	774	181	458	172	186	477	388	2054	262	701	617	160	332	197	291
ENAMEL EXTENSION UM1 (+= ASU 1-3)	**%**	7.80	2.20	6.80	0.00	8.00	0.00	53.20	9.70	54.60	49.70	24.90	45.90	50.90	43.70	22.50	36.10	20.10	7.80	9.20	5.00	3.50
	n	371	229	503	99	387	15	718	278	522	328	289	936	699	3016	315	746	741	193	797	240	289

ROOT NUMBER UP1 (+= ASU 2+)	**%**	40.70	45.90	57.10	66.70	61.10	20.00	27.20	24.50	24.90	6.90	31.30	4.90	6.70	14.30	43.20	38.60	33.60	55.60	42.40	30.20	46.20
	n	317	194	468	87	386	15	645	241	506	375	278	1022	693	2849	299	845	808	196	642	278	299
ROOT NUMBER UM2 (+= ASU 3+)	**%**	57.40	61.20	78.60	82.90	84.50	75.00	65.00	46.90	68.90	50.80	47.00	37.40	41.50	55.90	73.00	77.40	49.50	73.40	80.90	55.40	75.10
	n	265	227	364	82	341	16	591	254	495	260	247	836	523	2054	196	752	739	184	644	260	297
ODONTOME P1-P2 (+= ASU +)	**%**	0.80	0.00	0.20	0.00	0.40	0.00	5.50	0.40	5.00	2.10	0.60	6.20	6.50	4.40	2.80	2.50	2.30	1.20	3.00	0.00	2.80
	n	246	111	545	56	531	86	639	260	462	95	155	372	371	1787	213	564	572	170	336	119	218
4-CUSPED LM1 (-= ASU 4-)	**%**	7.80	10.00	10.00	0.00	1.20	0.80	0.20	0.00	0.30	0.00	3.10	0.00	0.00	0.00	0.40	0.70	1.20	0.00	0.40	4.50	1.90
	n	217	170	250	47	346	133	538	214	314	90	195	355	332	1847	248	418	417	148	235	66	210
GROOVE PATTERN LM2 (+= ASU Y)	**%**	27.20	21.00	30.60	32.80	45.70	71.90	7.60	32.10	13.10	18.60	22.20	20.00	11.80	9.80	18.40	17.50	18.80	21.20	12.70	39.20	26.80
	n	257	319	402	67	392	89	646	290	352	145	270	529	498	2473	348	587	501	160	465	102	254
CUSP NUMBER LM1 (+= ASU 6+)	**%**	8.30	16.90	7.70	44.70	18.80	4.70	35.90	46.70	42.70	50.00	20.50	50.40	50.30	55.10	40.30	32.50	53.50	45.30	61.70	15.20	49.50
	n	217	130	352	47	362	85	538	214	314	90	195	355	322	1847	248	418	417	148	235	166	210
CUSP NUMBER LM2 (+= ASU 5+)	**%**	28.90	15.60	33.60	88.00	70.00	93.20	79.20	71.30	86.40	93.50	45.80	94.80	95.60	91.40	67.80	69.70	66.80	79.50	90.30	40.90	50.00
	n	284	225	381	75	370	88	639	244	345	138	225	484	447	2462	314	555	461	161	413	93	234
DEFLECTING WRINKLE LM1 (+= ASU 2-3)	**%**	5.20	16.00	8.20	16.70	18.10	16.70	15.70	4.90	14.90	39.50	16.90	30.00	36.50	38.10	22.00	15.90	14.00	22.80	17.10	3.80	17.90
	n	154	75	267	30	298	60	343	162	262	81	142	230	192	1311	150	290	322	149	35	52	184
CUSP 7 LM1 (+= ASU 2-4)	**%**	4.50	5.00	9.40	43.70	26.50	26.40	7.90	3.10	5.70	6.00	9.90	8.50	6.80	8.50	7.50	7.30	7.10	5.80	5.30	7.00	12.40
	n	291	179	414	71	385	87	721	285	382	151	272	565	473	2756	370	588	495	175	294	100	267
TOME'S ROOT LP1 (+= ASU 3-5)	**%**	5.90	6.60	8.60	38.70	23.00	0.00	14.10	3.20	10.00	10.10	17.30	3.40	9.30	19.90	21.60	22.20	16.20	17.50	27.30	7.20	16.90
	n	270	168	372	49	217	15	248	282	200	99	196	493	494	1833	172	307	372	125	383	126	160
ROOT NUMBER LC (+= ASU 2+)	**%**	5.70	6.10	2.30	0.00	0.00	0.00	0.00	1.00	1.20	0.00	3.00	0.30	0.00	0.70	0.50	1.10	0.40	1.00	0.00	0.00	0.00
	n	314	214	347	33	192	14	401	203	335	206	260	733	500	2404	204	568	528	196	409	100	200
ROOT NUMBER LM1 (+= ASU 3+)	**%**	0.60	0.00	1.20	7.60	0.40	0.00	28.30	3.40	24.20	22.30	2.50	31.10	16.50	6.50	8.20	14.10	8.60	2.90	4.90	0.00	3.20
	n	357	198	337	92	240	15	604	377	429	238	242	871	741	3276	400	652	628	204	612	157	251
ROOT NUMBER LM2 (+= ASU 2+)	**%**	72.00	79.20	88.30	91.50	96.40	71.40	60.20	90.2	67.10	64.50	53.70	68.80	61.30	67.20	76.60	73.30	68.70	83.40	93.50	83.80	93.80
	n	318	269	333	82	225	15	548	336	407	220	242	772	659	2703	282	630	617	211	523	142	242

Appendix VI – Trait Frequency Charts

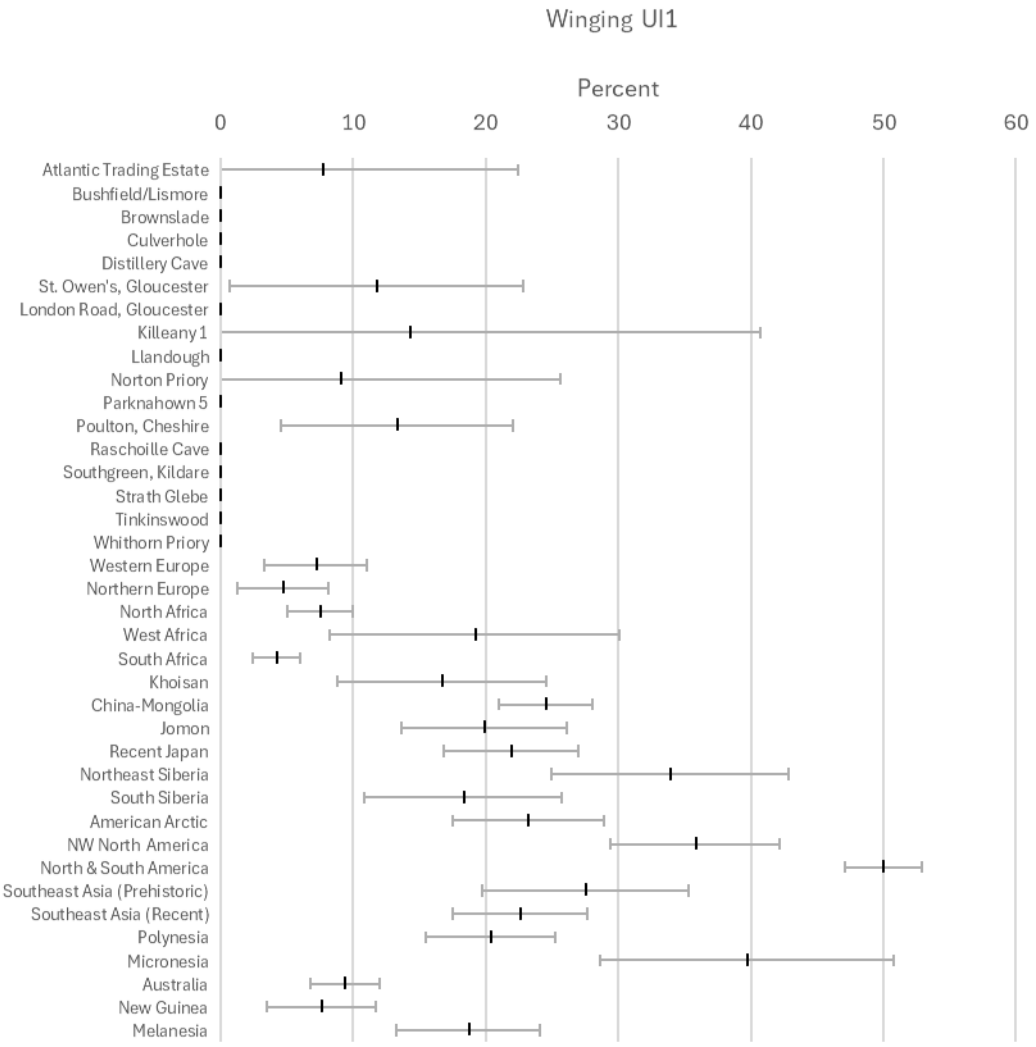

Figure 32: Winging trait frequency variation among British and Irish samples and global populations (trait frequency represented by vertical line with horizontal bars showing ±2 standard errors).

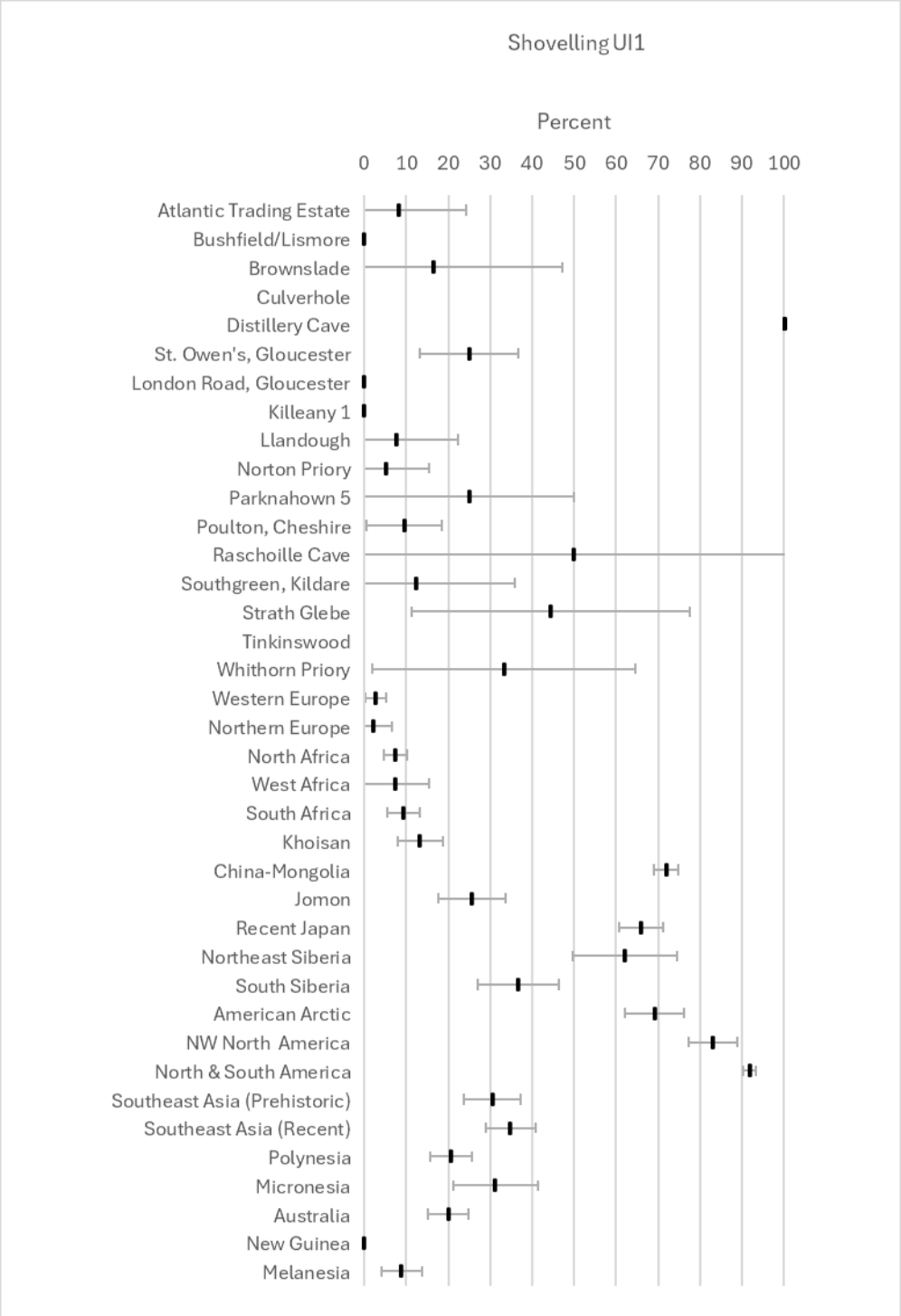

Figure 33: Shovelling trait frequency variation among British and Irish samples and global populations (trait frequency represented by vertical line with horizontal bars showing ±2 standard errors).

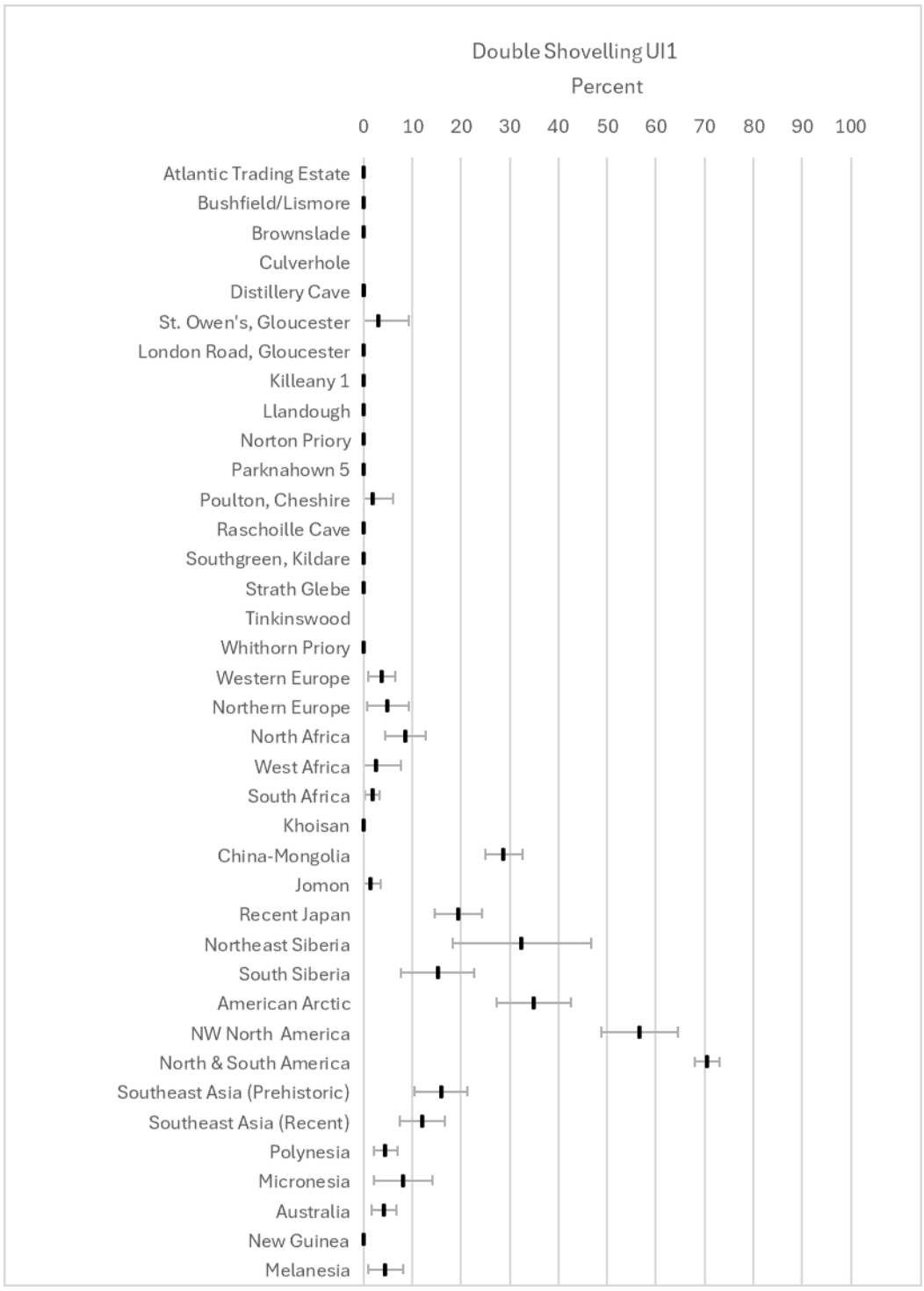

Figure 34: Double shovelling trait frequency variation among British and Irish samples and global populations (trait frequency represented by vertical line with horizontal bars showing ±2 standard errors).

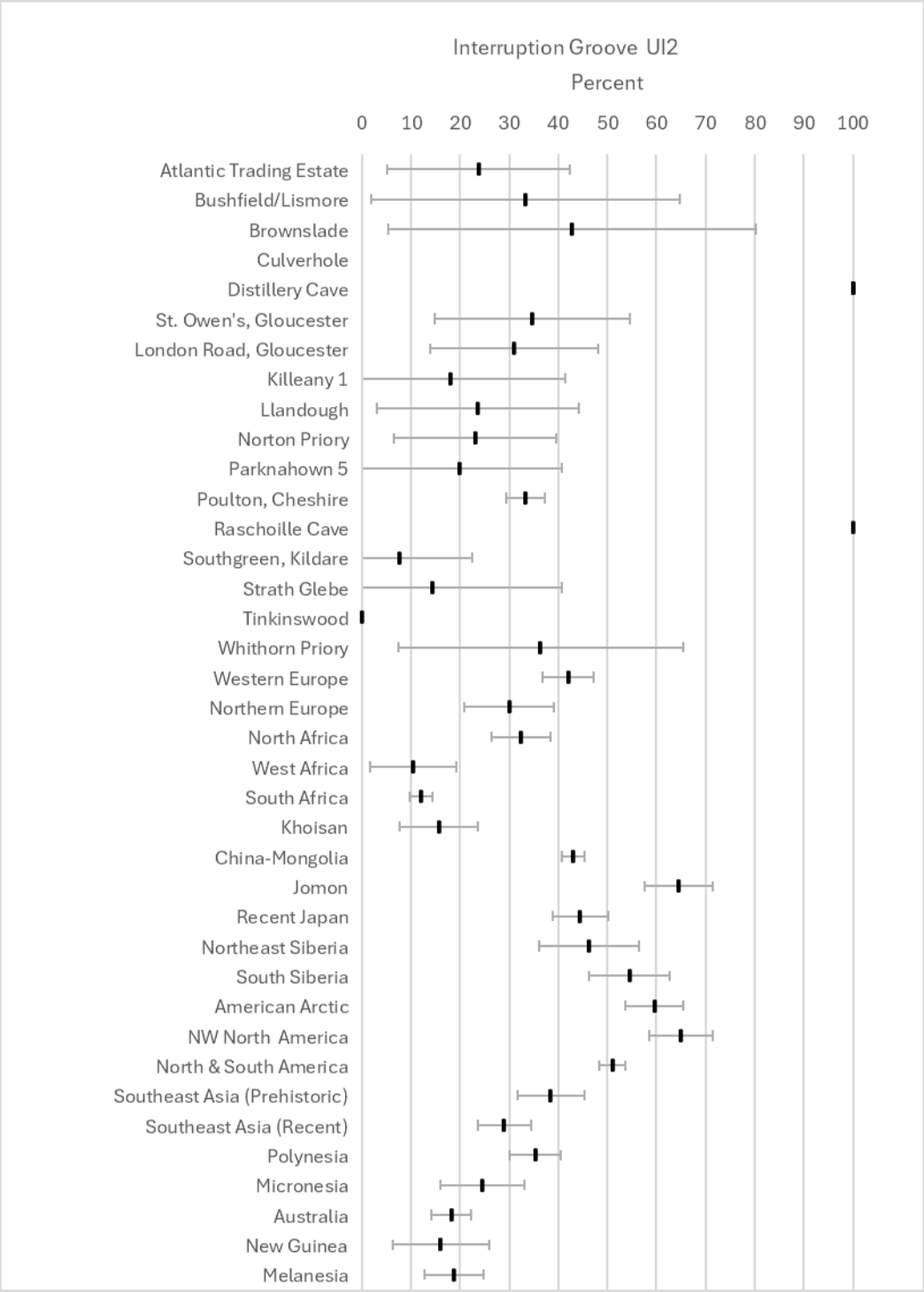

Figure 35: Interruption groove UI2 trait frequency variation among British and Irish samples and global populations (trait frequency represented by vertical line with horizontal bars showing ±2 standard errors).

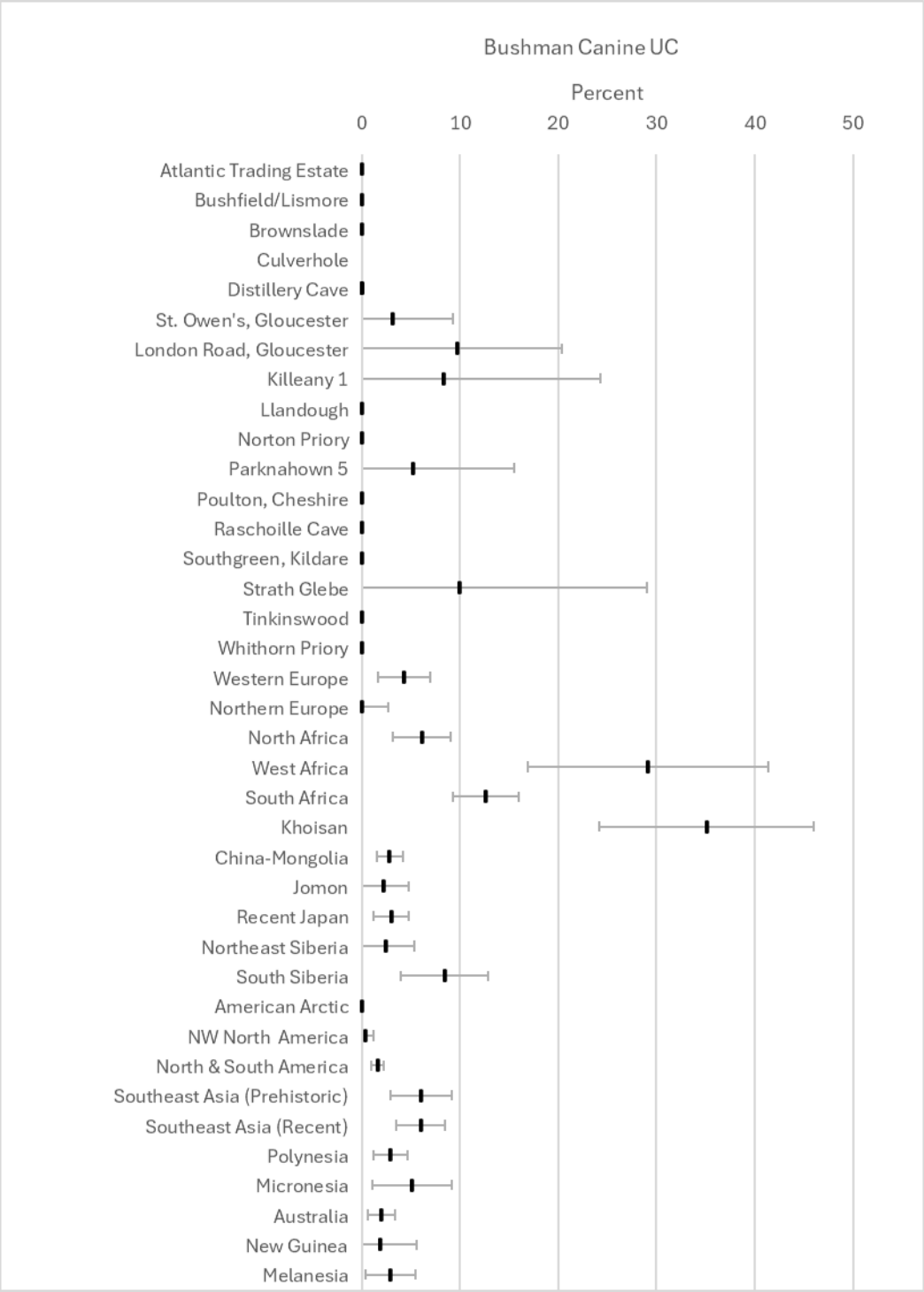

Figure 36: Bushman canine UC trait frequency variation among British and Irish samples and global populations (trait frequency represented by vertical line with horizontal bars showing ±2 standard errors).

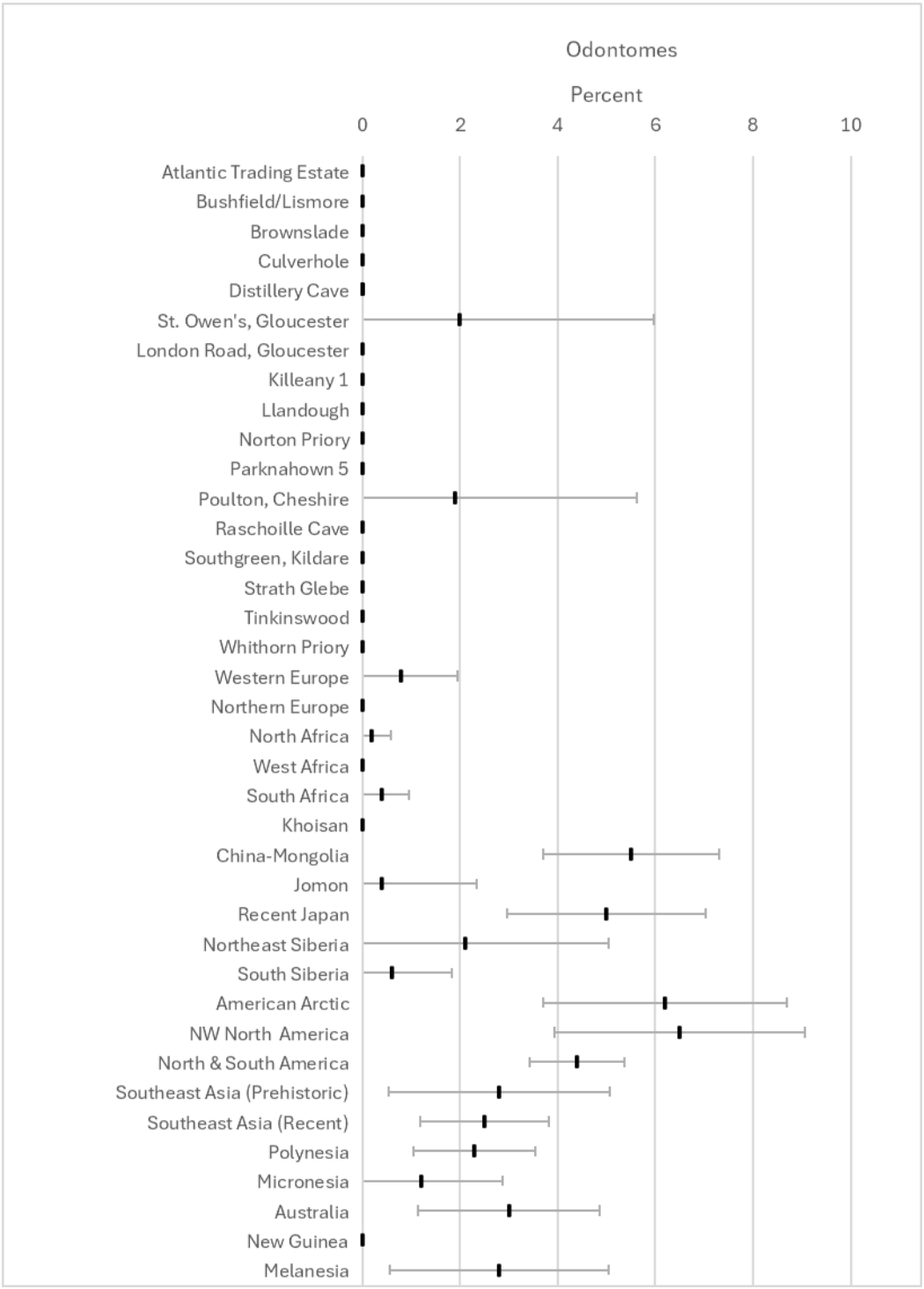

Figure 37: Odontomes trait frequency variation among British and Irish samples and global populations (trait frequency represented by vertical line with horizontal bars showing ±2 standard errors).

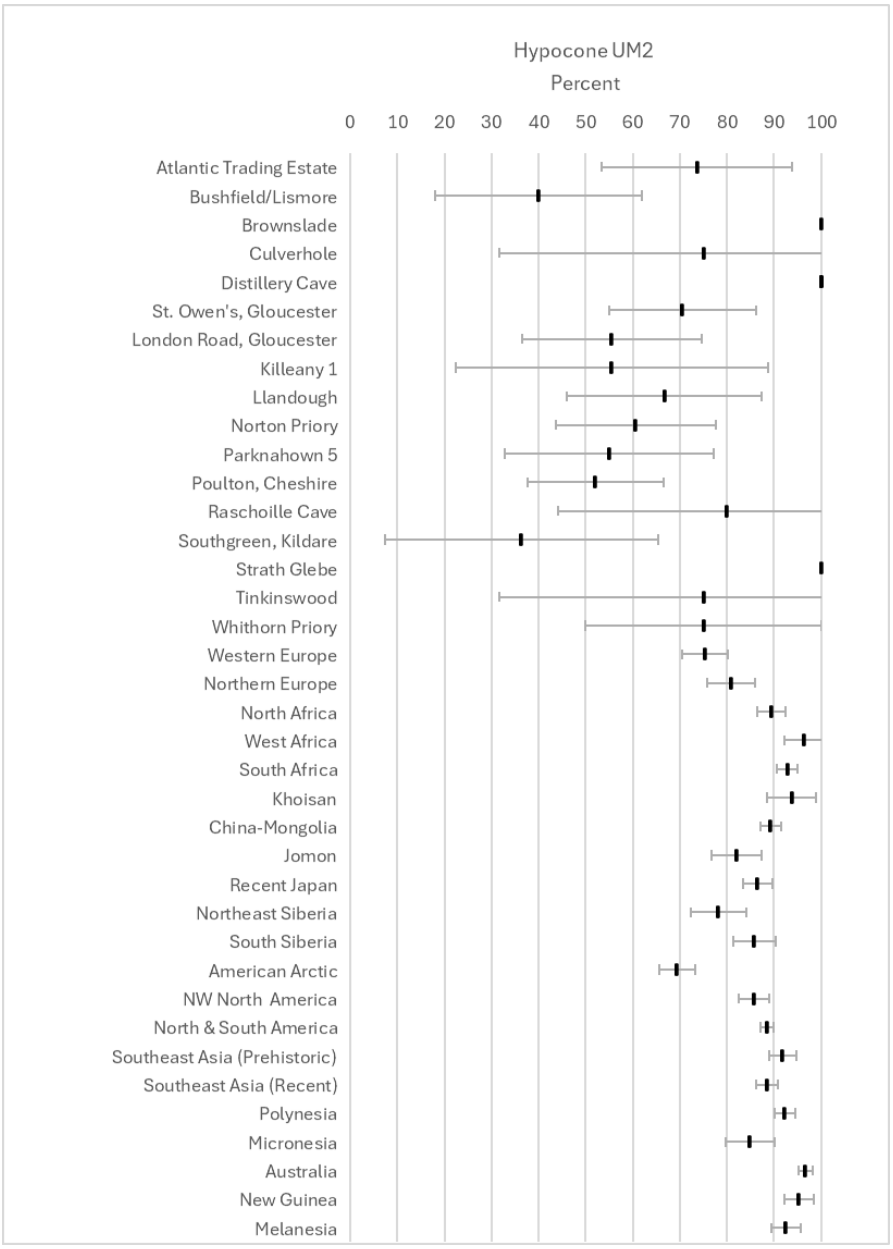

Figure 38: Hypocone UM2 trait frequency variation among British and Irish samples and global populations (trait frequency represented by vertical line with horizontal bars showing ±2 standard errors).

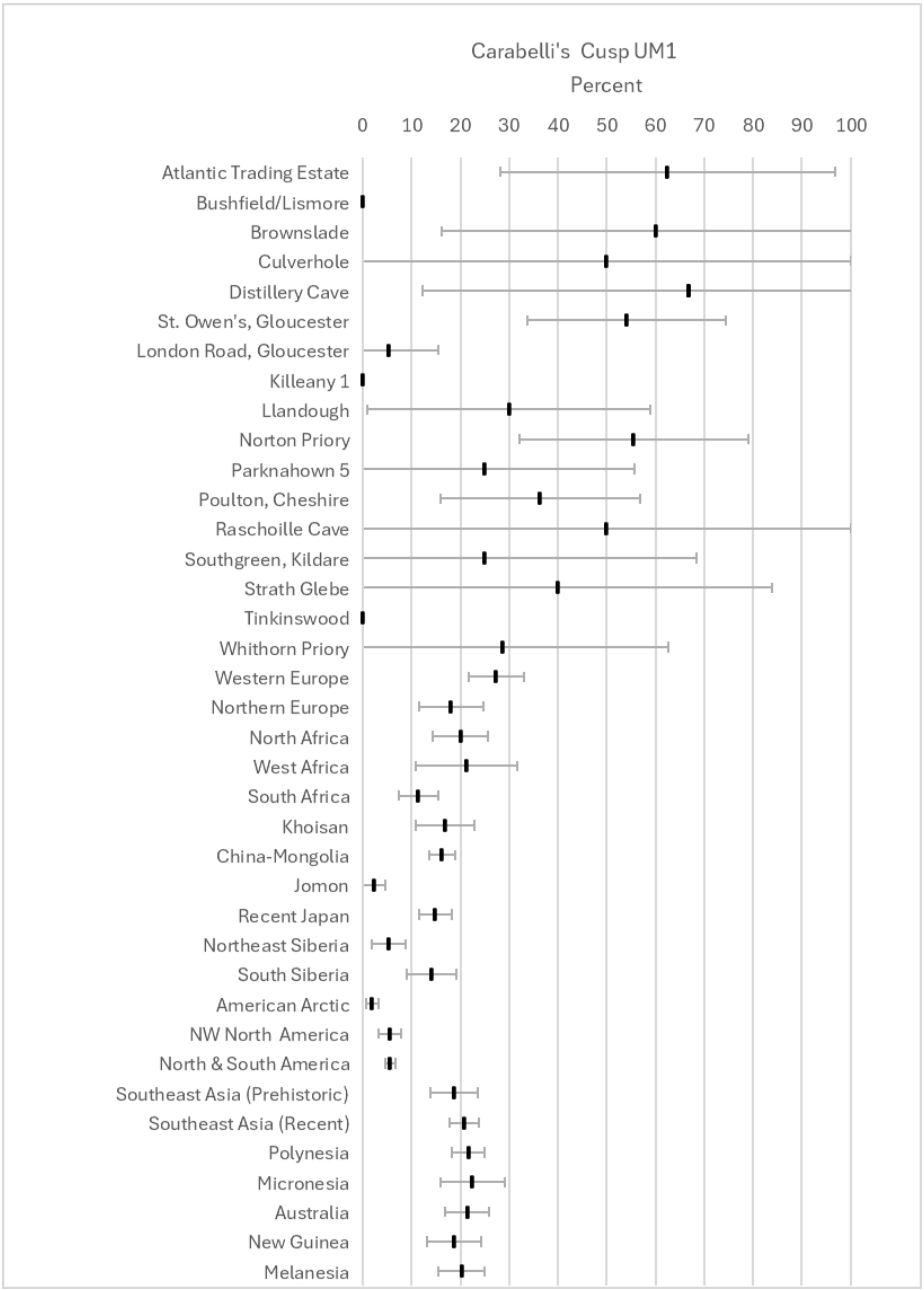

Figure 39: Carabelli's cusp UM1 trait frequency variation among British and Irish samples and global populations (trait frequency represented by vertical line with horizontal bars showing ±2 standard errors).

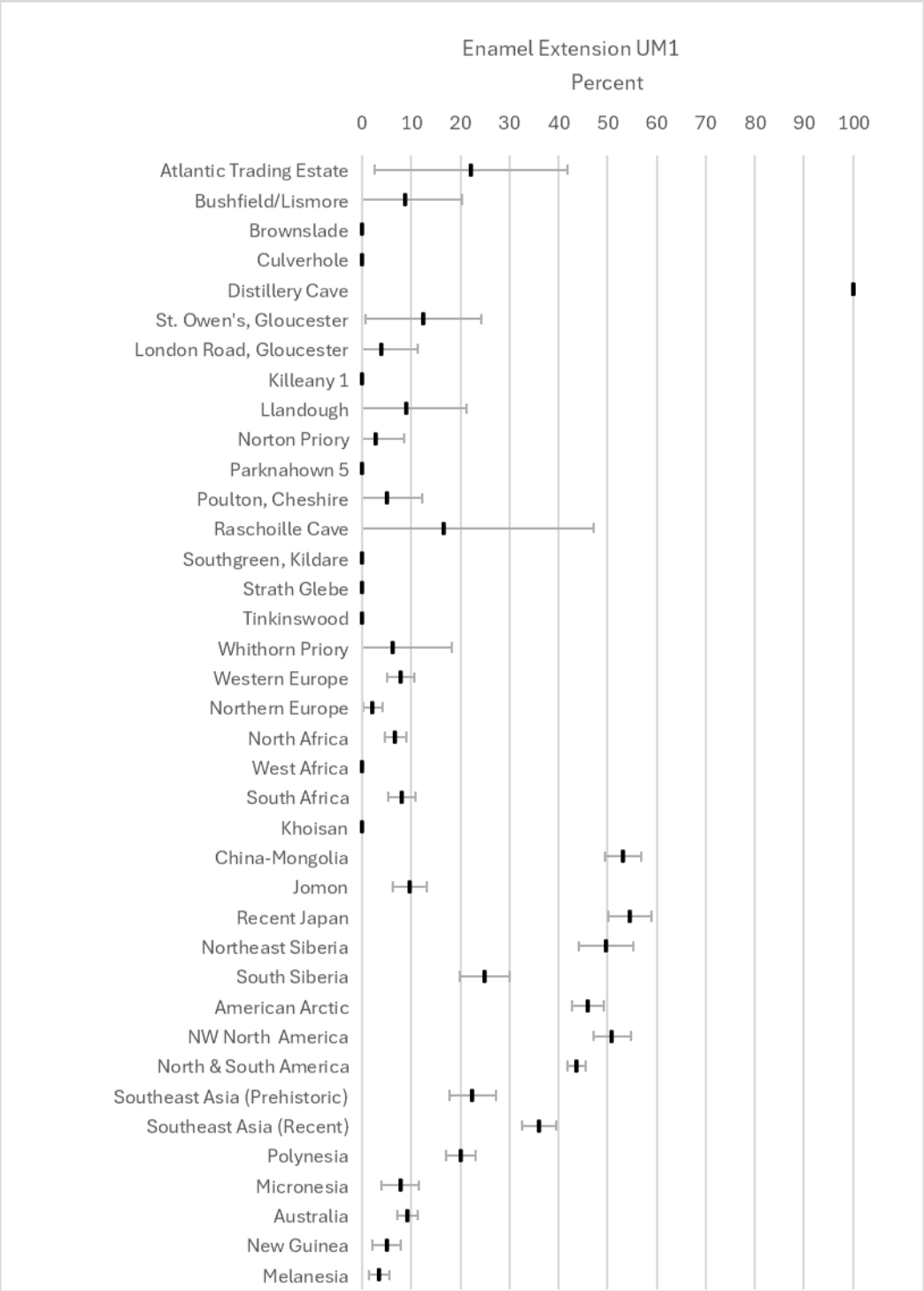

Figure 40: Enamel Extension UM1 trait frequency variation among British and Irish samples and global populations (trait frequency represented by vertical line with horizontal bars showing ±2 standard errors).

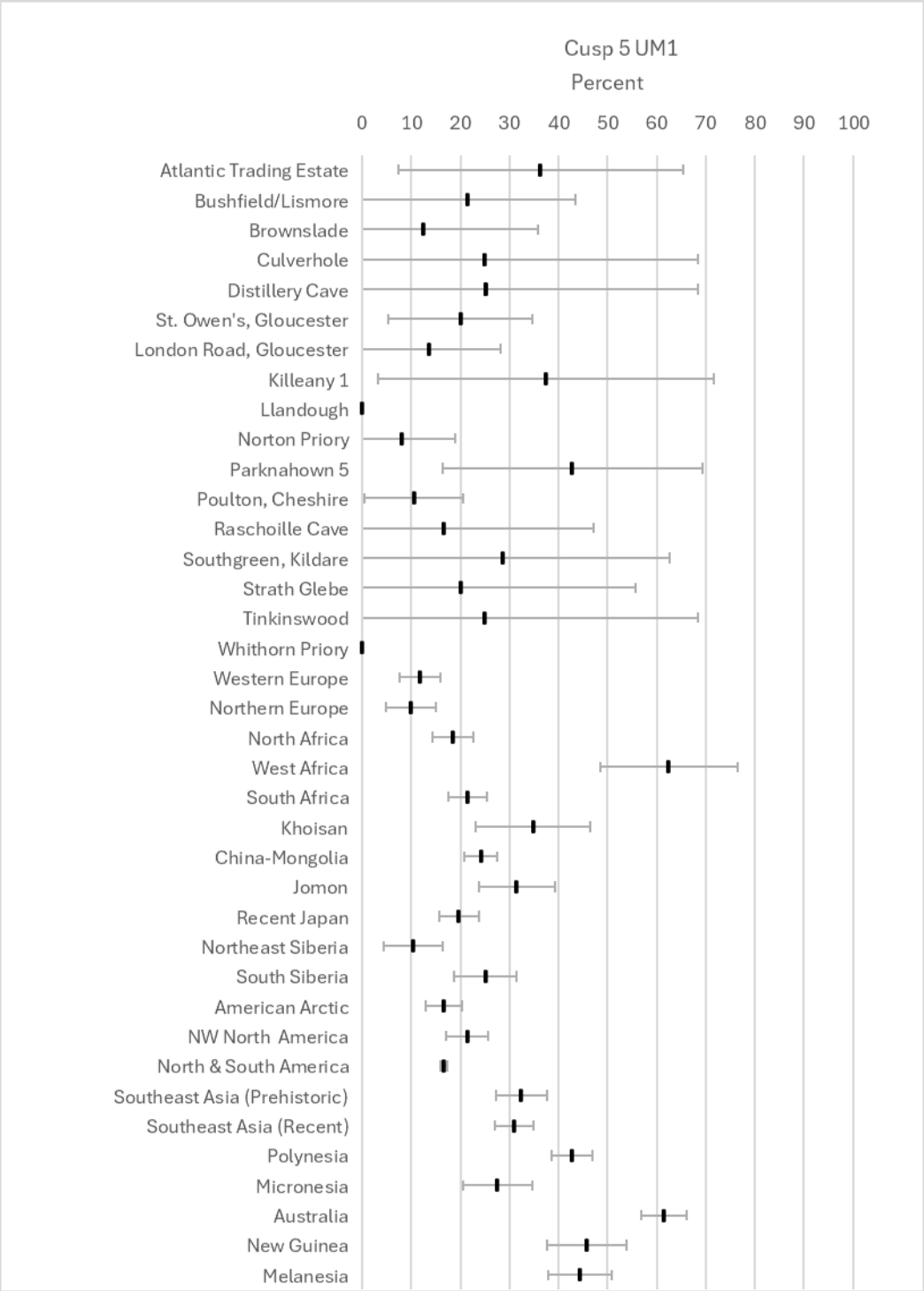

Figure 41: Cusp 5 UM1 trait frequency variation among British and Irish samples and global populations (trait frequency represented by vertical line with horizontal bars showing ±2 standard errors).

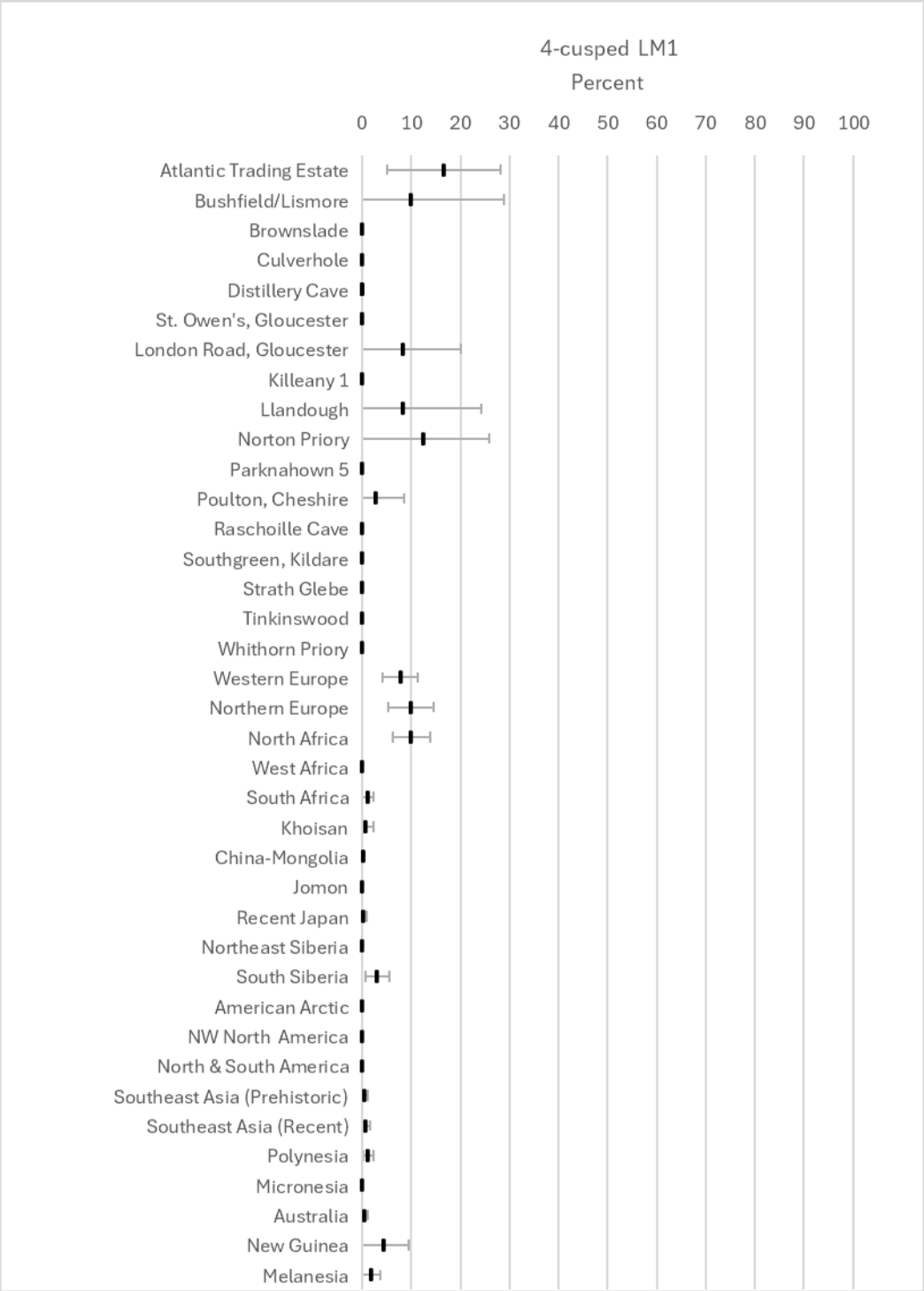

Figure 42: 4-cusped LM1 trait frequency variation among British and Irish samples and global populations (trait frequency represented by vertical line with horizontal bars showing ±2 standard errors).

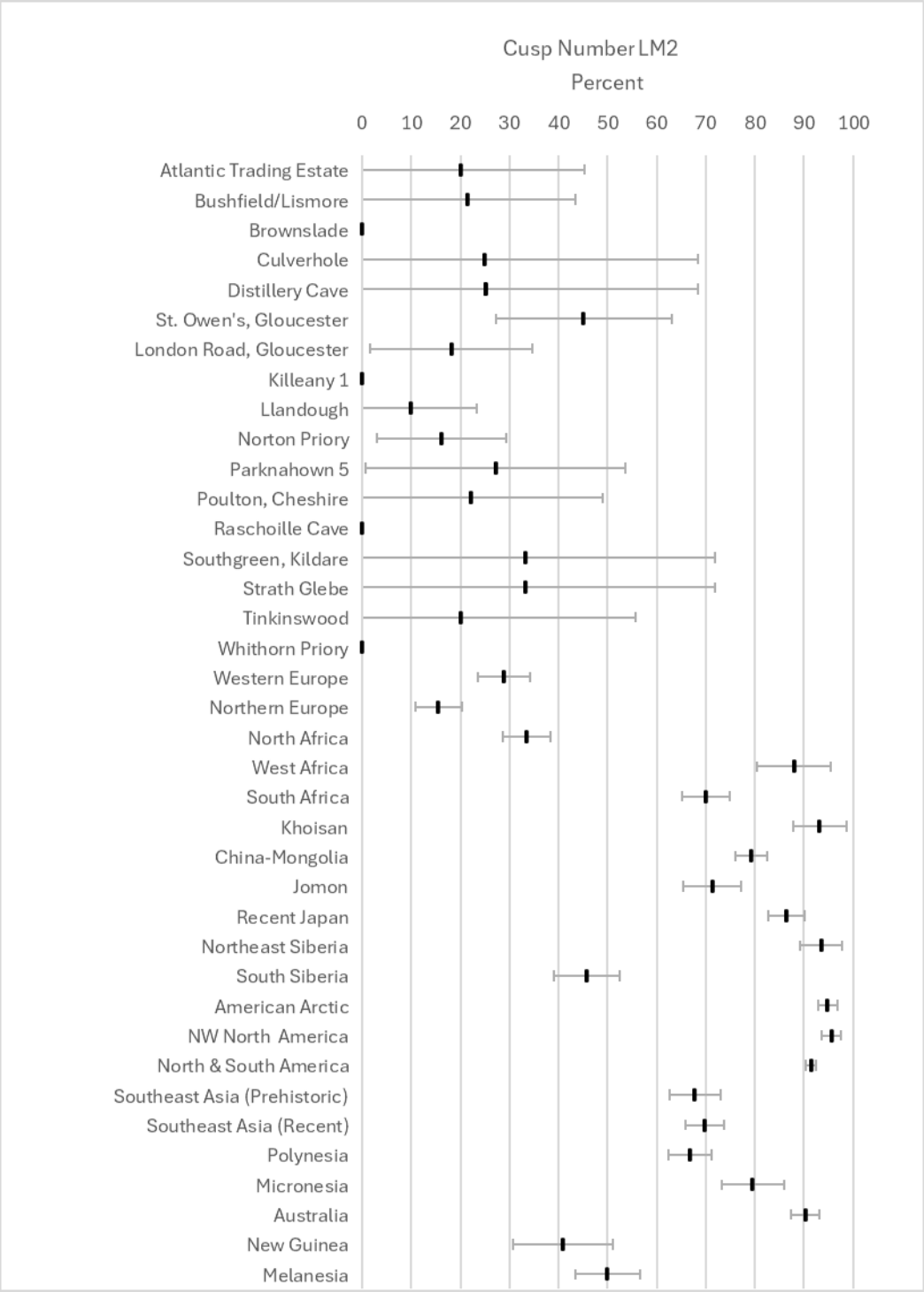

Figure 43: Cusp number LM2 trait frequency variation among British and Irish samples and global populations (trait frequency represented by vertical line with horizontal bars showing ±2 standard errors).

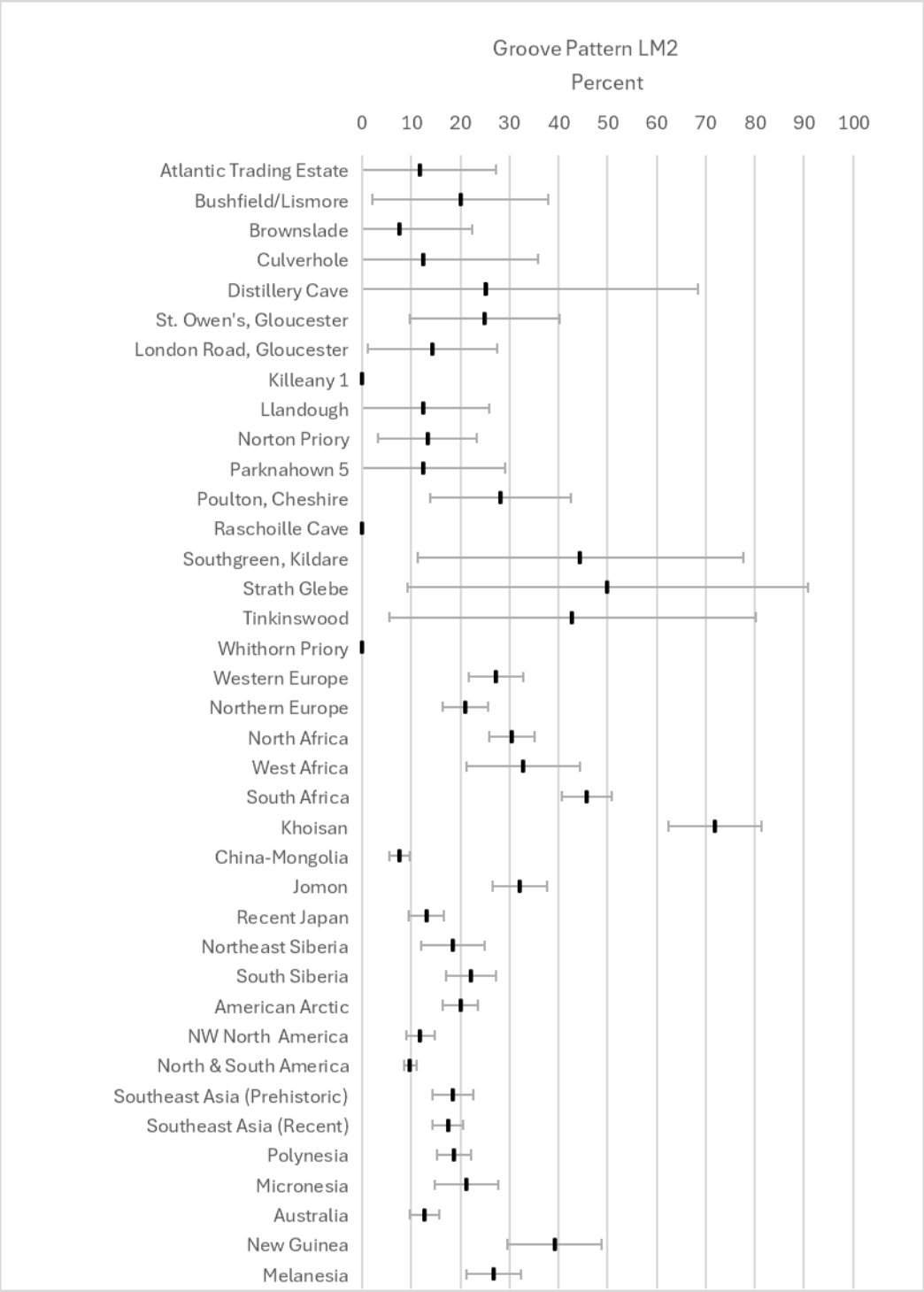

Figure 44: Groove Pattern LM2 trait frequency variation among British and Irish samples and global populations (trait frequency represented by vertical line with horizontal bars showing ±2 standard errors).

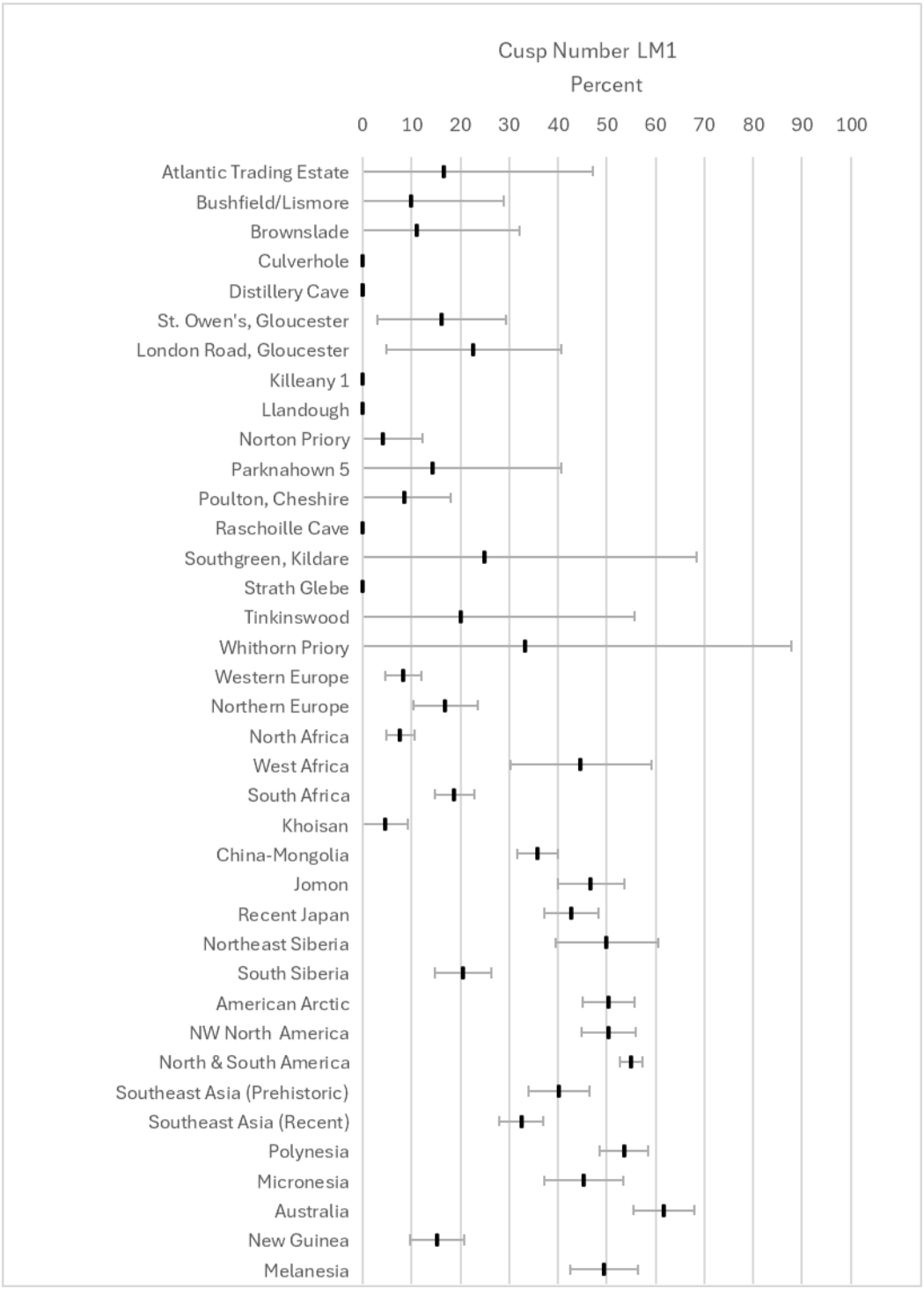

Figure 45: Cusp number LM1 trait frequency variation among British and Irish samples and global populations (trait frequency represented by vertical line with horizontal bars showing ±2 standard errors).

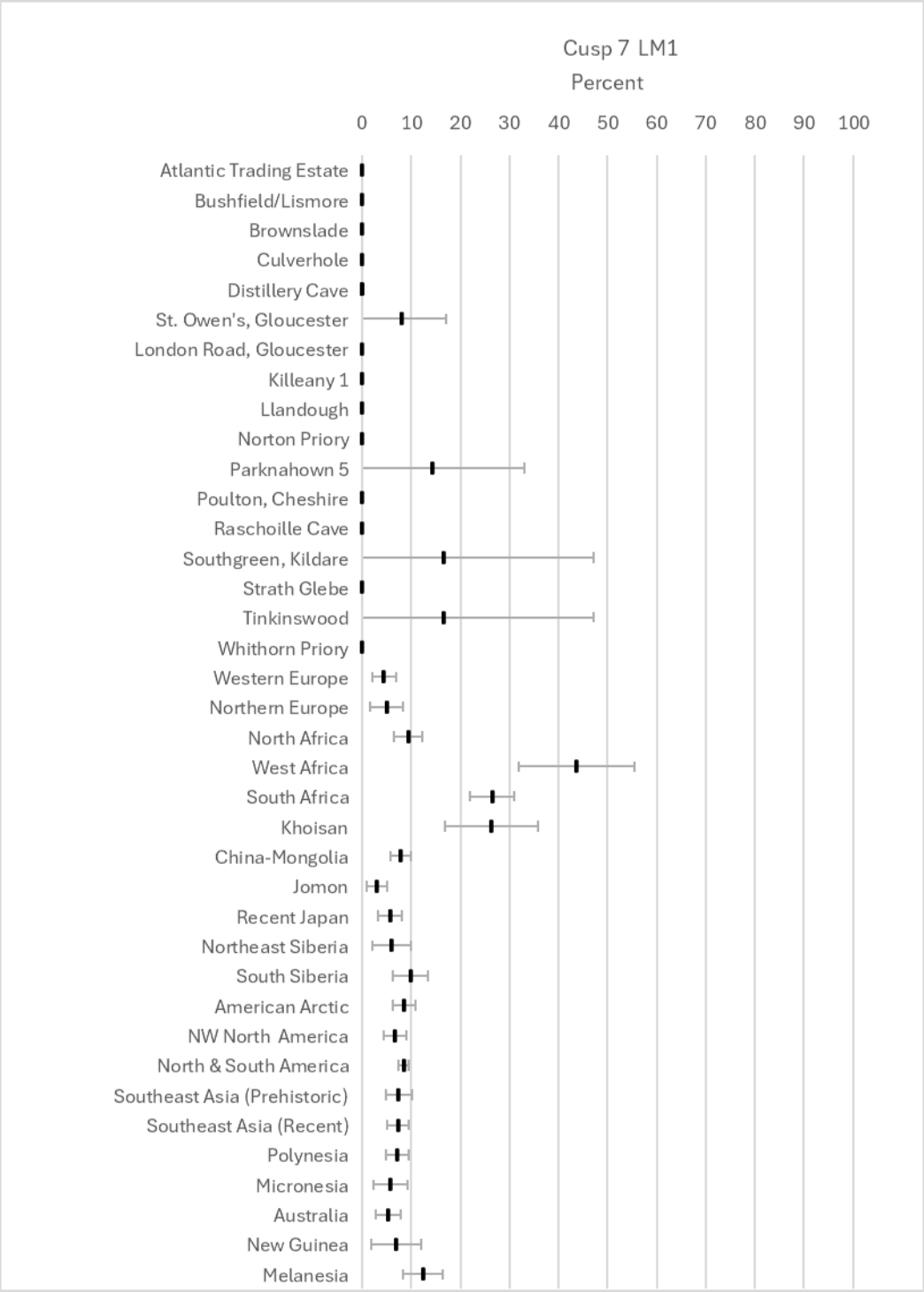

Figure 46: Cusp 7 LM1 trait frequency variation among British and Irish samples and global populations (trait frequency represented by vertical line with horizontal bars showing ±2 standard errors).

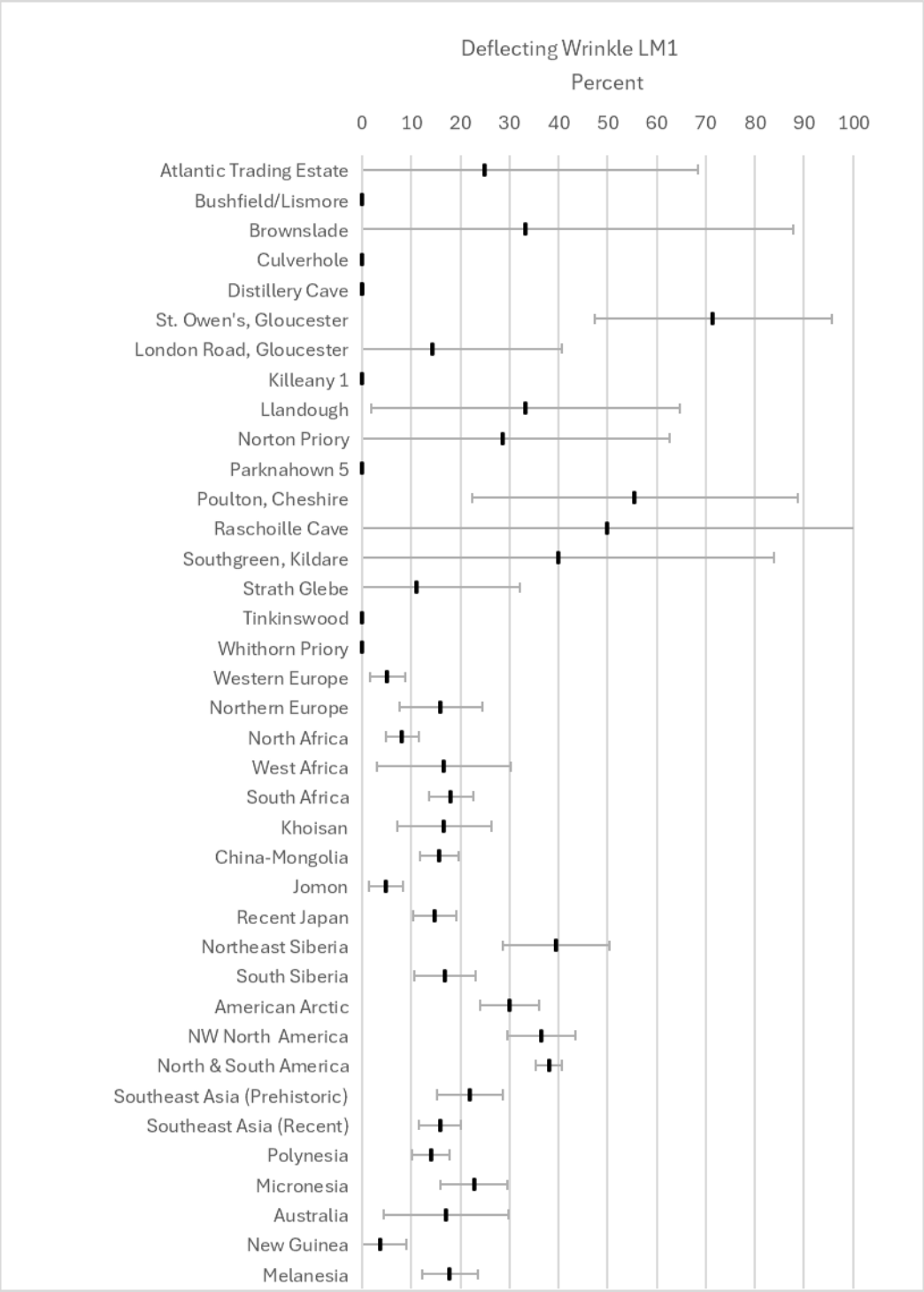

Figure 47: Deflecting Wrinkle LM1 trait frequency variation among British and Irish samples and global populations (trait frequency represented by vertical line with horizontal bars showing ±2 standard errors).

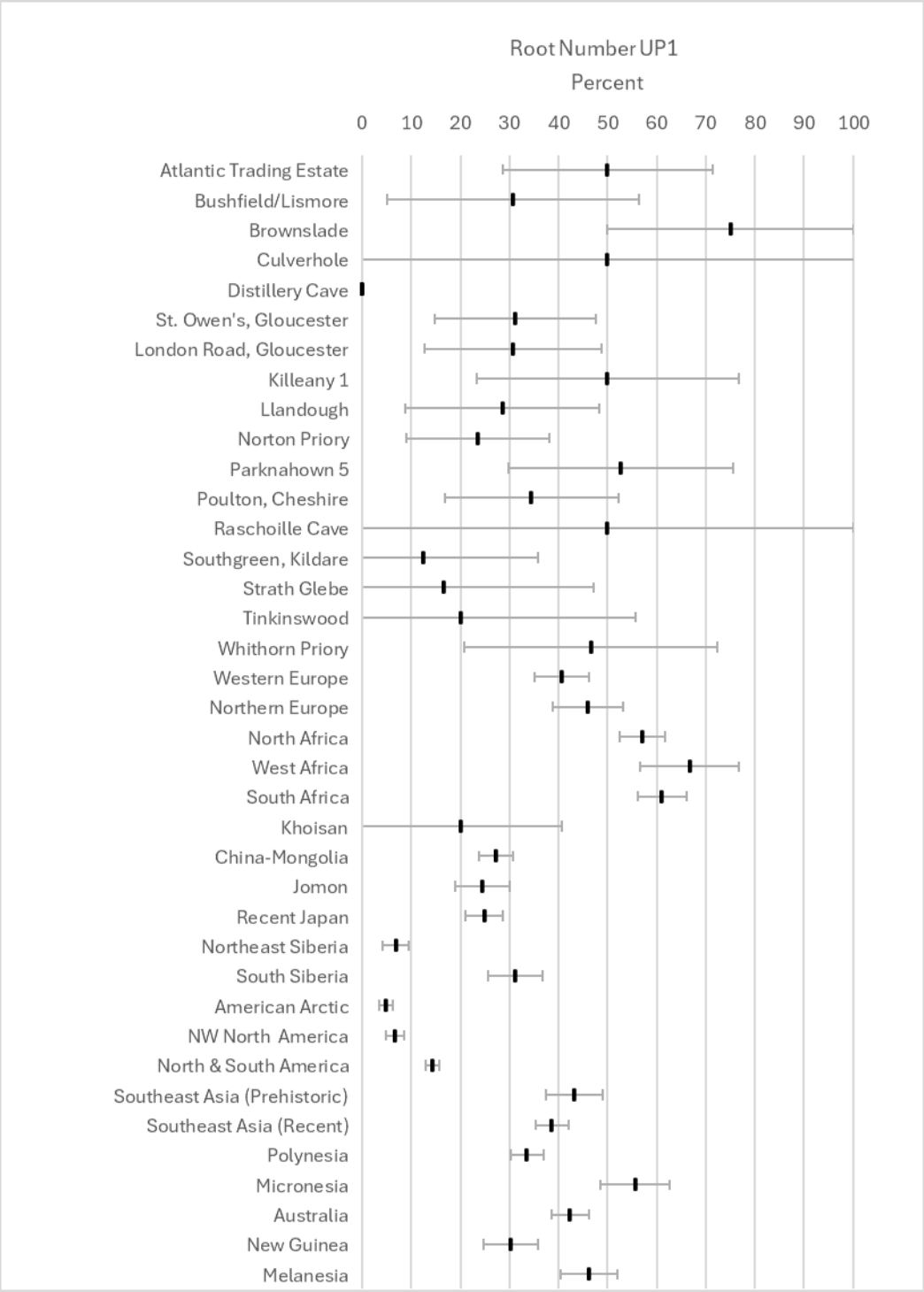

Figure 48: Root number UP1 trait frequency variation among British and Irish samples and global populations (trait frequency represented by vertical line with horizontal bars showing ±2 standard errors).

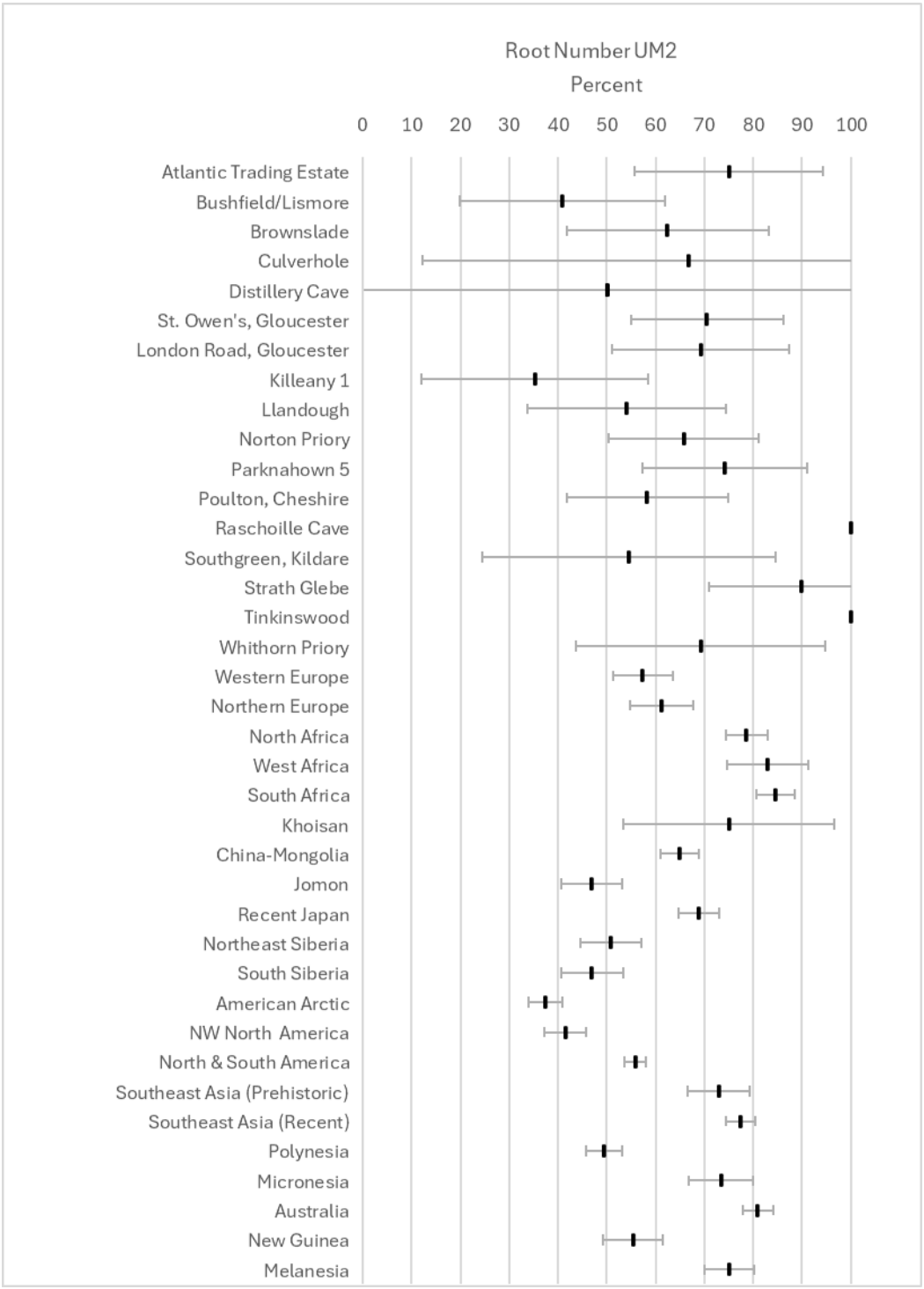

Figure 49: Root number UM2 trait frequency variation among British and Irish samples and global populations (trait frequency represented by vertical line with horizontal bars showing ±2 standard errors).

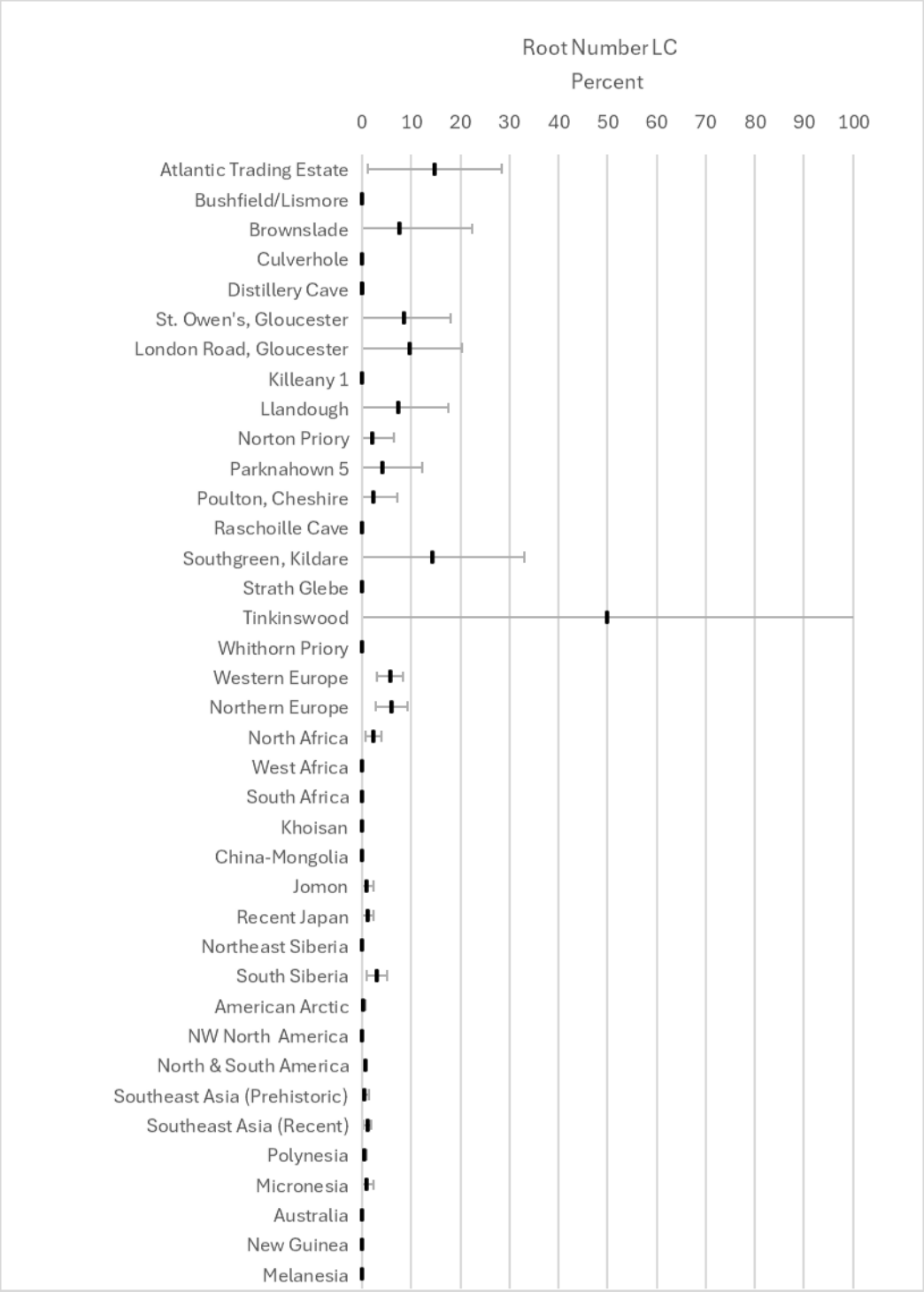

Figure 50: Root number LC trait frequency variation among British and Irish samples and global populations (trait frequency represented by vertical line with horizontal bars showing ±2 standard errors).

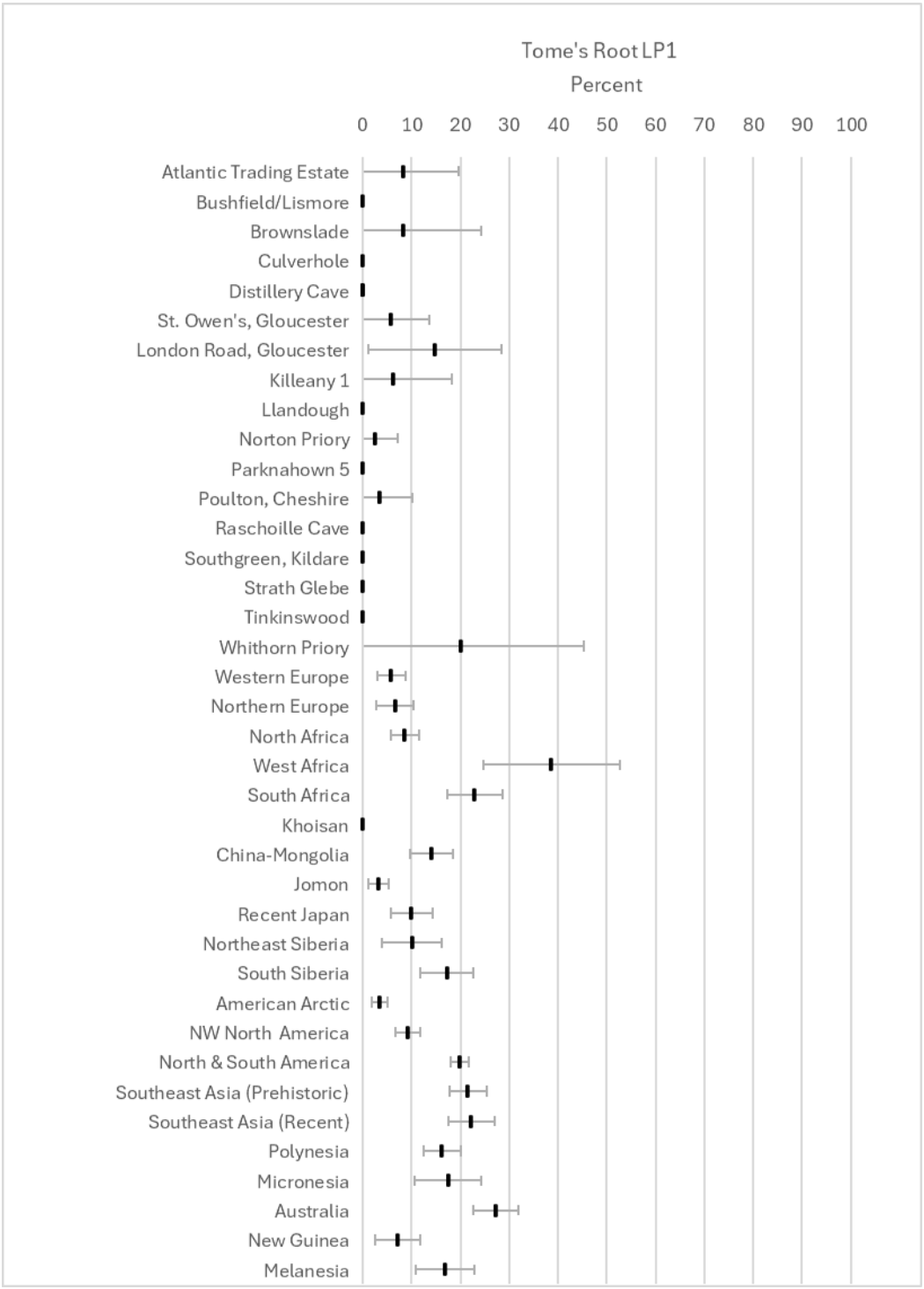

Figure 51: Tomes' Root LP1 trait frequency variation among British and Irish samples and global populations (trait frequency represented by vertical line with horizontal bars showing ±2 standard errors).

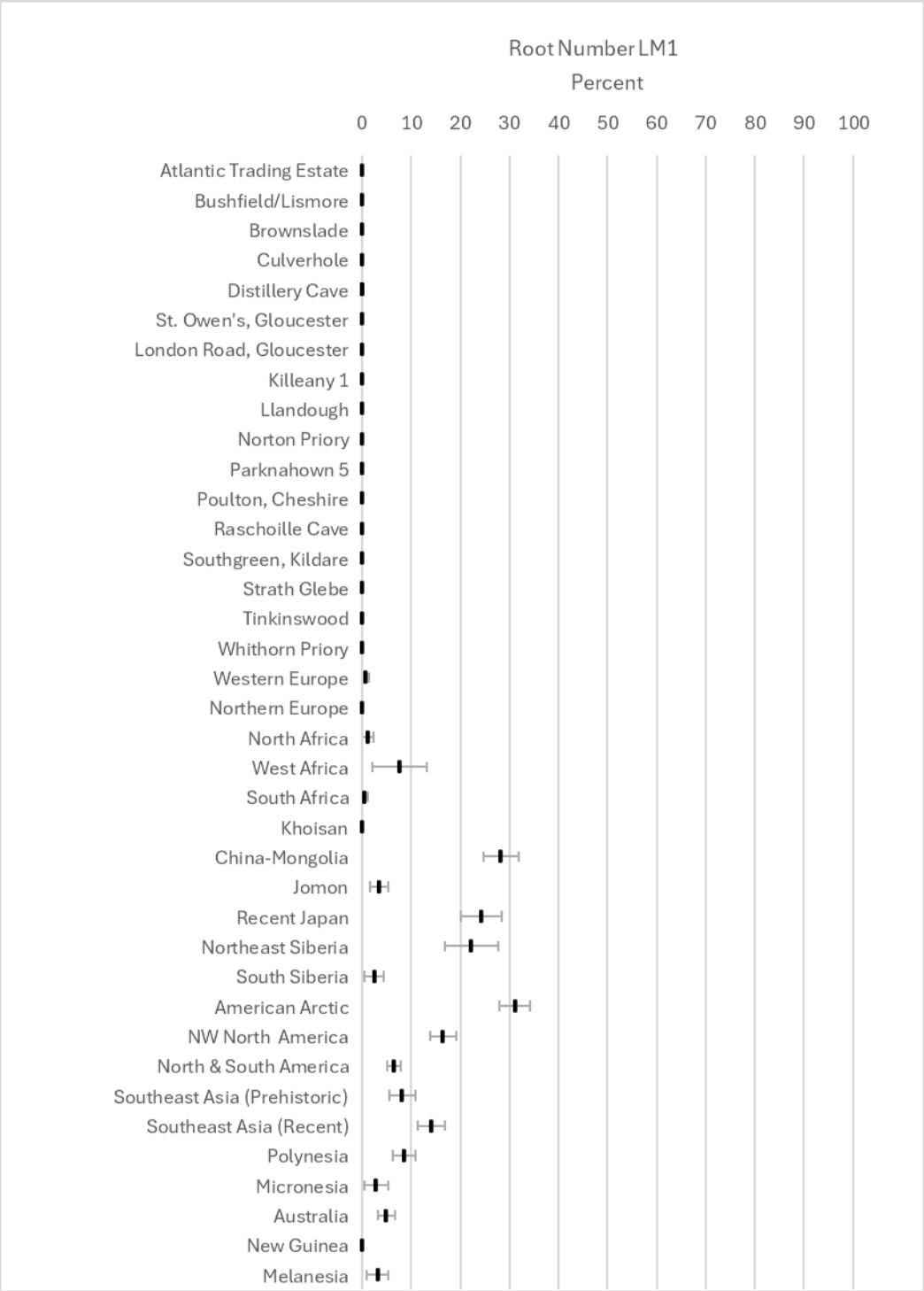

Figure 52: Root number LM1 trait frequency variation among British and Irish samples and global populations (trait frequency represented by vertical line with horizontal bars showing ±2 standard errors).

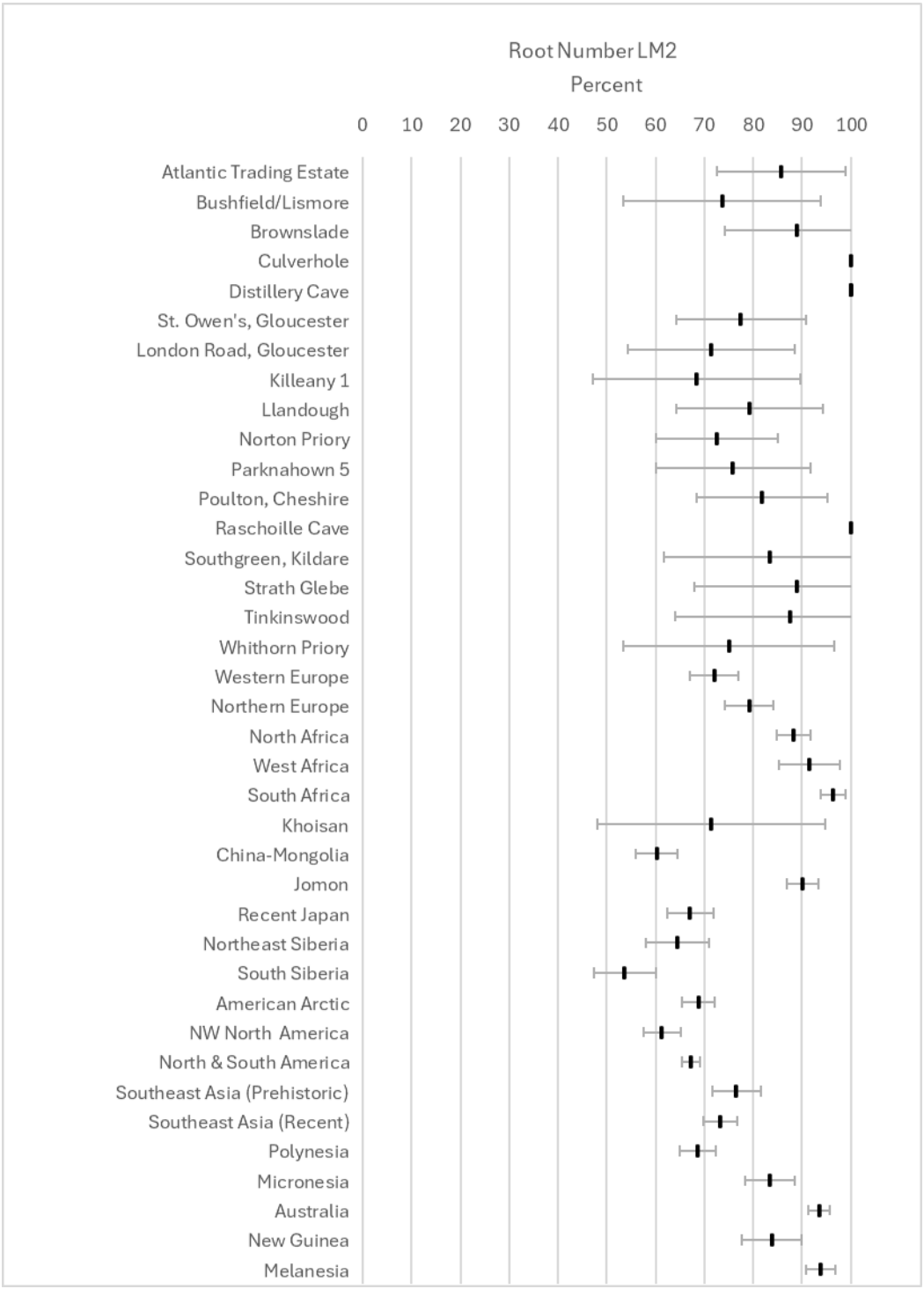

Figure 53: Root number LM2 trait frequency variation among British and Irish samples and global populations (trait frequency represented by vertical line with horizontal bars showing ±2 standard errors).